

**Cycloaddition reactions of imidazolium and phthalazinium
dicyanomethanide 1,3-dipoles: synthesis, mechanism
and the effect of water**

Eamon M. Moloney, B.Sc.

Thesis presented for the Ph.D. Degree
of the
National University of Ireland



Department of Chemistry, National University of Ireland, Galway
May 2017

Head of Department: Professor P.V. Murphy
Supervisors: Professor R.N. Butler, D.Sc.
Dr. Niall Geraghty

Table of Contents

Abstract	i
Acknowledgements	iii
Abbreviations	iv

Chapter 1

Introduction: azolium and azinium dicyanomethanide 1,3-dipoles

1.1	Introduction	1
1.2	Synthesis of azinium and azolium dicyanomethanide 1,3-dipoles	4
1.3	Structure of azinium and azolium 1,3-dipoles	6
1.4	Some cycloaddition reactions of azinium and azolium dicyanomethanide 1,3-dipoles	10
1.4.1	Reactions with symmetrical acetylenic dipolarophiles	10
1.4.2	Reactions with unsymmetrical acetylenic dipolarophiles	14
1.4.3	Reactions with alkenes	18
1.4.4	Double cycloadditions	21
1.5	Kinetic studies	22

Chapter 2

Synthetic and mechanistic studies on the cycloaddition reactions of imidazolium dicyanomethanide 1,3-dipoles and the 1-phenyl-1,2,4-triazolium-4-dicyanomethanide 1,3-dipole

2.1	Introduction	25
2.1.1	Frontier molecular orbital theory and Sustmann classification	26
2.1.2	Regiochemistry of 1,3-dipolar cycloadditions.	28
2.1.3	Azolium 1,3-dipoles	29
2.1.4	Imidazolium ylides	33
2.1.5	Project outline	38
2.2	Synthesis of imidazolium dicyanomethanide 1,3-dipoles	39
2.2.1	Synthesis of 1-methylimidazolium-3-dicyanomethanide 1,3-dipole 28	39
2.2.2	Synthesis of 1-benzylimidazolium-3-dicyanomethanide 1,3-dipole 112	41
2.2.3	Synthesis of 1-phenylimidazolium-3-dicyanomethanide 1,3-dipole 114	42
2.3	Cycloaddition reactions of imidazolium dicyanomethanide 1,3-dipoles with alkyne dipolarophiles	44
2.3.1	Cycloaddition reactions of 1,3-dipole 28 with symmetrical electron poor alkyne dipolarophiles (DMAD/DEAD)	44

2.3.2	Cycloaddition reactions of 1,3-dipole 28 with unsymmetrical electron poor alkyne dipolarophiles (MP/EP)	48
2.3.3	Cycloaddition reactions of 1,3-dipole 112 with symmetrical electron poor alkyne dipolarophiles (DMAD/DEAD)	51
2.3.4	Cycloaddition reactions of 1,3-dipole 112 with unsymmetrical electron poor alkyne dipolarophiles (MP/EP)	53
2.3.5	Cycloaddition reactions of 1,3-dipole 114 with symmetrical electron poor alkyne dipolarophiles (DMAD/DEAD)	56
2.3.6	Cycloaddition reactions of 1,3-dipole 114 with unsymmetrical electron poor alkyne dipolarophiles (MP/EP)	59
2.3.7	The rearrangement mechanism as proposed by Boekelheide and Fedoruk.	63
2.4	Cycloaddition reactions of imidazolium dicyanomethanide 1,3-dipoles with alkene dipolarophiles	64
2.4.1	Cycloaddition reaction of 1-methylimidazolium-3-dicyanomethanide 1,3-dipole 28 with <i>N</i> -phenylmaleimide 131	64
2.4.2	Reactions of 1-methylimidazolium-3-dicyanomethanide 1,3-dipole 28 and 1-benzylimidazolium-3-dicyanomethanide 1,3-dipole 112 with maleic anhydride 134	68
2.4.3	Reactions of 1-methylimidazolium-3-dicyanomethanide 1,3-dipole 28 with maleic anhydride 134 : theoretical analysis	72
2.5	Isolation and study of an initial cycloaddition adduct	74
2.5.1	Synthesis of 1-phenyl-1,2,4-triazole 145	75
2.5.2	Synthesis of 1-phenyl-1,2,4-triazolium-4-dicyanomethanide 142	76
2.5.3	Cycloaddition reaction of 1-phenyl-1,2,4-triazolium-4-dicyanomethanide 142 with DMAD 25 : isolation of the initial cycloadduct 143	77
2.5.4	Cycloaddition reaction of 1-phenyl-1,2,4-triazolium-4-dicyanomethanide 142 with DMAD 25 : generation of the ring expanded product 144	79
2.5.5	Cycloaddition reaction of 1-phenyl-1,2,4-triazolium-4-dicyanomethanide 142 with DMAD 25 : investigation of the ring expansion rearrangement by NMR spectroscopy	81
2.5.6	Mechanism of the rearrangement	86
2.6	Conclusion	88
2.7	Postscript	89
2.8	Experimental	91

Chapter 3

A study of synthesis, kinetics and water solvent effects in the reactions of phthalazinium-2-dicyanomethanide with *p*-substituted benzylidene acetones: comparisons with substituted styrenes and alkyl vinyl ketones

3.1	Introduction	117
3.1.1	The hydrophobic effect	118
3.1.2	Special hydrogen bonding	121
3.1.3	Polarity effects	124
3.1.4	“On Water” reactions	125
3.2	Synthesis of phthalazinium-2-dicyanomethanide 1,3-Dipole 45	128
3.3	Synthetic study of the reactions of phthalazinium-2-dicyanomethanide dipole 45 with <i>p</i>-substituted benzylidene acetone dipolarophiles in acetonitrile	129
3.3.1	Cycloaddition reaction of phthalazinium-2-dicyanomethanide 1,3-dipole 45 with benzylidene acetone 178	130
3.3.2	Cycloaddition reaction of phthalazinium-2-dicyanomethanide 1,3-dipole 45 with <i>p</i> -chlorobenzylidene acetone 181	133
3.3.3	Cycloaddition reaction of phthalazinium-2-dicyanomethanide 1,3-dipole 45 with <i>p</i> -tolylbenzylidene acetone 184	136
3.4	Kinetic investigation of the cycloaddition reactions of the phthalazinium-2-dicyanomethanide 1,3-dipole 45 with benzylidene acetone dipolarophiles	139
3.4.1	Water and polarity of the transition state: Hammett plots	140
3.5	Computational study	142
3.5.1	Calculations with 0-water and 4-water clusters	142
3.5.2	Plot of activation energy versus Hammett constants	144
3.5.3	Theoretical Hammett plot	145
3.5.4	Regiochemistry	146
3.5.5	Ionisation potential	148
3.6	Synthetic study of “on water” cycloaddition reactions of phthalazinium-2-dicyanomethanide 1,3-dipole 45	149
3.6.1	“On water” cycloaddition of phthalazinium dicyanomethanide 1,3-dipole 45 with <i>N</i> -phenylmaleimide 131	150
3.6.2	“On water” cycloaddition of phthalazinium-2-dicyanomethanide 1,3-dipole 45 with <i>p</i> -chlorobenzylidene acetone 181	152
3.7	Comparison with substituted styrenes	155
3.8	Comparison with alkyl vinyl ketones	159
3.9	Conclusion	162
3.10	Future work	163
3.11	Experimental	164
	References	175
	Publications	181

Abstract

The cycloaddition reactions of imidazolium-3-dicyanomethanide 1,3-dipoles with electron poor alkene and alkyne dipolarophiles were explored. The reactions of these azolium 1,3-dipoles with alkyne dipolarophiles generated unstable initial cycloadducts that rearranged *in situ* to yield ring expanded products. The imidazo[2,3-*a*]pyridine products were formed as loss of aromaticity in the initial fused cycloadduct drove the subsequent ring expansion rearrangement. Single regioisomers were produced when unsymmetrical dipolarophiles were used in the reactions.

An imidazo[2,3-*a*]pyridine product was also generated when the 1-methyl-imidazolium-3-dicyanomethanide 1,3-dipole was reacted with the electron poor alkene *N*-phenylmaleimide. However, imidazolium-3-dicyanomethanide 1,3-dipoles reacted with maleic anhydride to form novel ylide products. These Michael Addition reactions generated unstable intermediates that underwent *in situ* 1,2-rearrangement to form the new spirally twisted imidazolium ylide compounds.

The reaction of 1-phenyl-1,2,4-triazolium-4-dicyanomethanide 1,3-dipole with DMAD produced a stable initial cycloadduct that could be isolated under cold conditions. The initial cycloadduct easily underwent ring expansion rearrangement in solution at room temperature to form a 1,2,4-triazolo[4,5-*a*]pyridine product. Tracking the rearrangement by NMR spectroscopy revealed the presence of an intermediate that could be seen to develop and decline as the initial cycloadduct converted into the ring expanded product.

The cycloaddition reaction of the phthalazinium dicyanomethanide 1,3-dipole with benzylidene acetone dipolarophiles was also examined in both acetonitrile and water. New 1,2-substituted tetrahydropyrrolo[2,1-*a*]phthalazine derivatives were synthesized. The reactions produced two products, both with the aryl substituent on the C-2 position. The major product in each case had the aryl substituent in the *endo*-position.

The kinetics of the cycloaddition reactions of phthalazinium dicyanomethanide 1,3-dipole with benzylidene acetone dipolarophiles was also explored. Large rate accelerations were observed when the reactions were completed in aqueous acetonitrile rather than pure acetonitrile. Experimentally and theoretically derived Hammett plots ruled out increased polarity of the cycloaddition transition state as the cause of rate accelerations observed in the presence of water. The accelerations are most likely due to special hydrogen bonding effects.

Cycloaddition reactions involving solid phthalazinium dicyanomethanide 1,3-dipole and the solid dipolarophiles *p*-chlorobenzylidene acetone and *N*-phenylmaleimide were completed using pure water as the reaction solvent. The *p*-chlorobenzylidene acetone dipolarophile required liquefaction to allow the “on water” cycloaddition to proceed. Liquefaction of *N*-phenylmaleimide was not required as the dipolarophile had sufficient solubility in water to generate an oil layer. Solid-solid reactions have therefore been shown to be possible using the “on water” methodology.

Acknowledgments

Thanks to my parents, Francis and Marie, who supported me every step of the way.

My sincerest thanks to Prof. R.N. Butler whose guidance, patience and wisdom is both greatly appreciated and greatly missed. Ar dheis Dé go raibh a anam.

Many thanks to Dr. Niall Geraghty, who went above and beyond the call of duty in helping to bring this thesis to its completion.

My thanks to the technical staff of the department, particularly John Muldoon, Seamus Collier and Karen Costello.

My special thanks to Dearbhla for her level-headedness, patience and support.

Thanks to my outstanding lab mates- Aoife, John, Liam and Mark.

My thanks to the ladies and gentlemen of the Chemistry department who made my time in Galway such a joy. A special thanks to my housemates- Caroline & Paul; the “gentlemen”- Cormac, Kenneth, Stephen & Wayne; and the Chemhead ladies- Blaithín, Hilary & Sarah.

I gratefully acknowledge the receipt of an IRCSET postgraduate research scholarship.

Abbreviations

DEAD	Diethyl acetylenedicarboxylate
DEPT	Distortionless enhancement by polarization transfer
DFT	Density functional theory
DMAD	Dimethyl acetylenedicarboxylate
DMSO	Dimethyl sulfoxide
EP	Ethyl propiolate
EVK	Ethyl vinyl ketone
FMO	Frontier molecular orbital
GnCl	Guanidinium chloride
HFP	Hexafluoro-2-propanol
HOMO	Highest occupied molecular orbital
LUMO	Lowest unoccupied molecular orbital
MP	Methyl propiolate
MVK	Methyl vinyl ketone
NOEDS	Nuclear Overhauser enhanced differential spectroscopy
RORC	Ring opening, ring closing
TCNEO	Tetracyanoethylene oxide
TCNE	Tetracyanoethylene

Dedicated to my parents, Francis and Marie

Chapter 1

**Introduction: azolium and azinium
dicyanomethanide 1,3-dipoles**

1.1 Introduction

The 1,3-dipolar cycloaddition is an important reaction in organic synthesis, used to generate a wide variety of heterocyclic rings. The generality of the reaction was discovered by Huisgen in the 1960s.^{1, 2} A 1,3-dipole is a three atom π electron system with four π electrons delocalized over the three atoms.³ This three atom system can be made up of a variety of combinations of C, O, N and S. Cycloaddition to a 2π dipolarophile, a double or triple bond, generates a five membered heterocyclic ring (**Figure 1**).

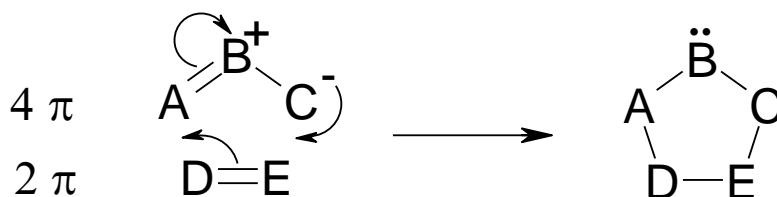


Figure 1

The 1,3-dipolar cycloaddition is useful in synthesis due to its high regio- and stereoselectivity. Concerted 1,3-dipolar cycloadditions are stereospecific. A large number of dienes and dipolarophiles are potential substrates for the reaction, leading to a considerable range of products. The reaction is characterized by high yields under relatively mild conditions. It also displays insensitivity to solvent polarity, as the rate of concerted reactions does not vary greatly on changing the polarity of the solvent.

The term 1,3-dipole is derived from the fact that it is not possible to write electron-paired resonance structures for 4π electrons delocalized over three atoms without using charges in the structure. These charges are delocalized and interchangeable. The molecules themselves are not particularly polar. Many 1,3-dipoles contain a heteroatom as the central atom. This can be formally sp or sp^2 hybridised depending upon whether or not there is a π bond orthogonal to the delocalized π system. This allows two categories of 1,3-dipoles to be defined. Those with an orthogonal π bond are linear in the ground state (**Figure 2**). This system can easily bend in the transition state, facilitating cycloaddition reactions with dipolarophiles. Examples of

this class of dipole include benzonitrile oxide **1**, as well as azides, nitrile ylides and diazo compounds.

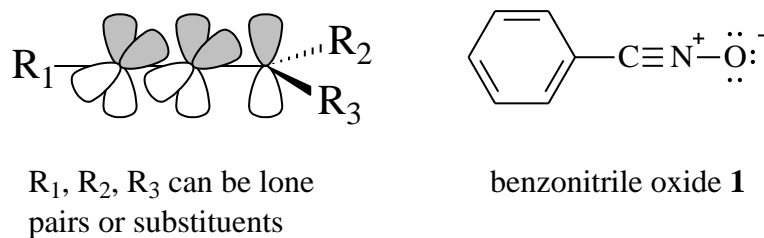


Figure 2

Those without orthogonal π bonds are bent in the ground state (**Figure 3**). C,N-diphenyl nitrene **2** is shown as an example. Other dipoles of this kind include azomethine ylides, carbonyl ylides and ozone.

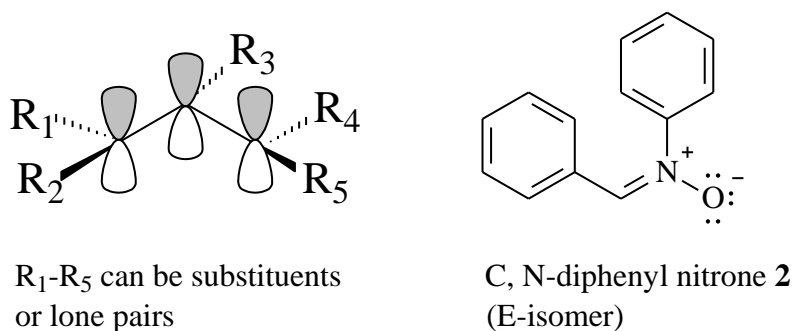


Figure 3

The stability of 1,3-dipoles varies with their ability to obtain octet stabilization. Dipoles containing an electron sextet at a carbon, nitrogen or oxygen atom are unstable. Stabilization is possible if a non-bonding pair of electrons can form an additional bond, thus relieving electron deficiency (**Table 1**).

Table 1: 1,3-Dipoles with octet stabilization

sextet structure	↔	octet structure	
	↔		nitrile ylides (nitrilium methanides)
	↔		nitrile oxides
	↔		azomethine ylides (iminium methanides)
	↔		nitron

If the central atom of the 1,3-dipole is a carbon, then internal octet stabilization is prevented by the lack of an available free electron pair. These 1,3-dipoles exist as short lived intermediates which can be trapped by reaction with *in situ* dipolarophiles.

Table 2: 1,3-Dipoles without octet stabilization

sextet structure	↔	octet structure	
	↔		imino carbenes
	↔		keto carbenes
	↔		imino nitrenes
	↔		vinyl nitrenes

1.2 Synthesis of azinium and azolium dicyanomethanide 1,3-dipoles

Dicyanomethanide 1,3-dipoles were first reported by Linn and Webster in the 1960s.^{4, 5} The first examples of this class of 1,3-dipole were based on six membered heterocycles. Stable azinium dicyanomethanide 1,3-dipoles were generated from pyridine **3**, pyrazine **4**, and isoquinoline **5**. Boekelheide⁶ used a similar procedure to generate dicyanomethanide 1,3-dipoles from five membered rings such as 1-methylimidazole **6** and thiazole **7** (Figure 4).

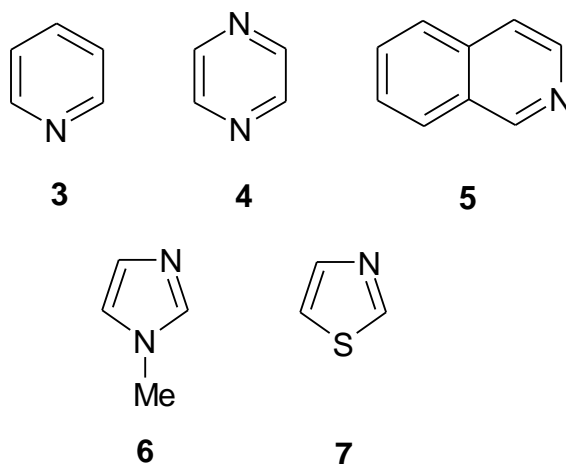
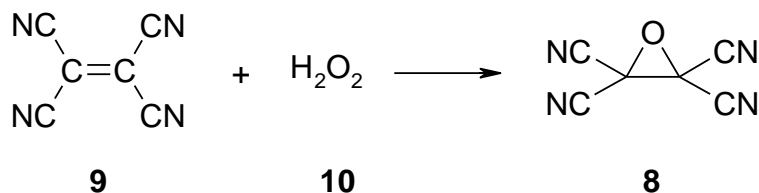


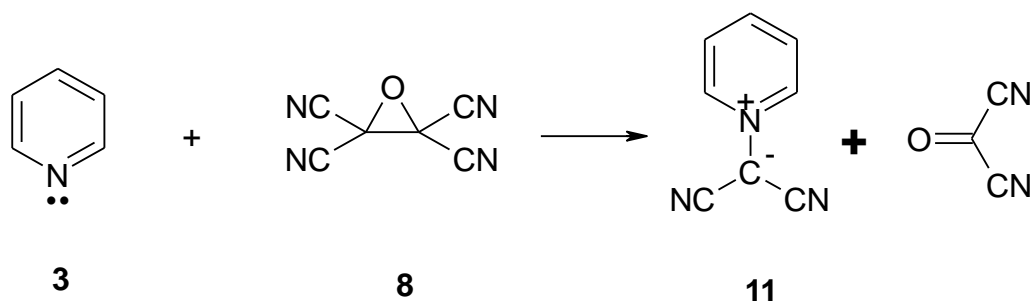
Figure 4

Synthesis of these dicyanomethanide 1,3-dipoles involves treatment of a tertiary aromatic base with tetracyanoethylene oxide **8** (TCNEO). TCNEO **8** can be produced⁵ by treating a cooled solution of tetracyanoethylene **9** with aqueous H₂O₂ **10** (Scheme 1).



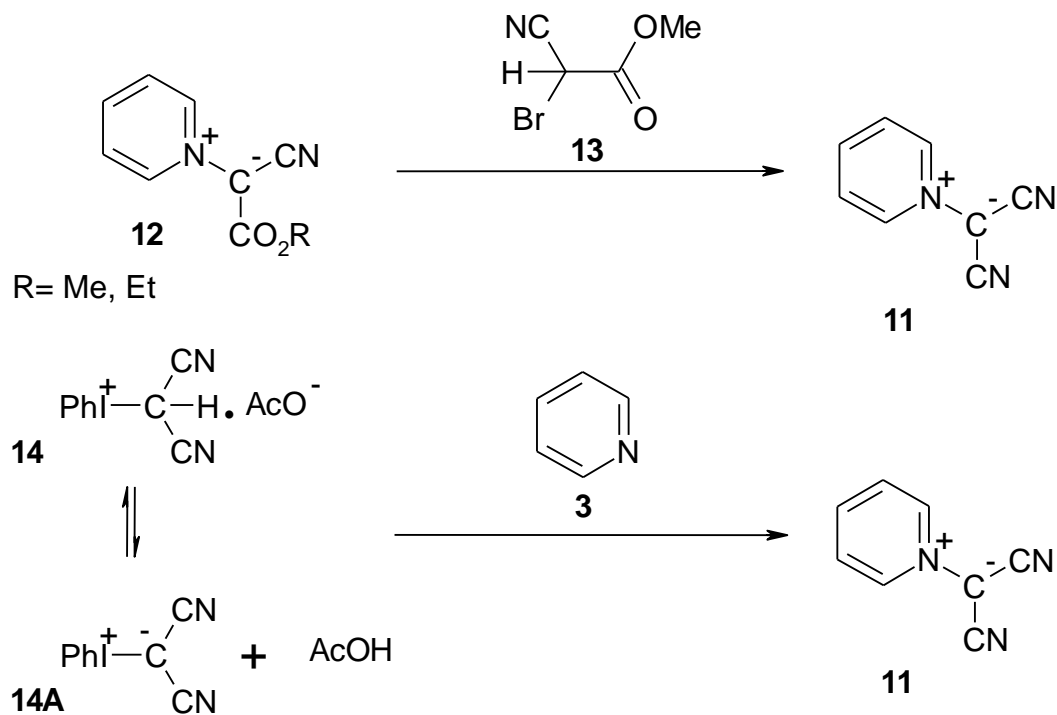
Scheme 1

In contrast with normal epoxides, TCNEO **8** is not attacked by electrophilic reagents due to the presence of the strongly electron withdrawing cyano groups. It does however react readily with nucleophilic reagents. Formation of the ylides involves nucleophilic attack by a pyridine-type nitrogen of the aromatic base on the oxirane ring (**Scheme 2**). The reactivity of a heterocycle towards TCNEO **8** is governed by two key factors⁷- the nucleophilicity of the nitrogen atom and the steric hindrance around the nitrogen atom. The nucleophilicity of a heterocycle depends on its structure and on the electrophile it is attacking. However, its variation generally parallels the basicity, and basic pKa values have been used as a guide to nucleophilicity. It has been shown that the nucleophilic reactivity of aromatic heterocycles with five- or six-membered rings increases monotonically with basic pKa.⁸



Scheme 2

The reactivity of heterocycles towards TCNEO **8** is therefore found to increase with basicity and decrease with steric hindrance. Only one dicyanomethanide group can be transferred to diazine and diazole rings as its presence lowers the nucleophilic electron density at the second ring nitrogen. Several alternative methods of dicyanomethanide 1,3-dipole synthesis have been proposed. Leonte and Zugravescu⁹ generated the pyridinium dicyanomethanide 1,3-dipole **11** by treating the pyridinium alkoxy carbonyl cyanomethanides **12** with methyl bromocyanacetate **13** (**Scheme 3**). Phenyliodonium dicyanomethanide¹⁰ **14a** or its conjugate acid **14** has also been used to transfer a dicyanomethanide group to pyridine **3**, as well as various substituted pyridine and isoquinoline heterocycles (**Scheme 3**).



Scheme 3

1.3 Structure of azinium and azolium 1,3-dipoles

The first structural study on an azinium 1,3-dipole was reported by Bugg *et al.*^{11, 12} The X-ray crystal structure of pyridinium dicyanomethanide 1,3-dipole **11** proved to be non-planar. The observed dimensions of the molecule are shown below (**Figure 5**). The C-C and C-N bond lengths displayed by the pyridine ring were shown to be similar¹³ to bond lengths associated with pyridine **3**.

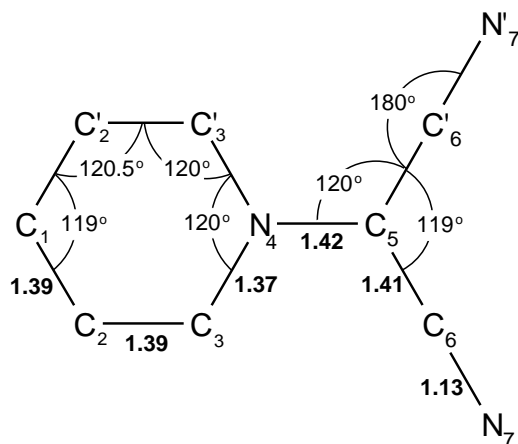


Figure 5: Bond distances (Å) and angles in pyridinium dicyanomethanide **11**. (bond distances quoted to two decimal places only)

The two cyano groups were found to be inclined, with the carbon and nitrogen atoms being 0.08 Å and 0.13 Å from the pyridinium ring plane respectively. The C(5)-C(6)-N(7) unit therefore makes an angle of 3° with respect to this plane. Computational studies by Karzazi *et al.*¹⁴ have shown that planarity in cycloimmonium ylides is determined by the size of the electron withdrawing groups bound to the ylidic carbon. Dicyanomethanide 1,3-dipoles, bearing two small cyano groups, display a small angle between the pyridinium plane (P1) and the anion plane (P2). Replacement of one of the cyano groups with a more bulky CONH₂ group to form amidocyano-pyridinium methanide **15** (**Figure 6**), causes the angle between P1 and P2 to increase to 15.45°. When two bulky groups are bound to the ylidic carbon, as in di-trifluoroacetyl-pyridinium methanide **16** (**Figure 6**), P1 is almost perpendicular to P2 (97°).

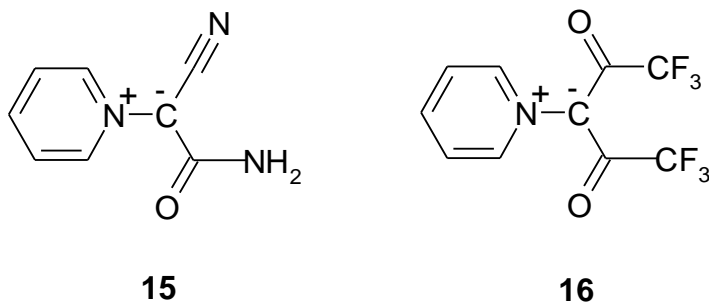


Figure 6

The value of 1.13 Å for the pyridinium dicyanomethanide 1,3-dipole **11** C(6)-N(7) bond is shorter than for a normal C-N triple bond (**Figure 5**). The bond length is similar to those measured for the dicyanomethanide groups of related zwitterions such as the tributylphosphine adduct of 4-chlorobenzylidenemalonitrile **17** and carbanions such as the lithium/hexamethylphosphoric triamide complex of malononitrile **18** (**Figure 7**). This indicates that the dicyanomethanide group of **11** possesses substantial anionic character. IR data also supports this conclusion, as the cyano stretching bands of **11** (2182, 2145 cm⁻¹)¹⁵ are considerably lower than those of molecules containing typical nitrile groups (2280-2220 cm⁻¹).¹⁶ Azolium dicyanomethanide 1,3-dipoles show similar cyano stretching bands.

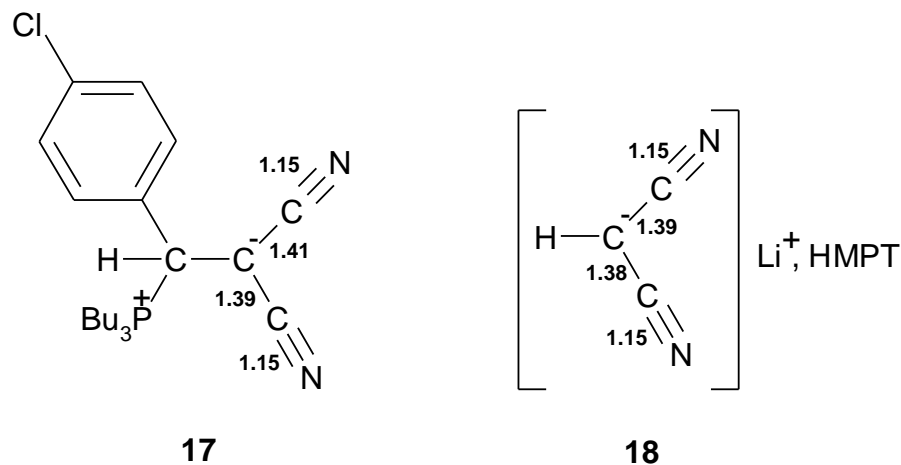


Figure 7: Selected experimental bond lengths (Å)

Independent computational studies^{15, 17} have shown that the ylidic carbon of **11** is insignificantly charged, while the ylidic nitrogen bears a small positive charge. It has also been concluded from these calculations that the cyano groups are negatively charged. Azinium 1,3-dipoles are highly stable species, with characteristically high melting points. The strong delocalization of positive charge on the aromatic ring and negative charge on the carbanion is the primary reason for the stability of dicyanomethanide 1,3-dipoles. Other factors which determine cycloimmonium ylide stability,¹⁸ such as the Coulomb attraction and the resonance interaction between the heterocycle and the negative carbanion system may also contribute to the dipole stability. It is of interest that the corresponding unsubstituted-azinium and azolium

methanide (CH_2^-) 1,3-dipoles, obtained by treating trimethylsilylmethyl trifluoromethane sulfonate salts with CsF ,¹⁹⁻²¹ e.g. **19** and **20**, have only fleeting existence and must be generated in the presence of excess dipolarophile in order to achieve useful synthesis (**Figure 8**).

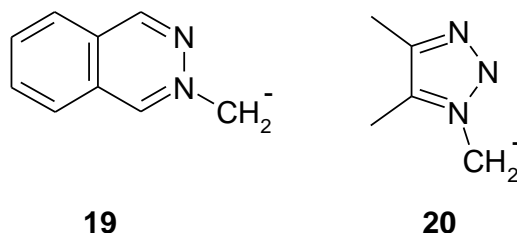


Figure 8

Also of interest in the structure of compound **11** is the length of the N(4)-C(5) bond (**Figure 5**). The experimental value obtained, 1.42 Å, is shorter than that expected for a single $\text{C}(\text{sp}^2)\text{-N}(\text{sp}^2)$ bond. Matsumoto^{22, 23} has investigated the factors affecting this bond length in some detail. Electron withdrawing groups increase the double bond character of the ylidic C-N bond. This is borne out by X-ray crystallographic studies²² on 4-methylpyridinium dicyanomethanide 1,3-dipole **21** and 4-acetylpyridinium dicyanomethanide 1,3-dipole **22**, which display slightly longer (1.427 Å) and slightly shorter ylidic C-N bond lengths (1.415 Å), respectively, than the parent pyridinium dicyanomethanide 1,3-dipole **11**. The diazinium dicyanomethanides display even shorter ylidic C-N bonds, pyridazinium dicyanomethanide 1,3-dipole **23** having a bond length of 1.403 Å while pyrazinium dicyanomethanide 1,3-dipole **24** has a bond length of 1.404 Å (**Figure 9**).

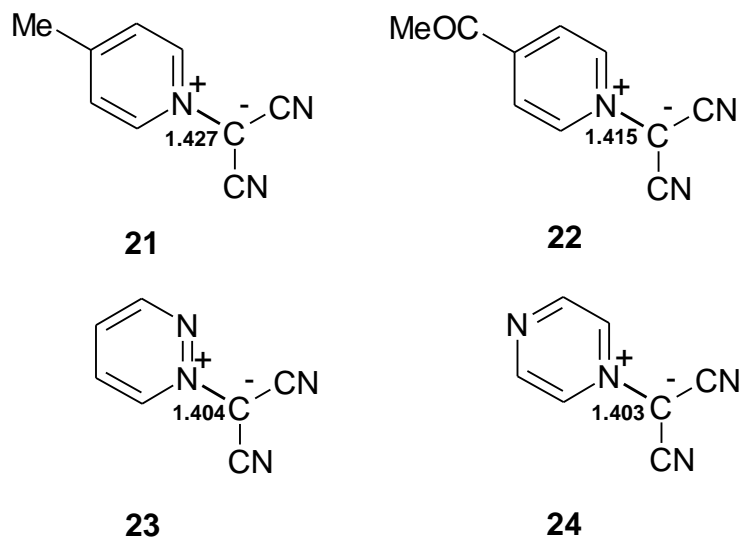
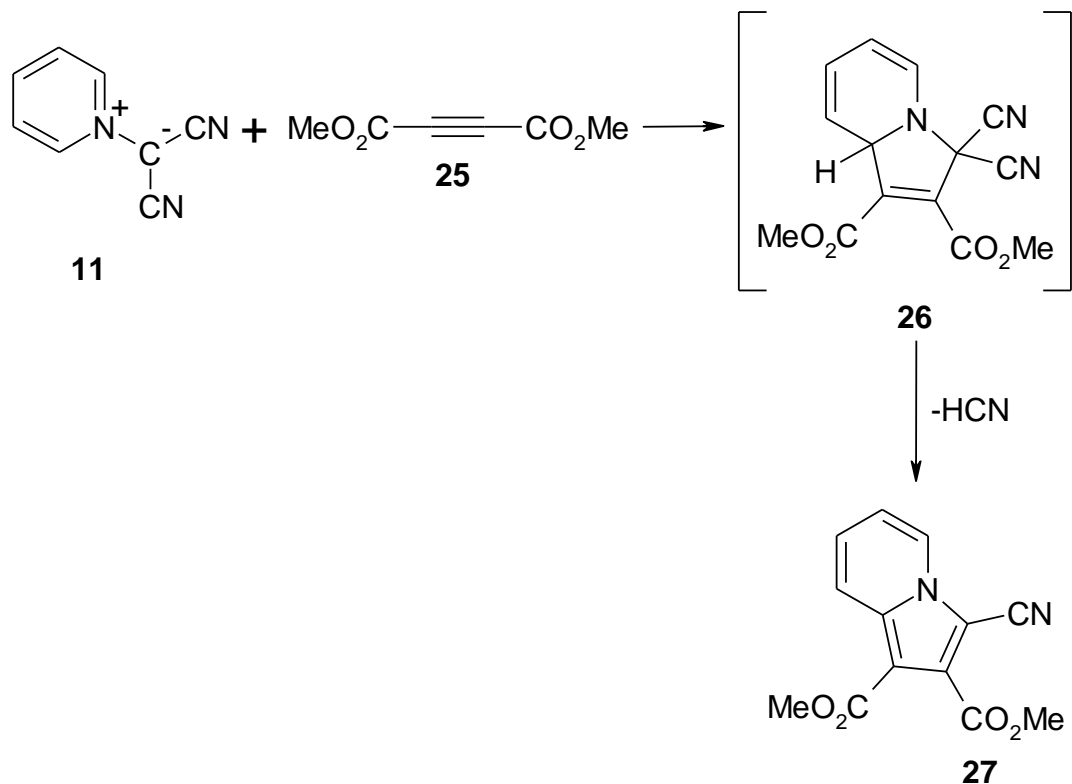


Figure 9: Experimental ylidic C-N bond lengths (Å)

1.4 Some cycloaddition reactions of azinium and azolium dicyanomethanide 1,3-dipoles

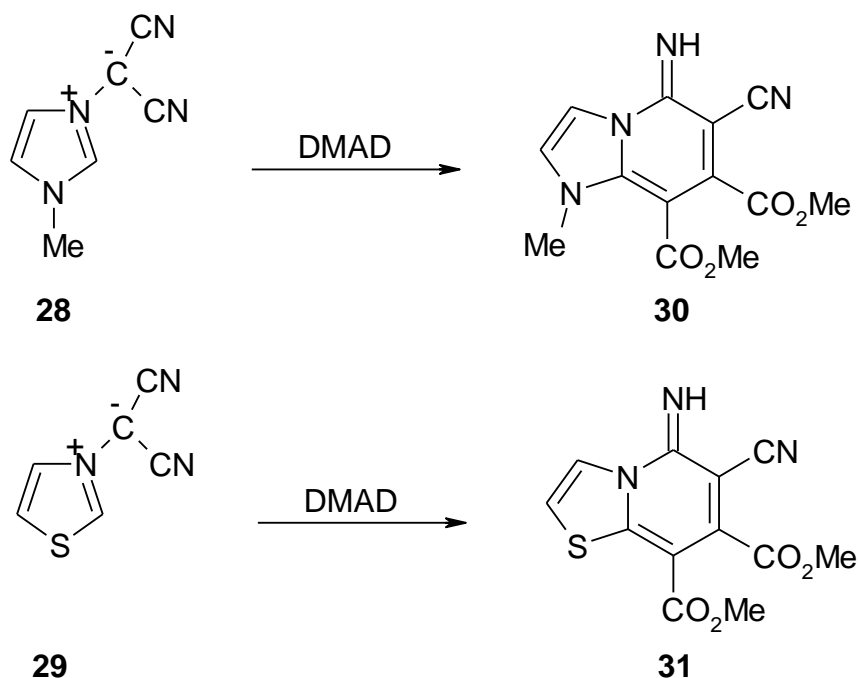
1.4.1 Reactions with symmetrical acetylenic dipolarophiles

Linn and Webster's⁵ first cycloadditions with dicyanomethanide 1,3-dipoles involved the use of dimethyl acetylenedicarboxylate **25** (DMAD) as dipolarophile. The reaction of pyridinium dicyanomethanide **11** with DMAD **25** yielded a single product **27** in 48% yield. The expected initial cycloadduct **26** was not observed as 1,4-elimination occurred to generate **27** with *in situ* loss of HCN (**Scheme 4**).



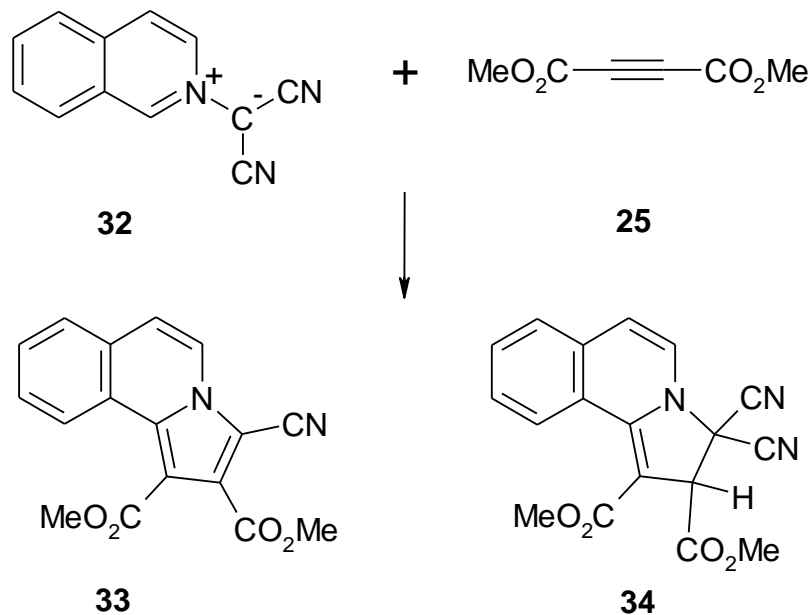
Scheme 4

The first cycloaddition reactions of azolium dicyanomethanide 1,3-dipoles were reported by Boekelheide and Fedoruk.⁶ The 1-methylimidazolium dicyanomethanide 1,3-dipole **28** and thiazolium dicyanomethanide 1,3-dipole **29** were reacted with DMAD **25**. In both cases, a single ring-expanded product was obtained (**Scheme 5**). The structures of products **30** and **31** were assigned on the basis of their ¹H NMR and UV spectra. The mechanism of this intriguing ring-expansion rearrangement will be the subject of more detailed discussion in Chapter 2.



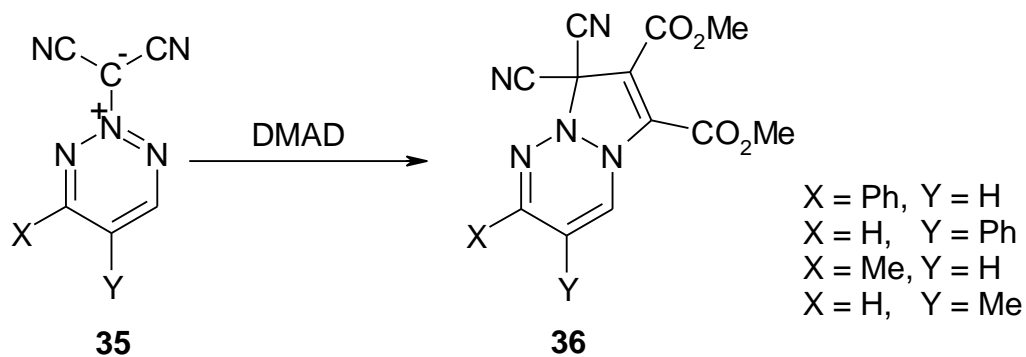
Scheme 5

Linn and Webster⁵ also studied the reaction of isoquinolinium dicyanomethanide **32** with DMAD **25**. Two products were isolated, both 1:1 adducts. Product **33** was formed in a similar manner to **27**, by *in situ* elimination of HCN from the direct cycloadduct (**Scheme 6**). However, the second product was originally assigned the wrong structure. On the basis of the ring-expanded products obtained by Boekelheide⁶ it was assumed that a similar rearrangement had occurred. Re-examination of this reaction by Basketter and Plunkett²⁴ led to the conclusion that the second product of the reaction is in fact compound **34** (**Scheme 6**). Kobayashi²⁵ subsequently confirmed the structure of **34**. This product is formed as the initial cycloadduct undergoes a 1,3-H shift, thereby restoring conjugation. This 1,3-H shift is not allowed suprafacially by Woodward and Hoffman HOMO orbital symmetry and may be solvent assisted. A 1,2-elimination of HCN from product **34** does not occur under the conditions studied and the product is stable.



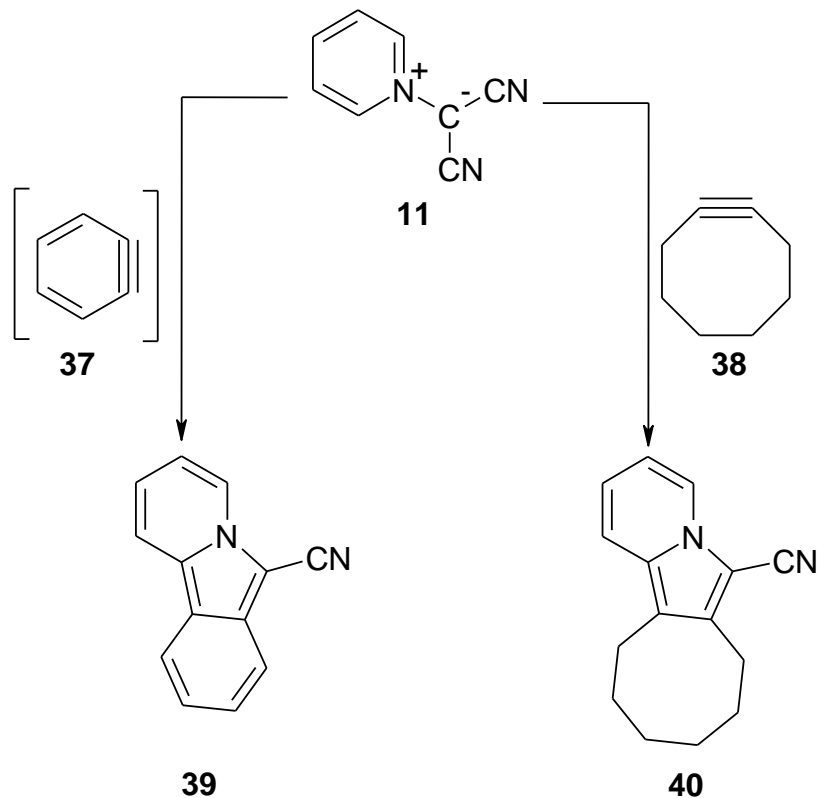
Scheme 6

Mättner and Neunhoeffler²⁶ succeeded in isolating the initial cycloadducts formed in the reactions between various substituted 1,2,3-triazinium-2-dicyanomethanide 1,3-dipoles **35** and DMAD **25**. The reactions, which were carried out under solvent free conditions, yielded bicyclic compounds **36** that were stable under inert gas at 0°C (**Scheme 7**). The compounds proved to be unstable in solution, as rearrangement followed by oxidation led to destruction of the triazine ring.



Scheme 7

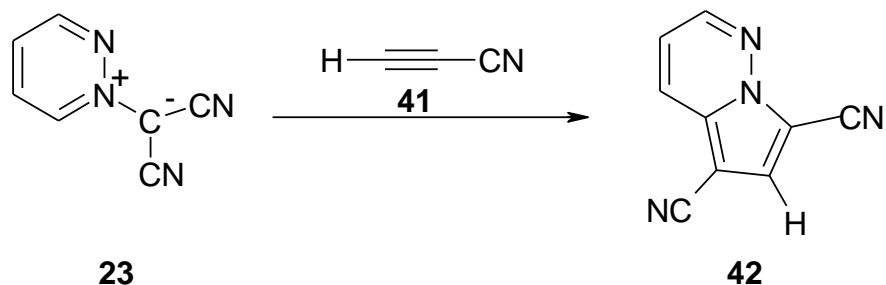
The pyridinium dicyanomethanide **11** has also been reacted with electron rich dipolarophiles. Matsumoto has treated the 1,3-dipole **11** with benzyne²⁷ **37**, and cyclooctyne²⁸ **38** (Scheme 8). The products **39** and **40** arose from *in situ* elimination of HCN after the cycloaddition step. These reactions have been described as HOMO_{dipole}-LUMO_{dipolarophile} controlled without any mechanistic study.^{27, 28}



Scheme 8

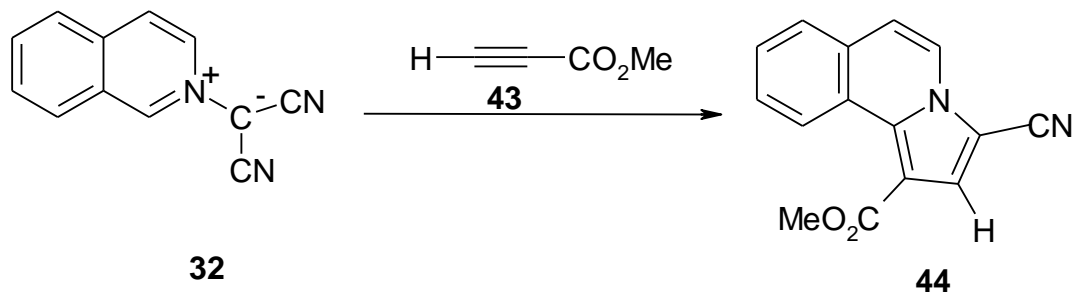
1.4.2 Reactions with unsymmetrical acetylenic dipolarophiles

The reaction of pyridazinium dicyanomethanide **23** with cyanoacetylene **41** was investigated by Sasaki *et al.*²⁹ (Scheme 9). The initial cycloadduct proved unstable, and *in situ* elimination of HCN yielded the final product **42** in 30% yield. Only one regioisomer was obtained.



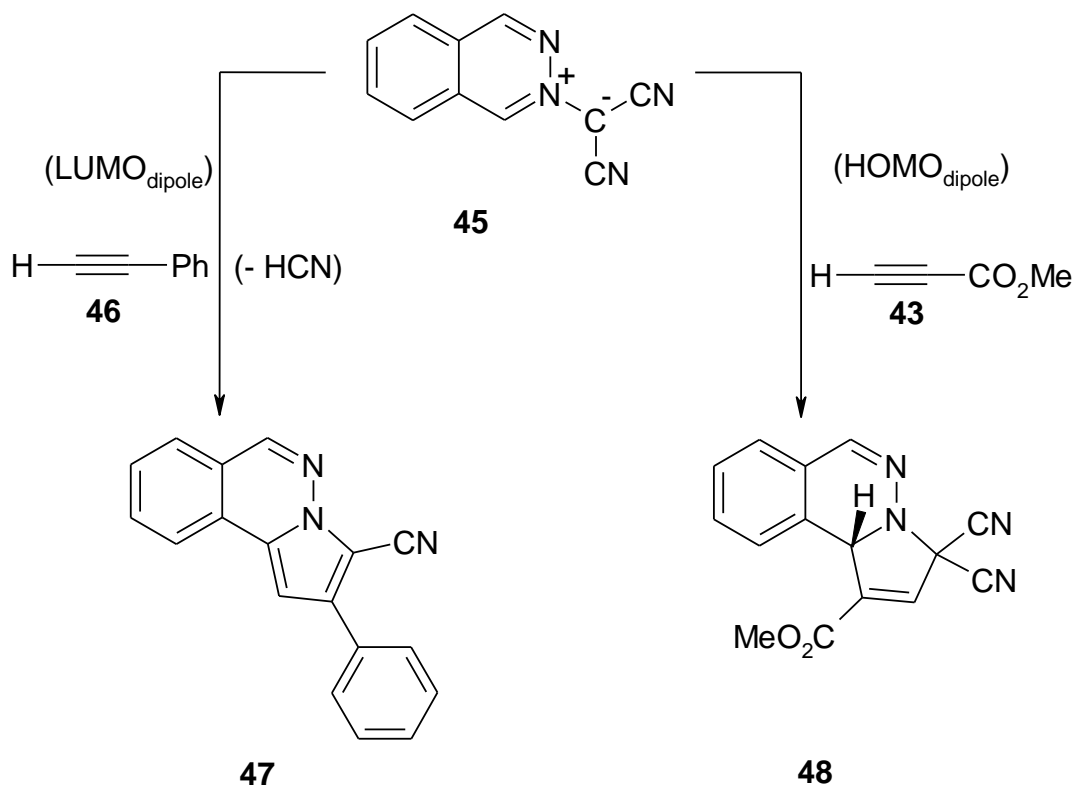
Scheme 9

The reaction of isoquinolinium dicyanomethanide 1,3-dipole **32** with methyl propiolate (MP) **43** was investigated separately by Basketter and Plunkett²⁴ and Matsumoto.³⁰ Both isolated a single regioisomer **44** (Scheme 10). The unsubstituted terminus of the dipolarophile was attached to the dicyanomethanide terminus of the 1,3-dipole. The initial cycloadduct was unstable, and so *in situ* elimination of HCN occurred. The regiochemistry is consistent with HOMO_{dipole}-LUMO_{dipolarophile} control.



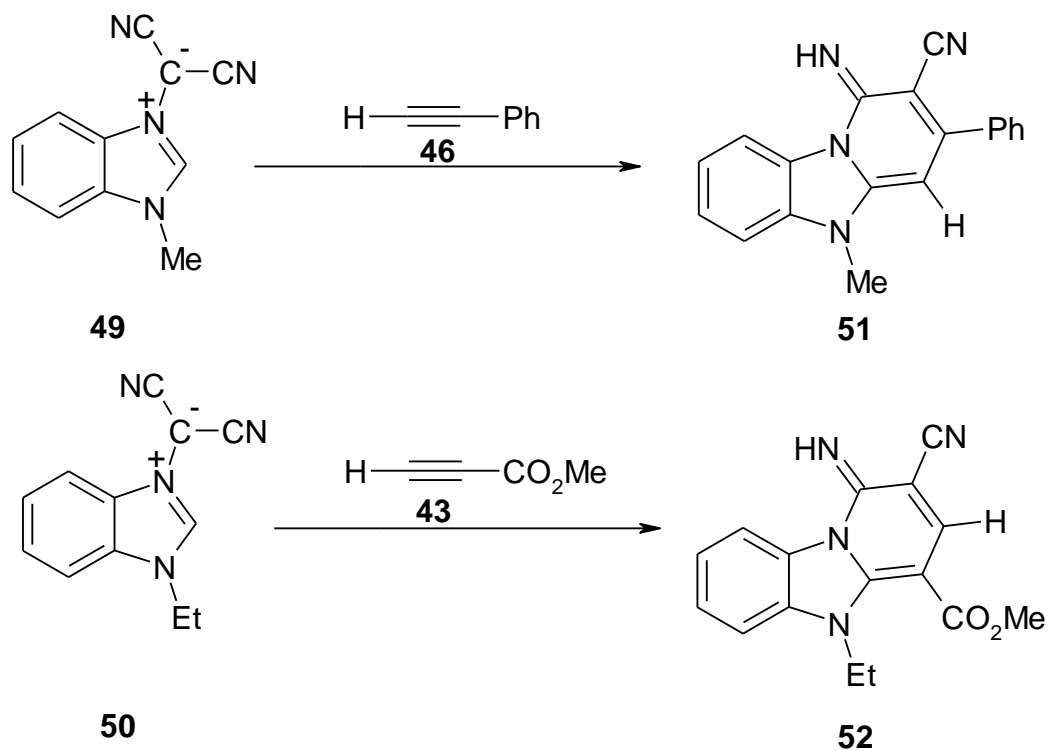
Scheme 10

The phthalazinium-2-dicyanomethanide 1,3-dipole **45** has been extensively studied in these laboratories.³¹⁻³⁴ It has been determined that dipole **45** is a Sustmann type II dipole. It can react *via* normal or inverse electron demand. The change in mechanism³³ is accompanied by a change in regiochemistry (Scheme 11). The reaction between 1,3-dipole **45** and the electron rich dipolarophile phenyl acetylene **46** is LUMO_{dipole} controlled and generates a single product (Scheme 11). However, the reaction of **45** with the electron poor dipolarophile methyl propiolate **43** is HOMO_{dipole} controlled and produces a single compound **48**.³³



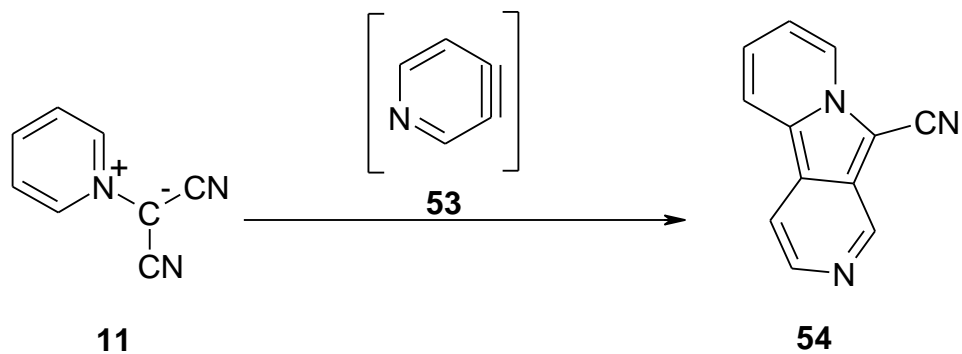
Scheme 11

Elguero *et al.*³⁵ have investigated the reactions of *N*-substituted benzimidazolium dicyanomethanide 1,3-dipoles **49** and **50** with unsymmetrical dipolarophiles. 1-Methylbenzimidazolium dicyanomethanide 1,3-dipole **49** was reacted with the electron rich dipolarophile phenyl acetylene **46** to yield the single regioisomer **51** in 8% yield (Scheme 12). The reaction of 1-ethylbenzimidazolium dicyanomethanide 1,3-dipole **50** with the electron poor dipolarophile methyl propiolate also yielded a single regioisomer **52**, in 25% yield (Scheme 12). Both structures arose from a complex ring-expansion rearrangement in the initial cycloadduct.



Scheme 12

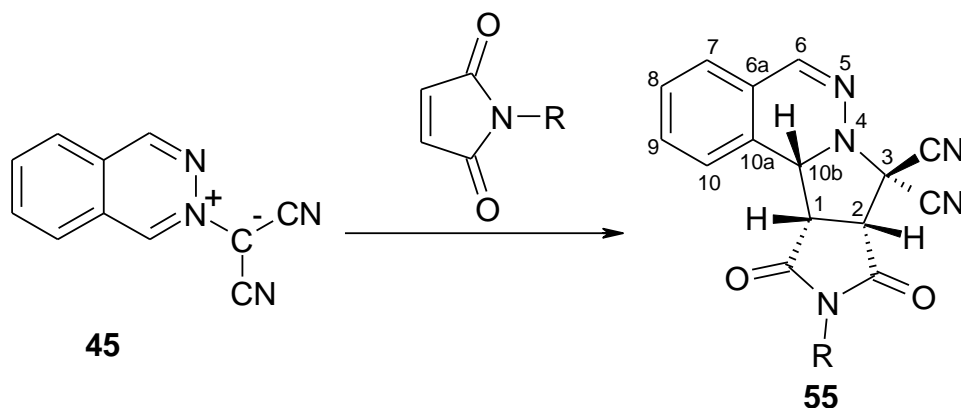
Matsumoto³⁶ has reacted pyridinium dicyanomethanide 1,3-dipole **11** with the unsymmetrical electron rich dipolarophile 3,4-pyridyne **53** (Scheme 13). Only one regioisomer **54**, generated from *in situ* loss of HCN from the cycloadduct, was isolated. The product was obtained in 27% yield.



Scheme 13

1.4.3 Reactions with alkenes

The stereochemistry of the cycloaddition reactions of phthalazinium-2-dicyanomethanide 1,3-dipole **45** has been investigated using various alkene dipolarophiles. Treatment of **45** with electron poor *N*-substituted maleimides³³ led to the isolation of single products **55** displaying *endo* stereochemistry (**Scheme 14**). The stereochemistry was assigned by nuclear Overhauser enhancement difference spectra (NOEDS). An X-ray crystal structure of the product obtained from the reaction of **45** with *N*-(*t*-butyl) maleimide confirmed the assigned structure (**Figure 10**). The presence of the *t*-butyl group did not influence the stereochemical outcome nor did a variety of other R groups.



Scheme 14

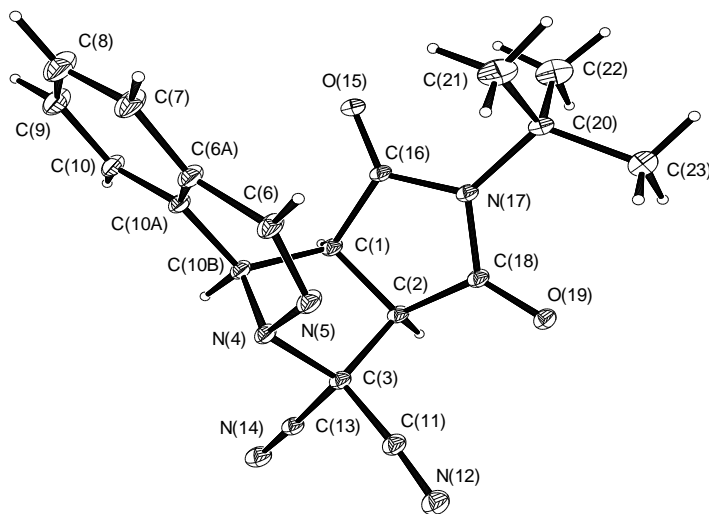
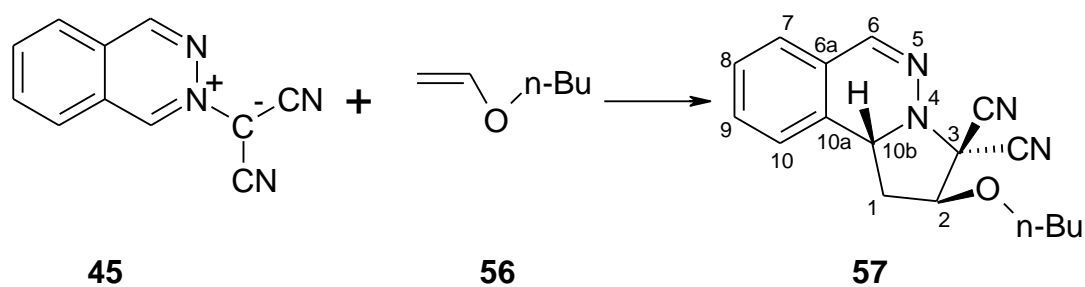
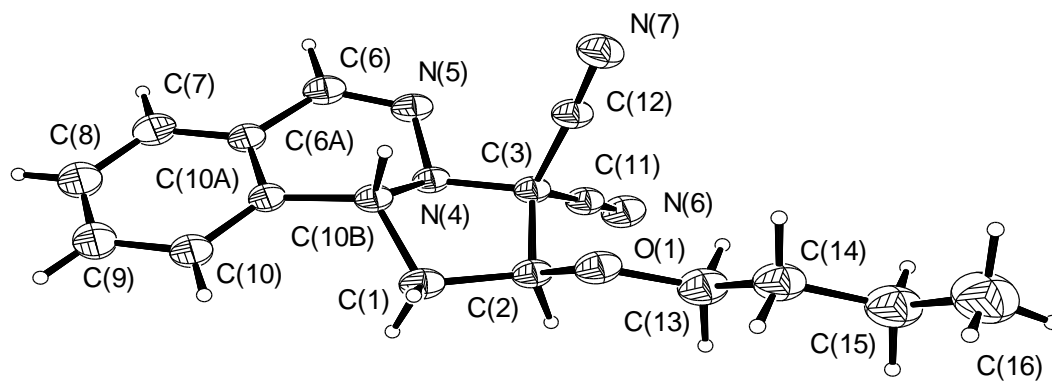


Figure 10: X-Ray crystal structure of compound **55** (R=*t*Bu)

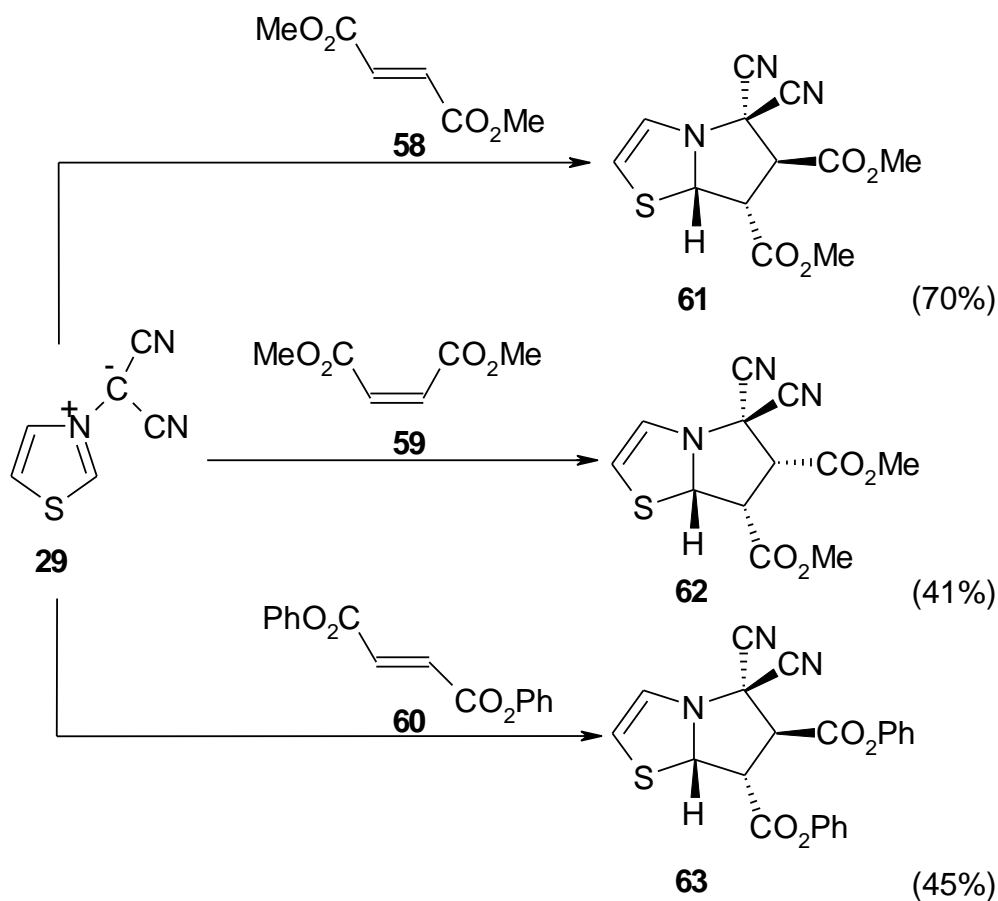
Phthalazinium-2-dicyanomethanide 1,3-dipole **45** has also been treated with a number of unsymmetrical olefinic dipolarophiles.³³ The reaction of **45** with the electron rich dipolarophile *n*-butyl vinyl ether **56** led to the isolation of a single regioisomer **57** in 86% yield (**Scheme 15**). This product displays the same regiochemistry as the products obtained from unsymmetrical electron rich alkynes. The stereochemistry on the C-2 position was found to be *exo* on the basis of NOEDS. This was later confirmed with an X-ray crystal structure (**Figure 11**).



Scheme 15

Figure 11: X-ray crystal structure of compound **57**

Tsuge *et al.*³⁷ have explored the reactions of the thiazolium dicyanomethanide 1,3-dipole **29** with dimethyl fumarate **58**, dimethyl maleate **59** and *trans*-1,2-dibenzoyl ethylene **60**. The reactions yielded only the *endo* stereoisomers **61**, **62**, **63** (Scheme 16).

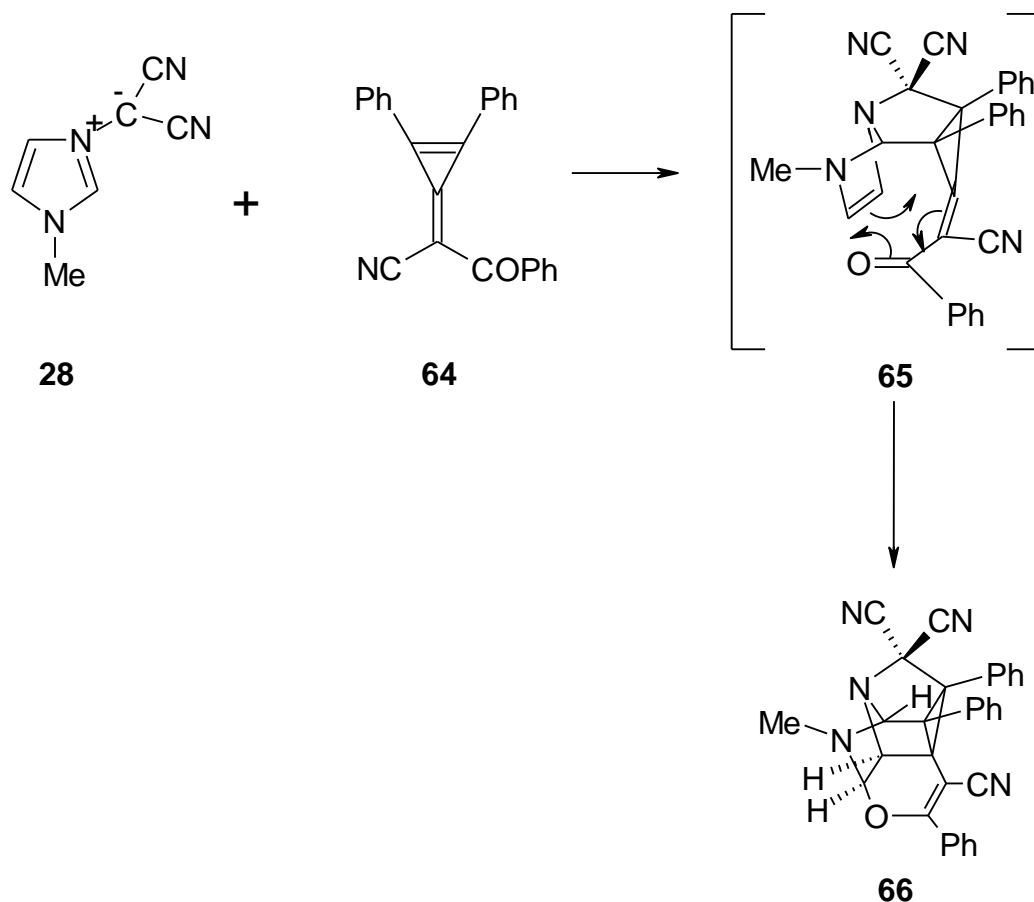


Scheme 16

Reactions between thiazolium dicyanomethanide 1,3-dipole **29** and *N*-substituted maleimides were found to yield mixtures of the *endo* and *exo* isomers. It was concluded that the *endo* product was isomerising into the *exo* product.³⁸

1.4.4 Double cycloadditions

The reactions of dicyanomethanide 1,3-dipoles with methylene cyclopropenes bearing unsaturated substituents at the 4-position are of interest as they provide the first examples of double cycloadditions that include at least one 1,3-dipolar cycloaddition.³⁷ The reaction of 1-methylimidazolium dicyanomethanide **28** with 2-benzoyl-2-(1',2'-diphenyl-3'-cyclopropenylylidene) acetonitrile **64** yields a single pentacyclic caged structure³⁹ **66** in 76% yield (**Scheme 17**).



Scheme 17

The first step is the stereo- and regiospecific 1,3-dipolar cycloaddition of **28** across the endocyclic double bond of **64**. The cycloadduct **65** formed is unstable due to the loss of aromaticity in the imidazolium ring. An intramolecular Diels-Alder reaction subsequently occurs across the newly formed olefinic double bond, yielding the cage

compound **66**. The thiazolium dicyanomethanide 1,3-dipole⁴⁰ **29** and pyridinium dicyanomethanide 1,3-dipole⁴¹ **11** have been reported to react with **64** to form similar products.

1.5 Kinetic studies

Kinetic studies on dicyanomethanide 1,3-dipoles are quite rare. Sauer *et al.*⁴² have reported on kinetic investigations of various monocyclic and bicyclic dicyanomethanide 1,3-dipoles. The reactions of the substituted dihydropyridazinium dicyanomethanide 1,3-dipole **67** with cyclooctyne **38**, ynamine **68** and DMAD **25** were studied (**Figure 12**).

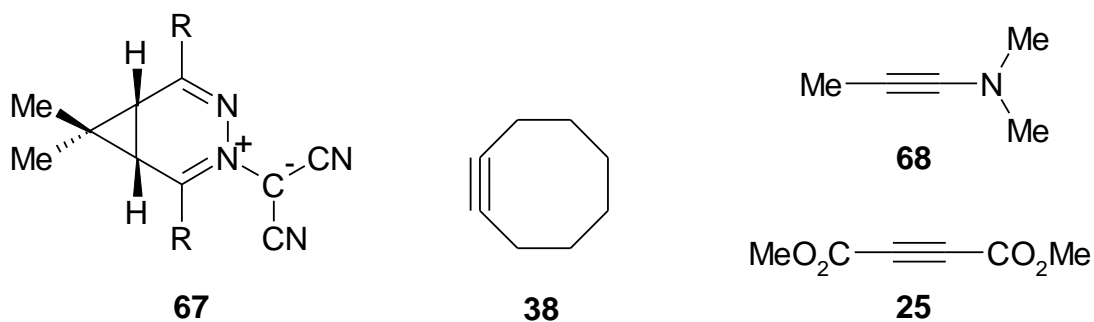


Figure 12

Table 3: Kinetic rate data for 1,3-dipoles **67a-e** with dipolarophiles **25**, **38** and **68** in dioxane; values for k_2 (dm³ mol⁻¹ s⁻¹)/10⁻⁴

1,3-Dipole 67	Cyclooctyne 38	Ynamine 68	DMAD 25
a. R= -C ₆ H ₄ -OMe	122	574	2.94
b. R= -C ₆ H ₄ -Me	240	1210	3.96
c. R= -C ₆ H ₅	436	2140	4.02
d. R= -C ₆ H ₄ -Cl	799	5180	5.11
e. R= -C ₆ H ₄ -CF ₃	2080	15300	7.72

The 1,3-dipoles **67a-e** (**Table 3**) react preferentially with electron rich dipolarophiles such as **38** and **68**. There is a marked decline in the rate constants for the reactions with the electron poor DMAD **25**. Variation of the dipole substituents has a profound effect on the reaction rates. The dipoles **67a-b** bearing electron donating substituents display slower rates than those with electron withdrawing substituents **67d-e**. It can therefore be concluded that these cycloadditions are under $\text{LUMO}_{\text{dipole}}\text{-HOMO}_{\text{dipolarophile}}$ control. The small positive Hammett ρ -values obtained for these reactions suggest that the reactions are inverse electron demand cycloadditions (**Table 4**) involving the $\text{LUMO}_{\text{dipole}}\text{-HOMO}_{\text{dipolarophile}}$ interaction. Electron withdrawing substituents enhance the reactions by lowering the $\text{LUMO}_{\text{dipole}}$ energy level. The 1,3-dipoles **67a-e** are therefore Sustmann type III.

Table 4: The Hammett ρ -values for the cycloadditions of **67a-e** with cyclooctyne **38**, ynamine **68** and DMAD **25**

Dipolarophile	Hammett ρ -value
Cyclooctyne 38	1.44
Ynamine 68	1.69
DMAD 25	0.46

Extensive kinetic studies^{34, 43, 44} have been undertaken in this Department on the phthalazinium-2-dicyanomethanide 1,3-dipole **45** and the pyridazinium dicyanomethanide 1,3-dipole **23**. The former was found to be a Sustmann type II case while the later was a Sustmann type I species, reacting only with electron poor dipolarophiles. In particular, the effect of water on cycloaddition rates was examined. The introduction of water as cosolvent into cycloaddition reactions of pyridazinium dicyanomethanide **23** and phthalazinium-2-dicyanomethanide **45** in acetonitrile gave small initial rate enhancements followed by larger rate increases as the mole fraction of the solvent mixture approached pure water. The influence of water on the rates was about 10 times larger for some dipolarophiles, and these dipolarophiles, which were mainly vinyl ketones, were classified as water-super because of this. Other dipolarophiles, such as vinyl esters and vinyl nitriles showed

smaller water effects and were classed as water-normal. One of the aims of this thesis (Chapter 3) was to explore whether water-induced changes in the polarity of the cycloaddition transition state might contribute to the distinction between water-super and water normal reactions for a fixed 1,3-dipole.

Azinium and azolium 1,3-dipoles are synthetically important molecules as the loss of aromaticity in their fused cycloadducts often leads to interesting rearrangements. Typically, the initial cycloadducts of azinium dicyanomethanide 1,3-dipoles re-establish aromaticity by the *in situ* elimination of HCN (**Scheme 4**). The loss of aromaticity in the fused cycloadducts of azolium 1,3-dipoles drives an interesting ring-expansion rearrangement (**Scheme 5**). The mechanism of this intriguing rearrangement has received very little attention in the literature. Another aim of this thesis was to explore the synthetic and mechanistic features of the cycloadditions and subsequent ring expansions of 1,3-dipole **28** and some related molecules (**Figure 13**).

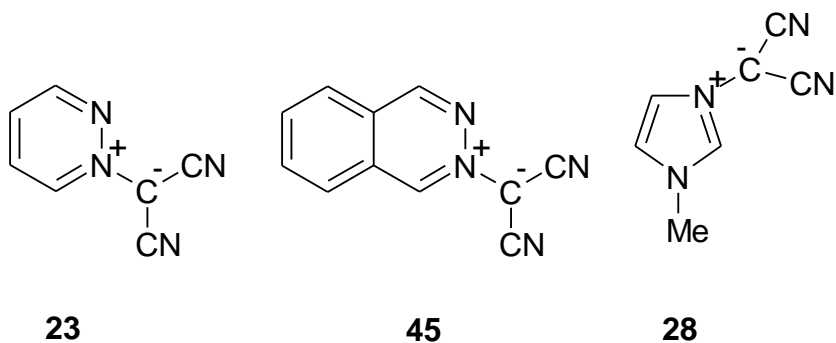


Figure 13

Chapter 2

**Synthetic and mechanistic studies on the
cycloaddition reactions of imidazolium
dicyanomethanide 1,3-dipoles and the 1-phenyl-
1,2,4-triazolium-4-dicyanomethanide 1,3-dipole**

2.1 Introduction

Cycloaddition reactions are among the most important reactions in all of organic chemistry. The generation of new ring systems is of particular importance to the pharmaceutical industry, which strives to create novel biologically active molecules. The hetero Diels-Alder and the Huisgen 1,3-dipolar cycloaddition are fundamental chemical reactions which may be used in the construction of heterocyclic rings.

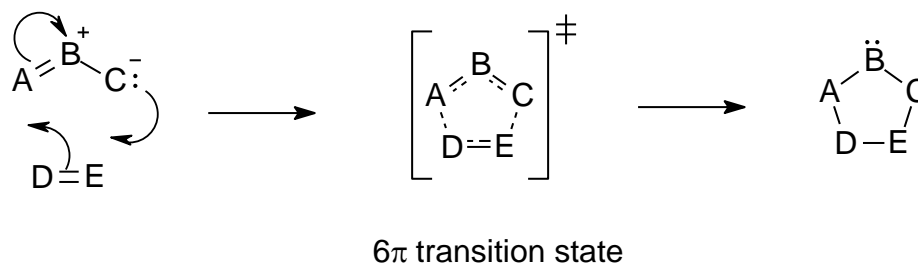
The Diels-Alder reaction⁴⁵ involves the cycloaddition of a conjugated 4π 1,3-diene and a 2π dienophile to form a six membered ring (**Figure 14**). The discoverers of the reaction, Otto Diels and Kurt Alder, received the Nobel Prize for their work in 1950. The 1,3-dipolar cycloaddition was pioneered by Huisgen in the 1960s^{1, 2} and is a remarkably efficient and versatile reaction used in the construction of five-membered heterocycles. Such heterocycles are subunits found in numerous natural products and in many pharmaceuticals. The reaction is capable of generating complex structures with new chiral centres, making it an invaluable tool for asymmetric synthesis.



Figure 14

The majority of 1,3-dipolar cycloadditions are considered to be concerted reactions that proceed in accordance with the Evans principle.⁴⁶ This states that thermal pericyclic reactions take place preferentially *via* an aromatic transition state. The mechanism can be viewed in terms of the Frontier Molecular Orbital (FMO) Theory approach⁴⁷ similar to the Diels-Alder reaction. The reactions are characterized by high negative entropies⁴⁸ and moderate enthalpies,⁴⁹ indicating a highly ordered

transition state. The reaction rate is typically unaffected by changes in solvent polarity.⁵⁰ The cycloaddition reaction is generally thought to proceed through an asynchronous transition state in which one of the new σ -bonds is more developed than the other (**Figure 15**).

**Figure 15**

An alternative to the one step concerted cycloaddition was proposed by Firestone⁵¹ who suggested that a diradical intermediate was formed which rapidly closed stereospecifically if generated in the correct conformation. This theory is generally not accepted⁵² as FMO provides a better explanation for the reactivity and regioselectivity of these reactions on the basis of the concerted ($\pi 4s + \pi 2s$) mechanism. However stepwise cycloadditions involving both biradical intermediates⁵³ and zwitterionic intermediates⁵⁴ have been discovered. Huisgen⁵⁵ has demonstrated that a spectrum of 1,3-dipolar mechanisms exist, ranging from fully concerted to two-step processes. However the majority are asynchronous concerted reactions and it is only in cases with specially selected substituents that the two-step reactions are encountered.

2.1.1 Frontier molecular orbital theory and Sustmann classification

Frontier molecular orbital theory is a powerful tool for understanding the different reactivities of 1,3-dipoles with different dipolarophiles. In FMO theory,⁴⁷ only the highest occupied molecular orbitals (HOMO) and the lowest unoccupied molecular orbitals (LUMO) of both reactants are considered during bond formation. The theory can only be applied to a reaction with a concerted mechanism which proceeds through a single transition state. No intermediates are formed and the symmetry of

Chapter 2

the frontier orbitals is conserved in the change to products. Any other orbital interactions between the occupied and unoccupied orbitals of the reactants are ignored. Generally, the HOMO of one reactant reacts with the LUMO of the other. The favoured interaction occurs between those orbitals with the lowest HOMO-LUMO energy gap.

The actual energy of the frontier orbitals is determined by both the skeletal atoms and the substituents of the molecule in question. Electron withdrawing groups such as ketones and esters lower the energies of molecular orbitals. Electron donating groups, on the other hand, raise the energies of the molecule's orbitals. Different substituents can therefore play a significant role in the outcome of a reaction.

Sustmann^{56, 57} has classified 1,3-dipolar cycloadditions into three categories based on the relative FMO energies of the dipole and the dipolarophile (**Figure 16**).

- Type I:** HOMO_{dipole}-LUMO_{dipolarophile} interaction is dominant.
(normal electron demand)
- Type II:** Both HOMO-LUMO gaps are approximately equal.
(neutral electron demand)
- Type III:** LUMO_{dipole}-HOMO_{dipolarophile} interaction is dominant.
(inverse electron demand)

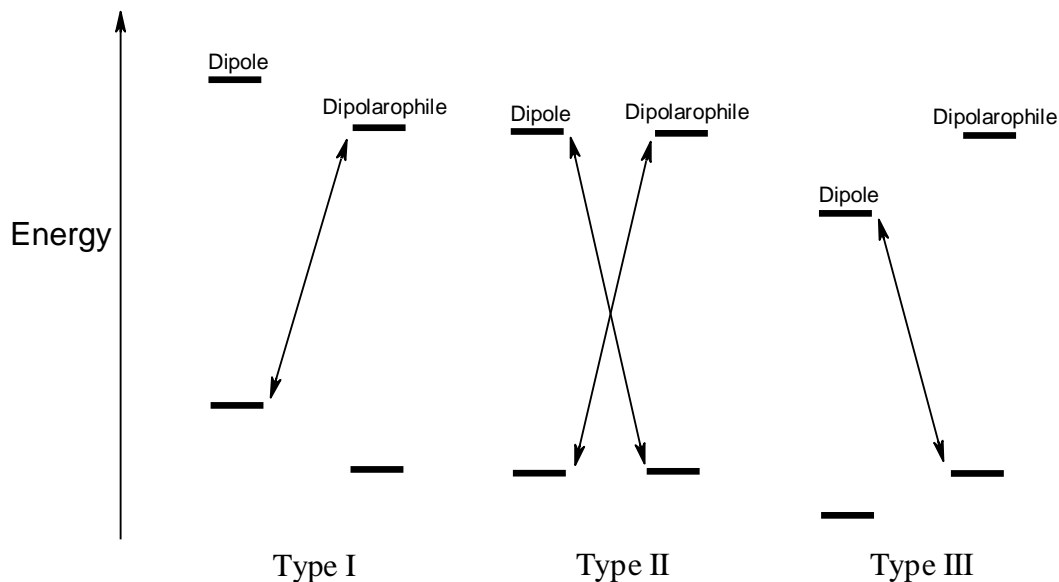


Figure 16: Sustainmann classification of 1,3-dipolar cycloadditions

2.1.2 Regiochemistry of 1,3-dipolar cycloadditions

A 1,3-dipolar cycloaddition can potentially produce a mixture of products. Regiochemistry is concerned with the way in which the dipolarophile adds onto the 1,3-dipole. In the case of an unsymmetrical dipolarophile, there may be two regioisomers (**Figure 17**).

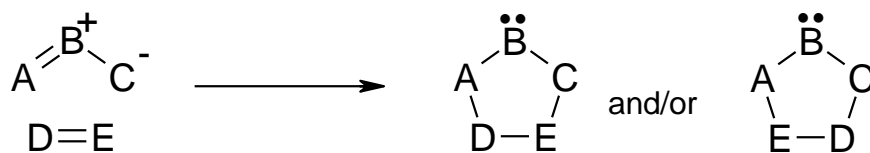
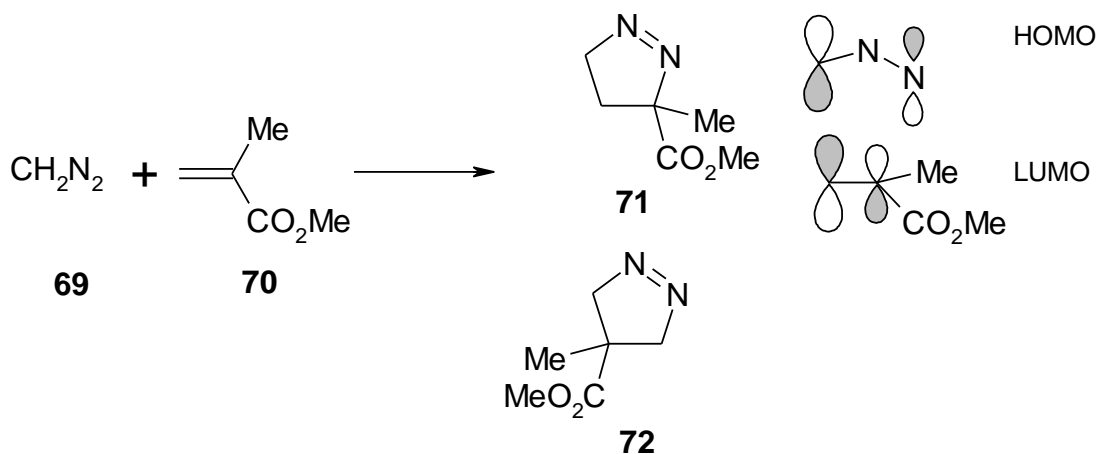


Figure 17

However, most 1,3-dipolar cycloadditions are highly selective and give only one of the two possible regioisomers. Two key pieces of information are required in order to determine the preferred product of a 1,3-dipolar cycloaddition.

- The dominant HOMO-LUMO interaction between the two reactants
- The orbital coefficients of the reactants

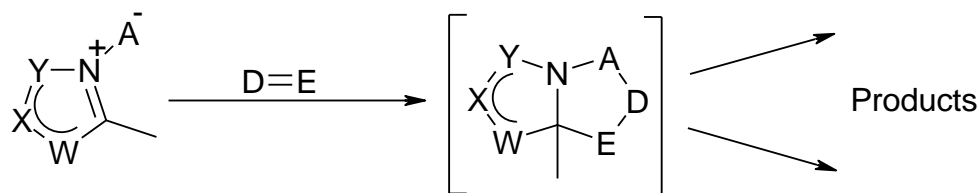
In the addition of diazomethane **69** to methyl methacrylate **70** the dominant interaction is $\text{HOMO}_{\text{dipole}}\text{-LUMO}_{\text{dipolarophile}}$. The reaction can potentially produce two regioisomers,³ compounds **71** and **72** (**Scheme 18**). However, only compound **71** is isolated as the dominant frontier orbitals both have larger atomic orbital coefficients on the CH_2 carbons rather than at the other termini. In cycloaddition reactions the bonding of atoms with the largest atomic orbital coefficients leads to a more stable transition state, and so is favoured energetically.



Scheme 18

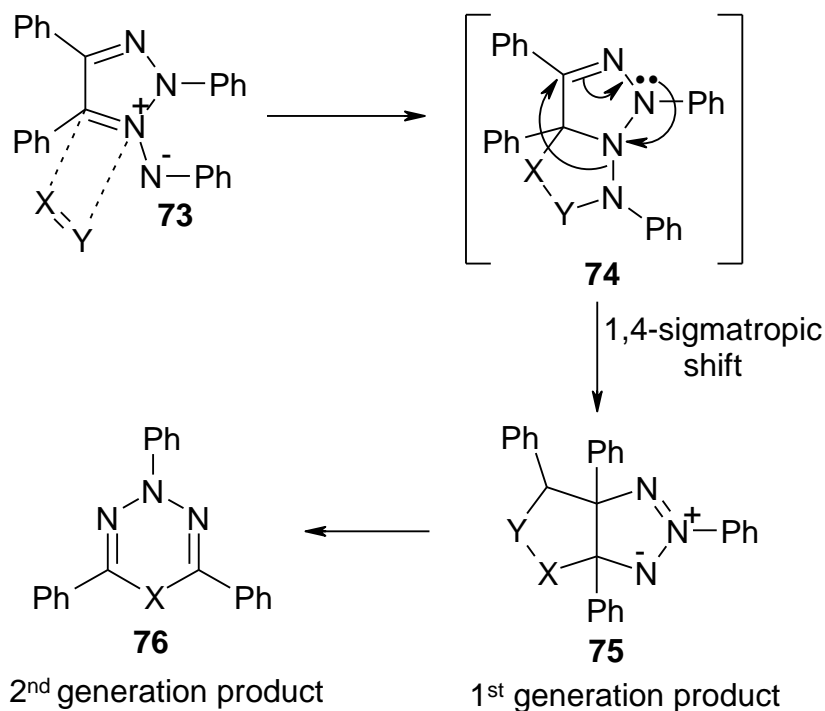
2.1.3 Azolium 1,3-dipoles

The scope of 1,3-dipoles has been further extended by the development of 1,3-dipoles where two of the four π -electrons are part of an azole ring. Azolium 1,3-dipoles are of interest because the loss of azole aromaticity in the fused cycloadducts derived from them often leads to unexpected rearrangements (**Scheme 19**).



Scheme 19

In many cases, the initial 1,3-dipolar cycloaddition is followed by multi-step rearrangements. The complexity of these rearrangements was not always appreciated in the early reports, and so many products were erroneously described as the simple primary adducts. The 1,3-dipolar cycloadditions of various azolium 1,3-dipoles have been studied extensively in these labs.⁵⁸⁻⁶⁰ The reactions of the 1,2,3-triazolium-1-aminide 1,3-dipole **73** with a range of dipolarophiles involve interesting rearrangements (**Scheme 20**).^{59, 61, 62}

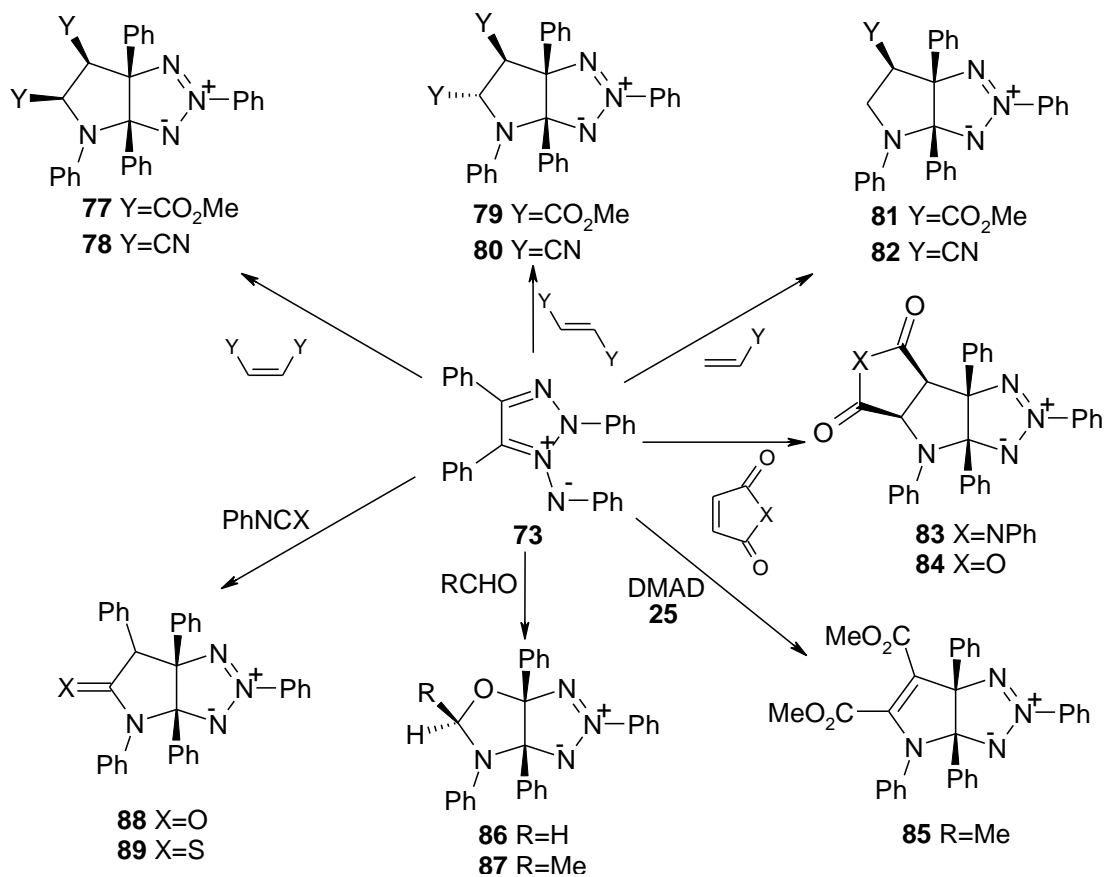


Scheme 20

The initial cycloadduct **74** (**Scheme 20**) is particularly unstable due to the presence of the extremely labile exocyclic N-N bond. The adduct undergoes 1,4-sigmatropic rearrangement to give the fused structure **75**, referred to as the first generation product. This may in turn be converted into the second generation product **76** if structural changes occur *in situ* or are induced. The 1,4-sigmatropic rearrangement is a nitrogen analogue⁶³ of the ubiquitous 1,5-rearrangements of 1,3-diene systems allowed by Woodward-Hoffmann HOMO symmetry. In the C-analogue, four π -electrons are delocalised over four C-atoms, leading to a 1,5-migration over two π -

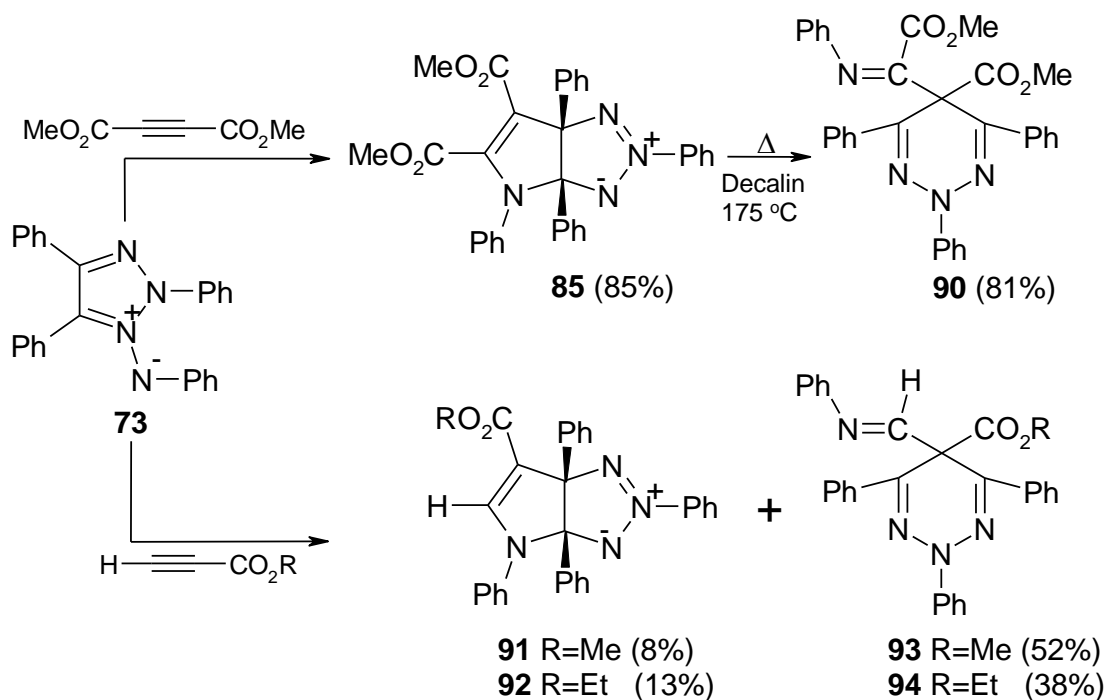
bonds. In the heteroanalogue, the four π -electrons are delocalised over three atoms, thus causing the 1,4-shift instead of the 1,5-migration.

The 1,2,3-triazolium-1-aminide **73** is a type I 1,3-dipole⁶⁴ and reacts with a wide range of 2π systems, examples of which are shown below (**Scheme 21**).^{59, 61, 62} The reactions show a high degree of stereo- and regioselectivity in all cases.



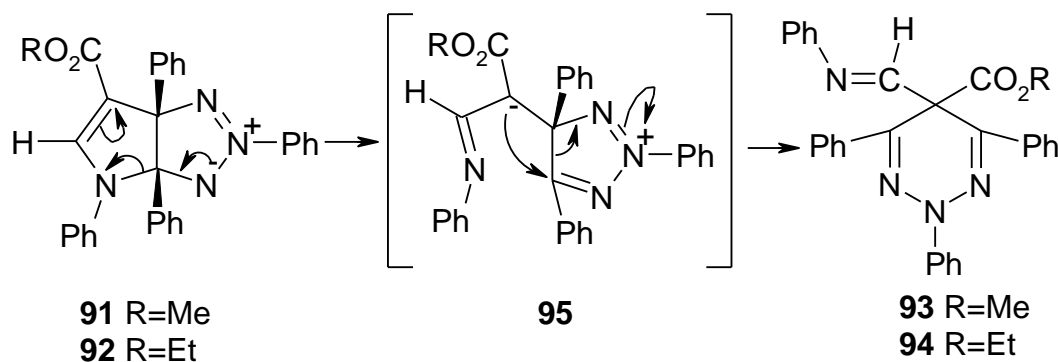
Scheme 21

In some cases, further rearrangements can be induced in the first generation products.⁵⁹ Compound **85**, produced using DMAD **25** as dipolarophile, can be converted into the second generation product **90** on heating in decalin at 175 °C (**Scheme 22**).⁶⁵



Scheme 22

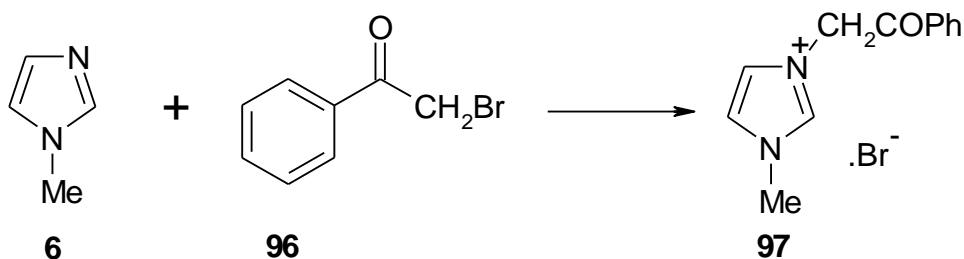
However, when the unsymmetrical alkyne dipolarophiles methyl propiolate and ethyl propiolate were reacted with the 1,3-dipole **73** a mixture of first and second generation products was obtained (Scheme 22).⁶⁶ The second generation products **93** and **94** were found to be the major products. In each case the reaction proved to be regioselective. The first generation products **91** and **92** possess a H atom at C-5 and a double bond at C-5 and C-6 and are highly labile, rearranging *in situ* with ring expansion. The proposed mechanism⁶⁷ involves a dipolar intermediate **95** which arises from heterolytic cleavage of the C(3a)-N(4) bond in the first generation product (Scheme 23). Compound **85** is stable due to the presence of a carboxymethyl group instead of a H atom at C-5, and so further heating is required to induce rearrangement.



Scheme 23

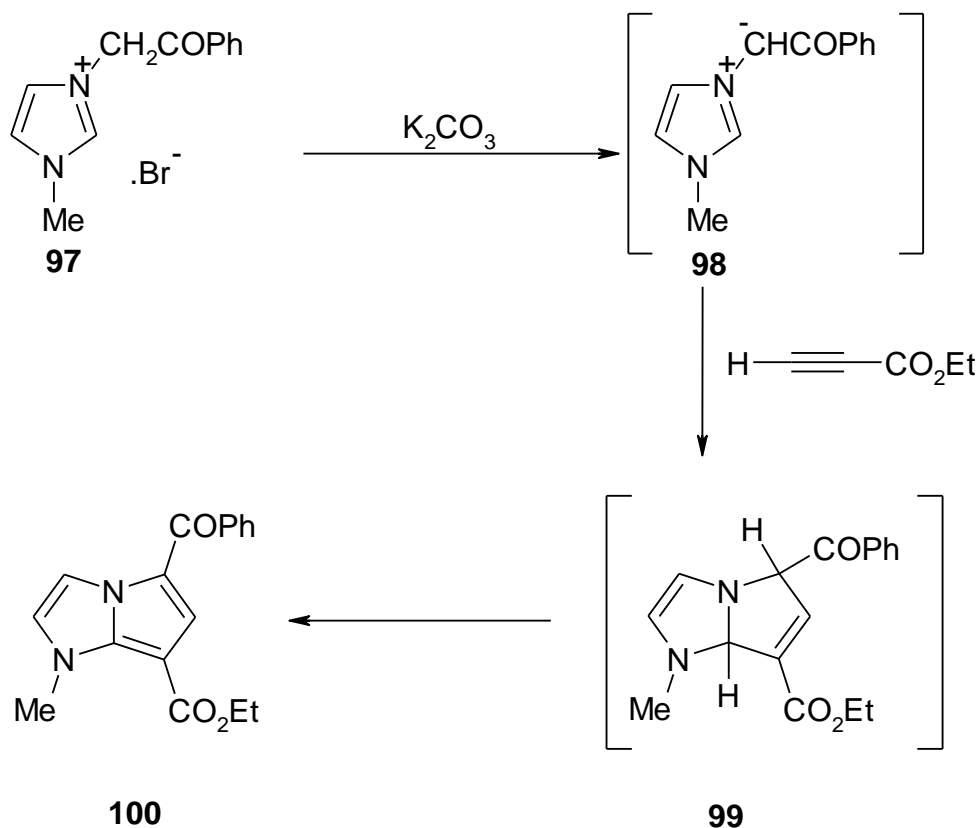
2.1.4 Imidazolium ylides

Boekelheide and Fedoruk pioneered the use of imidazolium 1,3-dipoles in cycloaddition reactions. The first reported⁶ imidazolium ylide was synthesized by the treatment of 1-methylimidazole **6** with phenacyl bromide **96** which yielded 1-methyl-3-phenacylimidazolium bromide **97** (Scheme 24).



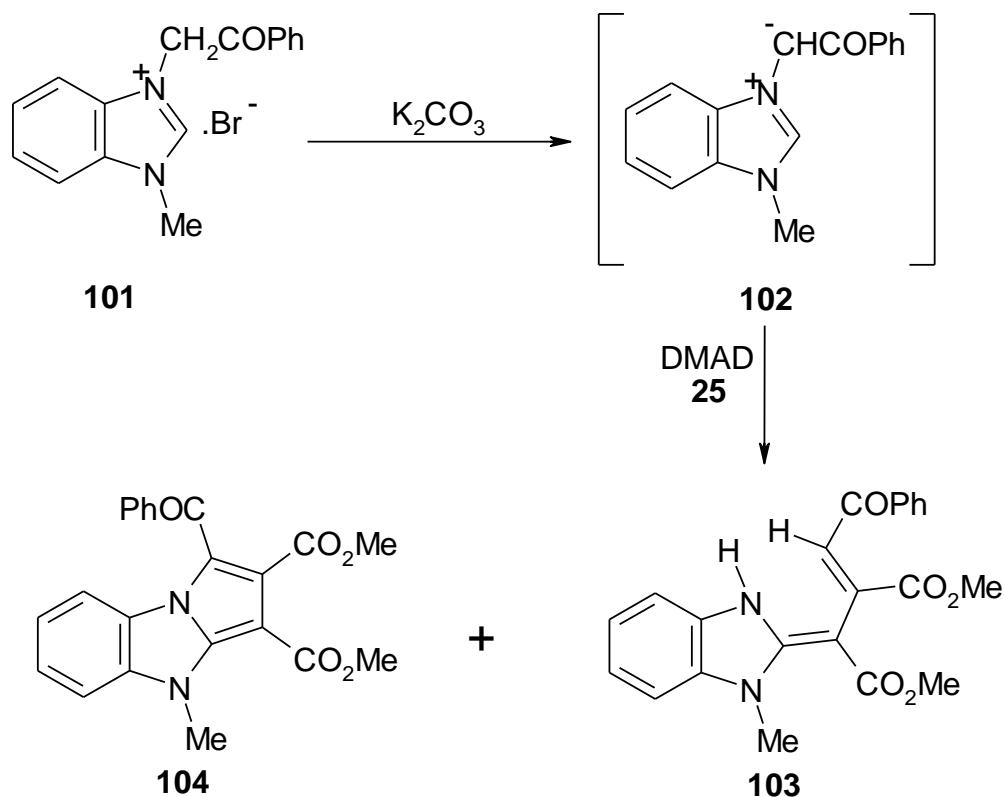
Scheme 24

The ylide **98** was then generated by treating a solution of the imidazolium bromide **97** in dimethylformamide with anhydrous potassium carbonate. The ylide **98** proved to be unstable, and could not be isolated. Instead, it was trapped *in situ* by reaction with ethyl propiolate (Scheme 25). The initial cycloadduct **99** formed from this cycloaddition also proved to be unstable, as dehydrogenation gave rise to the aromatised 1,3a-diazapentalene **100**. A single regioisomer was isolated.



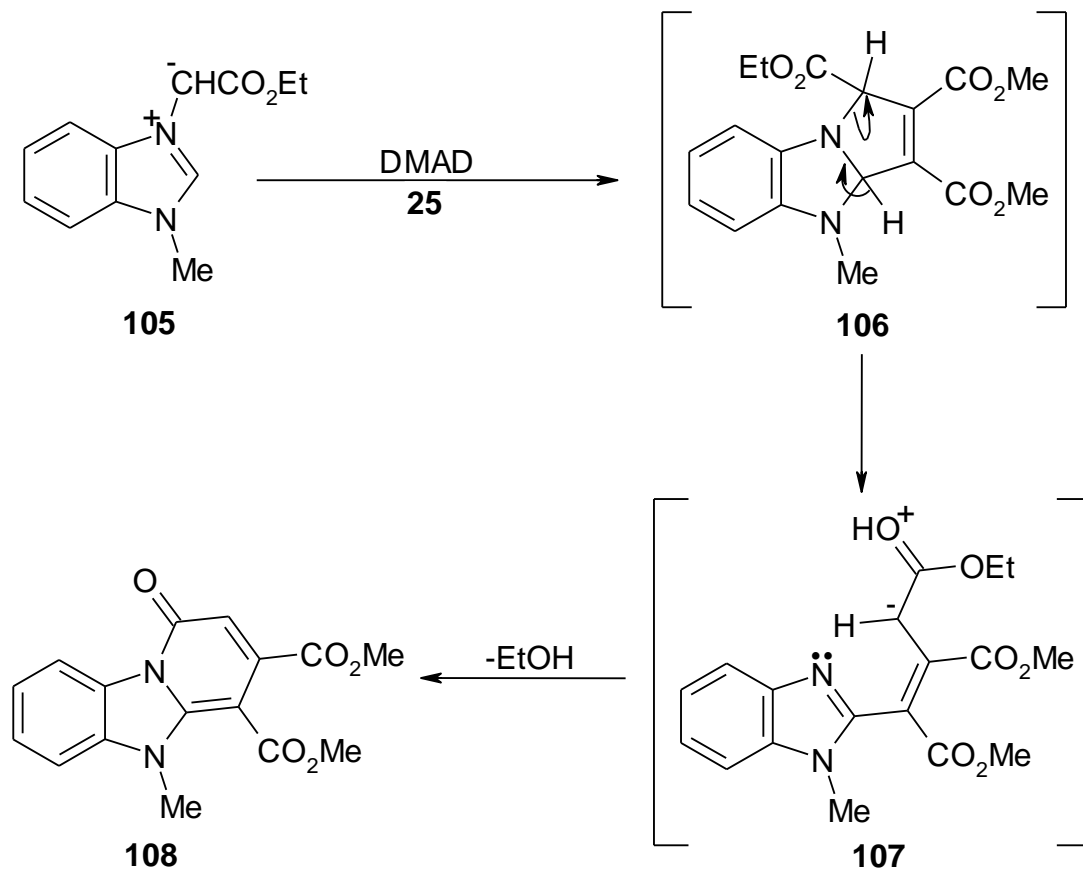
Scheme 25

The reactions of substituted benzimidazolium methanides⁶⁸ demonstrate the range of products that can arise due to rearrangement of the initial cycloadduct. Treatment of 1-methyl-3-phenacylbenzimidazolium bromide **101** with base generates the corresponding benzimidazolium methanide 1,3-dipole **102**. This can be trapped *in situ* with DMAD **25** to yield a mixture of **103** and **104** (Scheme 26). These products are formed following rearrangement of the initial cycloadduct. This rearrangement may occur due to oxidation arising from the presence of excess dipolarophile or ring opening to form an intermediate.



Scheme 26

Treating the corresponding 1-methyl-3-ethoxycarbonylmethyl benzimidazolium bromide **105** with DMAD **25** under the same conditions generates an initial cycloadduct which undergoes loss of a molecule of ethanol to produce the stable final product. This compound has been the subject of some confusion. Initially, Ogura and Kikuchi⁶⁸ proposed that compound **108** was the final product of the reaction (Scheme 27). The proposed mechanism involves ring opening of the initial cycloadduct **106** to generate **107**, which subsequently loses ethanol in a nucleophilic ring closure (Scheme 27). The authors reported that the mechanism was similar to that proposed by Boekelheide and Fedoruk⁶ for the reaction of 1-methylimidazolium-3-dicyanomethanide 1,3-dipole **28** with DMAD **25** (Scheme 5).



Scheme 27

This was disputed by Zugravescu,⁶⁹ who alternatively proposed the novel structure **109** on the basis of UV, IR and ¹H NMR data (Figure 18).

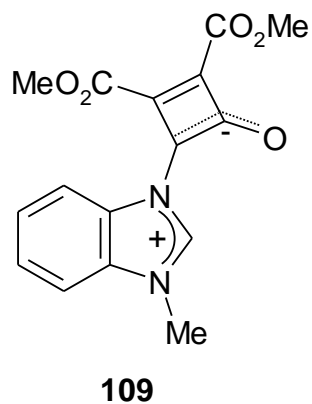
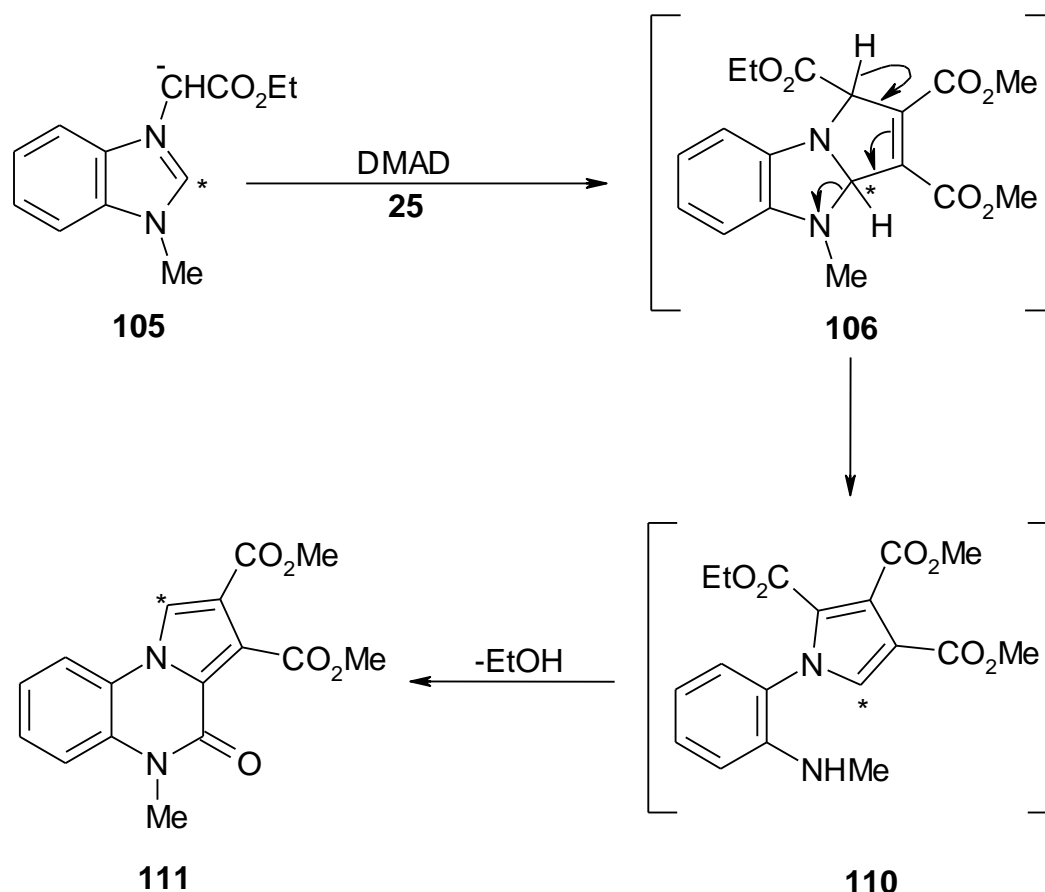


Figure 18

Both of these structures were subsequently disproved by Meth-Cohn,⁷⁰ on the basis of a ¹³C NMR spectrum of the product. The ¹³C NMR data immediately ruled out the benzimidazole-type structure **109** as no low field signal characteristic of the C-2 of benzimidazole was observed. The 1,3-dipole **105** was also prepared with a ¹³C label at the 2-position. The product obtained from the reaction this dipole contained a labelled CH group with long range coupling to two ester groups and one quaternary carbon (**Scheme 28**). Meth-Cohn⁷⁰ proposed that the initial cycloadduct **106** is converted into the pyrrole **110**, following the tautomeric shift of an acidic proton. This intermediate **110** can then cyclise to the pyrroloquinoxaline **111** with loss of ethanol (**Scheme 28**).



*Labelled Carbon

Scheme 28

2.1.5 Project outline

Our long standing interest in the rearrangements of azolium 1,3-dipoles led us to explore the imidazolium dicyanomethanide 1,3-dipole system in more detail. Having previously confirmed the structure of the ring expanded products by X-Ray crystallography, we explored the generality of this rearrangement by synthesizing a series of similar compounds. The regiochemistry of these reactions was investigated by the use of unsymmetrical dipolarophiles. Further interesting results were observed by using alkenes as dipolarophiles. The reactions of 1-methylimidazolium-3-dicyanomethanide 1,3-dipole **28** and 1-benzylimidazolium-3-dicyanomethanide 1,3-dipole **112** with maleic anhydride yielded interesting structures that provided new insights into this intriguing rearrangement. In order to probe the reaction mechanism it was necessary to isolate the initial cycloadduct, and then monitor the rearrangement by spectroscopic methods. Elguero³⁵ has previously isolated the initial cycloadduct from the reaction of an azolium dicyanomethanide 1,3-dipole and DMAD **25**. Studying this reaction allowed us to both confirm Elguero's original assignment and to follow the rearrangement of the initial cycloadduct by ¹H NMR and ¹³C NMR spectroscopy. Tracking the conversion of initial cycloadduct to ring-expanded product shed new light on this intriguing rearrangement.

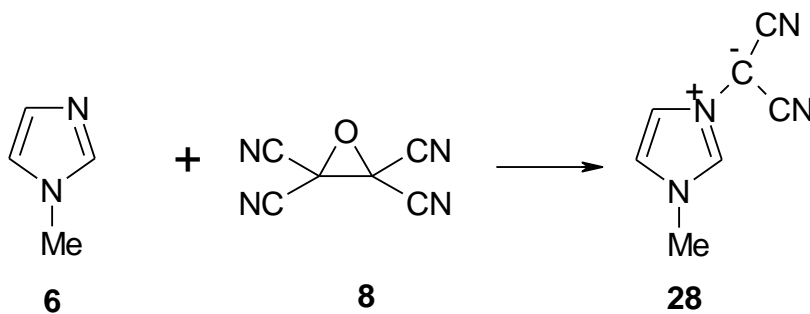
2.2 Synthesis of imidazolium dicyanomethanide 1,3-dipoles

As discussed previously (**Section 1.2**), tetracyanoethylene oxide (TCNEO) **8** has been used to generate a wide variety of azinium and azolium dicyanomethanide 1,3-dipoles.^{4-7, 26} TCNEO **8** can be efficiently synthesized^{4, 5} by the action of hydrogen peroxide **10** on tetracyanoethylene (TCNE) **9** (**Scheme 1**). A solution of TCNE **9** in acetonitrile was cooled to -5 °C and treated dropwise with an equimolar amount of H₂O₂ **10** (30%), such that the temperature of the reaction remained below 12 °C. Following completion of the addition, the reaction mixture was stirred for a further 5 min before being diluted with ice-cold water. This caused the precipitation of TCNEO **8** as a white solid which was collected by filtration. TCNEO **8** slowly evolves hydrogen cyanide when exposed to moist air at room temperature, and so must be used quickly.

2.2.1 Synthesis of 1-methylimidazolium-3-dicyanomethanide 1,3-dipole

28

The procedure described by Boekelheide⁶ was used to prepare 1-methylimidazolium-3-dicyanomethanide 1,3-dipole **28**. A cooled solution of TCNEO **8** in ethyl acetate was treated dropwise with an equimolar amount of 1-methylimidazole **6**, neat or in ethyl acetate, such that the reaction temperature remained below 10 °C (**Scheme 29**). Following addition of the heterocyclic base, the dipole separated from solution as a pale brown solid in 65% yield, and was collected by filtration. The structure was supported by IR, ¹H and ¹³C NMR spectroscopy.



Scheme 29

The IR spectrum contained two strong cyano bands at 2180 and 2134 cm^{-1} . In the ^1H NMR spectrum, the proton of C-2 showed the greatest deshielding and appeared at δ 9.08. Only one signal at 123.2 ppm was observed for the two cyano groups in the ^{13}C NMR spectrum. Theoretical calculations carried out in collaboration with Professor Luke Burke of Rutgers University have indicated⁷¹ that barrier of rotation in the exocyclic N-C bond is less than 1 kcal/mol. This suggests that resonance form **28A** is the appropriate suitable representation of the ylide, as only one ^{13}C NMR signal would be expected for the equivalent cyano groups. If the resonance form **28B** represented the structure of the 1,3-dipole, then the ^{13}C NMR spectrum would be expected to show separate signals for the cyano groups, which would be non-equivalent (**Figure 19**).

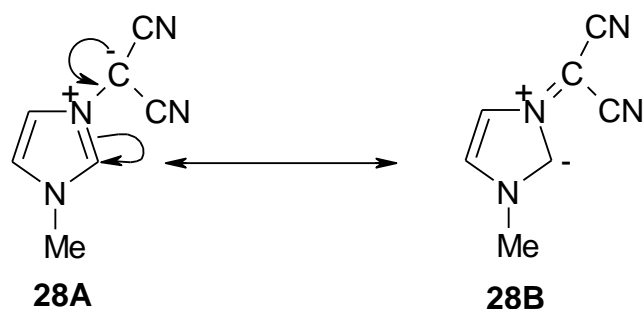


Figure 19

In the ^{13}C NMR spectrum a very weak signal at 60.3 ppm was observed for the methanide carbon. These signals are typically quite weak and have not been widely reported.⁷² A pulse delay of 3 seconds and a large number of scans (17,000) were required to detect the signal.

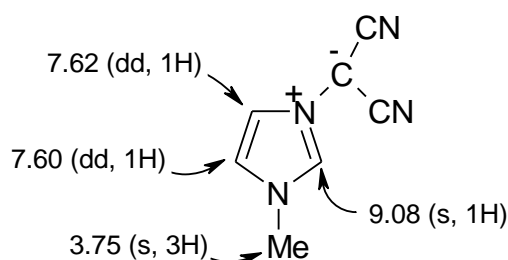
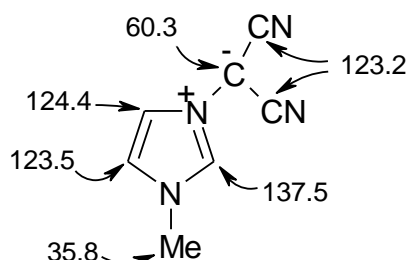
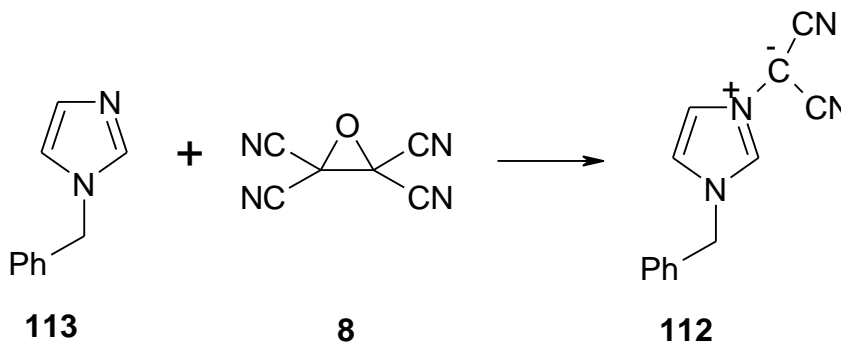
^1H NMR (DMSO- d_6) ^{13}C NMR (DMSO- d_6)

Figure 20: ^1H NMR and ^{13}C NMR assignments for compound **28**

2.2.2 Synthesis of 1-benzylimidazolium-3-dicyanomethanide 1,3-dipole **112**

The 1-benzylimidazolium-3-dicyanomethanide 1,3-dipole **112** has not been reported in the literature to date. It was prepared by treating a cooled solution of 1-benzylimidazole **113** in ethyl acetate with TCNEO **8** also in cooled ethyl acetate. (**Scheme 30**).



Scheme 30

The product precipitated from solution as a brown solid in 73% yield. The structure was supported by IR, ^1H and ^{13}C NMR spectroscopy. Two strong cyano bands at 2160 and 2180 cm^{-1} were observed in the IR spectrum. In the ^1H NMR spectrum, the proton on C-2 showed the greatest deshielding and appeared at δ 9.33. The two cyano groups are equivalent, and so only one cyano signal at 123.0 ppm appeared in the ^{13}C NMR spectrum. Despite extensive efforts, the methanide carbon signal was not detected. It is possible that the carbon is relaxing at a very slow rate, and because

of this the signal may be too weak to be seen due to saturation. The NMR assignments are shown below (**Figure 21**).

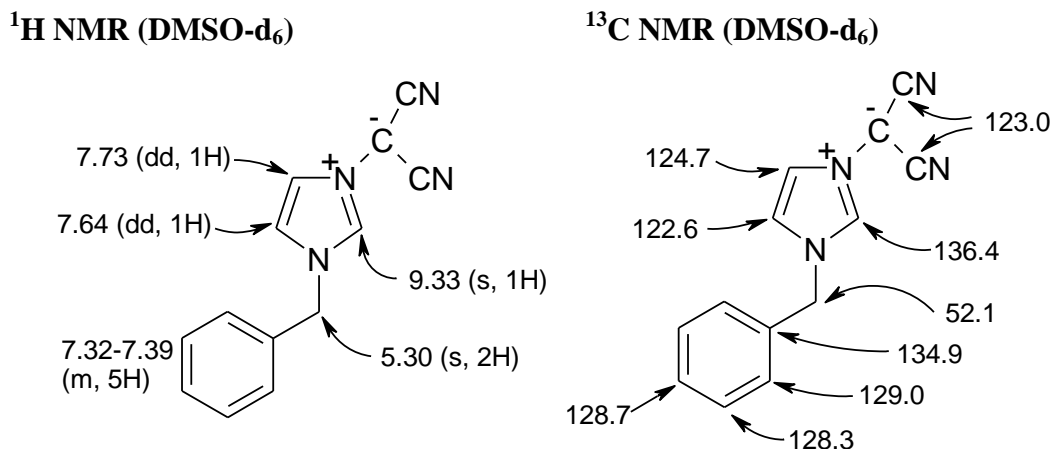
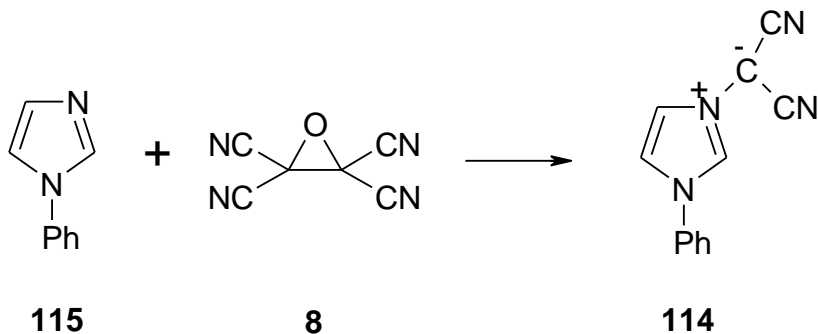


Figure 21: ^1H NMR and ^{13}C NMR assignments for compound **112**

2.2.3 Synthesis of 1-phenylimidazolium-3-dicyanomethanide 1,3-dipole **114**

The 1-phenylimidazolium-3-dicyanomethanide 1,3-dipole **114** was first synthesized by Elguero *et al.*⁷ The 1,3-dipole **114** was generated by treating a solution of 1-phenylimidazole **115** in cooled ethyl acetate with a solution of TCNEO **8**, also in cooled ethyl acetate (**Scheme 31**).



Scheme 31

Compound **114** precipitated from solution as an off-white solid in 81% yield. The structure was supported by IR, ^1H and ^{13}C NMR spectroscopy. Two strong cyano bands were observed at 2175 and 2114 cm^{-1} in the IR spectrum. In the ^1H NMR

spectrum, the hydrogen at C-2 appeared the most deshielded at δ 9.75. The two cyano groups gave one signal at 123.3 ppm in the ^{13}C NMR spectrum. The methanide carbon signal was not observed despite numerous attempts to locate it. The NMR assignments are shown below (**Figure 22**).

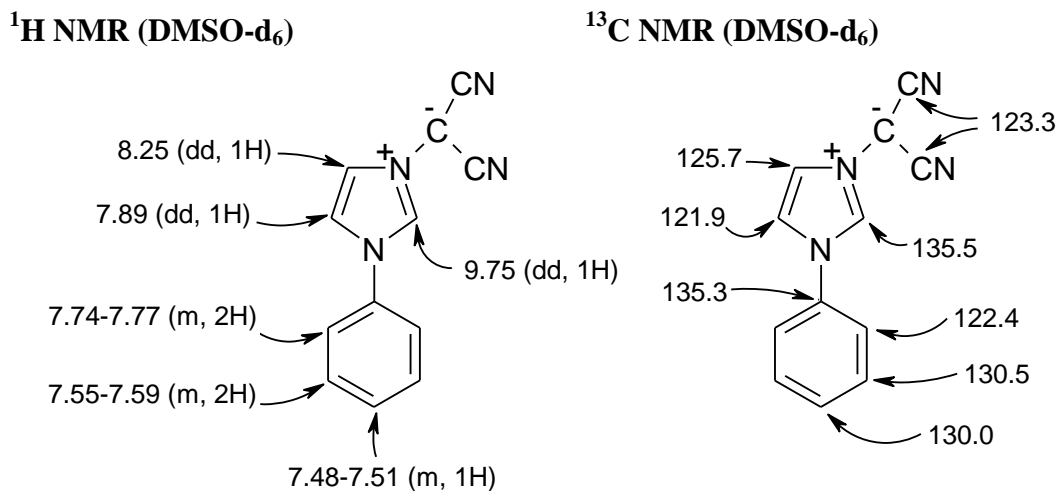


Figure 22: ^1H NMR and ^{13}C NMR assignments for compound **114**

2.3 Cycloaddition reactions of imidazolium dicyanomethanide 1,3-dipoles with alkyne dipolarophiles

2.3.1 Cycloaddition reactions of 1,3-dipole **28** with symmetrical electron poor alkyne dipolarophiles (DMAD/DEAD)

The first reported cycloaddition reaction⁶ of 1-methylimidazolium-3-dicyanomethanide **28** involved treatment of a solution of the ylide in dimethylformamide with neat DMAD **25** (Section 1.4.1, Scheme 5). The product was isolated as a yellow crystalline solid in 70% yield following column chromatography. Spectroscopic analysis of the product indicated that a substituted imidazo[2,3-*a*]pyridine ring system had been generated. We repeated this reaction using acetonitrile as solvent. After stirring for 1 h at room temperature, the product precipitated from solution and was collected by filtration. Recrystallisation from ethanol afforded compound **30** in 81% yield.

The melting point obtained agreed with the data presented in the original study.⁶ The ¹H NMR spectrum previously reported⁶ was also in agreement with that recorded by us (Figure 25). In both studies the N-H signal was not observed. However no ¹³C NMR data (Figure 25) have previously been published for this compound. The structure of compound **30** features a characteristic structural signature, an embedded enediamine unit involving atoms C-8, C-8a, N-1 and N-4 (Figure 23). Vinylic resonance has a profound effect on the ¹³C NMR spectrum of compound **30**. The enamine α -carbon, C-8a, is exceptionally deshielded, and appeared at 146.3 ppm in the ¹³C NMR spectrum. Conversely, C-8, the β -carbon is extremely shielded, and appeared at 88.7 ppm.

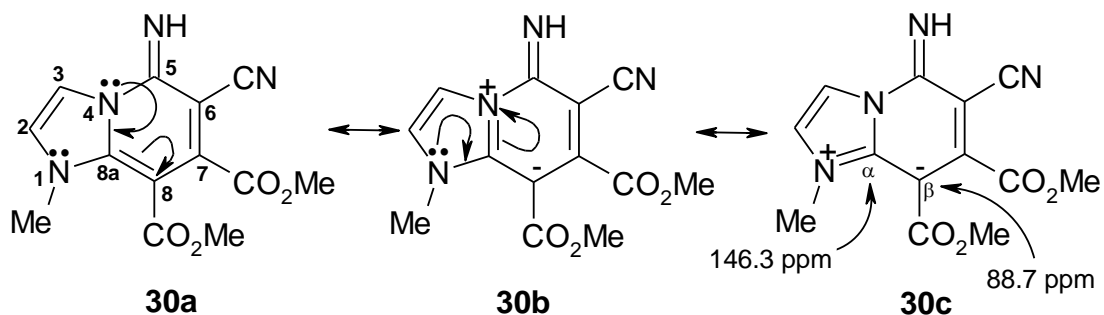


Figure 23

The IR spectrum contained bands at 1610 (C=N), and 3293 cm^{-1} (NH), confirming the presence of the imine group and consequently ring-expansion. The IR spectrum also showed bands at 1736 and 1709 cm^{-1} , corresponding to the two carbonyl groups. In related compounds, the higher absorbance has been assigned³⁵ to the ester group attached to C-7, which is conjugated with the electron withdrawing cyano group. Determination of the X-Ray crystal structure⁷¹ of 1-methyl-5-imino-6-cyano-7,8-dimethoxycarbonyl imidazo[2,3-*a*]pyridine **30** provided conclusive proof for the structural assignment (**Figure 24**).

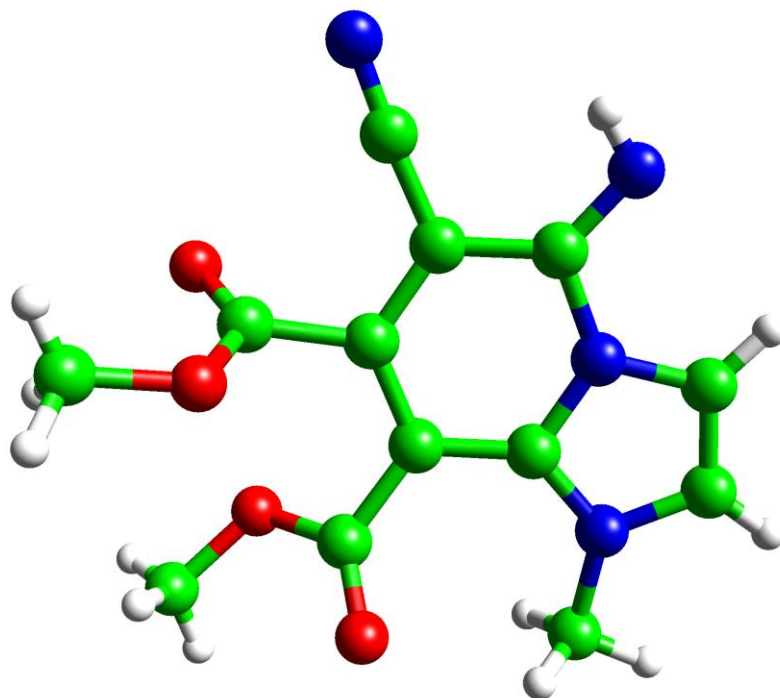
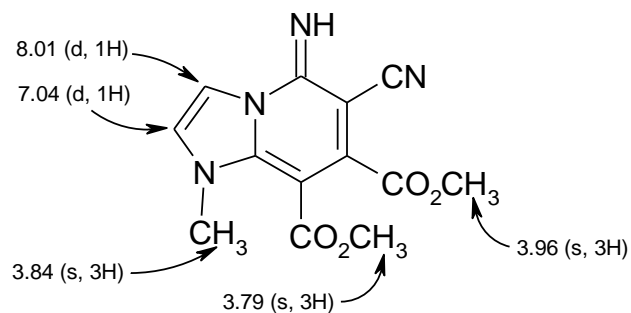


Figure 24: X-Ray crystal structure of compound **30**

The original structural assignment is therefore proven to be correct. Boekeleide's⁶ proposed structure, based on rather limited data, was a remarkable and intuitive assignment.

¹H NMR (CDCl₃)



¹³C NMR (CDCl₃)

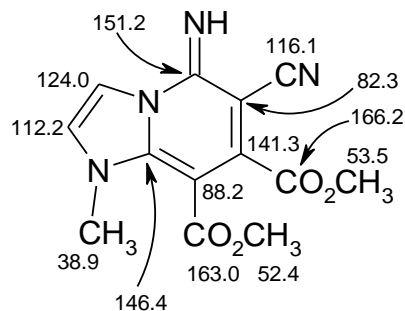
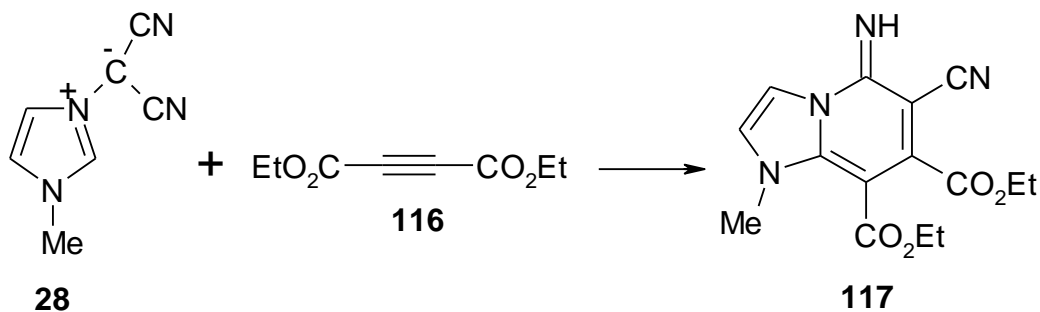


Figure 25: ¹H NMR and ¹³C NMR assignments for compound **30**

The reaction between 1-methylimidazolium-3-dicyanomethanide **28** and DEAD **116** yielded a similar ring expanded product, compound **117** (**Scheme 32**). A solution of **28** in acetonitrile was treated with DEAD **116** and the solution stirred at room temperature for 2 h. The solvent was then removed under reduced pressure and the residue crystallized from methanol to give compound **117** in 51% yield.



Scheme 32

The structure of **117** was confirmed by ^1H NMR, ^{13}C NMR and IR spectroscopy. The IR spectrum was similar to that of compound **30**, containing a characteristic NH band at 3291 cm^{-1} and a cyano band at 2207 cm^{-1} . The ^1H NMR spectrum (**Figure 27**) was also similar to that of compound **30**, with the imidazole protons H-2 and H-3 both appearing as doublets at δ 7.04 and 7.99 respectively (**Figure 27**). The assignments of H-2 and H-3 were supported by NOEDS (**Figure 26**).

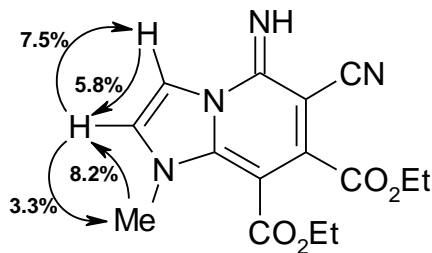


Figure 26: NOEDS enhancements of compound **117** in CDCl_3

In the ^{13}C NMR spectrum (**Figure 27**), the characteristic enediamine signals appeared at 88.7 ppm for C-8 and 146.3 ppm for C-8a (**Figure 27**).

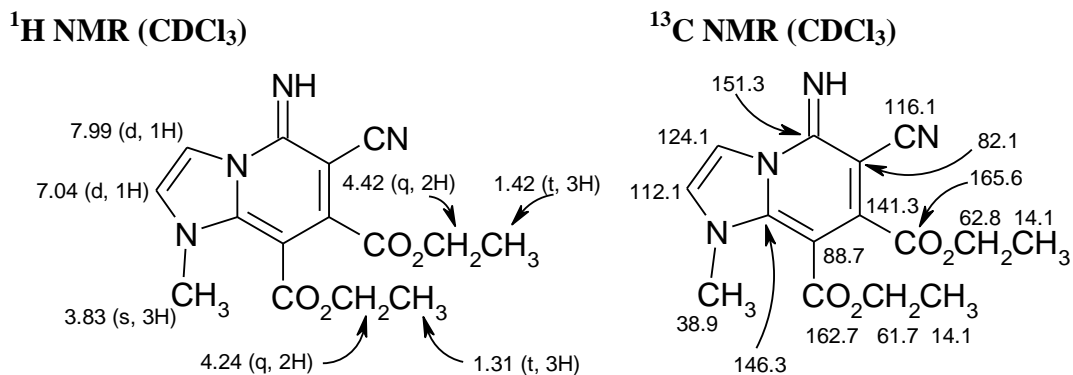
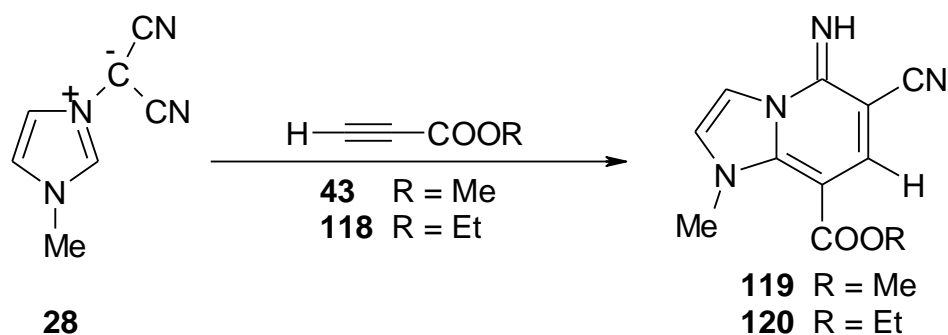


Figure 27: ¹H NMR and ¹³C NMR assignments for compound **117**

2.3.2 Cycloaddition reactions of 1,3-dipole **28** with unsymmetrical electron poor alkyne dipolarophiles (MP/EP)

The 1-methylimidazolium-3-dicyanomethanide 1,3-dipole **28** was treated with methyl propiolate **43** in acetonitrile at 0-5 °C (**Scheme 33**). A single product, compound **119**, was isolated in 52% yield by fractional crystallization from diethyl ether. The structural assignment of compound **119** was supported by IR, ¹H NMR and ¹³C NMR spectroscopy.



Scheme 33

The IR spectrum featured bands corresponding to an NH bond at 3107 and cyano group at 2204 cm⁻¹. The ¹H NMR spectrum (**Figure 28**) contained two doublets at δ 7.01 and 8.01, corresponding to H-2 and H-3, respectively. The signal for H-7 appeared at δ 8.05. The ¹³C NMR spectrum contained a single carbonyl signal at 163.2 ppm and a signal at 142.3 ppm corresponding to C-7. The embedded

enediamine unit was also identifiable in the spectrum, with C-8 appearing at 90.0 ppm and C-8a at 141.9 ppm (**Figure 28**).

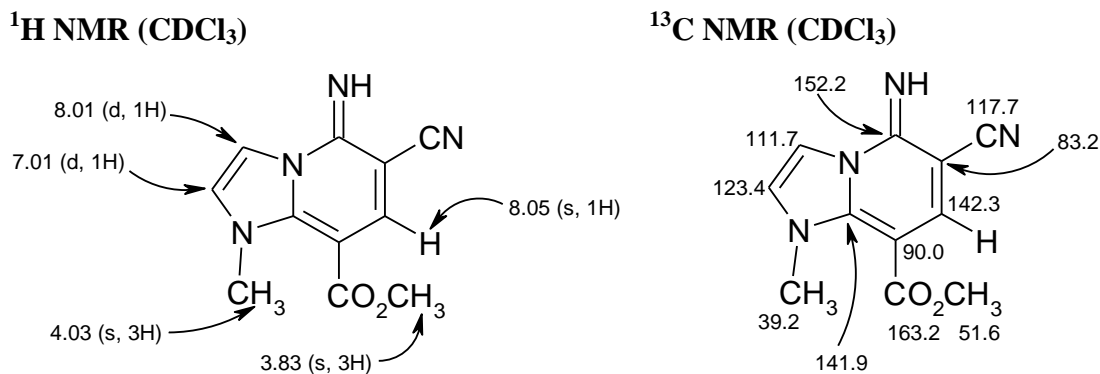


Figure 28: ¹H NMR and ¹³C NMR assignments for compound **119**

Treatment of the 1,3-dipole **28** with ethyl propiolate (EP) **118** also led to the isolation of a single regioisomer **120** in 33% yield (**Scheme 33**). The structural assignment of compound **120** (**Figure 29**) was supported by IR, ¹H NMR and ¹³C NMR spectroscopy. The ¹H NMR spectrum was similar to that of **119**, possessing a singlet at δ 8.05 corresponding to H-7. In the ¹³C NMR spectrum, the carbonyl carbon and C-7 appeared at 163.2 and 142.8 ppm, respectively. The signals for C-8 and C-8a appeared at 90.6 and 142.3 ppm, respectively (**Figure 29**).

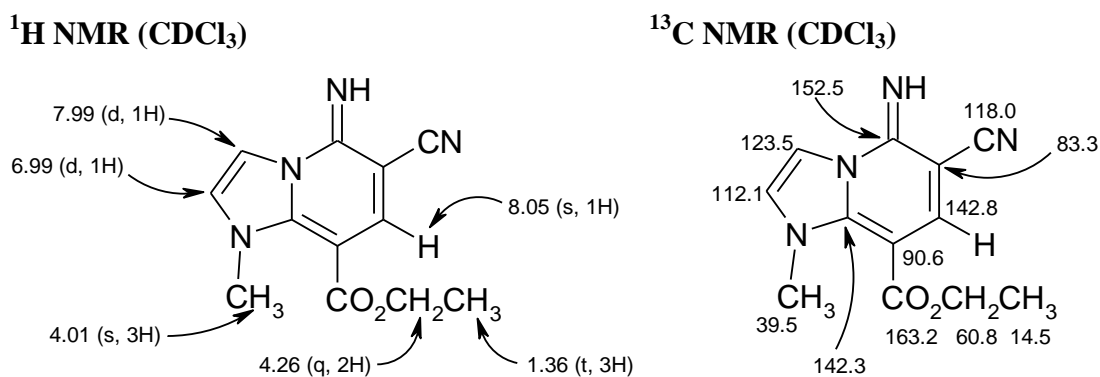


Figure 29: ¹H NMR and ¹³C NMR assignments for compound **120**

IR data were used to help determine the structures of **119** and **120** (Table 5): both compounds contained a single carbonyl stretching frequency at 1689 and 1696 cm^{-1} , respectively. These absorbances correspond to the lower frequency carbonyl absorbances observed for the related compounds with two ester groups, **30** and **117**. The higher of the two carbonyl stretching frequencies in **30** and **119** is assigned to the carbonyl on C-7, as this is conjugated with the electron withdrawing cyano group. Therefore in all the cases the lower stretching frequency arises from the ester group on C-8, allowing the structure of **119** and **120** to be determined.

The ^{13}C NMR spectra of **119** and **120** also supported the assignment of regiochemistry. The C-7 signal was significantly stronger than the C-8 signal in both ^{13}C NMR spectra which indicated a hydrogen atom was attached to C-7. This was confirmed by distortionless enhancement by polarization transfer (DEPT) spectra. Therefore the regiochemistry observed in these reactions is that whereby the unsubstituted terminus of the dipolarophile is attached to the dicyanomethanide terminus of the 1,3-dipolarophile. This is consistent with investigations conducted by Elguero *et al.*³⁵

Table 5: Carbonyl stretching frequencies for the products arising from the reactions of 1-methylimidazolium-3-dicyanomethanide 1,3-dipole **28** with alkyne dipolarophiles

Compound	Dipolarophile	Dipole	IR/ cm^{-1} (νCO)	
			C7 CO_2R	C8 CO_2R
30	DMAD 25	28	1736	1708
119	MP 43	28	-	1689
117	DEAD 116	28	1739	1697
120	EP 118	28	-	1696

The assignments of H-2 and H-3 in the ^1H NMR spectra were supported by NOEDS (Figure 30).

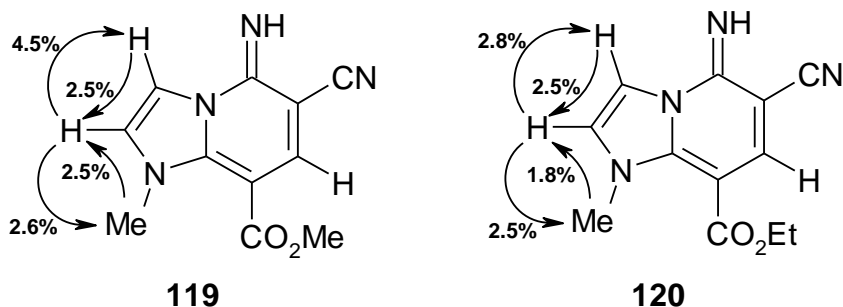
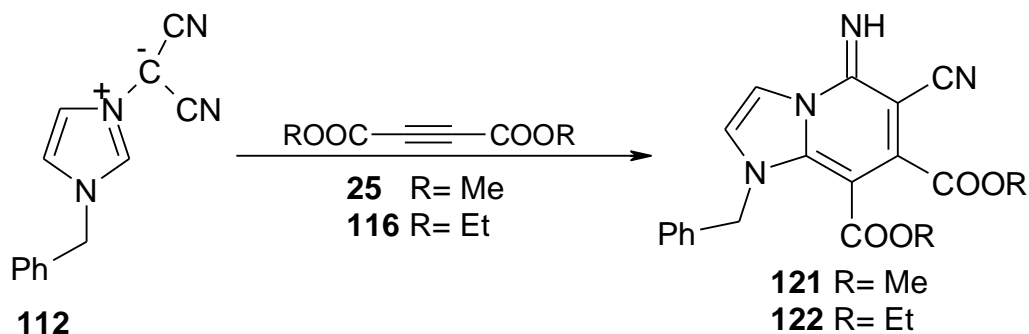


Figure 30: NOEDS enhancements of compounds **119** and **120** in CDCl_3

2.3.3 Cycloaddition reactions of 1,3-dipole **112** with symmetrical electron poor alkyne dipolarophiles (DMAD/DEAD)

An ice-cold solution of the 1-benzylimidazolium-3-dicyanomethanide 1,3-dipole **112** in DMF was treated with DMAD **25**, and then left to stand at 0 °C for 4 h. The mixture was subsequently added to cooled water, causing precipitation of compound **121** in 53% yield as a yellow solid (**Scheme 34**). The structural assignment of compound **121** was supported by IR, ^1H NMR and ^{13}C NMR spectroscopy.



Scheme 34

The IR spectrum of compound **121** displayed stretching frequencies of 3305 (NH), 2208 ($\text{C}\equiv\text{N}$) and 1615 cm^{-1} ($\text{C}=\text{N}$). These are characteristic of a ring-expanded product. In the ^1H NMR spectrum (**Figure 31**), the methoxy protons appeared as singlets at δ 3.63 and 3.91. The imidazole protons, H-2 and H-3, appeared at δ 7.02 and 8.00, respectively. Each of the signals was a doublet with a J value of 1.8 Hz. The ^{13}C spectrum (**Figure 31**) included two signals at 163.3 and 166.1 ppm

corresponding to the two carbonyl groups present. The embedded enediamine unit was also evident, with C-8 appearing at 89.1 ppm and C-8a at 146.1 ppm.

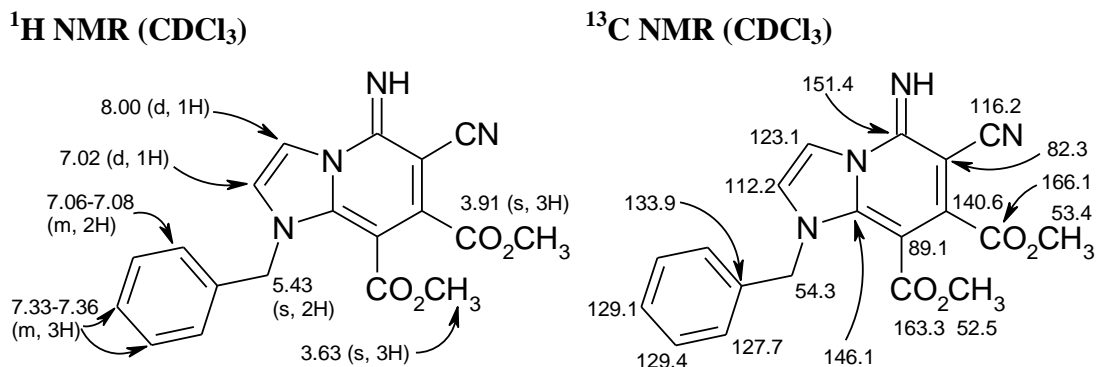


Figure 31: ^1H NMR and ^{13}C NMR assignments for compound **121**

Compound **122** was prepared by treating solution of 1-benzylimidazolium-3-dicyanomethanide 1,3-dipole **112** in ice-cold acetonitrile with an equimolar amount of DEAD **116**. The mixture was allowed to stir at 0 °C for 4 h. Compound **122** separated from solution as a yellow precipitate in 42% yield (**Scheme 34**). The assignment of compound **122** was supported by IR, ^1H NMR and ^{13}C NMR spectroscopy.

The IR spectrum of compound **122** displayed the characteristic ring-expanded product bands at 3303 (NH), 2204 ($\text{C}\equiv\text{N}$) and 1620 cm^{-1} ($\text{C}=\text{N}$). The ^1H NMR spectrum featured two doublets at δ 7.07 and 8.07, corresponding to H-2 and H-3, respectively (**Figure 32**). The assignments of these signals were supported by NOEDS (**Figure 33**). In the ^{13}C NMR spectrum, the enediamine carbons appeared at 146.0 (C8a) and 89.3 ppm (C-8) (**Figure 32**). The spectrum also contained signals at 151.3 ppm due to the imine carbon and at 116.0 ppm attributable to the carbon of the cyano group.

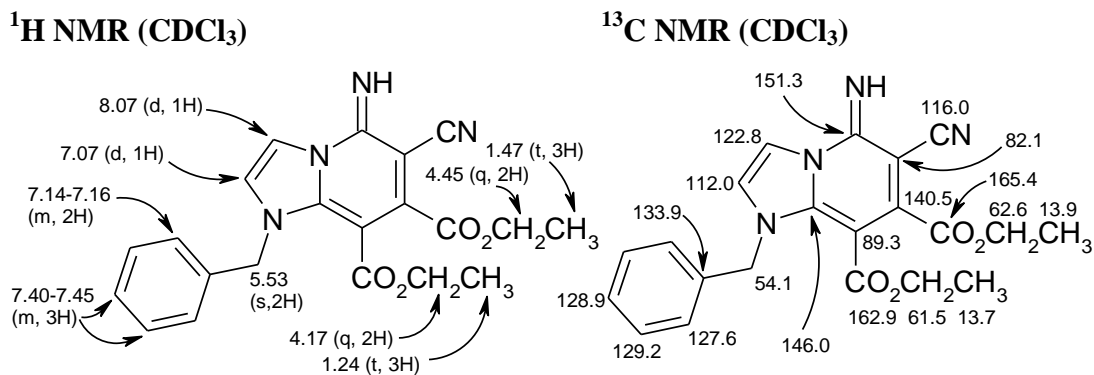


Figure 32: ^1H NMR and ^{13}C NMR assignments for compound **122**

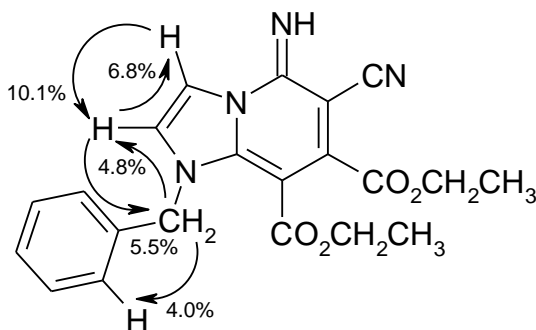
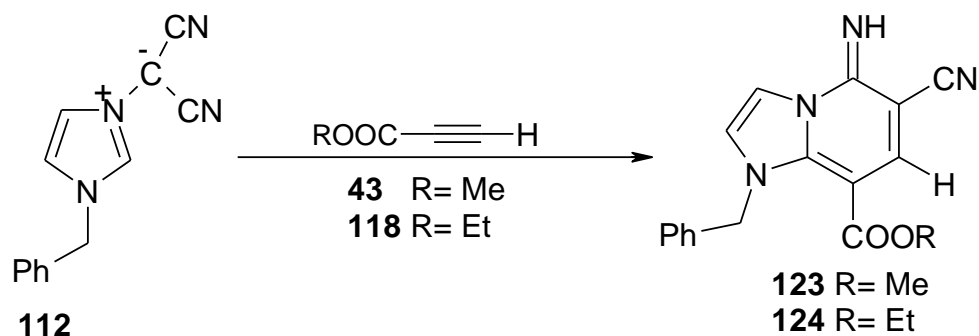


Figure 33: NOEDS enhancements of compound **122** in CDCl_3

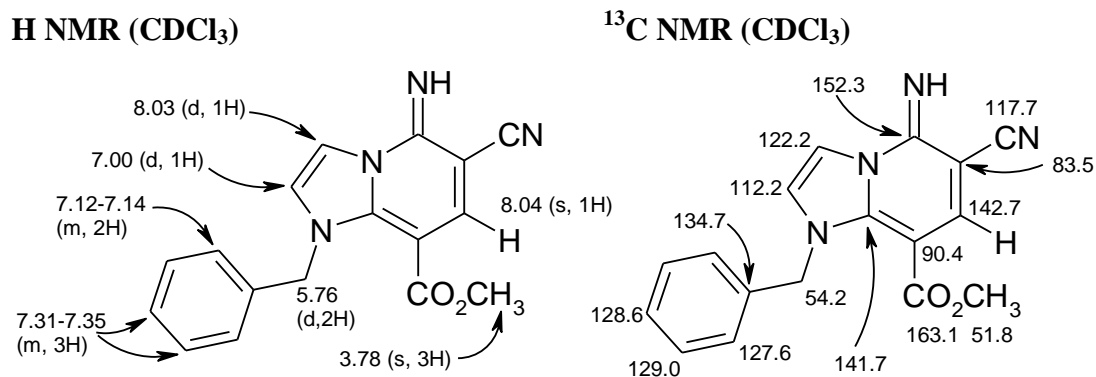
2.3.4 Cycloaddition reactions of 1,3-dipole **112** with unsymmetrical electron poor alkyne dipolarophiles (MP/EP)

A solution of 1-benzylimidazolium-3-dicyanomethanide 1,3-dipole **112** in acetonitrile was treated with an equimolar amount of MP **43** (Scheme 35). The mixture was allowed to stir at ambient temperature for 48 h, during which time compound **123** separated from solution as a buff precipitate in 48% yield. The structural assignment of compound **123** was supported by IR, ^1H NMR and ^{13}C NMR spectroscopy.



Scheme 35

The IR spectrum featured bands corresponding to a NH bond at 3292 cm^{-1} and a cyano group at 2203 cm^{-1} . The spectrum also contained a band at 1694 cm^{-1} corresponding to the methoxy group at the C-7 position. The ^1H NMR spectrum (**Figure 34**) contained doublets at δ 7.00 and 8.03, corresponding to H-2 and H-3, respectively. The signal for H-7 appeared slightly further downfield at δ 8.04 (**Figure 34**). The assignments of the ^1H NMR signals of **123** were supported by NOEDS (**Figure 35**). The ^{13}C NMR spectrum contained a single carbonyl signal at 163.1 ppm and a signal at 142.7 ppm corresponding to C-7. The embedded enediamine unit was also identifiable in the spectrum, with C-8 appearing at 90.4 ppm and C-8a at 141.7 ppm (**Figure 34**).

Figure 34: ^1H NMR and ^{13}C NMR assignments for compound **123**

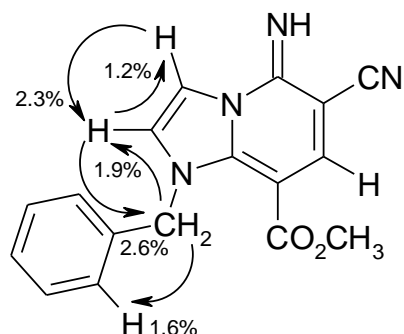
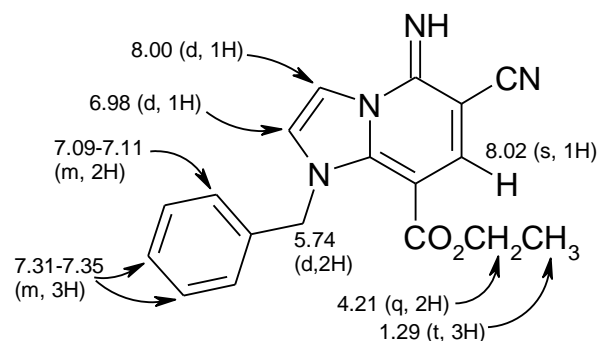


Figure 35: NOEDS enhancements of compound **123** in CDCl_3

Treatment of 1-benzylimidazolium-3-dicyanomethanide 1,3-dipole **112** with an equimolar amount of EP **118** in acetonitrile led to the isolation of compound **124**. The mixture was stirred at ambient temperature for 51 h. The solvent was then removed under reduced pressure, yielding a sticky brown solid. Fractional crystallization from diethyl ether gave **124** as a pale yellow solid in 27% yield, together with an orange gum. The orange gum was subjected to a Soxhlet extraction with ether which afforded further **124** in 36% yield.

^1H NMR (CDCl_3)



^{13}C NMR (CDCl_3)

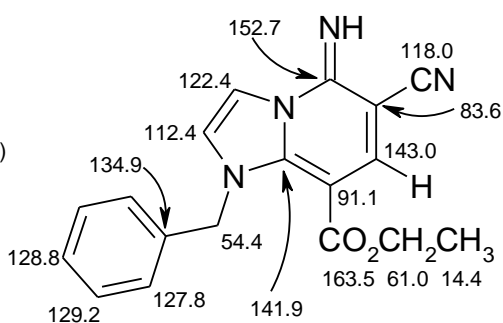


Figure 36: ^1H NMR and ^{13}C NMR assignments for compound **124**

The structural assignment of compound **124** was supported by IR, ^1H NMR and ^{13}C NMR spectroscopy. The ^1H NMR spectrum was similar to that of **123**, possessing a singlet at δ 8.02 corresponding to H-7 and doublets at δ 6.98 (H-2) and 8.00 (H-3). The ^{13}C NMR spectrum contained signals at 163.5 (carbonyl group) and 143.0 ppm

(C-7). The signals for C-8 and C-8a appeared at 91.1 and 141.9 ppm respectively, (Figure 36).

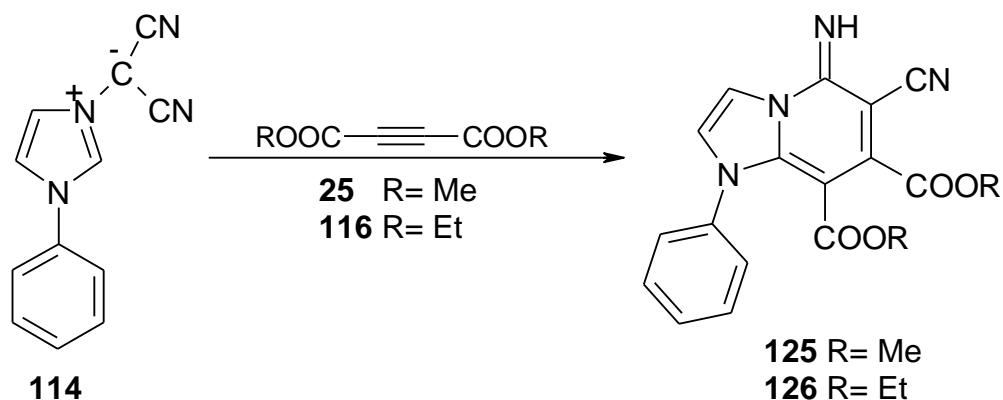
IR data, specifically carbonyl stretching frequencies, were used, as before, to help determine the regiochemistry of these reactions (Table 6). The assignment was also supported by ^{13}C NMR spectra which showed the presence of a hydrogen at C-7 in compounds **123** and **124**, and its absence in products **121** and **122**. The assignment of C-7 was confirmed by DEPT spectra.

Table 6: Carbonyl stretching frequencies for the products arising from the reactions of 1-benzylimidazolium-3-dicyanomethanide 1,3-dipole **112** with alkyne dipolarophiles

Compound	Dipolarophile	Dipole	IR/cm ⁻¹ (νCO)	
			C7 CO ₂ R	C8 CO ₂ R
121	DMAD 25	112	1720	1704
123	MP 43	112	-	1694
122	DEAD 116	112	1727	1698
124	EP 118	112	-	1682

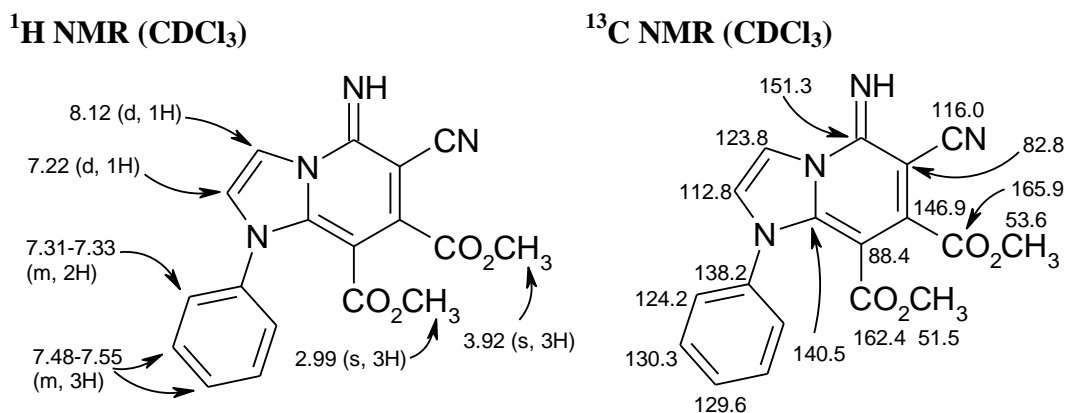
2.3.5 Cycloaddition reactions of 1,3-dipole **114** with symmetrical electron poor alkyne dipolarophiles (DMAD/DEAD)

A solution of 1-phenylimidazolium-3-dicyanomethanide 1,3-dipole **114** in acetonitrile was treated with an equimolar amount of DMAD **25**. The mixture was stirred at ambient temperature for 3.5 h. The solvent then was removed under reduced pressure at room temperature to yield a brown gum which solidified overnight. Crystallisation from hot ethanol yielded compound **125** in 67% yield (Scheme 36). The structural assignment of compound **125** was supported by IR, ^1H NMR and ^{13}C NMR spectroscopy.



Scheme 36

The IR spectrum contained the three characteristic bands of a ring expanded product- 3320 (NH), 2206 ($\text{C}\equiv\text{N}$) and 1617 cm^{-1} ($\text{C}=\text{N}$). The two carbonyl groups afforded signals at 1724 and 1696 cm^{-1} . The ^1H NMR spectrum (**Figure 37**) featured two doublets at δ 7.22 and 8.12, corresponding to H-2 and H-3, respectively (**Figure 37**). NOEDS was used to confirm these assignments, however no enhancement was found from the phenyl ring to the imidazole ring protons (**Figure 38**). In the ^{13}C NMR spectrum, the enediamine carbons appeared at 140.5 (C-8a) and 88.4 ppm (C-8) (**Figure 37**). The spectrum also contained a signal at 151.3 ppm due to the imine carbon and at 116.0 ppm attributable to the carbon of the cyano group.

Figure 37: ^1H NMR and ^{13}C NMR assignments for compound **125**

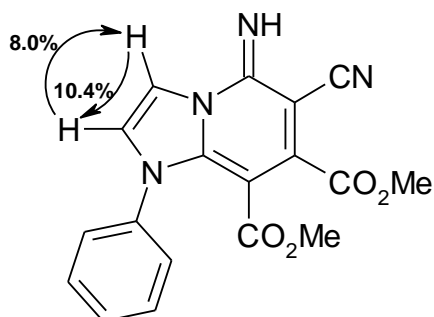


Figure 38: NOESY enhancements of compounds **125** in CDCl_3

Compound **126** was produced by treating a solution of 1-phenylimidazolium-3-dicyanomethanide 1,3-dipole **114** in acetonitrile with an equimolar amount of DEAD **116** (Scheme 36). The mixture was stirred at ambient temperature for 3.5 h. The solvent was then removed under reduced pressure at room temperature, yielding a brown gum which solidified overnight. Crystallisation from hot ethanol yielded compound **126** in 55% yield.

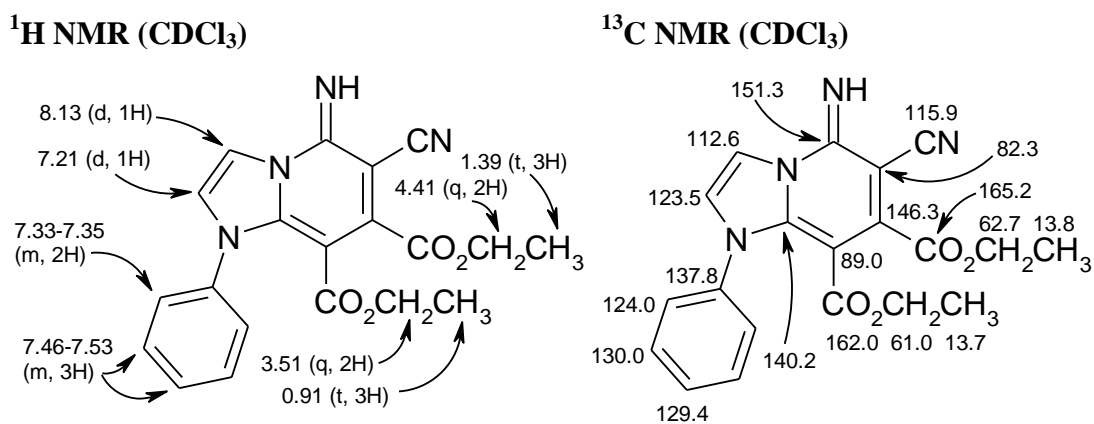


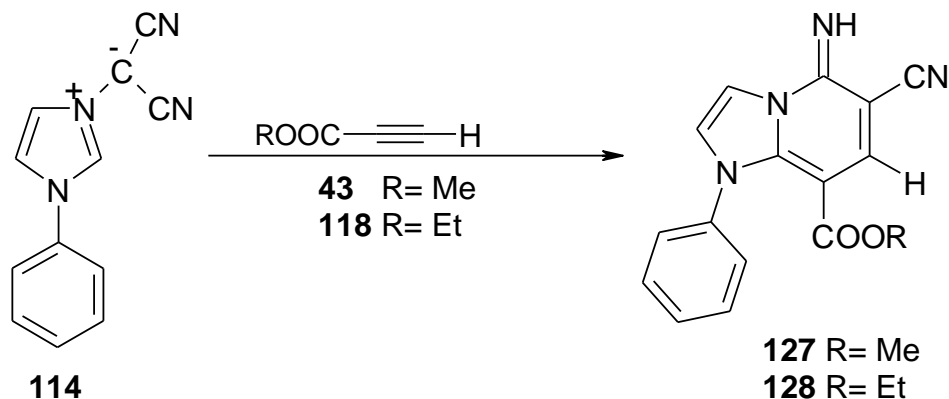
Figure 39: ^1H NMR and ^{13}C NMR assignments for compound **126**

The structural assignment of compound **126** was supported by IR, ^1H NMR and ^{13}C NMR spectroscopy. The IR spectrum of compound **126** displayed the characteristic ring-expanded product bands at 3296 (NH), 2206 ($\text{C}\equiv\text{N}$) and 1615 cm^{-1} ($\text{C}=\text{N}$). The ^1H NMR spectrum featured two doublets at δ 7.23 and 8.16, corresponding to H-2 and H-3, respectively (Figure 39). In the ^{13}C NMR spectrum, the enediamine carbons appeared at 140.2 (C-8a) and 89.0 ppm (C-8) (Figure 39). The spectrum

also contained a signal at 151.3 ppm due to the imine carbon and at 115.9 ppm due to the carbon of the cyano group.

2.3.6 Cycloaddition reactions of 1,3-dipole **114** with unsymmetrical electron poor alkyne dipolarophiles (MP/EP)

A solution of 1-phenylimidazolium-3-dicyanomethanide 1,3-dipole **114** in acetonitrile was treated with an equimolar amount of MP **43** (Scheme 37). The mixture was stirred at ambient temperature for 48 h. Compound **127** separated from solution as a buff precipitate in 25% yield. The assignment of compound **127** was supported by IR, ^1H NMR and ^{13}C NMR spectroscopy.



Scheme 37

The IR spectrum featured bands corresponding to the NH bond at 3341 cm^{-1} and cyano group at 2198 cm^{-1} . The spectrum also contained a band at 1688 cm^{-1} corresponding to the carbomethoxy group at the C-8 position. The ^1H NMR spectrum (Figure 40) contained doublets at δ 7.17 and 8.16, corresponding to H-2 and H-3, respectively. The signal for H-7 appeared as a singlet at δ 8.01 ppm (Figure 40). The ^{13}C NMR spectrum contained a carbonyl signal at 163.0 ppm and a signal at 143.3 ppm corresponding to C-7. The embedded enediamine unit was also identifiable in the spectrum, with C-8 appearing at 90.3 ppm and C-8a at 141.4 ppm (Figure 40).

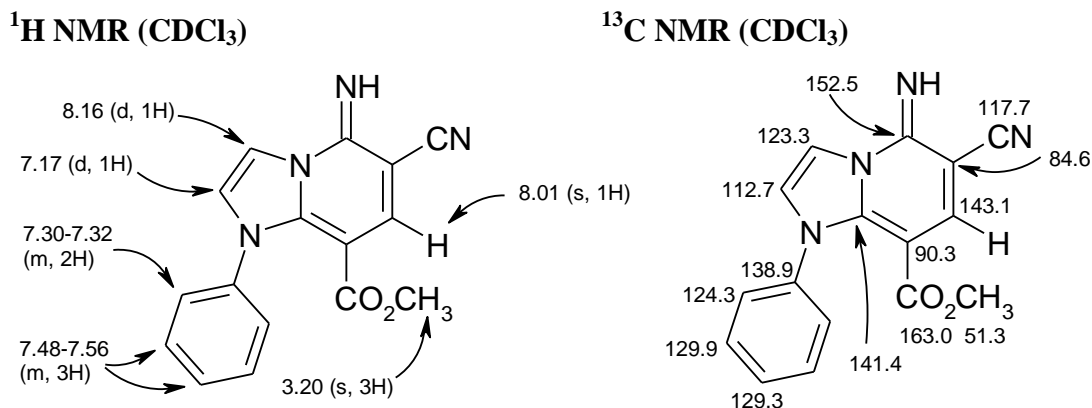


Figure 40: ¹H NMR and ¹³C NMR assignments for compound **127**

A solution of 1-phenylimidazolium-3-dicyanomethanide 1,3-dipole **114** in acetonitrile was treated with ethyl propiolate **118**. The mixture was stirred at ambient temperature for 51 h. Solvent was removed under reduced pressure to yield a dark brown solid, which was recrystallized from ethanol to yield pure **128** in 44% yield.

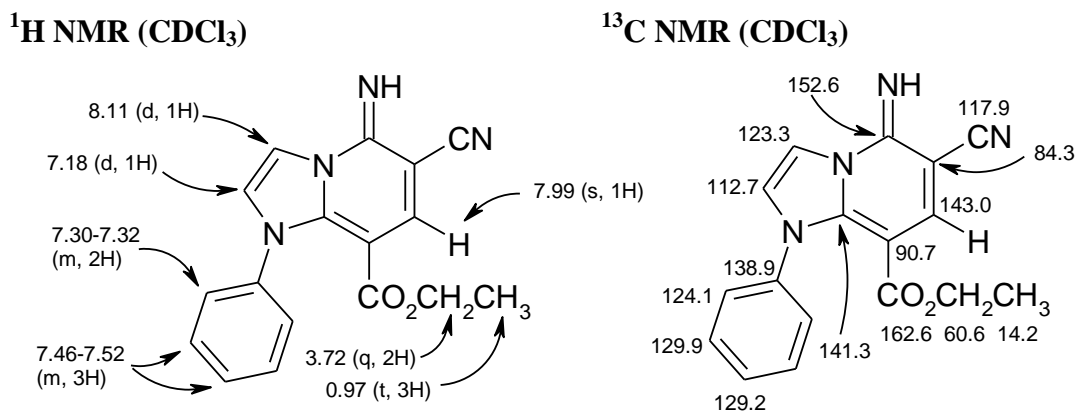


Figure 41: ¹H NMR and ¹³C NMR assignments for compound **128**

The structural assignment of compound **128** was supported by IR, ¹H NMR and ¹³C NMR spectroscopy. The IR spectrum contained the characteristic ring-expanded product bands at 3314 (NH), 2205 (C≡N) and 1622 cm⁻¹ (C=N). The spectrum also displayed a single carbonyl band at 1683 cm⁻¹. The ¹H NMR spectrum (**Figure 41**) possessed a singlet at δ 7.99 corresponding to H-7. Doublets at δ 7.18 and 8.11 corresponded to H-2 and H-3, respectively. NOEDS was used to help determine

these assignments, however again no enhancement was found from the phenyl ring to the imidazole ring protons (**Figure 42**). In the ^{13}C NMR spectrum (**Figure 41**), the carbonyl group appeared at 162.6 ppm, while C-7 was present at 143.0 ppm. The signals for C-8 and C-8a appeared at 90.7 and 141.3 ppm, respectively (**Figure 41**).

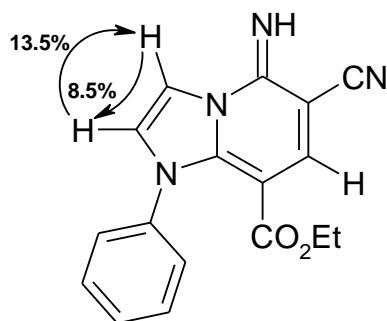


Figure 42: NOEDS enhancements of compound **128** in CDCl_3

IR data, specifically carbonyl stretching frequencies, were again used to help determine the regiochemistry of these reactions (**Table 7**). The ^{13}C NMR spectra of **127** and **128** also contained signals for C-7 that were significantly stronger than the C-8 signals, indicating that a hydrogen atom was attached to C-7. This was confirmed by a DEPT spectrum.

Table 7: Carbonyl stretching frequencies for the products arising from the reactions of 1-phenylimidazolium-3-dicyanomethanide 1,3-dipole **114** with alkyne dipolarophiles

Compound	Dipolarophile	Dipole	IR/ cm^{-1} (νCO)	
			C7	C8
125	DMAD 25	114	1724	1696
127	MP 43	114	-	1688
126	DEAD 116	114	1730	1710
128	EP 118	114	-	1683

The structural assignments of the products arising from unsymmetrical dipolarophiles are also supported by ^1H NMR data (**Table 8**, **Table 9**). The products

derived from the symmetrical dipolarophile DMAD (**30**, **121**, **125**) contain two carbomethoxy groups. The chemical shift of the methoxy group of the ester attached to C-7 would not be expected to vary widely in the ^1H spectra of these compounds. These groups are too far away to be influenced by changes in the imidazole portion of the molecule. Conversely the methoxy group of the ester attached to C-8 would be expected to vary as it is adjacent to the imidazole portion of the cycloadduct. The carboxymethoxy group attached to C-8 is influenced by the nearby methyl, benzyl or phenyl group. As a result the methoxy attached to the ester group on C-8 in **125** is more shielded than the corresponding methoxy in **30** due to shielding from the imidazole substituent. The variation in the methoxy ^1H NMR shifts for the unsymmetrical products **117**, **123** and **127** indicates that this methoxy is part of an ester group attached to C-8 and so is subject to influence from the adjacent imidazole portion of the compound. Similar trends are observed in the ^1H NMR for the CH_2 signals of the ethoxy groups in the products derived from DEAD and EP (**Table 9**).

Table 8: Comparison of methoxy ^1H NMR shifts of cycloadducts derived from the reactions of imidazolium 1,3-dipoles with DMAD and MP

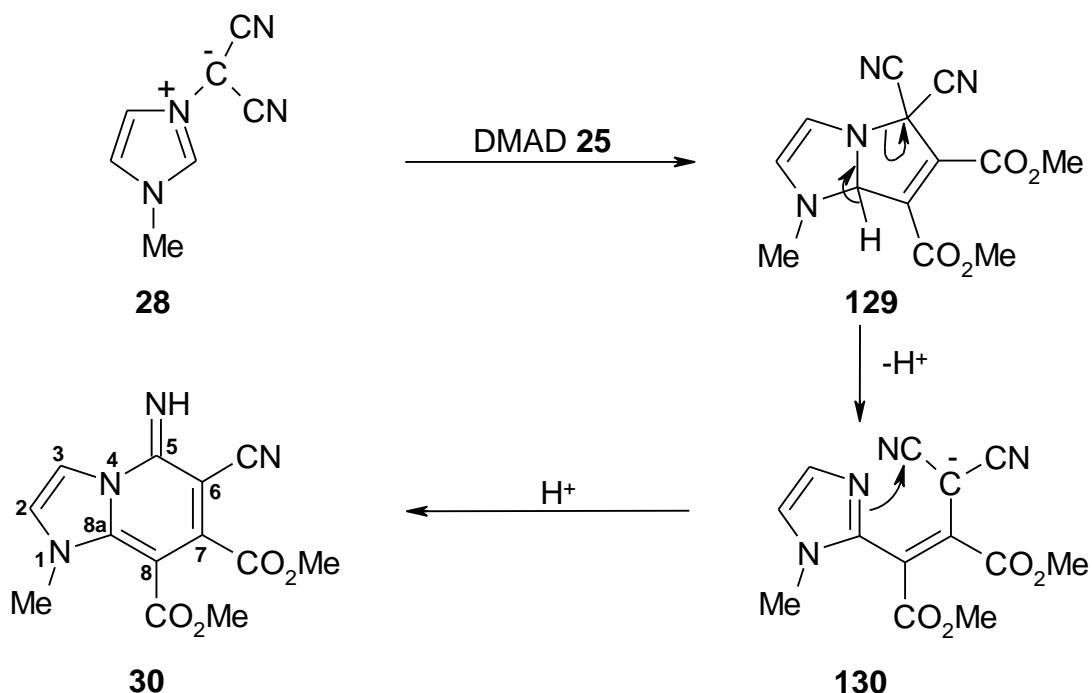
Substituent	Compound	Dipolarophile	Dipole	^1H NMR /ppm (CH_3)	
				C7	C8
Methyl	30	DMAD 25	28	3.96	3.79
Methyl	117	MP 43	28	-	3.83
Benzyl	121	DMAD 25	112	3.91	3.63
Benzyl	123	MP 43	112	-	3.78
Phenyl	125	DMAD 25	114	3.92	2.99
Phenyl	127	MP 43	114	-	3.20

Table 9: Comparison of ethoxy CH₂ ¹H NMR shifts of cycloadducts derived from the reactions of imidazolium 1,3-dipoles with DEAD and EP

Substituent	Compound	Dipolarophile	Dipole	¹ H NMR /ppm (CH ₂)	
				C7	C8
Methyl	119	DEAD 116	28	4.42	4.24
Methyl	120	EP 118	28	-	4.26
Benzyl	122	DEAD 116	112	4.45	4.17
Benzyl	124	EP 118	112	-	4.21
Phenyl	126	DEAD 116	114	4.41	3.51
Phenyl	128	EP 118	114	-	3.72

2.3.7 The rearrangement mechanism as proposed by Boekelheide and Fedoruk

The products derived from the reactions of imidazolium 1,3-dipoles **28**, **112** and **114** with acetylenic dipolarophiles confirm the generality of the Boekelheide-Fedoruk rearrangement. In their 1968 paper, Boekelheide and Fedoruk⁶ proposed a mechanism for the formation of the ring expanded product **30** from the reaction of 1,3-dipole **28** and DMAD **25** (Scheme 38). The mechanism involves the conversion of the initial cycloadduct **129** into an anion intermediate **130** which subsequently rearranges into the ring expanded product **30**. The anion is formed through loss of the bridgehead H-7a proton and cleavage of the N-4/C-5 bond. Attack by the delocalised N-4 anion on a nitrile carbon leads to the ring expanded final product **30**. The proposed rearrangement is therefore an E1cb type process followed by a 6-*exo-dig* ring closure. This mechanism provides a credible explanation for the formation of **30**, but the results of subsequent reactions prompted us to reassess the mechanism.

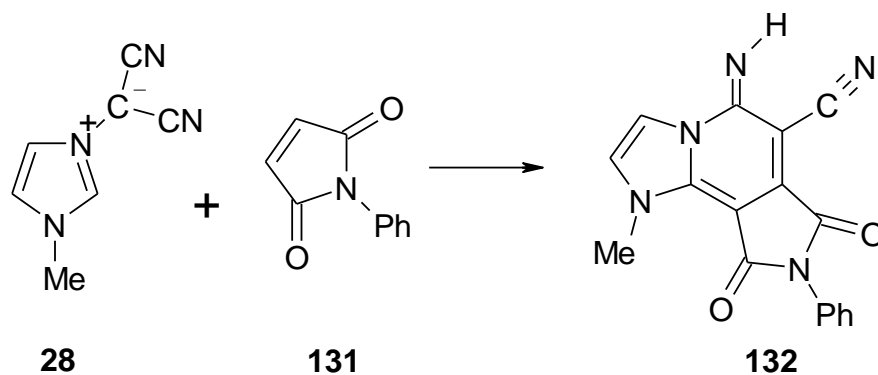


Scheme 38

2.4 Cycloaddition reactions of imidazolium dicyanomethanide 1,3-dipoles with alkene dipolarophiles

2.4.1 Cycloaddition reaction of 1-methylimidazolium-3-dicyanomethanide 1,3-dipole **28** with *N*-phenylmaleimide **131**

In an effort to further probe this interesting ring expansion mechanism, it was decided to investigate the reactions of the imidazolium 1,3-dipoles with alkene dipolarophiles. The reaction of 1-methylimidazolium-3-dicyanomethanide 1,3-dipole **28** with *N*-phenylmaleimide **131** in acetonitrile at ambient temperature yielded compound **132** in 77% yield (**Scheme 39**). The product precipitated from solution after 2 h as a dark orange solid. The structural assignment of compound **132** was supported by IR and 1H and ^{13}C NMR spectra.



Scheme 39

The IR spectrum contained bands characteristic of a ring expanded product. The bands at 3307 (NH), 2209 ($\text{C}\equiv\text{N}$), and 1614 cm^{-1} ($\text{C}=\text{N}$) were similar to those observed in the ring-expanded products derived from the imidazolium 1,3-dipoles and alkyne dipoles. Two amido carbonyl stretching frequencies at 1759 and 1708 cm^{-1} were also observed. The product proved to be very insoluble in organic solvents, and so DMSO-d_6 was used to obtain NMR spectra. The ^1H NMR spectrum (**Figure 43**) featured the N-Me group at δ 4.28, while H-2 and H-3 were present at δ 8.16 and 8.44, respectively. The remaining signals in the spectrum correspond to the aromatic protons of the phenyl ring. The protons due to the maleimide ring were not observed, which is proof that ring expansion has occurred. The highly insoluble nature of the product made obtaining a complete ^{13}C NMR spectrum difficult. Despite extensive efforts one weak signal proved elusive and was not observed. The missing signal is tentatively assigned to C-6, and is expected to be found between 80 ppm and 90 ppm. A signal for the C-6 carbon was observed in the ^{13}C NMR spectra of all other imidazo[2,3-a]pyridine products, though these compounds display superior solubilities in deuterated solvents. The main signals obtained for **132** are shown below (**Figure 43**).

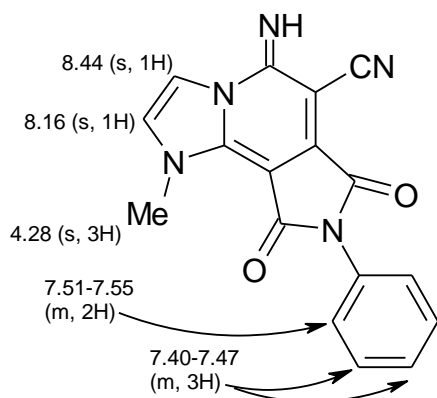
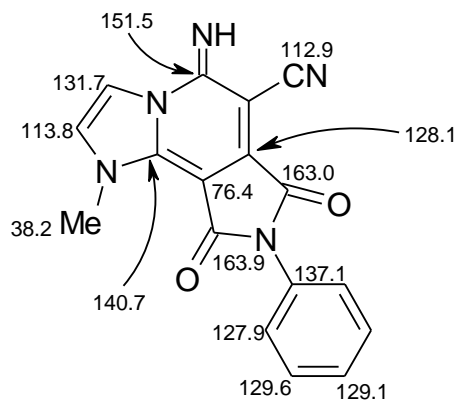
^1H NMR (DMSO- d_6) ^{13}C NMR (DMSO- d_6)

Figure 43: ^1H NMR and ^{13}C NMR assignments for compound **132**

Conclusive proof of the structure of **132** has been obtained from previous work in NUI Galway.⁷³ Exhaustive repetitive recrystallizations of compound **132** from acetonitrile eventually yielded crystals suitable for X-ray analysis. The X-ray structure of the orange plate-like crystals revealed **132** to be a flat molecule with the 5-imino proton *syn* coplanar with the 6-cyano group at a distance of 2.809 Å from the triple bond (**Figure 44**).

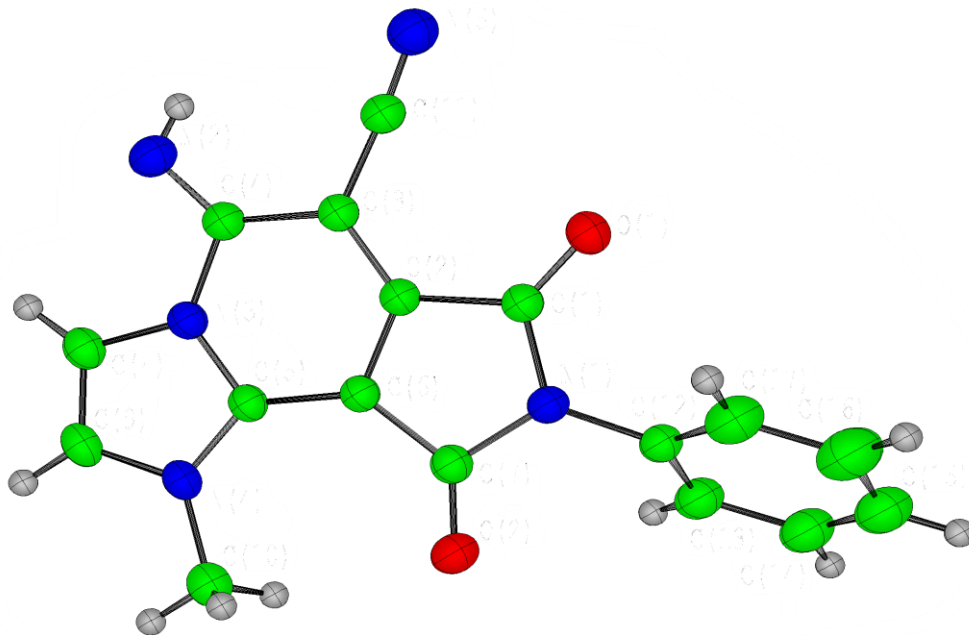
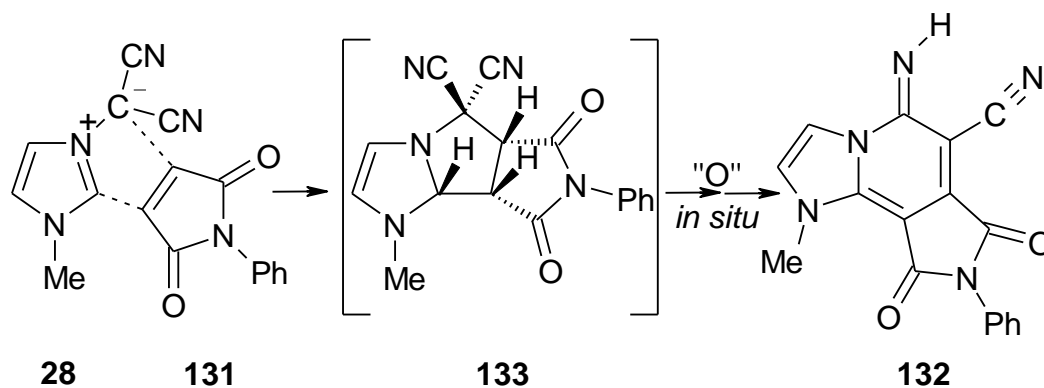


Figure 44: X-Ray crystal structure of compound **132**

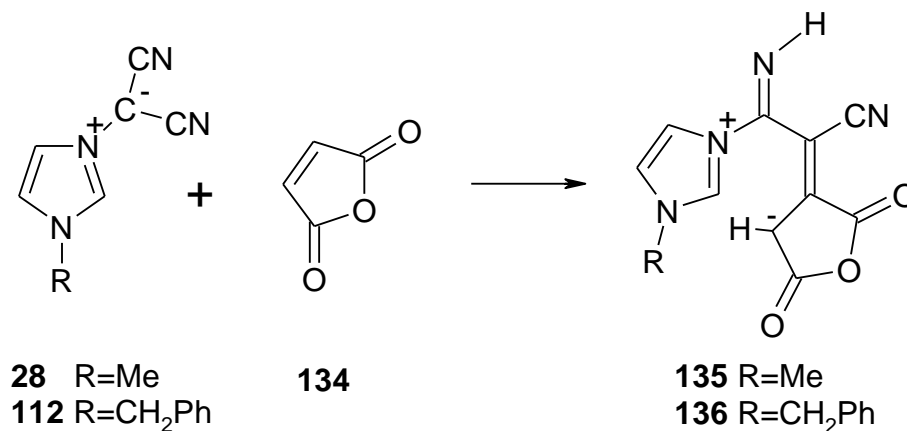
The reaction of 1-methylimidazolium-3-dicyanomethanide 1,3-dipole **28** with *N*-phenylmaleimide **131** therefore parallels the reaction of **28** with alkyne dipolarophiles. The initial cycloadduct formed in both sets of reactions is unstable, and so rearranges to form the ring-expanded product. In this case, the initial cycloadduct **133** is oxidised *in situ*, and so rearrangement occurs, yielding compound **132** (**Scheme 40**). The oxidation may be promoted by air, or by the maleimide present in the reaction mixture. Attempts to exclude air from the reaction by nitrogen purging the system and carrying out the reaction under a steady flow of nitrogen failed to prevent the oxidation, leading to isolation of compound **132** in all cases.⁷³



Scheme 40

2.4.2 Reactions of 1-methylimidazolium-3-dicyanomethanide 1,3-dipole **28** and 1-benzylimidazolium-3-dicyanomethanide 1,3-dipole **112** with maleic anhydride **134**

The reactions of 1-methylimidazolium-3-dicyanomethanide 1,3-dipole **28** and 1-benzylimidazolium-3-dicyanomethanide 1,3-dipole **112** with maleic anhydride **134** yielded altogether different compounds. The products of these reactions, ylides **135** and **136** (Scheme 41), were formed *via* apparent Michael reactions followed by 1,2-rearrangements. Despite the switch from a cycloaddition to Michael type reaction, the Boekelheide-Fedoruk rearrangement still occurred. These reactions therefore provide an interesting new perspective on the rearrangement.



Scheme 41

Compound **135** was formed when a solution of 1-methylimidazolium-3-dicyanomethanide 1,3-dipole **28** in acetonitrile was treated with a slight excess of maleic anhydride **134**, also in acetonitrile (**Scheme 41**). The mixture was stirred at ambient temperature for 3 h. The solvent was then removed under reduced pressure at a temperature below 35 °C. Addition of ether to the residue caused precipitation of the product **135** as a green solid in 70% yield. Evaporation of the ethereal solution led only to isolation of an oily residue from which no product was isolated. The structural assignment of compound **135** was supported by IR, ¹H NMR and ¹³C NMR spectroscopy. Compound **135** was initially stable at ambient temperature, but decomposed on standing to an imidazole containing gum.

The IR spectrum contained characteristic bands at 3330 (N-H) and 2175 cm⁻¹ (C≡N). The two carbonyl groups afforded signals at 1792 and 1734 cm⁻¹. The NMR spectra of the product clearly indicated the presence in the product of the simple intact imidazolium unit, an imine unit bonded to the imidazole N-3 and an altered maleic anhydride unit (**Figure 45**). The ¹H NMR spectrum featured singlets at δ 7.53, 7.58 and 8.84. These signals correspond to the imidazolium ring protons H-2, H-3 and H-5, respectively. A singlet further up field at δ 5.12 has been assigned to the proton attached to the C⁺ carbon of the maleic anhydride moiety. The intact imidazolium ring was also evident in the ¹³C NMR spectrum (**Figure 45**), the ring carbons appearing at 120.7, 123.4 and 136.3 ppm. The spectrum also contained a signal at 149.6 ppm due to the imine carbon and at 118.3 ppm attributable to the carbon of the cyano group. The C⁺ of the maleic anhydride unit was observed at 92.1 ppm. The signal for the C-7 carbon appeared at 59.7 ppm, though it was quite weak and proved to be elusive at first. It was eventually observed by increasing the pulse delay to 5 seconds and scanning the sample in excess of 9000 times.

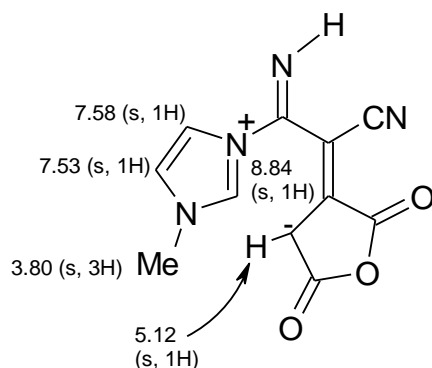
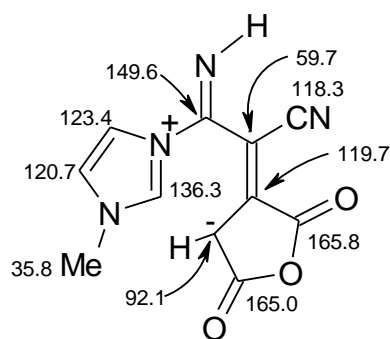
^1H NMR (DMSO- d_6) ^{13}C NMR (DMSO- d_6)

Figure 45: ^1H NMR and ^{13}C NMR assignments for compound **135**

Compound **136** was generated by treating a solution of 1-benzylimidazolium-3-dicyanomethanide 1,3-dipole **112** with maleic anhydride **134** (Scheme 41). The mixture was stirred at 50 °C for 27 h under nitrogen. Evaporation of the solvent under reduced pressure at ambient temperature yielded compound **136** as a sticky brown solid in 86% yield. The structural assignment of compound **136** was supported by ^1H NMR and ^{13}C NMR spectra. The product decomposed on standing to an imidazole containing gum, and so had to be analysed rapidly upon isolation.

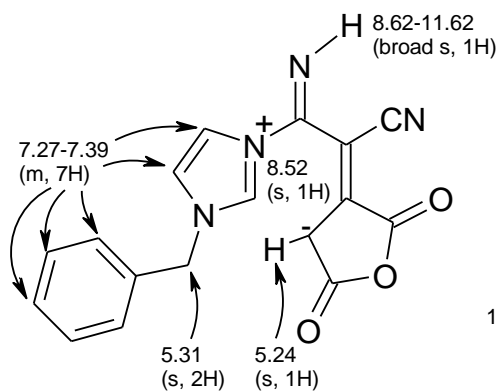
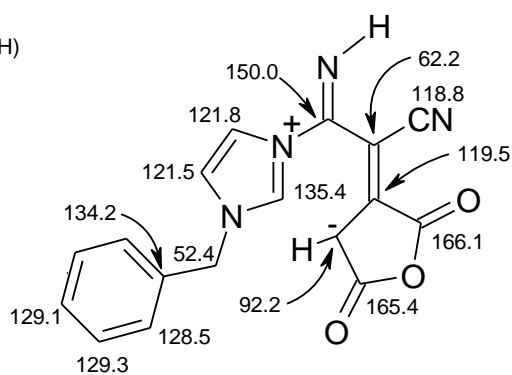
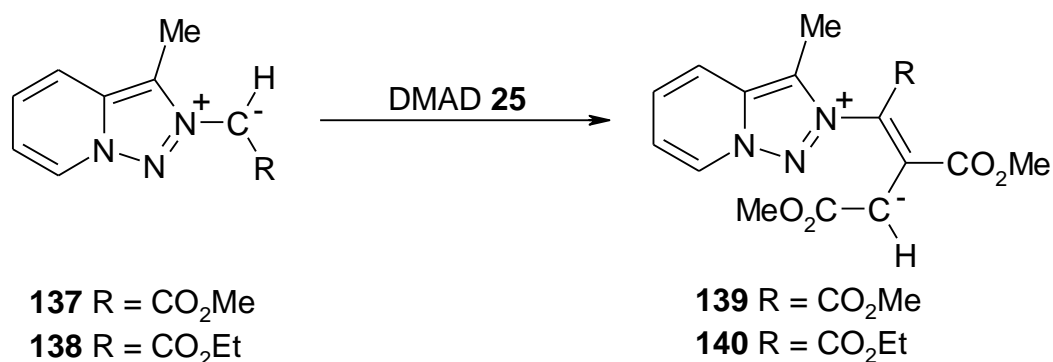
 ^1H NMR (CD_3CN) ^{13}C NMR (CD_3CN)

Figure 46: ^1H NMR and ^{13}C NMR assignments for compound **136**

The ^1H NMR spectrum contained a singlet at δ 8.52 corresponding to imidazolium H-5 (**Figure 46**). The signals for the remaining imidazolium ring protons, H-2 and H-3, were part of a series of multiplets at δ 7.27-7.39 which also included signals for the protons associated with the benzyl group's phenyl ring. The signal at δ 5.24 corresponded to the proton attached to C $^-$ carbon of the maleic anhydride moiety. The ^{13}C NMR spectrum demonstrated the presence of the intact imidazolium ring linked to the altered maleic anhydride unit. The imidazolium ring carbons were present at 121.5 (C-2), 121.8 (C-3) and 135.4 ppm (C-5) (**Figure 46**). The imine carbon appeared at 150.0 ppm and the cyano carbon at 118.8 ppm. The C $^-$ of the maleic anhydride was observed at 92.2 ppm. In keeping with compound **135**, the signal for C-7 was very weak and difficult to detect. However, increasing the pulse delay to 4 seconds and scanning the sample in excess of 12,800 times allowed the signal to be observed at 62.2 ppm.

Structures of this type⁷⁴ have previously been reported in the literature. The ylides **137** and **138** were reacted with DMAD **25** in acetonitrile to yield adducts **139** and **140** respectively (**Scheme 42**). The ^{13}C NMR spectra reported for these ylide products indicate that the C $^-$ carbon appears at 84.5 ppm for **139** and 79.0 ppm for **140**.

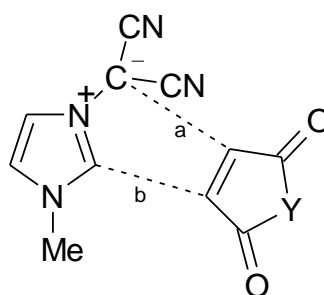


Scheme 42

2.4.3 Reactions of 1-methylimidazolium-3-dicyanomethanide 1,3-dipole **28** with maleic anhydride **134**: theoretical analysis

The unusual nature of the products arising from these reactions prompted us to carry out a theoretical study in collaboration with Professor Luke Burke of Rutgers University at Camden. Calculated transition states for the reactions of 1-methylimidazolium-3-dicyanomethanide 1,3-dipole **28** with maleic anhydride **134**, maleimide and *N*-phenylmaleimide **131** are presented below (**Table 10**).

Table 10: Calculated reaction energies (ΔE_R), activation energies (E_a) and distances



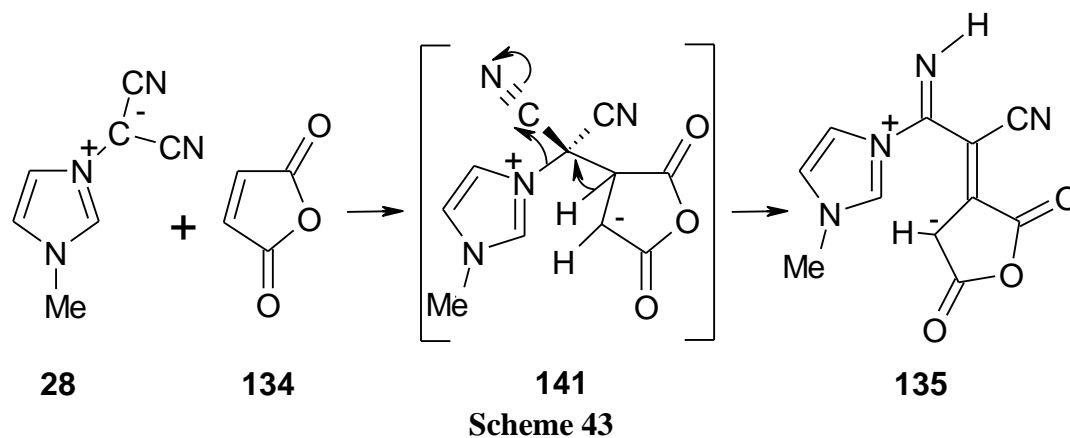
Entry	Y	Cycloaddition Reactions		Cycloadducts		Transition States		
			ΔE_R (kJ mol ⁻¹)	<i>a</i> (Å)	<i>b</i> (Å)	E_a (kJmol ⁻¹)	<i>a</i> (Å)	<i>b</i> (Å)
1	O	<i>endo</i>	-5.94	1.600	1.633	44.60	1.794	2.719
2	O	<i>exo</i>	-5.95	1.603	1.604	57.38	2.050	2.132
3	O	E_{diff}	0.01	-	-	-12.78	-	-
4	O	<i>exo/endo</i>	1.00	-	-	0.01	-	-
5	NH	<i>endo</i>	-18.12	1.596	1.618	52.77	1.914	2.430
6	NH	<i>exo</i>	-25.53	1.597	1.592	54.90	2.194	2.046
7	NH	E_{diff}	6.41	-	-	-2.13	-	-
8	NH	<i>exo/endo</i>	12.02	-	-	0.44	-	-
9	NPh	<i>endo</i>	-17.81	1.598	1.620	49.43	2.122	2.100
10	NPh	<i>exo</i>	-23.00	1.595	1.592	56.89	2.193	2.056
11	NPh	E_{diff}	5.19	-	-	-7.46	-	-
12	NPh	<i>exo/endo</i>	7.48	-	-	0.06	-	-

Compound **132** is the product from the cycloaddition reaction of 1-methylimidazolium-3-dicyanomethanide 1,3-dipole **28** and *N*-phenylmaleimide **131** (**Scheme 40**). Theoretical calculations of the transition state for this reaction indicate

that a normal Huisgen cycloaddition takes place. Both new bonds in the transition state are almost equally developed (a : 2.122 Å, b : 2.100 Å) and the activation energy (E_a) is lower by 7.46 kJmol⁻¹ for *endo* approach of the dipolarophile rather than *exo* (**Table 10, entries 9, 11**).

This contrasts with the transition state calculations for the reaction of 1-methylimidazolium-3-dicyanomethanide 1,3-dipole **28** and maleic anhydride **134**. The activation energy is also lower for the *endo* transition state, but only one new bond is formed in this case (a : 1.794 Å, b : 2.719 Å) (**Table 10, entry 1**). The theoretical calculations indicate that the transition state structure is twisted such that the maleic anhydride unit spirals under the imidazole ring. A normal cycloaddition where both new bonds are well formed would have an activation energy of 12.79 kJ/mol⁻¹ higher and involve an unfavoured *exo* transition state (**Table 10, entry 3**).

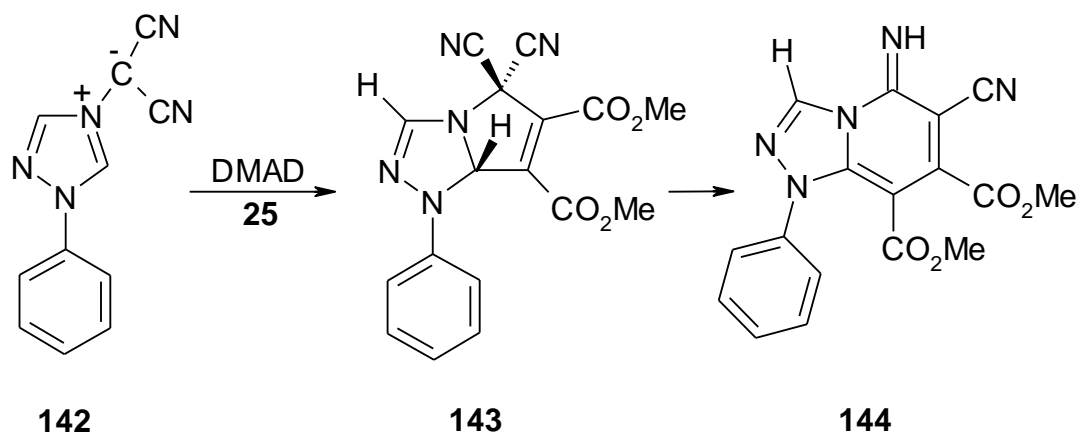
Therefore the theoretical results agree well with experimental observations. Dipole **28** reacts with *N*-phenylmaleimide **131** *via* a Huisgen cycloaddition addition to yield the unstable cycloadduct **133** which ultimately rearranges to yield the ring expanded product **132** (**Scheme 40**). With maleic anhydride **134** the reaction changes to a potentially two step cycloaddition, but the second step fails to complete. Instead a Michael reaction takes place, though once again the initial adduct **141** proves to be unstable. The adduct undergoes a Boekelheide-Fedoruk type rearrangement to give the ylide product **135**. This more stable conjugated product may potentially be formed by a 1,2-shift of the N-C bond and an intermolecular H-shift (**Scheme 43**). The rearrangement could also parallel the Steven's Rearrangement⁷⁵ which involves short lived caged diradicals.



The mechanism proposed by Boekelheide and Fedoruk, however (**Scheme 38**), does not adequately explain the formation of products **135** and **136**. The reaction of maleic anhydride **134** with **28** and **112** indicate that ring expansion is not necessarily part of the Boekelheide-Fedoruk rearrangement. The originally proposed mechanism also involves loss of the imidazole H-5 proton, though this does not occur in the formation of these products. Therefore the unusual ylide product arising from these reactions prompted us to reassess the rearrangement mechanism as originally proposed by Boekelheide and Fedoruk.

2.5 Isolation and study of an initial cycloaddition adduct

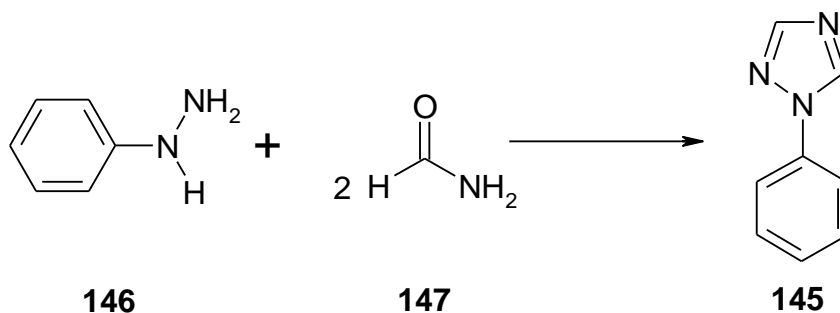
It was felt that NMR spectroscopy could be used to help increase our understanding of the rearrangement process. Central to this approach was the isolation and investigation of an initial cycloadduct. The only initial cycloadduct isolated for this class of reactions to date was discovered by Elguero.³⁵ The reaction of 1-phenyl-1,2,4-triazolium-4-dicyanomethanide 1,3-dipole **142** with DMAD **25** yields a cycloadduct intermediate **143** that can be easily transformed into the ring expanded product **144** with gentle heating (**Scheme 44**). Revisiting this cycloadduct intermediate proved to be crucial to our understanding of the ring expansion reaction.



Scheme 44

2.5.1 Synthesis of 1-phenyl-1,2,4-triazole 145

The compound 1-phenyl-1,2,4-triazole **145** was produced by heating phenylhydrazine **146** in an excess of formamide **147** (Scheme 45). The resulting reaction mixture was then diluted with water and the product extracted with diethyl ether. Column chromatography afforded the product as a white solid in 43% yield, along with recovered starting materials **146** and **147**.



Scheme 45

The structure of **145** was confirmed by IR, ^1H NMR and ^{13}C NMR spectra which were found to be in agreement with those in the literature.⁷⁶⁻⁷⁸

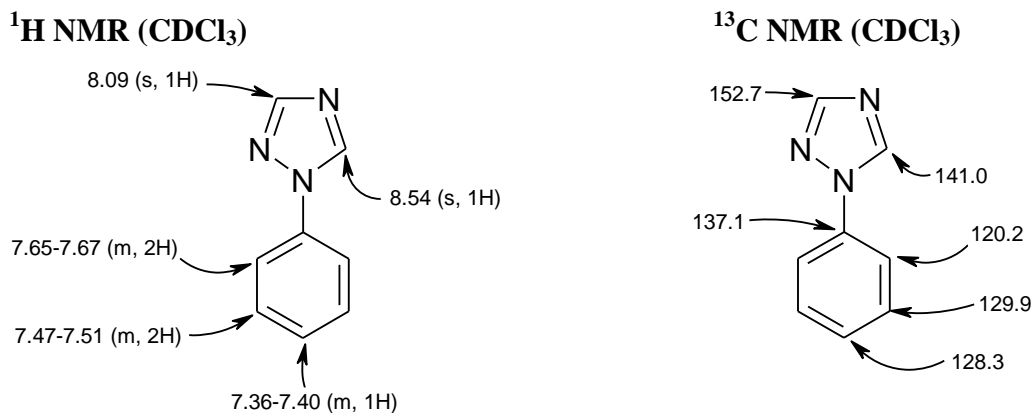
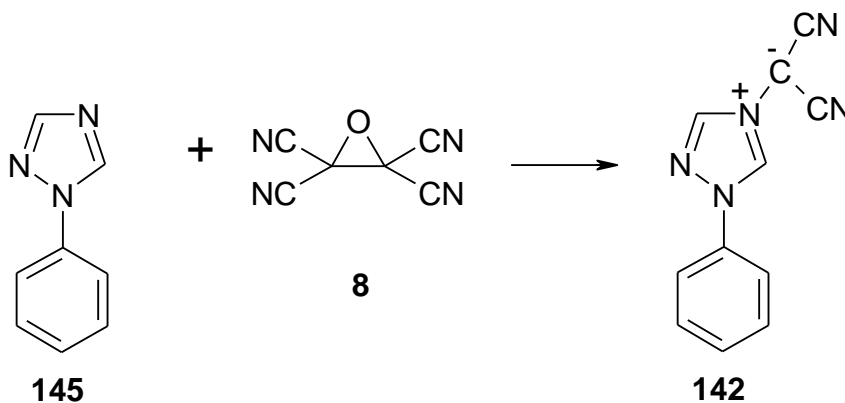


Figure 47: ¹H NMR and ¹³C NMR assignments for compound **145**

2.5.2 Synthesis of 1-phenyl-1,2,4-triazolium-4-dicyanomethanide **142**

The procedure described by Elguero⁷ was used to generate the 1-phenyl-1,2,4-triazolium-4-dicyanomethanide 1,3-dipole **142**. A mixture of 1-phenyl-1,2,4-triazole **145** and TCNEO **8** in ether was stirred at room temperature for 3 days, yielding the ylide in 23% (**Scheme 46**), along with recovered **145**.



Scheme 46

The lower reactivity of **145** towards TCNEO **8**, relative to the imidazole heterocycles, can be explained by its low basic pK_a value of 1.9.⁷ The reactivity of heterocycles towards TCNEO **8** increases with basicity and decreases with steric hindrance. The structure of compound **142** was confirmed by IR, ¹H NMR and ¹³C NMR spectroscopy. Two strong cyano bands at 2128 and 2184 cm⁻¹ were observed in the IR spectrum. In the ¹H NMR spectrum, the proton of C-5 showed the greatest deshielding and appeared at δ 10.86. The two cyano groups are NMR chemical shift

equivalent, and so only one cyano signal at 122.6 ppm appeared in the ^{13}C NMR spectrum. Despite extensive efforts, the methanide carbon signal was not observed in ^{13}C NMR spectrum (**Figure 48**).

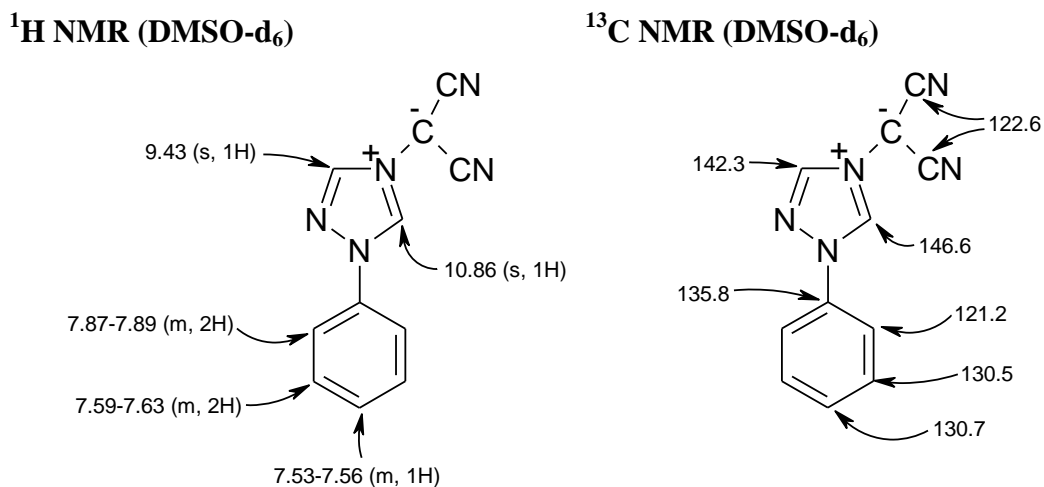


Figure 48: ^1H NMR and ^{13}C NMR assignments for compound **142**

2.5.3 Cycloaddition reaction of 1-phenyl-1,2,4-triazolium-4-dicyanomethanide **142** with DMAD **25**: isolation of the initial cycloadduct **143**

The procedure outlined by Elguero³⁵ was used to isolate the initial cycloadduct **143** formed in the reaction between of 1-phenyl-1,2,4-triazolium-4-dicyanomethanide 1,3-dipole **142** and DMAD **25**. A solution of 1-phenyl-1,2,4-triazolium-4-dicyanomethanide 1,3-dipole **142** in DMF (cooled to 0 °C) was treated with DMAD **25** and allowed to stand at 0 °C for 4.5 h. The resulting mixture was filtered through a cooled funnel, and the filtrate added to ice-cold water. The resulting brown precipitate was collected on a jacketed sintered glass funnel at -5 °C and washed with cooled ethanol and diethyl ether. The crude cycloadduct product **143** was isolated as a brown solid in 71% yield. The assignment of compound **143** was supported by ^1H and ^{13}C NMR spectra.

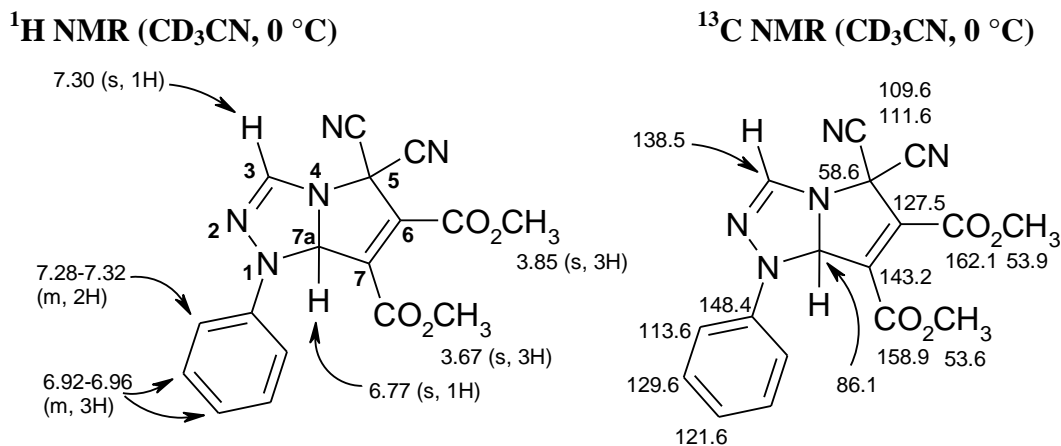


Figure 49: ^1H NMR and ^{13}C NMR assignments for compound **143**

The ^1H and ^{13}C NMR spectra of the initial cycloadduct were measured at $0\text{ }^\circ\text{C}$ due to the ease with which the ring expansion rearrangement occurs in solution. The compound could not be purified further following isolation due to its propensity for rearrangement. CD_3CN was used in NMR experiments rather than CDCl_3 as in the original Elguero study. However, the ^1H NMR spectrum closely matched that previously reported. The ^1H contained four singlet signals corresponding to the two methyl groups (δ 3.85 and 3.66), the H-3 proton (δ 7.30) and the H-7a proton (δ 6.77) (**Figure 49**).

Our ^{13}C NMR spectrum benefited from the availability of a higher field NMR spectrophotometer than that used by Elguero in the early 1980s and so weaker signals not previously found were observed. Thus all carbons were accounted for in our ^{13}C NMR spectrum. Separate signals were observed for both cyano groups (111.6 ppm and 109.6 ppm) and the C-5 carbon was detected at 58.6 ppm (**Figure 49**). We also observed the bridgehead carbon C-7a at 86.1 ppm which had not previously been reported. Slightly different shifts were observed for the phenyl ring carbons, but the ^{13}C NMR spectra were in agreement with one another, and the structure originally proposed by Elguero is confirmed to be correct, namely the only reported un-rearranged cycloadduct from an azolium dicyanomethanide 1,3-dipole.

Further support of the structure was provided by theoretical calculations carried out in collaboration with Professor Luke Burke of Rutgers University. A set of predicted NMR shifts for the ^1H and ^{13}C NMR spectra of the initial cycloadduct was found to be in good agreement with both our own (**Figure 49**) and Elguero's experimentally observed values (**Figure 50**).

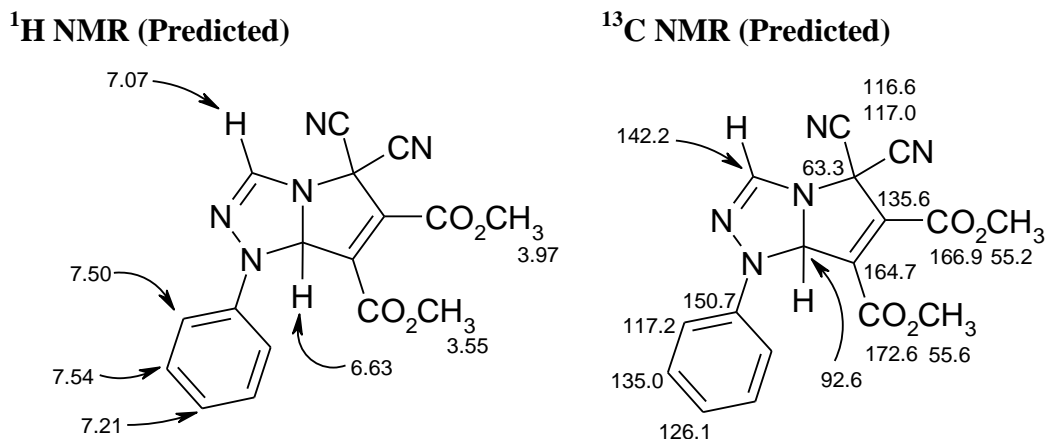


Figure 50: Predicted ^1H NMR and ^{13}C NMR assignments for **143** (See **Figure 49**)

Therefore, in contrast with the reactions of the imidazolium 1,3-dipoles, the reaction of 1-phenyl-1,2,4-triazolium-4-dicyanomethanide 1,3-dipole **142** with DMAD **25** leads to the isolation of the initial cycloadduct **143**. Studying the rearrangement of this compound was critical to our understanding of the rearrangement mechanism.

2.5.4 Cycloaddition reaction of 1-phenyl-1,2,4-triazolium-4-dicyanomethanide **142** with DMAD **25**: generation of the ring expanded product **144**

The initial cycloadduct **143** is unstable, and rearranges in solution to the ring expanded product **144** (**Scheme 44**). This rearrangement occurs readily at room temperature. In order to ensure full conversion to the desired ring expanded product, a solution of **143** in acetonitrile was stirred at 50 °C for 2 h and then ambient temperature for a further 50 h to ensure full conversion. Removal of the solvent

under reduced pressure yielded the ring expanded product **144** as a yellow crystalline solid in 80% yield.

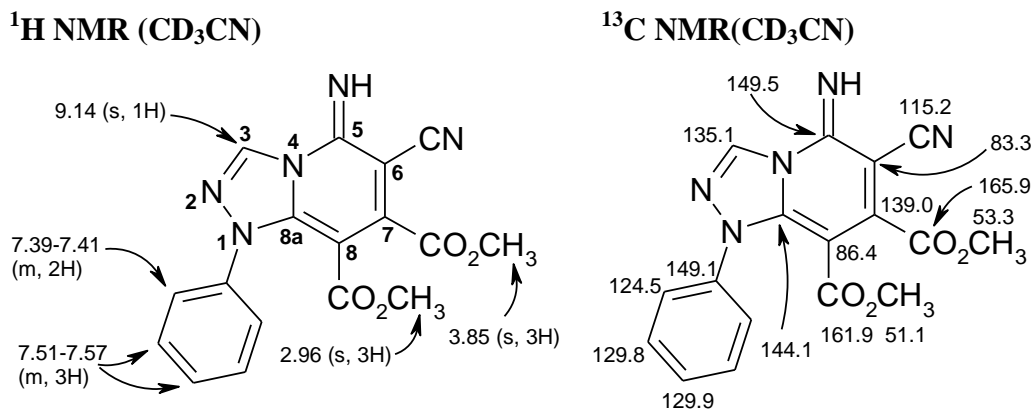


Figure 51: ^1H NMR and ^{13}C NMR assignments for compound **144**

The assignment of compound **144** was supported by IR, ^1H NMR and ^{13}C NMR spectroscopy. The IR spectrum displayed the characteristic ring-expanded product bands at 3316 (NH), 2204 ($\text{C}\equiv\text{N}$) and 1624 cm^{-1} ($\text{C}=\text{N}$). The ^1H NMR spectrum contained three singlets corresponding to H-3 and the two carboxymethyl groups (**Figure 51**). The carboxymethyl group attached to C-8 is considerably more shielded (δ 2.96 ppm) than that associated with C-7 (δ 3.85). This is potentially due to shielding effects of the phenyl ring, similar to those observed in the products from the reactions of 1-phenylimidazolium-3-dicyanomethanide 1,3-dipole **114** and alkyne dipolarophiles. Another point to note is that H-3 and the phenyl ring protons are all deshielded relative to the initial cycloadduct **143**, probably due to aromatisation of the core fused ring system.

The ^{13}C NMR spectrum features the embedded enediamine unit indicative of ring expansion (**Figure 51**). The enamine α -carbon C-8a is highly deshielded and appears at 144.1 ppm. Conversely C-8 the β -carbon is extremely shielded and appears at 86.4 ppm. This is in contrast with the initial cycloadduct **143** where C-7 (143.2 ppm) was far more deshielded than the bridgehead carbon C-7a (86.1 ppm). As was observed

in the ^1H NMR spectrum, the phenyl ring carbons were found to have shifted downfield relative to the initial cycloadduct **143**.

Both the IR and ^1H NMR spectra agreed well with those previously reported by Elguero for compound **144**.³⁵ However ^{13}C NMR data for **144** was not reported in the original study, preventing us from making a direct comparison. The ^1H and ^{13}C NMR spectra acquired for **144** do agree well with the predicted spectra developed in conjunction with Professor Luke Burke (**Figure 52**).

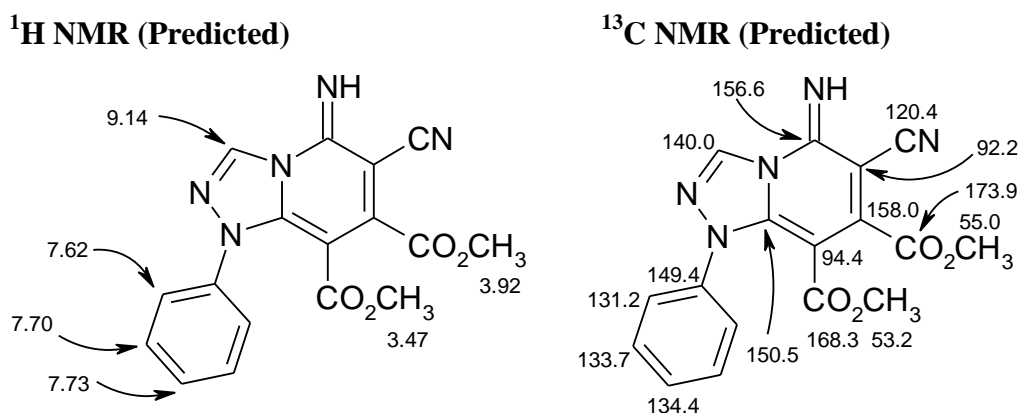


Figure 52: Predicted ^1H NMR and ^{13}C NMR assignments for compound **144**

Hence the reaction of 1-phenyl-1,2,4-triazolium-4-dicyanomethanide 1,3-dipole **142** with DMAD **25** initially generates the direct cycloadduct **143** which is converted quite easily to the ring expanded product **144**. This system is therefore ideally suited to investigating the mechanism of this intriguing rearrangement.

2.5.5 Cycloaddition reaction of 1-phenyl-1,2,4-triazolium-4-dicyanomethanide **142** with DMAD **25**: investigation of the ring expansion rearrangement by NMR spectroscopy

Having isolated and confirmed the structures of both the initial cycloadduct **143** and ring expanded product **144**, our efforts turned to investigating the rearrangement mechanism. A sample of cycloadduct **143** was dissolved in CD_3CN at $0\text{ }^\circ\text{C}$ and the ^1H NMR spectrum recorded. The sample was kept cold in the NMR spectrometer

chamber using liquid nitrogen. The sample temperature was then raised to typical probe temperature (19 +/- 1 °C) and ¹H NMR spectra measured at 30 min intervals over 16 h. Unsurprisingly, over this period the signals of the initial cycloadduct **143** were seen to decline, while those of the ring expanded product **144** grew. At the end of the experiment all traces of compound **143** were gone, and only compound **144** was present in the sample.

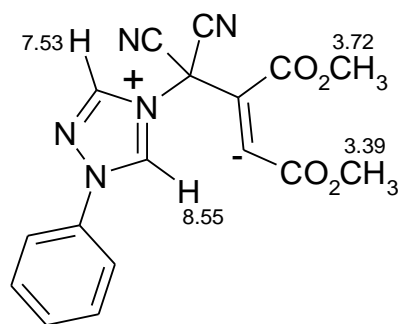
The ¹H NMR spectra also revealed the presence of an intermediate **148** which was seen to develop once the solution had been raised to probe temperature (**Figure 54, 55**). The intermediate displayed four simple singlet signals. Two carboxymethyl groups were identified at δ 3.39 and 3.72. Signals corresponding to the two triazole ring protons were initially observed at δ 7.53 and 8.55. The signal at δ 8.55 was found to drift upfield during the course of the experiment. The signal at δ 7.53 became impossible to track over the course of the rearrangement due to its overlap with developing aromatic protons.

Shortly after this intermediate appeared signals characteristic of the ring expanded product **144** were observed. After about 6 h the intermediate reached its maximum concentration. At this point the initial cycloadduct, the intermediate and the ring expanded product were all present in similar concentrations. As the experiment progressed the ring expanded product began to dominate, and finally full conversion to **144** was observed.

In the 30 min intervals between ¹H NMR scans, ¹³C NMR spectra were collected. Due to the large number of close and overlapping signals, assignments based on these spectra are tenuous. However, a number of signals we believe to be associated with the intermediate **148** were observed (**Figure 53**). The two methyl groups appeared at 52.1 ppm and 52.3 ppm while the triazole ring carbons appeared at 137.5 ppm and 138.0 ppm.

We believe that the structure of this intermediate is an azolium ylide type structure that may be similar to that of compounds **135** and **136**, formed in the separate reactions between 1-methylimidazolium-3-dicyanomethanide 1,3-dipole **28** and 1-benzylimidazolium-3-dicyanomethanide 1,3-dipole **112** and maleic anhydride **134** (**Scheme 41**). The ylide **148** contains resonance-stabilised termini, an intact triazole ring and two carboxymethyl groups (**Scheme 47, Figures 54, 55**).

^1H NMR (CD_3CN)



^{13}C NMR (CD_3CN)

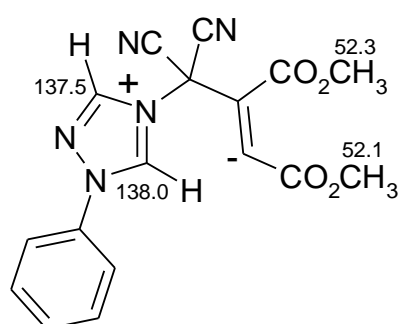
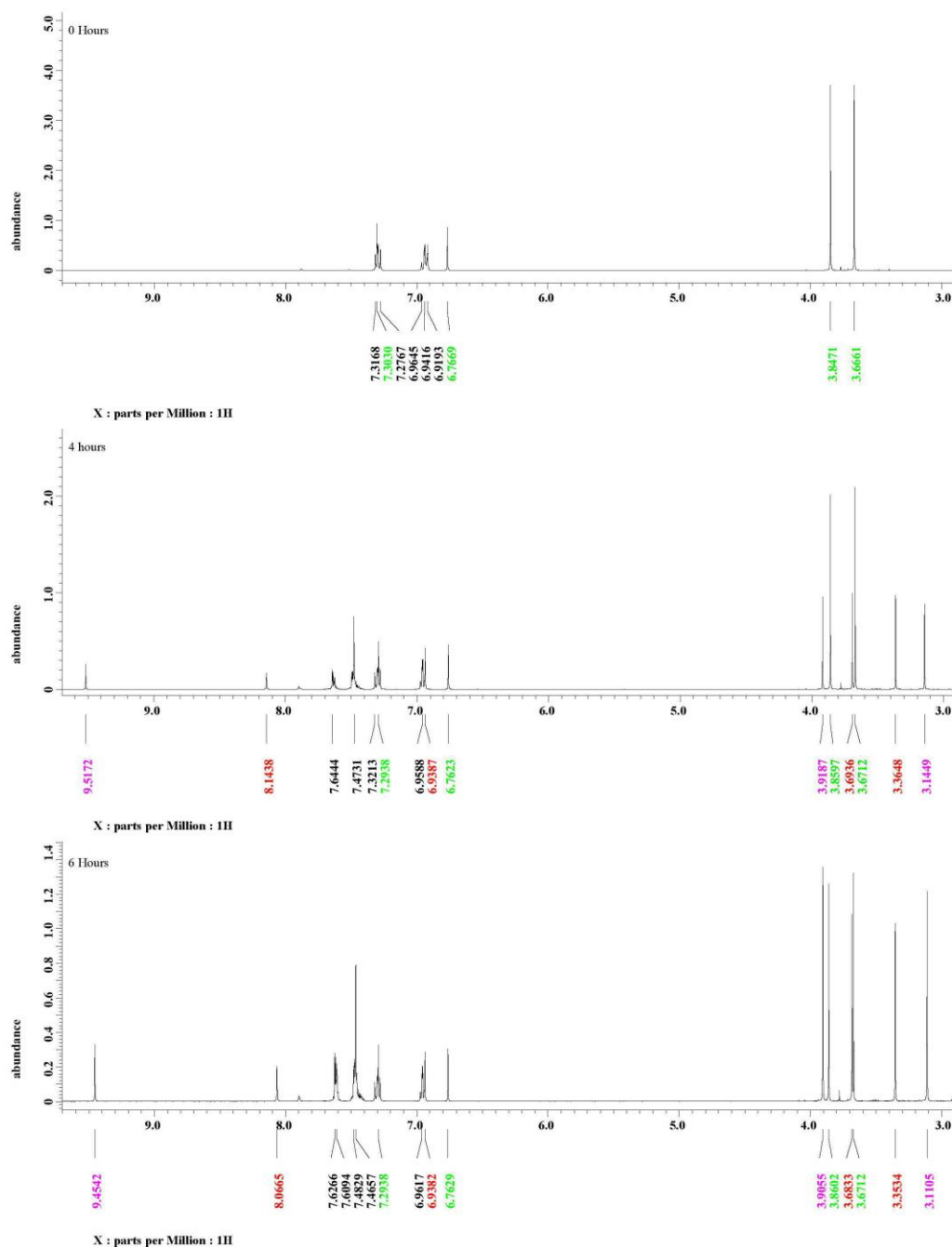


Figure 53: ^1H NMR and ^{13}C NMR assignments for possible intermediate **148**

Chapter 2



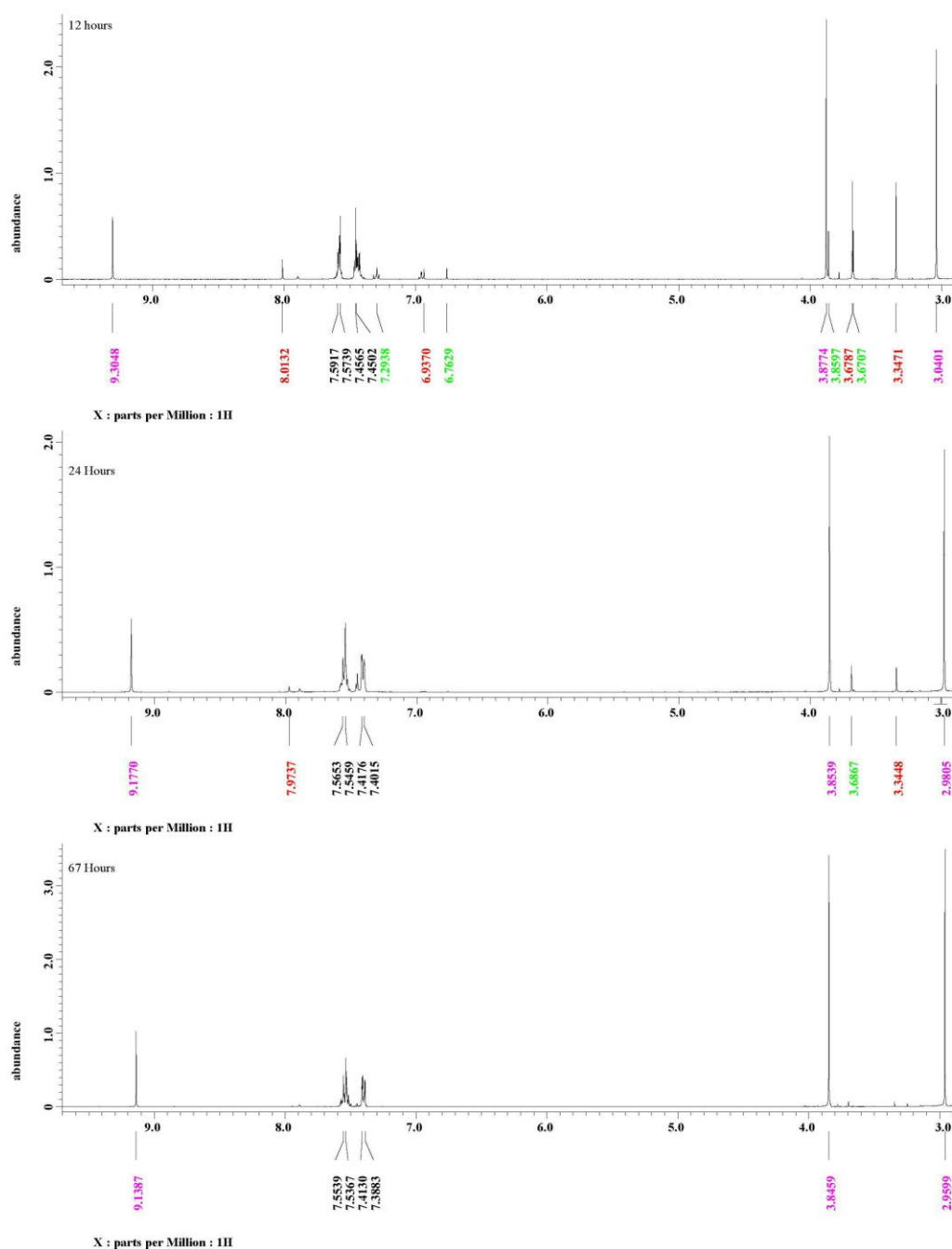
Note 1: Key signals for initial cycloadduct **143** highlighted in green

Note 2: Key signals for intermediate **148** highlighted in red

Note 3: Key signals for ring-expanded product **144** highlighted in pink

Figure 54: ¹H NMR spectra of conversion of **143** to **144** via **148**- 0, 4 and 6 h

Chapter 2



Note 1: Key signals for initial cycloadduct **143** highlighted in green

Note 2: Key signals for intermediate **148** highlighted in red

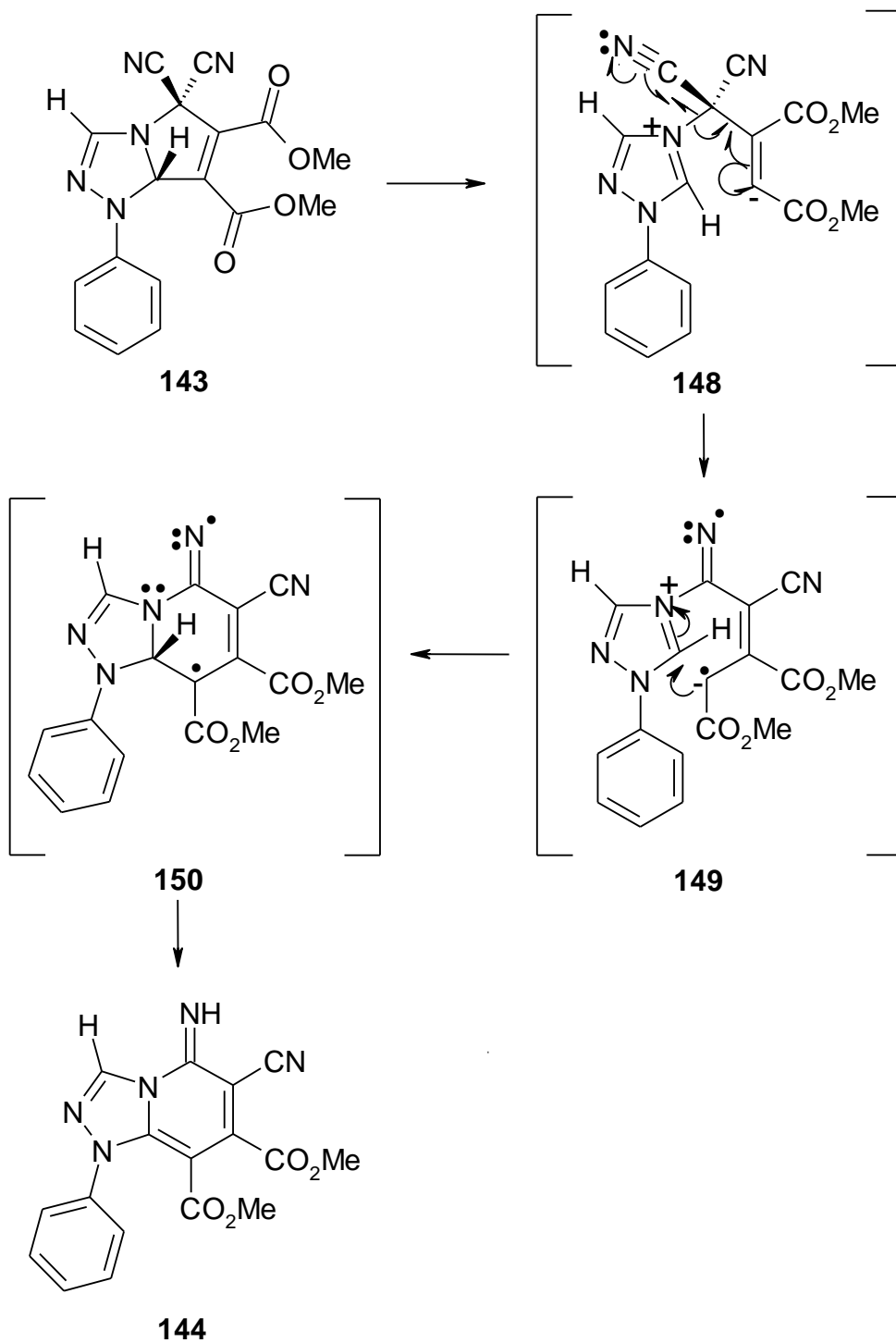
Note 3: Key signals for ring-expanded product **144** highlighted in pink

Figure 55: ¹H NMR spectra for conversion of **143** to **144** via **148**- 12, 24 and 67 h

2.5.6 Mechanism of the rearrangement

Our study of the reactions of the Boekelheide-Fedoruk rearrangement leads us to believe that the originally proposed mechanism does not capture the full complexity of the rearrangement. This is apparent from the ylide products **135** and **136** which are formed *via* Boekelheide-Fedoruk rearrangement of an initial Michael adduct (**Scheme 41**). This rearrangement occurs without ring expansion or loss of the imidazole H-4 proton. The mechanism as proposed by Boekelheide and Fedoruk requires that both these events take place. The transformation of **143** into **144** may proceed *via* an intermediate **148** that possesses a similar structure to the ylides **135** and **136**.

The presence of the two triazole ring protons suggests that the intermediate may have been formed by ring opening of the C(7)-C(7a) bond. In parallel with the formation of **135** and **136** this may undergo 1,2-rearrangement to the ylide diradical **149** which then ring closes (RORC) to form **150** which aromatises to form the ring expanded product **144** (**Scheme 47**).



Scheme 47

2.6 Conclusion

We have investigated the reactions of imidazolium dicyanomethanide 1,3-dipoles with a variety of electron poor alkyne and alkene dipolarophiles. These reactions generate unstable initial cycloadducts that rearrange *in situ* to form the isolated ring-expanded products. We refer to this conversion of the initial cycloadduct to the ring-expanded product as the Boekelheide-Fedoruk rearrangement.

A series of ring-expanded compounds was synthesized by reacting the imidazolium dicyanomethanide 1,3-dipoles with both symmetrical and unsymmetrical dipolarophiles. The regiochemistry observed in these reactions is that whereby the unsubstituted terminus of the dipolarophile is attached to the dicyanomethanide terminus of the 1,3-dipole.

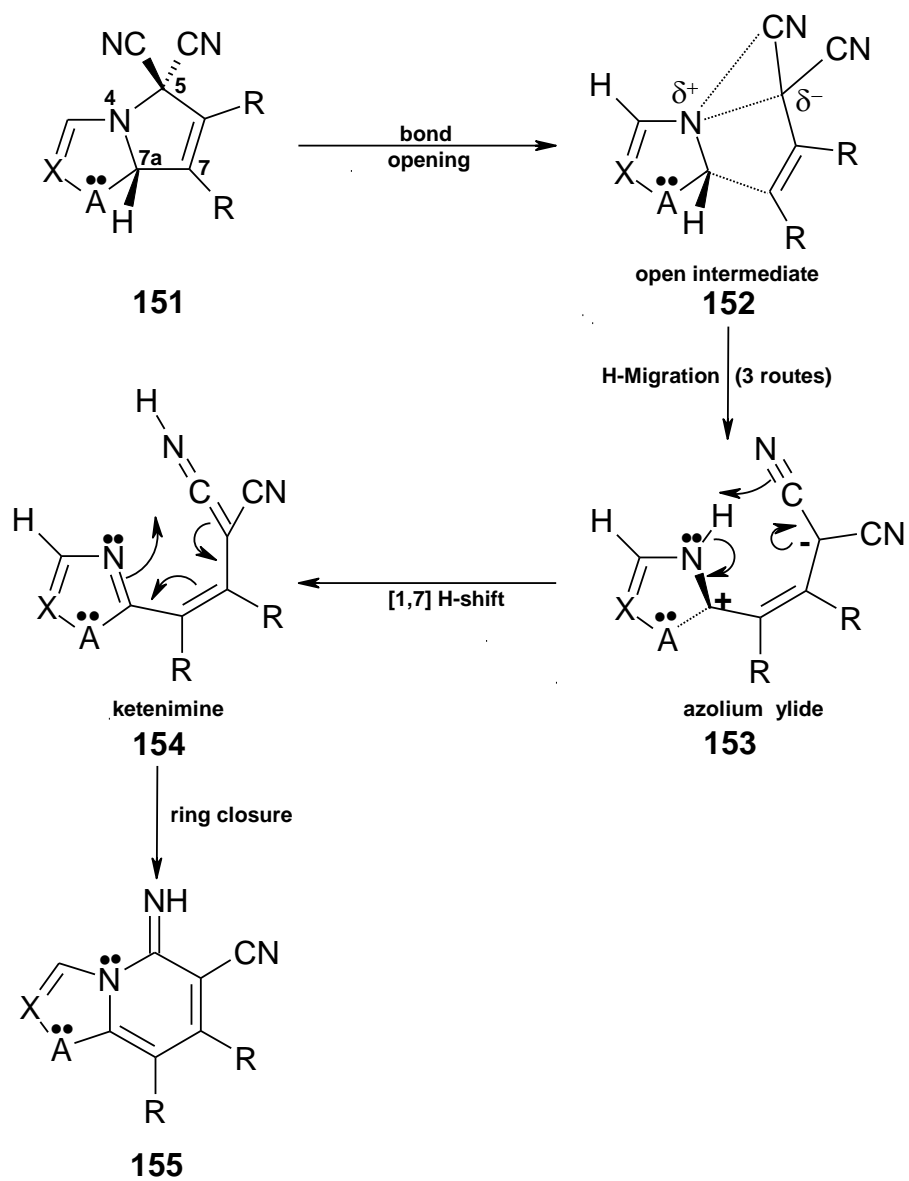
The reactions of the imidazolium dicyanomethanide 1,3-dipoles with alkene dipolarophiles also produced unstable intermediates that rearranged to generate the final product. The reaction of the 1-methylimidazolium-3-dicyanomethanide 1,3-dipole **28** with *N*-phenylmaleimide **131** provided a ring-expanded compound similar to the products formed by the reactions of the imidazolium dicyanomethanide 1,3-dipoles with alkyne dipolarophiles. However the reactions of imidazolium dicyanomethanide 1,3-dipoles with maleic anhydride **134** gave a new ylide product. The reaction proceeded *via* Michael Addition to form an unstable intermediate that underwent 1,2-rearrangement to form the novel ylide product.

The rearrangement mechanism was further probed using low temperature NMR spectroscopy to follow the conversion of an unstable, but isolatable, initial cycloadduct from a 1,2,4-triazole-4-dicyanomethanide to the final ring-expanded product. Combined with theoretical calculations, these experiments provide an interesting new perspective on the Boekelheide-Fedoruk rearrangement and reopen the question of its mechanism.

2.7 Postscript

Following completion of the work herein, a paper on it was published. During the intervening years, an in-depth computational study⁷⁹ of remaining questions concerning the rearrangement was carried out by Professors L.A. Burke and R.N. Butler. This study further highlighted the overall complexity of the reaction. The mechanism of the rearrangement of the cycloadduct is now considered to involve (i) opening of the N4-C5 bond in the cycloadduct; (ii) H-migration from imidazole C7a to N4 giving an azolium ylide intermediate; (iii) a 1,7-H-shift to give a ketenimine intermediate; (iv) ring closure to give the aromatic fused 5,6 ring structure (**Scheme 48**).

Computed NMR shifts as well as energies of intermediates and transitions states suggest that the transient intermediate detected herein for the 1,2,4-triazole case was the azolium ylide species **153** rather than the azolium ylide **148**. Ring opening of the C7-C7a bond did not prove to be thermodynamically viable once it was formed.



Scheme 48

2.8 Experimental

Melting points were measured on an Electrothermal apparatus. IR spectra were measured on a Perkin-Elmer Spectrum 1000 spectrophotometer. Microanalyses were measured on a Perkin-Elmer Model 240 CHN analyser. NMR spectra were measured on a JEOL GXFT 400 instrument with tetramethylsilane as an internal reference. Deuteriochloroform, hexadeuteriomethyl sulphoxide and acetonitrile-d₃ were used as solvents. ¹H NMR assignments were supported by selective proton decoupling and COSY spectra. *J* values are given in Hz. ¹³C NMR assignments were supported by DEPT spectra. Assignments of stereochemistry were determined by NOEDS. Solvents were purified according to literature procedures⁸⁰. Acetonitrile was HPLC grade and was used without purification.

Chemicals were purchased as follows:

Sigma-Aldrich: DMSO-d₆, acetonitrile-d₃, tetracyanoethylene, hydrogen peroxide (30%), formamide, phenylhydrazine, *N*-methylimidazole, *N*-benzylimidazole, *N*-phenylimidazole, DMAD, DEAD, methyl propiolate, ethyl propiolate, *N*-phenylmaleimide.

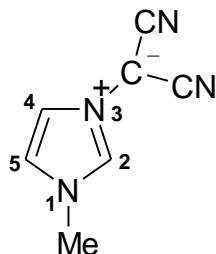
Lancaster: maleic anhydride.

Fluorochem: chloroform-d₁

Chapter 2

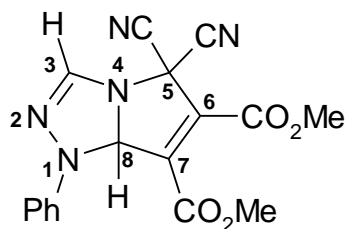
The numbering and naming system below is used in this chapter and has been accepted for publication.

1.3-Dipoles

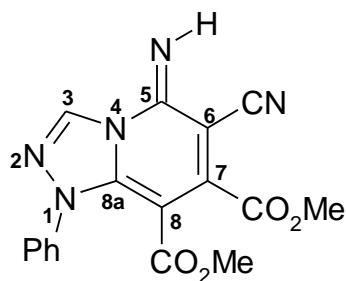


1-methylimidazolium-3-dicyanomethanide 1,3-dipole **28**

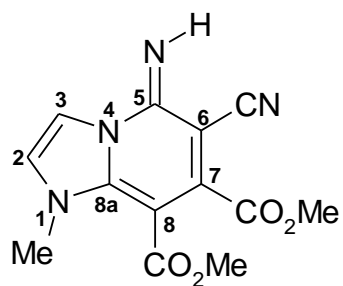
Cycloadducts



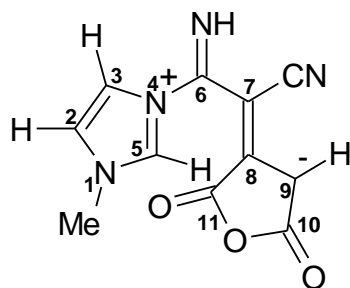
1-phenyl-5,5-dicyano-6,7-dimethoxycarbonyl-5,8-dihydropyrrolo[1,2-*d*]1,2,4-triazole **143**



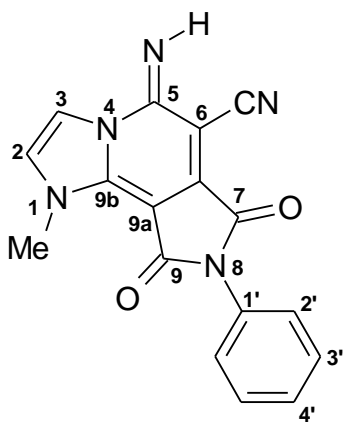
1-phenyl-5-imino-6-cyano-7,8-dimethoxycarbonyl-1,2,4-triazolo[4,5-*a*]pyridine **144**



1-methyl-5-imino-6-cyano-7,8-dimethoxycarbonyl imidazo[2,3-*a*]pyridine **30**



imidazolium ylide **135**



1-methyl-5-imino-6-cyano-7,9-(dicarboxy-*N*-phenylimido) imidazo[2,3-*a*]pyridine
132

Synthesis of tetracyanoethylene oxide **8**

A solution of tetracyanoethylene (3.00 g, 23 mmol) in acetonitrile (22 cm³) was cooled to -5 °C in an acetone-ice bath. Hydrogen peroxide (30%) (2.66 cm³, 23 mmol) was added drop-wise at such a rate that the temperature of the reaction remained between 10-12 °C. When addition was complete, the reaction mixture was stirred for a further 5 min and then diluted with ice cold water (150 cm³). The precipitated solid was collected by filtration and washed with water. The solid was left to dry on a suction pump for 1 h and then used immediately. The product was obtained as a white solid (2.53 g, 75%), mp 177-179 °C (sealed tube) (Lit.⁴, mp 177-178 °C); (Found C, 50.0; N, 38.7. C₆N₄O requires C, 50.0; N, 38.9%).

CAUTION: Both TCNE and TCNEO evolve hydrogen cyanide when exposed to water. All operations must be carried out in a fume hood.

Synthesis of 1-phenyl-1,2,4-triazole **145**

Phenylhydrazine (10.80 g, 9.83 cm³, 0.10 mol) in formamide (45 g, 40 cm³, 1.00 mol) was heated for 8 h at 160-170 °C. The resulting reaction mixture was added to 100 cm³ of water, and extracted using 5 x 100 cm³ portions of diethyl ether. The mixture was concentrated to an oil under vacuum, then placed neat on a flash column of silica (230-400 mesh ASTM), made up in dichloromethane. The column was eluted with dichloromethane and diethyl ether in the gradient 1:0 to 95:5 to give the product **145** as an oil which solidified to an off-white solid on cooling in ice. Compound **145**: (6.25 g, 43%), mp 41-43 °C (ethanol) (Lit.,^{77, 81} mp 46-47 °C); (Found C, 66.3; N, 5.0; H, 28.6. C₈H₇N₃ requires C, 66.2; H, 4.85; H, 28.95%); $\nu_{\max}/\text{cm}^{-1}$ 638, 790 (Ph); δ_{H} (CDCl₃) 7.36-7.40 (m, 1H, H-4'), 7.47-7.51 (m, 2H, H-3'), 7.65-7.67 (m, 2H, H-2'), 8.09 (s, 1H, H-3), 8.54 (s, 1H, H-5); δ_{C} (CDCl₃) 120.2 (C-2'), 128.3 (C-4'), 129.9 (C-3'), 137.1 (C-1'), 141.0 (C-5), 152.7 (C-3). δ_{H} (DMSO-d₆) 7.37-7.40 (m, 1H, H-4'), 7.51-7.55 (m, 2H, H-3'), 7.82-7.84 (m, 2H, H-2'), 8.21 (s, 1H, H-3), 9.27 (s, 1H, H-5); δ_{C} (DMSO-d₆) 119.9 (C-2'), 128.3 (C-4'), 130.3 (C-3'), 137.3 (C-1'), 142.8 (C-5), 153.0 (C-3).

Preparation of dicyanomethanide 1,3-dipoles

Synthesis of 1-methylimidazolium-3-dicyanomethanide 1,3-dipole **28**

To a solution of tetracyanoethylene oxide (1.74 g, 12.10 mmol) in ethyl acetate (15 cm³) at 0 °C, 1-methylimidazole (0.96 cm³, 12.10 mmol), also in ethyl acetate (3 cm³), was added drop-wise with stirring such that the reaction temperature remained below 10 °C. When the addition was complete a pale brown solid separated from the solution. The product **28** (1.15 g, 65%), mp 143-144 °C (from ethanol using Norit) (Lit.,⁶ mp 143-144 °C); was filtered off and washed with cold ethyl acetate. The filtrate rapidly turned dark brown. Attempts to isolate more product or starting material from the filtrate by removing the solvent under reduced pressure led to a brown sticky residue due to decomposition of TCNEO. Compound **28**: (Found: C, 57.45; H, 3.95; N, 38.2. C₇H₆N₄ requires C, 57.55; H, 4.1; N, 38.35%); $\nu_{\max}/\text{cm}^{-1}$ 2180 cm⁻¹ and 2134 cm⁻¹ (C≡N); δ_{H} NMR (DMSO-d₆): 3.75 (s, 3H, CH₃), 7.60 (dd, 2H, *J* 1.6, 1.9, H-4), 7.62 (dd, 2H, *J* 1.6, 1.9, H-5), 9.08 (s, 1H, H-2); δ_{C} NMR (DMSO-d₆): 35.8 (CH₃), 60.3 (C⁻) 123.2 (CN), 123.5 (C-5), 124.4 (C-4), 137.5 (C-2); (for C⁻ pulse delay, 3 seconds, 17,000 scans).

Synthesis of 1-benzylimidazolium-3-dicyanomethanide 1,3-dipole **112**

A solution of TCNEO (0.31 g, 2.15 mmol) in ethyl acetate (3 cm³) was cooled to 0 °C in an ice-bath and treated with a cooled solution of 1-benzylimidazole (0.34 g, 2.15 mmol) in ethyl acetate (3 cm³) dropwise with stirring. The mixture was stirred for a further 10 min in the ice-bath and then filtered to give the product **112** (0.35 g, 73%), mp 177-179 °C (ethanol). The filtrate rapidly turned dark brown. Attempts to isolate more product or starting material from the filtrate by removing the solvent under reduced pressure led to a brown sticky residue due to decomposition of TCNEO. Compound **112**: (Found: C, 70.1; H, 4.7; N, 25.3. C₁₃H₁₀N₄ requires C, 70.25; H, 4.55; N, 25.2%); $\nu_{\max}/\text{cm}^{-1}$ 2160, 2180 (C≡N); δ_{H} NMR (DMSO-d₆): 5.30 (s, 2H, benzyl CH₂), 7.32-7.39 (m, 5H, Ph), 7.64 (dd, *J* 1.6, 1.6, 1H, H-5), 7.73 (dd, 1H, *J* 1.6, 1.6, H-4), 9.33 (s, 1H, H-2); δ_{C} NMR (DMSO-d₆) 52.1 (benzyl CH₂),

122.6 (C-5), 123.0 (CN), 124.7 (C-4), 128.3 (C-3'), 128.7 (C-4'), 129.0 (C-2'), 134.9 (C-1'), 136.4 (C-2).

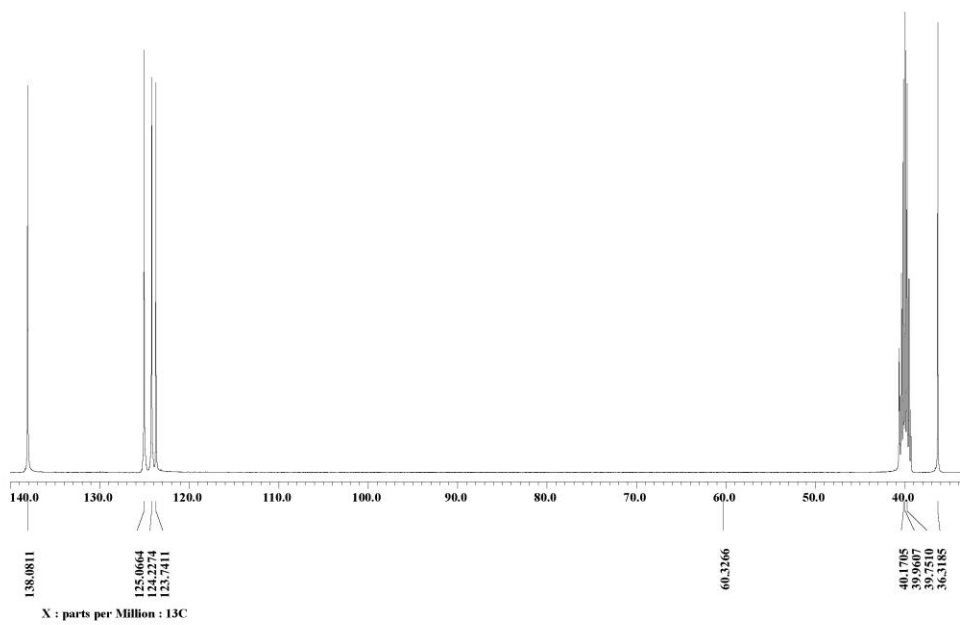
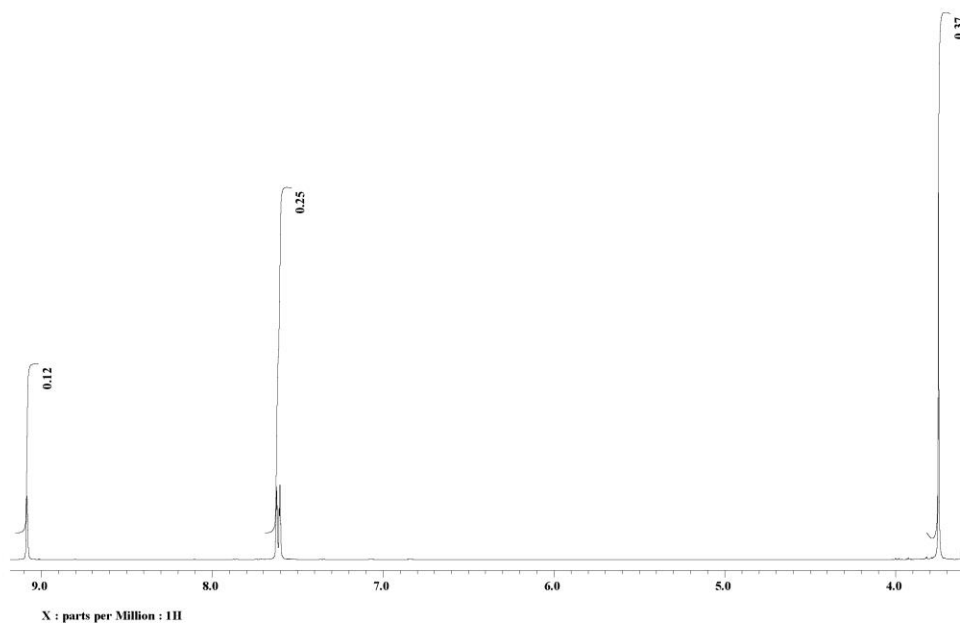
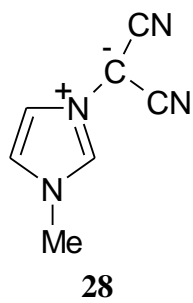
Synthesis of 1-phenylimidazolium-3-dicyanomethanide 1,3-dipole **114**

A solution of 1-phenylimidazole (0.95 cm³, 7.51 mmol) in ethyl acetate (12 cm³) was cooled to 0 °C in an ice-bath and treated with a cooled solution of TCNEO (1.08 g, 7.51 mmol) in ethyl acetate (8 cm³) dropwise with stirring. The mixture was stirred for a further 5 min in the ice-bath and then filtered to give the product **114** (1.27 g, 81%), mp 202-203 °C (ethanol) (Lit.⁷ 210-212 °C). The filtrate rapidly turned dark brown. Attempts to isolate more product or starting material from the filtrate by removing the solvent under reduced pressure led to a brown sticky residue due to decomposition of TCNEO. Compound **114**: (Found: C, 69.5; H, 3.8; N, 27.25. C₁₂H₈N₄ requires C, 69.2; H, 3.9; N, 26.9%); $\nu_{\max}/\text{cm}^{-1}$ 2175, 2114 (C≡N); δ_{H} (DMSO-d₆) 7.48-7.51 (m, 1H, H-4'), 7.55-7.59 (m, 2H, H-3'), 7.75-7.77 (m, 2H, H-2'), 7.89 (dd, 2H, *J* 1.8, 1.9, H-5), 8.25 (dd, 1H, *J* 1.6, 1.9, H-4), 9.73 (dd, 1H, *J* 1.6, 1.6, H-2); δ_{C} (DMSO-d₆) 121.9 (C-5), 122.4 (C-2'), 123.3 (C≡N), 125.7 (C-4), 130.0 (C-4'), 130.5 (C-3'), 135.3 (C-1'), 135.5 (C-2).

Synthesis of 1-phenyl-1,2,4-triazolium-4-dicyanomethanide 1,3-dipole **142**

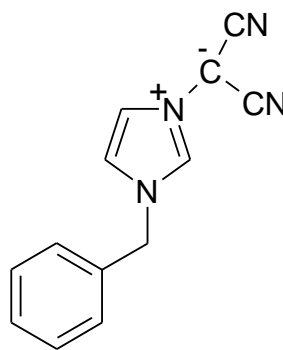
A solution of 1-phenyl-1,2,4-triazole (1.50 g, 16.40 mmol) in diethyl ether (50 cm³) was treated with TCNEO (1.48 g, 16.40 mmol), also in diethyl ether (50 cm³). The reaction mixture was stirred at room temperature for 72 h in a nitrogen rich atmosphere. During this time the product precipitated from solution and was collected by filtration to give a light brown solid, compound **142** (0.50 g, 23%), mp >300 °C (ethanol) (Lit.⁷ mp >260 °C); (Found: C, 62.9; H, 3.7; N, 33.45. C₁₁H₇N₅ requires C, 63.15; H, 3.4; N, 33.5%); $\nu_{\max}/\text{cm}^{-1}$ 2184, 2128 (C≡N); δ_{H} NMR (DMSO-d₆) 7.53-7.56 (m, 1H, Ph H-4'), 7.59-7.63 (m, 2H, H-3'), 7.87-7.89 (m, 2H, H-2'), 9.43 (s, 1H, H-3), 10.86 (s, 1H, H-5); δ_{C} (DMSO-d₆) 121.2 (C-2'), 122.6 (C≡N), 130.5 (C-3'), 130.7 (C-4'), 135.8 (C-1'), 142.3 (C-3), 146.6 (C-5).

Chapter 2

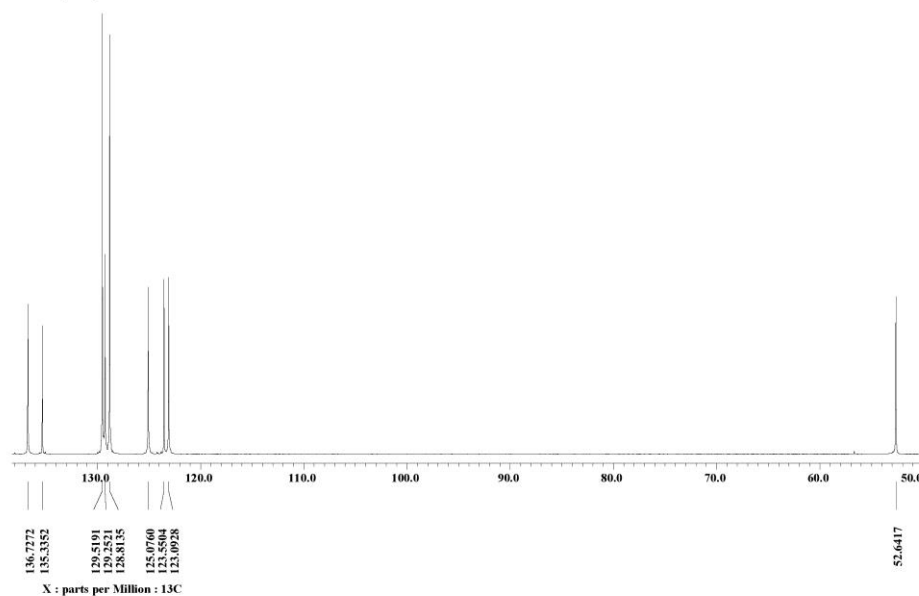
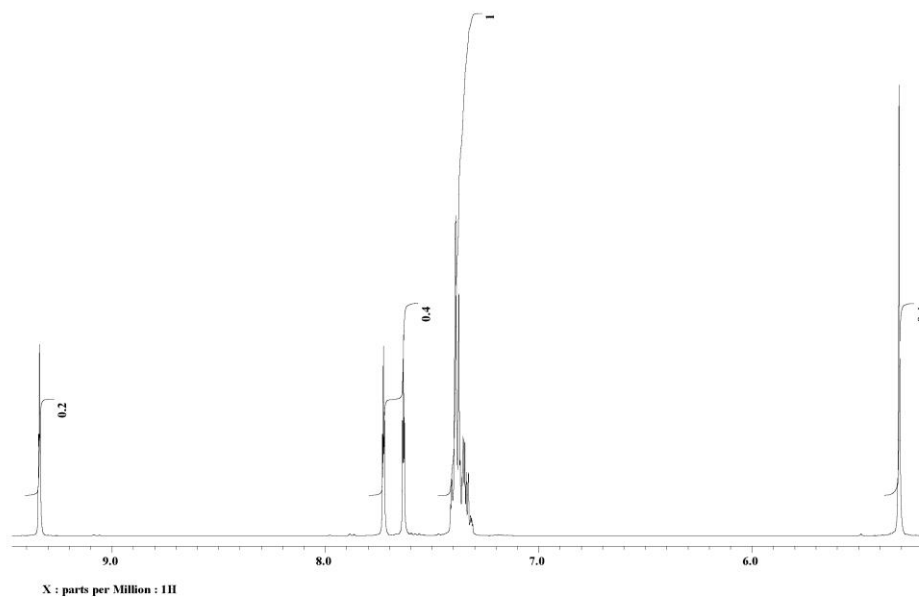


^1H and ^{13}C NMR spectra for product **28** in DMSO-d_6

Chapter 2



112



^1H and ^{13}C NMR spectra for product **112** in DMSO-d_6

1,3-Dipolar cycloaddition reactions

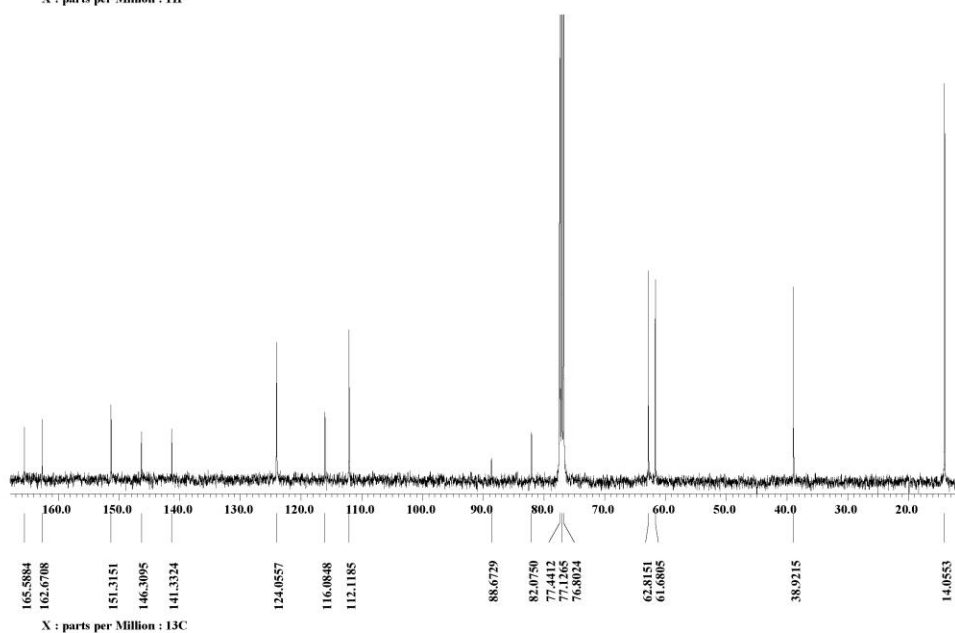
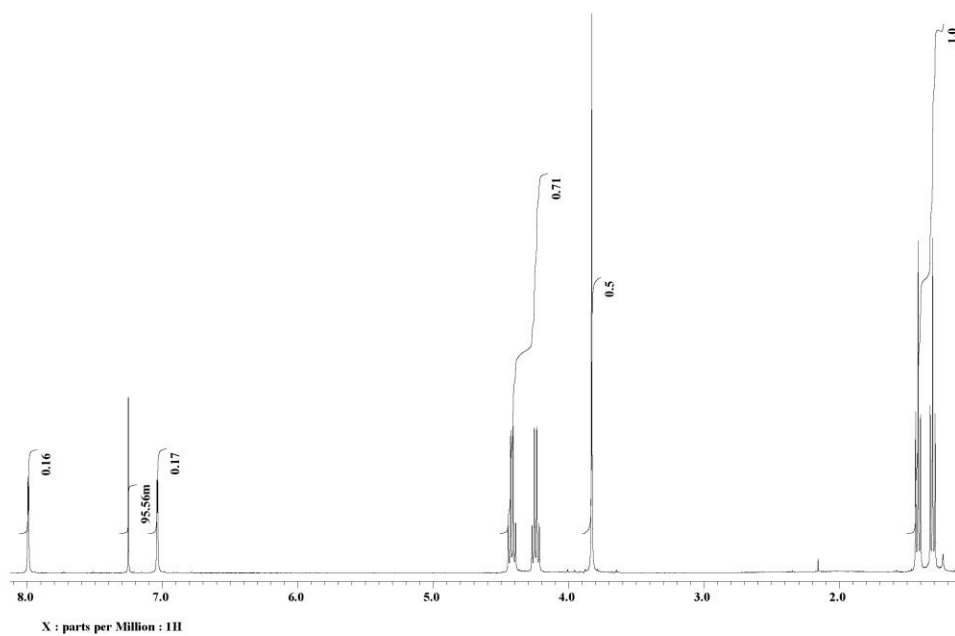
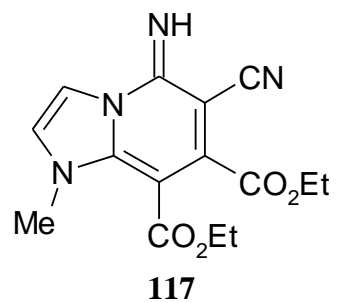
Synthesis of 1-methyl-5-imino-6-cyano-7,8-dimethoxycarbonyl imidazo[2,3-*a*]pyridine **30**

A solution of 1-methylimidazolium-3-dicyanomethanide (0.20 g, 1.37 mmol) in acetonitrile (5 cm³) was treated with DMAD (0.17 cm³, 1.38 mmol) and the solution stirred at room temperature for 1 h. During this time the product, compound **30** separated, (0.32 g, 81%), mp 190-192 °C (ethanol), (lit.⁶, mp 190-191 °C); (Found C, 54.3; H, 4.0; N, 19.55. C₁₃H₁₂N₄O₄ requires C, 54.2; H, 4.2; N, 19.4%); $\nu_{\max}/\text{cm}^{-1}$ 3293 (NH), 2204 (C≡N), 1736, 1709 (C=O), 1610 (C=N); δ_{H} (CDCl₃) 3.79 (s, 3H, OCH₃), 3.84 (s, 3H, NCH₃), 3.96 (s, 3H, OCH₃), 7.04 (d, 1H, *J* 2.3, H-2), 8.01 (d, 1H, *J* 2.3, H-3); δ_{C} (CD₃Cl₃) 38.9 (NCH₃), 52.4 (OCH₃), 53.5 (OCH₃), 82.3 (C-6), 88.2 (C-8), 112.2 (C-2), 116.1 (C≡N), 124.0 (C-3), 141.3 (C-7), 146.4 (C-8a), 151.2 (C-5), 163.0 (C=O), 166.2 (C=O).

Synthesis of 1-methyl-5-imino-6-cyano-7,8-diethoxycarbonyl imidazo[2,3-*a*]pyridine **117**

A solution of 1-methylimidazolium-3-dicyanomethanide (0.18 g, 1.23 mmol) in acetonitrile (5 cm³) was treated with DEAD (0.20 cm³, 1.23 mmol) and the solution stirred at room temperature for 2 h. The solvent was then removed under reduced pressure and the residue crystallized from methanol to give the product, compound **117**, (0.20 g, 51%), mp 129-130 °C (methanol). Evaporation of the methanolic filtrate led only to an oily brown residue and no further product was isolated. (Found C, 56.5; H, 4.9; N, 18.2. C₁₅H₁₆N₄O₄ requires C, 56.95; H, 5.1; N, 17.7%); $\nu_{\max}/\text{cm}^{-1}$ 3291 (NH), 2207(C≡N), 1739, 1697 (C=O), 1619 (C=N); δ_{H} (CDCl₃) 1.31 (t, 3H, *J* 7.1, CH₃), 1.42 (t, 3H, *J* 7.1, CH₃), 3.83 (s, 3H, N-CH₃), 4.24 (q, 2H, *J* 7.1, CH₂), 4.42 (q, 2H, *J* 7.1, CH₂), 7.04 (d, 1H, *J* 2.3, H-2), 7.99 (d, 1H, *J* 2.3, H-3); δ_{C} (CDCl₃) 14.1 (2 x CH₃), 38.9 (N-CH₃) 61.7 (CH₂), 62.8 (CH₂), 82.1 (C-6), 88.7 (C-8), 112.1 (C-2), 116.1 (C≡N), 124.1 (C-3), 141.3 (C-7), 146.3 (C-8a), 151.3 (C-5), 162.7 (C=O), 165.6 (C=O).

Chapter 2



^1H and ^{13}C NMR spectra for product **117** in CDCl_3

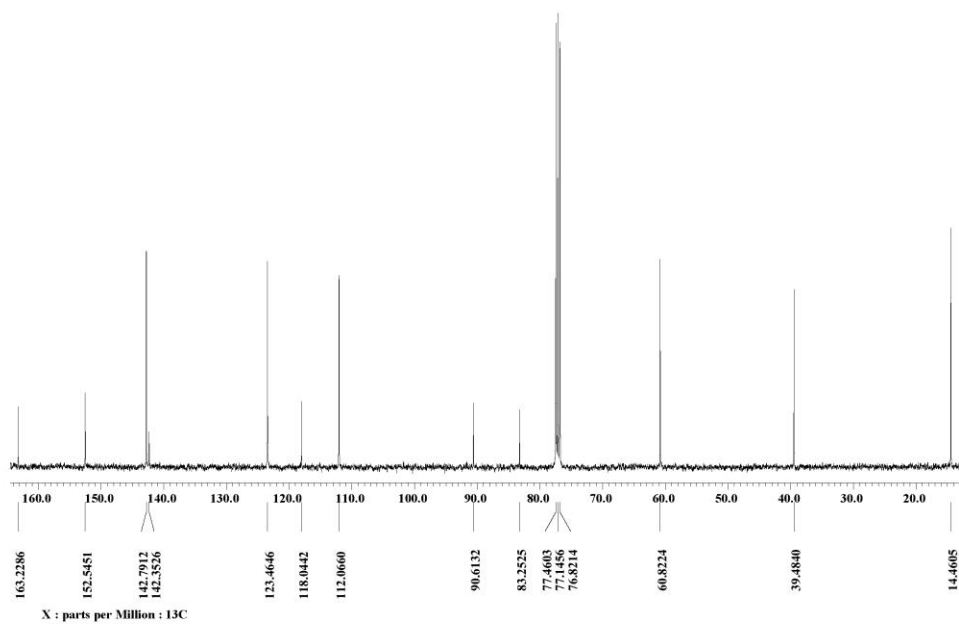
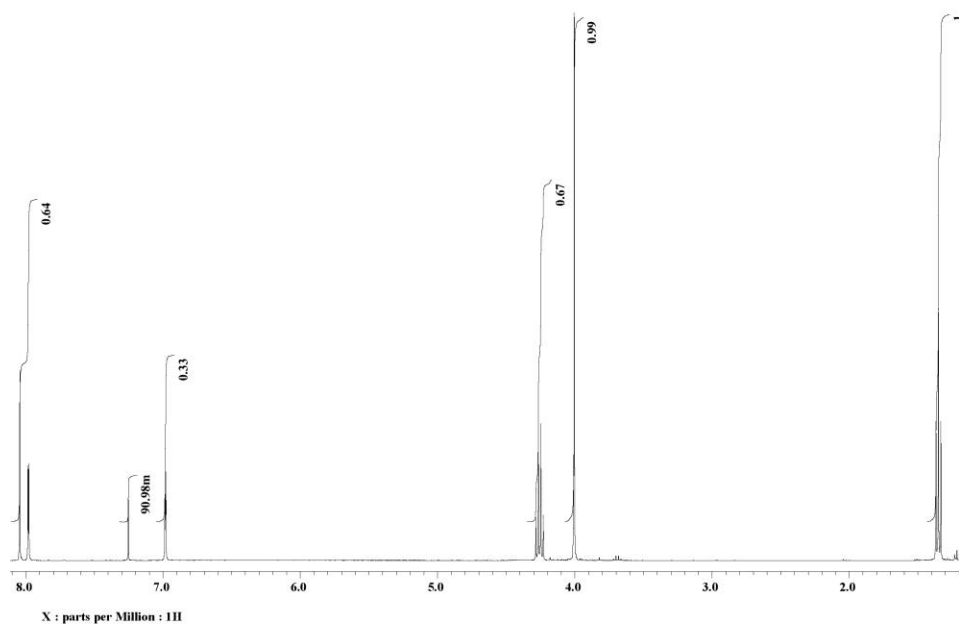
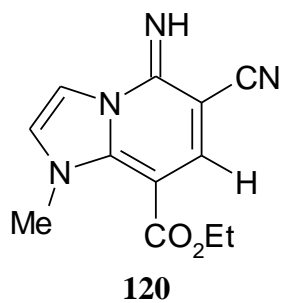
Synthesis of 1-methyl-5-imino-6-cyano-8-methoxycarbonyl imidazo[2,3-*a*]pyridine **119**

A solution of 1-methylimidazolium-3-dicyanomethanide (0.28 g, 1.92 mmol) in acetonitrile (5 cm³) was treated with MP (0.17 cm³, 1.92 mmol) and the solution stirred at 0-5 °C (ice-bath) for 72 h. The solvent was removed under reduced pressure to give a crude dark brown solid (0.42 g, 95%). Fractional crystallisation from diethyl ether gave **119** as a pale yellow solid (0.23 g, 52%) mp 155-157 °C (ethanol) and a dark red gum. (Found: C, 57.4; H, 4.5; N, 24.7. C₁₁H₁₀N₄O₂ requires C, 57.4; H, 4.4; N, 24.3 %); $\nu_{\max}/\text{cm}^{-1}$ 3107 (NH), 2204 (C≡N), 1723 (C=O), 1613 (C=N); δ_{H} (CDCl₃) 3.83 (s, 3H, OCH₃), 4.03 (s, 3H, N-CH₃), 7.01 (d, 1H, *J* 2.4, H-2), 8.01 (d, 1H, *J* 2.4, H-3), 8.05 (s, 1H, H-7); δ_{C} (CDCl₃) 39.2 (N-CH₃), 51.6 (OCH₃), 83.2 (C-6), 90.0 (C-8), 111.7 (C-3), 117.7 (C≡N), 123.4 (C-2), 141.9 (C-8a), 142.3 (C-7), 152.2 (C-5), 163.2 (C=O).

Synthesis of 1-methyl-5-imino-6-cyano-8-ethoxycarbonyl imidazo[2,3-*a*]pyridine **120**

A solution of 1-methylimidazolium-3-dicyanomethanide (0.20 g, 1.36 mmol) in acetonitrile (5 cm³) was treated with EP (0.138 cm³, 1.36 mmol) and the solution stirred at ambient temperature for 26 h. The solvent was removed under reduced pressure to give a crude dark brown solid (0.31 g, 93%). Crystallisation from hot ethanol gave **120** as a pale orange solid (0.11 g, 33%), mp 164-165 °C (ethanol); (Found: C, 58.8; H, 5.25; N, 23.0. C₁₂H₁₂N₄O₂ requires C, 59.0; H, 4.95; N, 22.9%); $\nu_{\max}/\text{cm}^{-1}$ 3314 (NH), 2205 (C≡N), 1695 (C=O), 1615 (C=N); δ_{H} (CDCl₃) 1.36 (t, 3H, *J* 7.1, CH₃), 4.01 (s, 3H, N-CH₃), 4.26 (q, 2H, *J* 7.1, CH₂), 6.99 (d, 1H, *J* 2.3, H-2), 7.99 (d, 1H, *J* 2.3, H-3), 8.05 (s, 1H, H-7); δ_{C} (CDCl₃) 14.5 (CH₃), 39.5 (N-CH₃), 60.8 (CH₂), 83.3 (C-6), 90.6 (C-8), 112.1 (C-2), 118.0 (C≡N), 123.5 (C-3), 142.3 (C-8a), 142.8 (C-7), 152.5 (C-5), 163.2 (C=O).

Chapter 2



^1H and ^{13}C NMR spectra for product **119** in CDCl_3

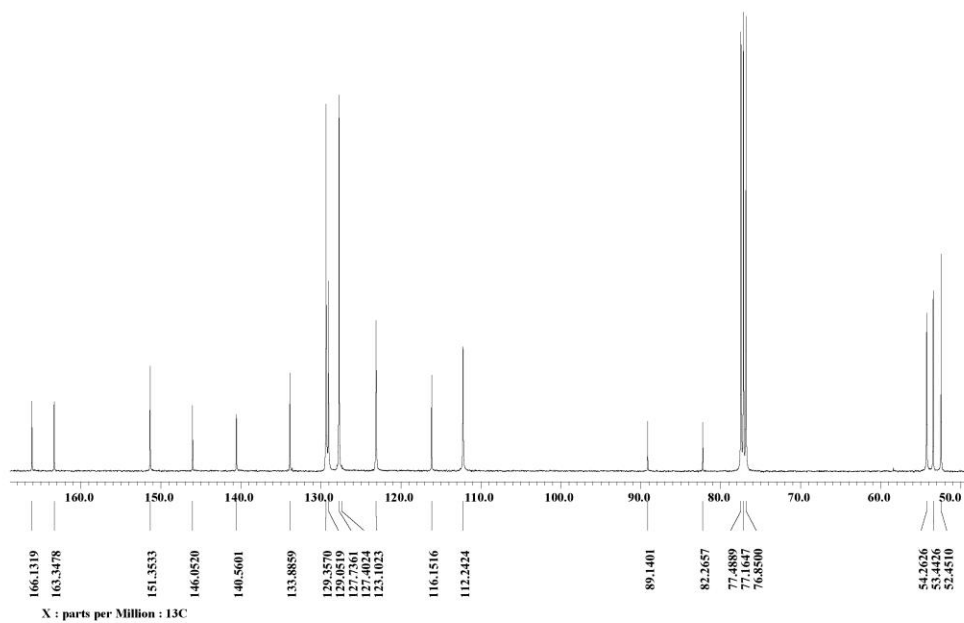
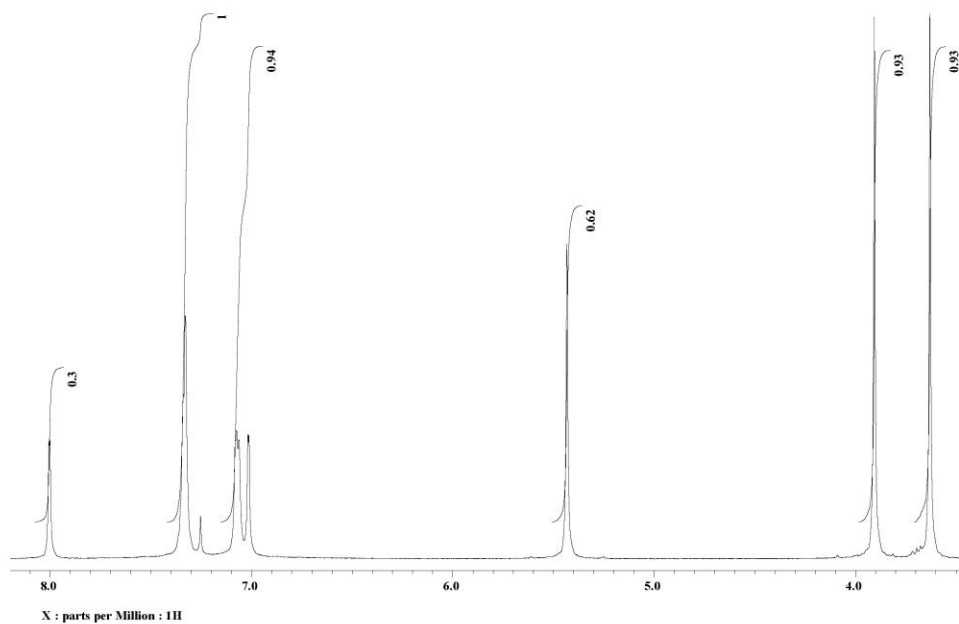
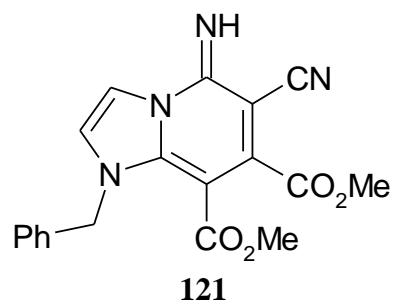
Synthesis of 1-benzyl-5-imino-6-cyano-7,8-dimethoxycarbonyl imidazo [2,3-*a*]pyridine **121**

A solution of 1-benzylimidazolium-3-dicyanomethanide 1,3-dipole (0.22 g, 1.00 mmol) in dimethyl formamide (5 cm³) was cooled to 0 °C, then treated with DMAD (0.123 cm³, 1.00 mmol). The mixture was allowed to stand at 0 °C for 4 h, and subsequently added to cooled water. Compound **121** precipitated as a yellow solid (0.19 g, 53%), mp 131-133 °C (ethanol); (Found: C, 62.3; H, 4.1; N, 15.8. C₁₉H₁₆N₄O₄ requires C, 62.6; H 4.4; N, 15.4%); $\nu_{\max}/\text{cm}^{-1}$ 3305 (NH), 2208 (C≡N), 1720, 1704 (C=O), 1615 (C=N); δ_{H} (CDCl₃) 3.63 (s, 3H, OCH₃), 3.91 (s, 3H, OCH₃), 5.43 (s, 2H, benzyl CH₂), 7.02 (d, 1H, *J* 1.8, H-2), 7.06-7.08 (m, 2H, H-2' of Ph), 7.33-7.36 (m, 3H, H-3' and H-4' of Ph), 8.00 (d, 1H, *J* 1.8, H-3); δ_{C} (CDCl₃) 52.5 (OCH₃), 53.4 (OCH₃), 54.3 (benzyl CH₂), 82.3 (C-6), 89.1 (C-8), 112.2 (C-2), 116.2 (C≡N), 123.1 (C-3), 127.7 (C-2'), 129.1 (C-4'), 129.4 (C-3'), 133.9 (C-1'), 140.6 (C-7), 146.1 (C-8a), 151.4 (C-5), 163.3 (C=O), 166.1 (C=O).

Synthesis of 1-benzyl-5-imino-6-cyano-7,8-diethoxycarbonyl imidazo [2,3-*a*]pyridine **122**

A solution of 1-benzylimidazolium-3-dicyanomethanide 1,3-dipole (0.30 g, 1.44 mmol) in acetonitrile (8 cm³) was cooled to 0 °C and treated with DEAD (0.232 cm³, 1.44 mmol). The mixture was allowed to stir at 0 °C for 4 h. Compound **122** separated from solution as a yellow solid (0.22 g, 42%), mp 153-155 °C (ethanol); (Found: C, 63.9; H, 4.65; N, 13.9. C₂₁H₂₀N₄O₄ requires C, 64.3; H, 5.1; N, 14.3%); $\nu_{\max}/\text{cm}^{-1}$ 3303 (NH), 2204 (C≡N), 1727, 1698 (C=O), 1620 (C=N); δ_{H} (CDCl₃) 1.24 (t, 3H, *J* 7.1, CH₃), 1.47 (t, 3H, *J* 7.1, CH₃), 4.17 (q, 2H, *J* 7.1, CH₂), 4.45 (q, 2H, *J* 7.1, CH₂), 5.53 (benzyl CH₂), 7.07 (d, 1H, *J* 2.2, H-2), 7.14-7.16 (m, 2H, H-2' of Ph), 7.40-7.45 (m, 3H, Ph H-3'and H-4' of Ph), 8.07 (d, 1H, *J* 2.2, H-3); δ_{C} (CDCl₃) 13.7 (CH₃), 13.9 (CH₃), 54.1 (benzyl CH₂), 61.5 (CH₂), 62.6 (CH₂), 82.1 (C-6), 89.3 (C-8), 112.0 (C-2), 116.0 (C≡N), 122.8 (C-3), 127.6 (C-2'), 128.9 (C-4'), 129.2 (C-3') 133.9 (C-1'), 140.5 (C-7), 146.0 (C-8a), 151.3 (C-5), 162.9 (C=O), 165.4 (C=O).

Chapter 2



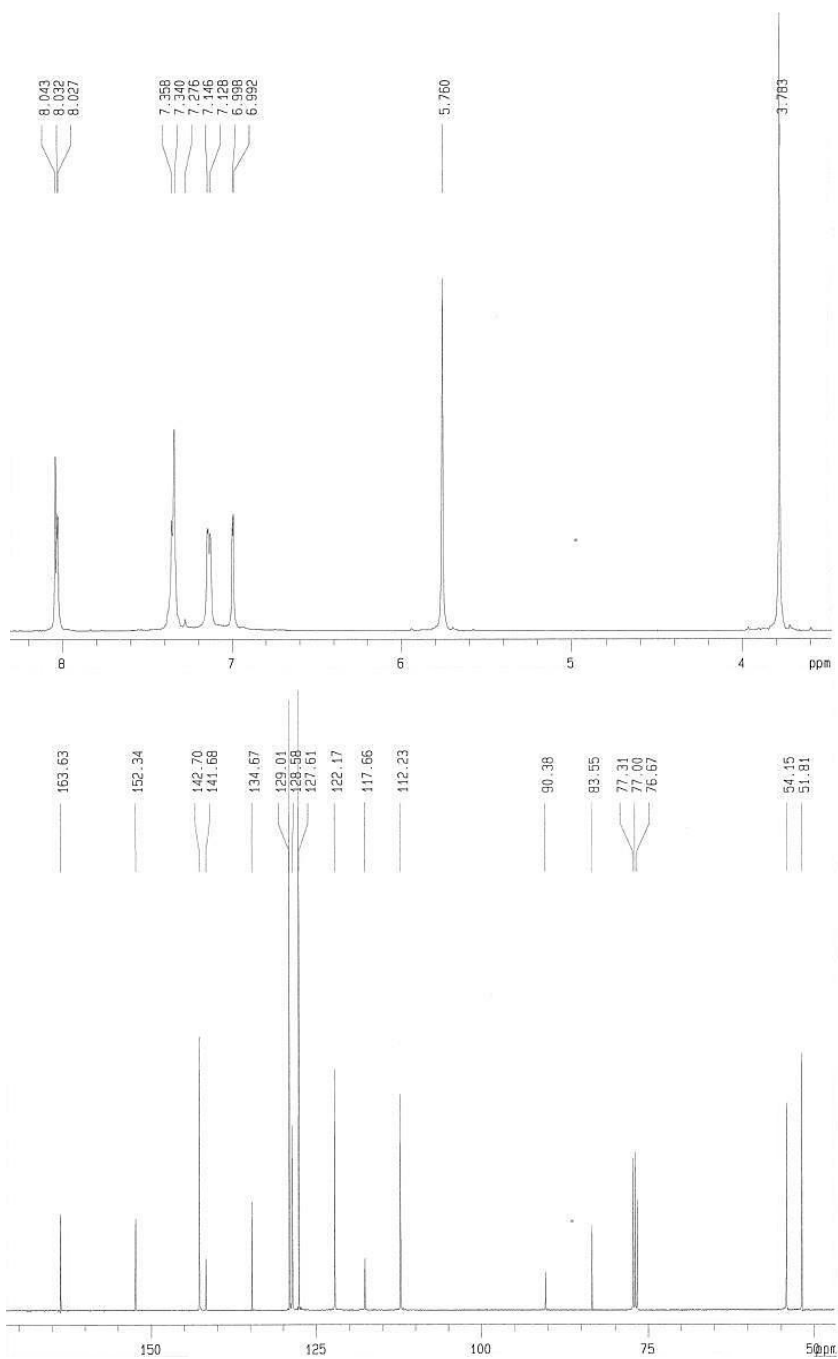
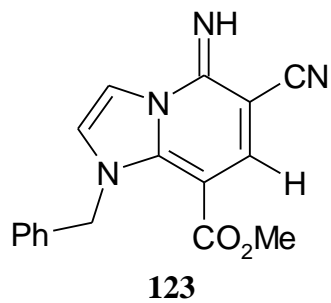
^1H and ^{13}C NMR spectra for product **121** in CDCl_3

Synthesis of 1-benzyl-5-imino-6-cyano-8-methoxycarbonyl imidazo[2,3-*a*]pyridine **123**

A solution of 1-benzylimidazolium-3-dicyanomethanide 1,3-dipole (0.30 g, 1.44 mmol) in acetonitrile (8 cm³) was treated with methyl propiolate (0.128 cm³, 1.44 mmol). The mixture was allowed to stir at ambient temperature for 48 h. Compound **123** separated from solution as a buff solid (0.21 g, 48%), mp 190-191 °C (ethanol); (Found: C, 66.8; H, 4.1; N, 18.2. C₁₇H₁₄N₄O₂ requires C, 66.7; H, 4.6; N, 18.3%); $\nu_{\max}/\text{cm}^{-1}$ 3292 (NH), 2203 (C≡N), 1694 (C=O), 1616 (C=N); δ_{H} (CDCl₃) 3.78 (s, 3H, OCH₃), 5.76 (s, 2H, benzyl CH₂), 7.00 (d, 1H, *J* 2.2, H-2), 7.12-7.14 (m, 2H, H-2' of Ph), 7.31-7.35 (m, 3H, H-3' and H-4' of Ph), 8.03 (d, 1H, *J* 2.2, H-3), 8.04 (s, 1H, H-7); δ_{C} (CDCl₃) 51.8 (OCH₃), 54.2 (benzyl CH₂), 83.5 (C-6), 90.4 (C-8), 112.2 (C-2), 117.7 (C≡N), 122.2 (C-3), 127.6 (C-2'), 128.6 (C-4'), 129.0 (C-3') 134.7 (C-1'), 141.7 (C-8a), 142.7 (C-7), 152.3 (C-5), 163.1 (C=O).

Synthesis of 1-benzyl-5-imino-6-cyano-8-ethoxycarbonyl imidazo[2,3-*a*]pyridine **124**

A solution of 1-benzylimidazolium-3-dicyanomethanide 1,3-dipole (0.39 g, 1.76 mmol) in acetonitrile (16 cm³) was treated with ethyl propiolate (0.178 cm³, 1.76 mmol). The mixture was stirred at ambient temperature for 51 h. The solvent was removed under reduced pressure, yielding a sticky brown solid. Fractional crystallization from diethyl ether gave **124** as a pale yellow solid (0.15 g, 27%), mp 133-134 °C (ethanol) and an orange gum. The orange gum was subjected to a Soxhlet extraction with ether which yielded further **124** (0.20 g, 36%). (Found: C, 67.1; H, 4.8; N, 17.4. C₁₈H₁₆N₄O₂ requires C, 67.5; H, 5.0; N, 17.5%); $\nu_{\max}/\text{cm}^{-1}$ 3289 (NH), 2206 (C≡N), 1682 (C=O), 1613 (C=N); δ_{H} (CDCl₃) 1.29 (t, 3H, *J* 7.1, CH₃), 4.21 (q, 2H, *J* 7.1, CH₂), 5.74 (s, 2H, benzyl CH₂), 6.98 (d, 1H, *J* 2.3, H-2), 7.09-7.11 (m, 2H, H-2' of Ph), 7.31-7.35 (m, 3H, H-3' and H-4' of Ph), 8.00 (d, 1H, *J* 2.3, H-3), 8.02 (s, 1H, H-7); δ_{C} (CDCl₃) 14.4 (CH₃), 54.4 (benzyl CH₂), 61.0 (CH₂), 83.6 (C-6), 91.1 (C-8), 112.4 (C-2), 118.0 (C≡N), 122.4 (C-3), 127.8 (C-2'), 128.8 (C-4'), 129.2 (C-3'), 134.9 (C-1'), 141.9 (C-8a), 143.0 (C-7), 152.7 (C-5), 163.5 (C=O).



¹H and ¹³C NMR spectra for product **123** in CDCl₃

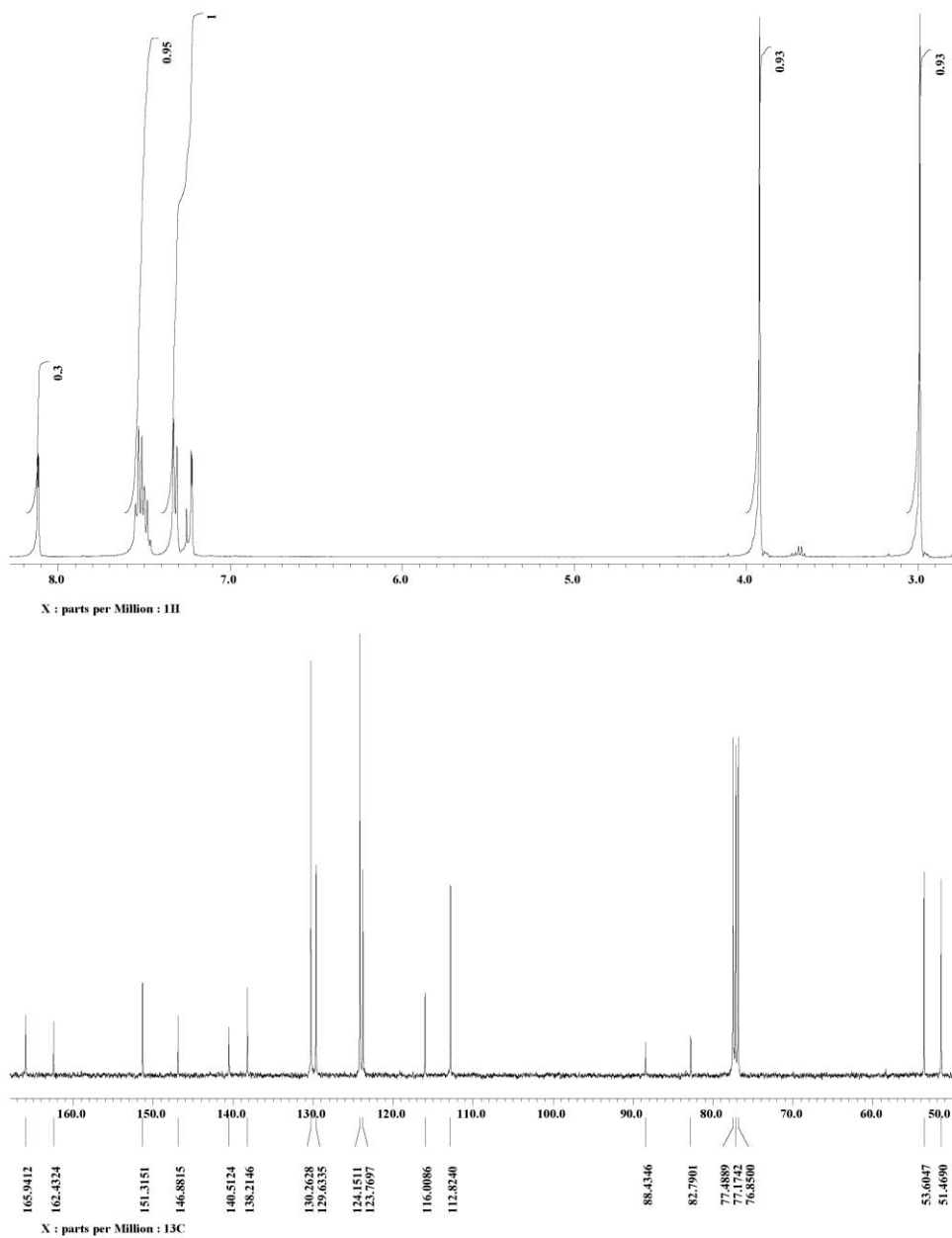
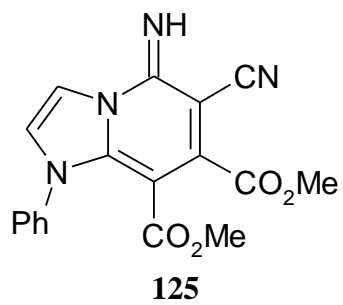
Synthesis of 1-phenyl-5-imino-6-cyano-7,8-dimethoxycarbonyl imidazo [2,3-*a*]pyridine **125**

A solution of 1-phenylimidazolium-3-dicyanomethanide 1,3-dipole (0.30 g, 1.44 mmol) in acetonitrile (26 cm³) was treated with DMAD (0.177 cm³, 1.44 mmol). The mixture was stirred at ambient temperature for 3.5 h. The solvent was removed under reduced pressure at room temperature yield a brown gum which solidified overnight. Crystallisation from hot ethanol yielded compound **125** (0.34 g, 67%), mp 176-177 °C (Lit.³⁵ 177-178 °C); (Found: C, 61.2; H, 4.1; N, 15.9. C₁₈H₁₄N₄O₄ requires C, 61.7; H, 4.0; N, 16.0%); $\nu_{\max}/\text{cm}^{-1}$ 3320 (NH), 2206 (C≡N), 1724, 1696 (C=O), 1617 (C=N); δ_{H} (CDCl₃) 2.99 (s, 3H, OCH₃), 3.92 (s, 3H, OCH₃), 7.22 (d, 1H, *J* 1.9, H-2), 7.31-7.33 (m, 2H, H-2' of N-Ph) 7.48-7.55 (m, 3H, H-3' and H-4' of N-Ph), 8.12 (d, 1H, *J* 1.9, H-3); δ_{C} (CDCl₃) 51.5 (OCH₃), 53.6 (OCH₃), 82.8 (C-6), 88.4 (C-8), 112.8 (C-2), 116.0 (C≡N), 123.8 (C-3), 124.2 (C-2'), 129.6 (C-4'), 130.3 (C-3'), 138.2 (C-1'), 140.5 (C-8a), 146.9 (C-7), 151.3 (C-5), 162.4 (C=O), 165.9 (C=O).

Synthesis of 1-phenyl-5-imino-6-cyano-7,8-diethoxycarbonyl imidazo [2,3-*a*]pyridine **126**

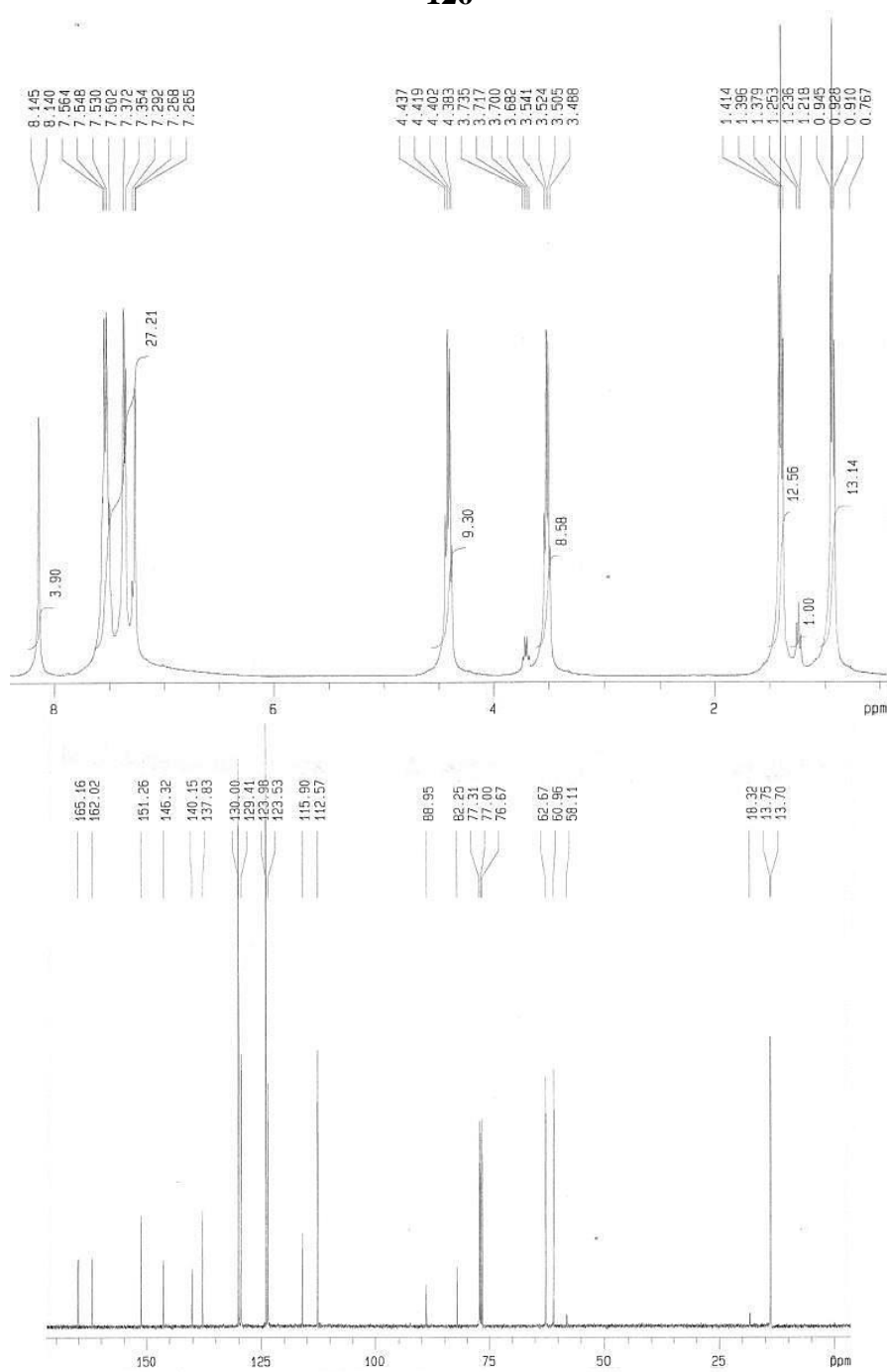
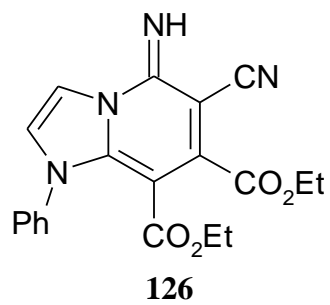
A solution of 1-phenylimidazolium-3-dicyanomethanide 1,3-dipole (0.20 g, 0.96 mmol) in acetonitrile (12 cm³) was treated with DEAD (0.154 cm³, 0.96 mmol). The mixture was stirred at ambient temperature for 3.5 h. The solvent was removed under reduced pressure at room temperature yield a brown gum which solidified overnight. Crystallisation from hot ethanol yielded compound **126** (0.20 g, 55%), mp 117-119 °C; (Found: C, 62.9; H, 4.5; N, 14.6. C₂₀H₁₈N₄O₄ requires C, 63.5; H, 4.8; N, 14.8%); $\nu_{\max}/\text{cm}^{-1}$ 3296 (NH), 2206 (C≡N), 1730, 1710 (C=O), 1615 (C=N); δ_{H} (CDCl₃) 0.93 (t, 3H, *J* 7.2, CH₃), 1.40 (t, *J* 7.1, 3H, CH₃), 3.52 (q, *J* 7.1, 2H, CH₂), 4.42 (q, 2H, *J* 7.2, CH₂), 7.23 (d, 1H, *J* 2.5, H-2), 7.35-7.37 (m, 2H, H-2' of N-Ph), 7.50-7.54 (m, 3H, H-3' and H-4' of N-Ph), 8.16 (d, *J* 2.5, 1H, H-3); δ_{C} (CDCl₃) 13.7 (CH₃), 13.8 (CH₃), 61.0 (CH₂), 62.7 (CH₂) 82.3 (C-6), 89.0 (C-8), 112.6 (C-2), 115.9 (C≡N), 123.5 (C-3), 124.0 (C-2'), 129.4 (C-4'), 130.0 (C-3'), 137.8 (C-1'), 140.2 (C-8a), 146.3 (C-7), 151.3 (C-5), 162.0 (C=O), 165.2 (C=O).

Chapter 2



¹H and ¹³C NMR spectra for product **125** in CDCl₃

Chapter 2



^1H and ^{13}C NMR spectra for product **126** in CDCl_3

Synthesis of 1-phenyl-5-imino-6-cyano-8-methoxycarbonyl imidazo[2,3-*a*]pyridine **127**

A solution of 1-phenylimidazolium-3-dicyanomethanide 1,3-dipole (0.20 g, 0.96 mmol) in acetonitrile (15 cm³) was treated with methyl propiolate (0.085 cm³, 0.96 mmol). The mixture was stirred at ambient temperature for 48 h. Compound **127** separated from solution as a buff precipitate (0.07 g, 25%), mp 198-200 °C (Lit.³⁵ 205-206 °C); (Found: C, 65.2; H, 4.1; N, 19.3. C₁₆H₁₂N₄O₂ requires C, 65.7; H, 4.1; N, 19.2%); $\nu_{\max}/\text{cm}^{-1}$ 3314 (NH), 2198 (C≡N), 1688 (C=O), 1621 (C=N); δ_{H} (CDCl₃) 3.20 (s, 3H, OCH₃), 7.17 (d, 1H, *J* 2.4, H-2), 7.30-7.32 (m, 2H, H-2' of N-Ph) 7.48-7.56 (m, 3H, H-3' and H-4' of N-Ph), 8.01 (s, 1H, H-7), 8.16 (d, 1H, *J* 2.4, H-3); δ_{C} (CDCl₃) 51.3 (CH₃), 84.6 (C-6), 90.3 (C-8), 112.7 (C-2), 117.7 (C≡N), 123.3 (C-3), 124.3 (C-2'), 129.3 (C-4'), 129.9 (C-3'), 138.9 (C-1'), 141.4 (C-8a), 143.1 (C-7), 152.5 (C-5), 163.0 (C=O).

Synthesis of 1-phenyl-5-imino-6-cyano-8-ethoxycarbonyl imidazo[2,3-*a*]pyridine **128**

A solution of 1-phenylimidazolium-3-dicyanomethanide 1,3-dipole (0.20 g, 0.96 mmol) in acetonitrile (15 cm³) was treated with ethyl propiolate (0.097 cm³, 0.96 mmol). The mixture was stirred at ambient temperature for 51 h. Solvent was removed under reduced pressure to yield a crude dark brown solid (0.29 g, 98%). This was recrystallized from ethanol to yield clean **128** (0.13 g, 44%) mp 191-192 °C (ethanol); (Found: C, 66.4; H, 4.2; N, 18.3. C₁₇H₁₄N₄O₂ requires C, 66.7; H, 4.6; N, 18.3%); $\nu_{\max}/\text{cm}^{-1}$ 3314 (NH), 2205 (C≡N), 1683 (C=O), 1622 (C=N); δ_{H} (CDCl₃) 0.97 (t, 3H, *J* 7.1, CH₃), 3.72 (q, 2H, *J* 7.1, CH₂), 7.18 (d, 1H, *J* 2.5, H-2), 7.30-7.32 (m, 2H, H-2' of N-Ph), 7.46-7.52 (m, 3H, H-3' and H-4' of N-Ph), 7.99 (s, 1H, H-7), 8.11 (d, 1H, *J* 2.5, H-3); δ_{C} (CDCl₃) 14.2 (CH₃), 60.6 (CH₂), 84.3 (C-6), 90.7 (C-8), 112.7 (C-2), 117.9 (C≡N), 123.3 (C-3), 124.1 (C-2'), 129.2 (C-4'), 129.9 (C-3'), 138.9 (C-1'), 141.3 (C-8a), 143.0 (C-7), 152.6 (C-5), 162.6 (C=O).

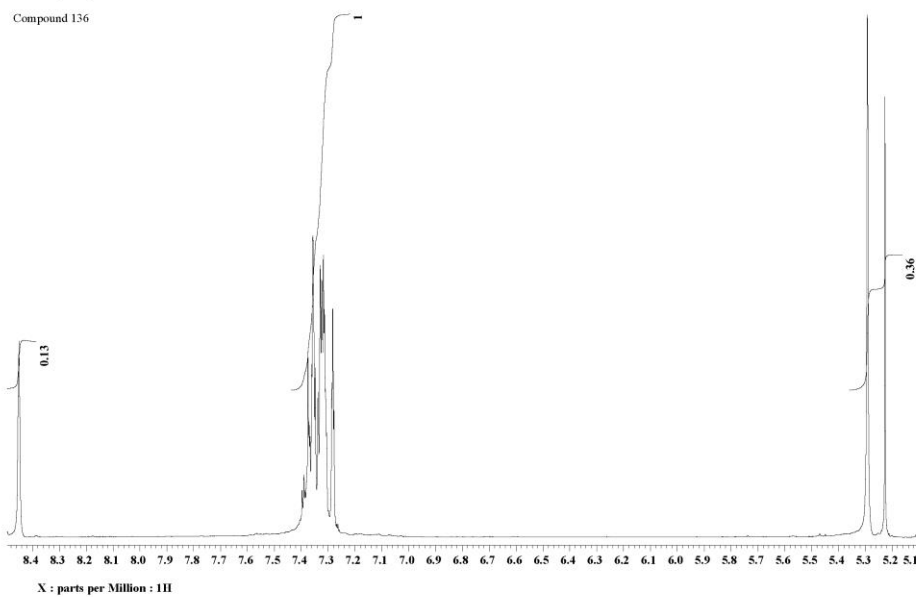
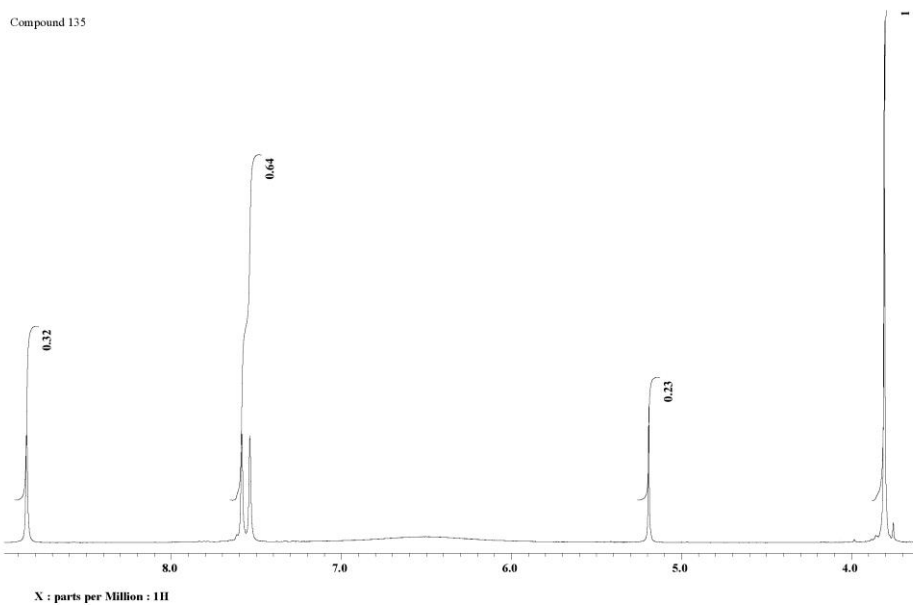
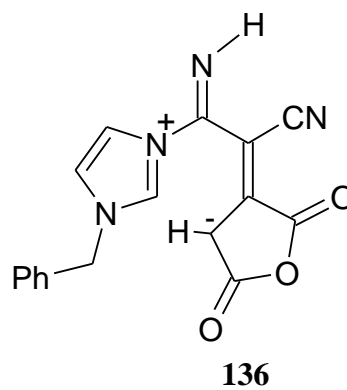
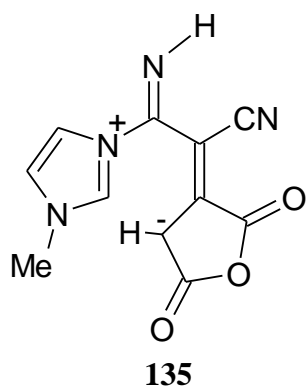
Reaction of 1-methylimidazolium-3-dicyanomethanide 1,3-dipole with maleic anhydride

A solution of 1-methylimidazolium-3-dicyanomethanide (0.48 g, 3.28 mmol) in acetonitrile (10 cm³) was treated with a solution of maleic anhydride (0.32 g, 3.26 mmol) in acetonitrile, and the mixture stirred at room temperature for 3 h. The solution was then evaporated under reduced pressure at a temperature below 35 °C. Addition of ether to the residue caused precipitation of the green product, compound **135** (0.58 g, 70%), mp 180-181 °C (from acetonitrile). Evaporation of the ethereal solution only led to isolation of an oily residue. (Found: C, 54.35; H, 3.60; N, 22.70. C₁₁H₈N₄O₃ requires C, 54.10; H, 3.30; N, 22.95%); $\nu_{\max}/\text{cm}^{-1}$ 3330 cm⁻¹(N-H), 2175 (C≡N), 1792, 1734 (C=O); δ_{H} NMR (DMSO-d₆) 3.80 (s, 3H, N-CH₃), 5.12 (s, 1H, H-9), 7.53 (s, 1H, H-2), 7.58 (s, 1H, H-3), 8.84 (s, 1H, H-5); δ_{C} NMR (DMSO-d₆) 35.8 (N-CH₃), 59.7 (C-7), 92.1 (C-9), 118.3 (C≡N), 119.7 (C-8), 120.7 (C-2), 123.4 (C-3), 136.3 (C-5), 149.6 (C-6), 165.0 (C=O), 165.8 (C=O); for C-7 pulse delay 5 s, >9000 scans).

Reaction of 1-benzylimidazolium-3-dicyanomethanide 1,3-dipole with maleic anhydride

A solution of 1-benzylimidazolium-3-dicyanomethanide (0.27 g, 1.21 mmol) in acetonitrile (10 cm³) was treated with a solution of maleic anhydride (0.12 g, 1.22 mmol) in acetonitrile (5 cm³), and the solution stirred for 27 h at 50 °C under N₂. The solution was then evaporated under reduced pressure at ambient temperature to yield compound **136** as a sticky brown solid (0.33 g, 86%); δ_{H} NMR (CD₃CN) 5.24 (s, 1H, H-9), 5.31 (s, 2H, CH₂), 7.27-7.39 (m, 7H, H-2, H-3 and Ph), 8.52 (s, 1H, H-5), 9.8 - 11.62 (broad s, 1H, NH); δ_{C} NMR (CD₃CN) 52.4 (CH₂), 62.2 (C-7), 92.2 (C-9), 118.8 (C≡N), 119.5 (C-8), 121.5 (C-2), 121.8 (C-3), 128.5 (C-2'), 129.1 (C-4'), 129.3 (C-3'), 134.2 (C-1'), 135.4 (C-5), 150.0 (C-6), 165.4 (C=O), 166.1 (C=O); (for C-7 pulse delay 4 s, 12,800 scans).

Chapter 2



^1H NMR spectra for product **135** (DMSO- d_6) and **136** (CD_3CN)

Reaction of 1-methylimidazolium-3-dicyanomethanide 1,3-dipole with *N*-phenylmaleimide

A solution of 1-methylimidazolium-3-dicyanomethanide (0.50 g, 3.42 mmol) in acetonitrile (8 cm³) was treated with a solution of *N*-phenylmaleimide (0.59 g, 3.42 mmol) in acetonitrile (5 cm³). The mixture was stirred at ambient temperature for 2 h during which time the product, compound **132** precipitated as an orange solid (0.84 g, 77%), mp >300 °C. Evaporation of the filtrate led a dark red gum and no further product was isolated. (Found: C, 64.0; H, 3.75; N, 22.4. C₁₇H₁₁N₅O₂ requires C, 64.35; H, 3.5; N, 22.1%); $\nu_{\max}/\text{cm}^{-1}$ 3307 (NH), 2209 (C≡N), 1759, 1708 (C=O), 1614 (C=N); δ_{H} (DMSO-d₆) 4.28 (s, 3H, CH₃), 7.40-7.47 (m, 3H, H-3' and H-4' of N-Ph), 7.51-7.55 (m, 2H, H-2' of N-Ph), 8.16 (s, 1H, H-2), 8.44 (s, 1H, H-3); δ_{C} (DMSO-d₆) 38.2 (N-CH₃), 76.4 (C-8), 112.9 (C≡N), 113.8 (C-2), 127.9 (C-2'), 128.1 (C-7), 129.1 (C-4'), 129.6 (C-3'), 131.7 (C-3), 137.1 (C-1'), 140.7 (C-8a), 151.5 (C-5), 163.0 (C=O), 163.9 (C=O).

Reaction of 1-phenyl-1,2,4-triazolium-4-dicyanomethanide 1,3-dipole with DMAD: isolation of the initial cycloadduct

Synthesis of 1-phenyl-5,5-dicyano-6,7-dimethoxycarbonyl-5,8-dihydropyrrolo[1,2-*d*]1,2,4-triazole **143**

A solution of 1-phenyl-1,2,4-triazolium-4-dicyanomethanide 1,3-dipole (0.37 g, 1.77 mmol) in DMF (20 cm³), cooled to 0 °C, was treated with DMAD (0.218 cm³, 1.77 mmol), and allowed to stand at 0 °C for 4.5 h. The resulting mixture was filtered through a cooled funnel, and the filtrate added to ice-cold water. The resulting brown precipitate was collected on a jacketed sintered glass funnel at -5 °C, washed with ethanol (10 x 1 cm³, 0 °C) and diethyl ether (3 x 1 cm³, 0 °C). The crude product **143** cannot be purified further since it affords **144** by simple crystallization. Compound **143**: (0.44 g, 71%); δ_{H} (CD₃CN, 0 °C) 3.67 (s, 3H, OCH₃), 3.85 (s, 3H, OCH₃), 6.77 (s, 1H, H-7a), 6.92 – 6.96 (m, 2H, H-3 and H-4' of N-Ph) 7.27 – 7.32 (m, 2H, H-2' of N-Ph), 7.30 (s, 1H, H-3); δ_{C} (CD₃CN, 0 °C) 53.6 (OCH₃), 53.9

(OCH₃), 58.6 (C-5), 86.1 (C-7a), 109.6, 111.6 (C≡N), 113.6 (C-2'), 121.6 (C-4'), 127.5 (C-6), 129.6 (C-3') 138.5 (C-3), 143.2 (C-7), 148.4 (C-1'), 159.0 (C=O), 162.1 (C=O).

δ_H (CDCl₃, -10 °C) 3.70 (s, 3H, OCH₃), 3.96 (s, 3H, OCH₃), 6.59 (s, 1H, H-7a), 6.98 – 7.02 (m, 2H, H-3 and H-4' of N-Ph), 7.11 (s, 1H, H-3), 7.30 – 7.34 (m, 2H, H-2' of N-Ph).

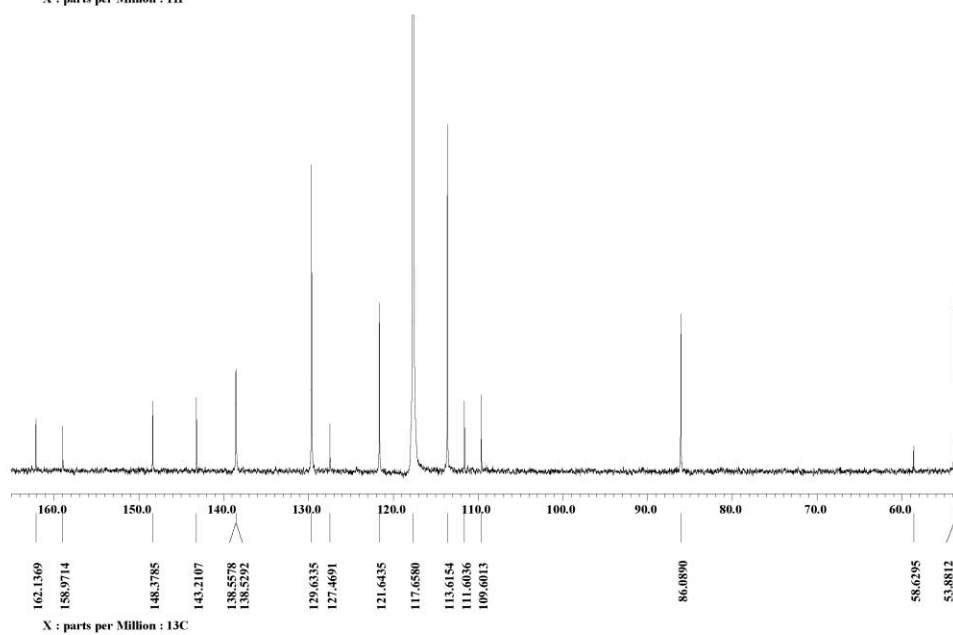
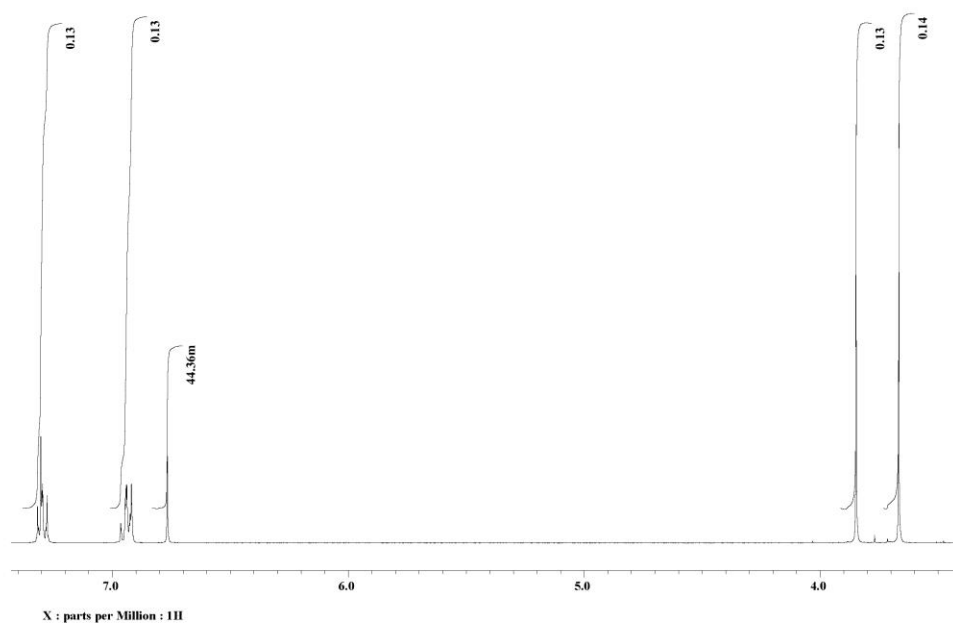
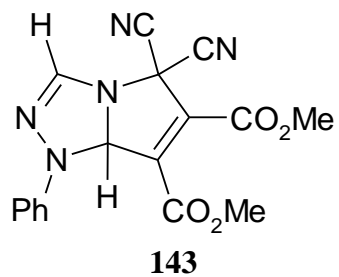
Reaction of 1-phenyl-1,2,4-triazolium-4-dicyanomethanide 1,3-dipole with DMAD: isolation of the ring expanded product

Synthesis of 1-phenyl-5-imino-6-cyano-7,8-dimethoxycarbonyl-1,2,4-triazolo[4,5-*a*]pyridine 144

A solution of **143** (0.20 g, 0.50 mmol) in CH₃CN (15 cm³) was stirred at 50 °C for 2 h and then ambient temperature for 50 h. Removal of the solvent under reduced pressure yielded compound **144** (0.16 g, 80%), mp 167 °C (lit.³⁵, mp 172-174 °C); (Found: C, 58.1; H, 3.8; N, 20.2. C₁₇H₁₃N₅O₄ requires C, 58.1; H, 3.7; N, 19.9%); ν_{max}/cm⁻¹ 3316 (NH), 2204 (C≡N), 1742, 1714 (C=O), 1624 (C=N); δ_H (CD₃CN) 2.96 (s, 3H, OCH₃), 3.85 (s, 3H, OCH₃), 7.39-7.41 (m, 2H, H-2' of N-Ph) 7.51-7.57 (m, 3H, H-3' and H-4' of N-Ph), 9.14 (s, 1H, H-3); δ_C (CD₃CN) 51.1 (OCH₃), 53.3 (OCH₃), 83.3 (C-6), 86.4 (C-8), 115.2 (C≡N), 124.5 (C-2'), 129.8 (C-3'), 129.9 (C-4'), 135.1 (C-3), 139.0 (C-7), 144.1 (C-8a), 149.1 (C-1'), 149.5 (C-5), 161.9 (C=O), 165.9 (C=O).

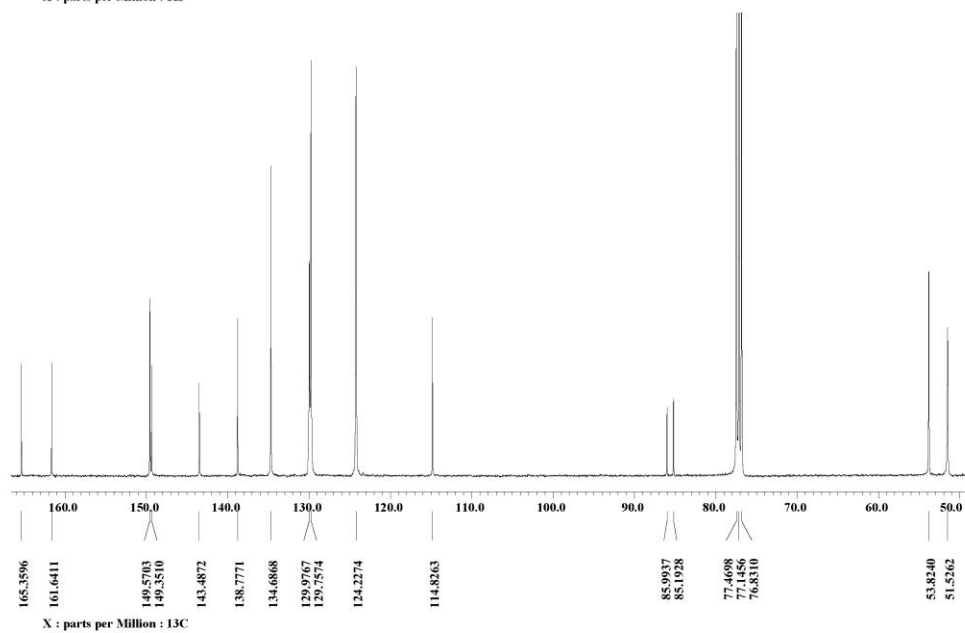
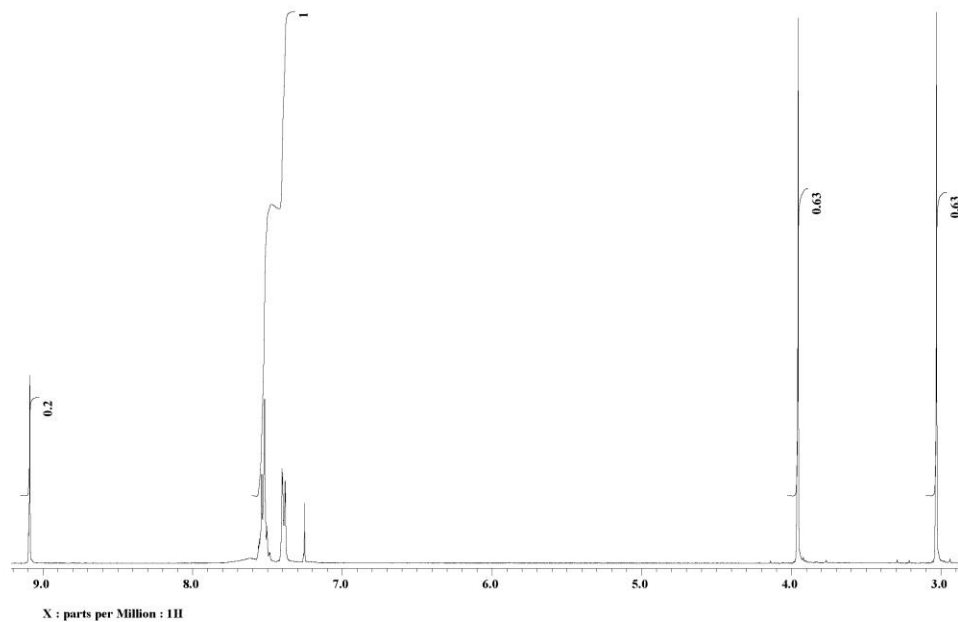
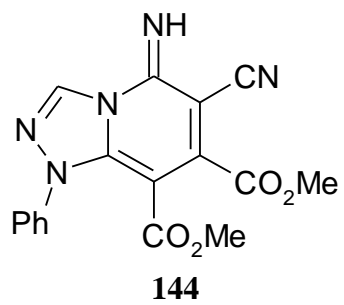
δ_H (CDCl₃) 3.03 (s, 3H, OCH₃), 3.96 (s, 3H, OCH₃), 7.38-7.40 (m, 2H, H-2' of N-Ph) 7.50-7.56 (m, 3H, H-3' and H-4' of N-Ph), 9.09 (s, 1H, H-3); δ_C (CDCl₃) 51.5 (OCH₃), 53.8 (OCH₃), 85.2 (C-6), 86.0 (C-8), 114.8 (C≡N), 124.2 (C-2'), 129.8 (C-3'), 130.0 (C-4'), 134.7 (C-3), 138.8 (C-7), 143.5 (C-8a), 149.4 (C-1'), 149.6 (C-5), 161.6 (C=O), 165.5 (C=O).

Chapter 2



^1H and ^{13}C NMR spectra for product **143** in CD_3CN at $0\text{ }^\circ\text{C}$

Chapter 2



^1H and ^{13}C NMR spectra for product **144** in CDCl_3

Chapter 3

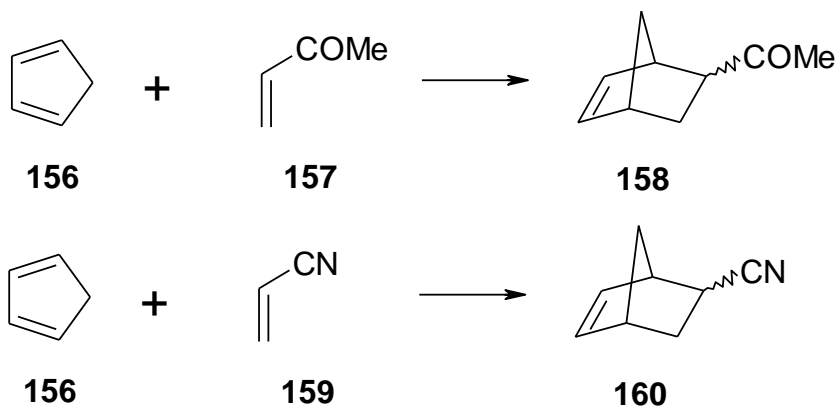
A study of synthesis, kinetics and water solvent effects in the reactions of phthalazinium-2-dicyanomethanide with *p*-substituted benzylidene acetones: comparisons with substituted styrenes and alkyl vinyl ketones

3.1 Introduction

Historically, chemists have avoided using water as a reaction medium for organic chemical reactions. Organic solvents have traditionally been selected based on their ability to dissolve reactants, thereby ensuring that the compounds are fully available for reaction. Water has also been eschewed in order to avoid hydrolysis and other unwanted interactions with reactants, intermediates and products.

However, interest in the use of water as a reaction solvent has greatly increased over the last number of years. In part, this can be associated with an increase in concern for the environment. Water is a green solvent, non-toxic, non-flammable and easily handled. Water is also abundantly available and relatively cheap to process. The replacement of organic solvents with water has the potential to have both positive environmental and financial impacts for the chemical industry.

The increased interest in water is also associated with the remarkable effects water can have on chemical reactions. Breslow⁸² was the first to report the increase in reaction rate associated with completing the Diels-Alder reaction in water. It was observed that the reaction of cyclopentadiene **156** and methyl vinyl ketone **157** to form compound **158** was more than 700 times faster in water than in the hydrocarbon solvent isooctane. Completing the reaction in methanol led to a modest 12-fold increase in rate over isooctane (**Scheme 49**). This suggested that the large rate increase in water was not simply due to a solvent polarity effect.



Scheme 49

The reaction of cyclopentadiene **156** with acrylonitrile **159** to form **160** was also investigated⁸² in various solvents (**Scheme 49**). A significant rate increase was observed on completing the reaction in water rather than isooctane. Once again, a more modest increase was observed on using methanol as solvent. Overall it was demonstrated that water had much more beneficial effect on the rate of the methyl vinyl ketone **157** reaction rather than the acrylonitrile **159** reaction (**Table 11**). Breslow⁸² proposed that the large rate acceleration observed was due to the hydrophobic effect.

Table 11: Kinetic data for the reactions of cyclopentadiene **156** with methyl vinyl ketone **157** and acrylonitrile **159**

Solvent	Additional Component	$k_2 / 10^{-5} (\text{M}^{-1}\text{s}^{-1})$ ^a	Relative Rate ^b
Cyclopentadiene 156 and methyl vinyl ketone 157 at 20 °C			
Isooctane	-	5.94	1.0
Methanol	-	75.5	12.0
Water	-	4400.0	740
Water	LiCl (4.86M)	10800.0	1818
Water	GnCl (4.86M)	4300	722
Cyclopentadiene 156 and acrylonitrile 159 at 30 °C			
Isooctane	-	1.9	1.0
Methanol	-	4.0	2.0
Water	-	59.3	31.0

^{a)} $\text{M}^{-1}\text{s}^{-1} = \text{dm}^3 \text{mol}^{-1}\text{s}^{-1}$ ^{b)} Relative to isooctane.

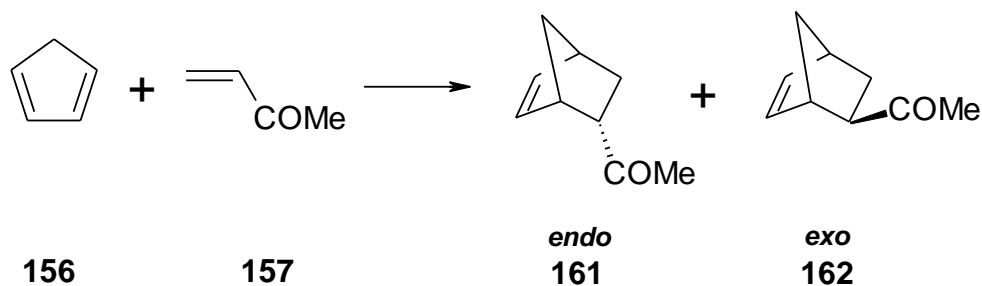
3.1.1 The hydrophobic effect

The hydrophobic effect is the tendency of non-polar species to aggregate in water solution so as to decrease the hydrocarbon-water interfacial area.⁸³ As such, it is specific example of solvophobicity. Breslow⁸⁴ has claimed that packing of the non-polar surfaces in the transition states of the reactions is favoured in water, thereby lowering the transition energies and increasing reaction rates.

Breslow has probed the hydrophobic effect by examining the effect of adding various salts to the reaction mixtures. Structure making salts, such as LiCl, were found to increase the hydrophobic effect by promoting electrostriction (increased structure making) of water. This decreases the solubility of organic molecules and thus promotes their association.⁸⁵ The effect parallels the technique of “salting out” used to drive the partition of an organic product into an organic layer during aqueous-organic solvent extractions by adding NaCl to the water. The increase in hydrophobic effect is accompanied by an increase in reaction rate. Completing the reaction of cyclopentadiene **156** with methyl vinyl ketone **157** in 4.86 molar LiCl solution increased the reaction rate 2.5 fold over that in pure water (**Table 11**).

Structure breaking salts (e.g. guanidinium chloride) had the opposite effect, causing a reduction in the hydrophobic effect. There was a 3 fold decrease in reaction rate when the reaction was completed in 4.86 molar GnCl solution versus the rate in pure water. Breslow⁸³ has suggested that the “salting in” effect observed with these salts is more complex than a simple structure breaking effect. The anti-hydrophobic effect of the salt is the result of directly solvating hydrocarbons rather than disrupting the water structure.

Breslow⁸⁶ has also demonstrated that completing reactions in water has the potential to influence the *endo/exo* ratio of products in a Diels-Alder reaction. The reaction of cyclopentadiene **156** with methyl vinyl ketone **157** (**Scheme 50**) displayed a large increase in the *endo/exo* ratio when completed in water (21.4) as opposed to excess cyclopentadiene **156** (3.85) or ethanol (8.5).



Scheme 50

Reactions with methyl acrylate **163**, dimethyl maleate **59** and methyl methacrylate **70** also display an increased preference for the *endo* cycloadduct in water (**Figure 56, Table 12**). The enhancements are not as large as experienced by methyl vinyl ketone **157**, but a clear trend of *endo*-isomer enhancement in water is apparent. Breslow⁸⁷ has suggested that hydrophobic effects favour the *endo* transition state due to its smaller exposed non-polar surface. The *endo*-transition states for these reactions are more compact than the *exo*-transition states, and so are more favoured when water is used as the reaction solvent.

This conclusion is supported by the impact of salts on the *endo/exo* ratio of reaction of cyclopentadiene **156** with methyl vinyl ketone **157** (**Scheme 50**). Adding LiCl to the reaction mixture increased the preference for the *endo* isomer by increasing the hydrophobic effect. The presence of guanidinium chloride had the opposite effect, leading to a decrease in the *endo-exo* ratio. Therefore the *endo-exo* ratio of this reaction in water can be manipulated by using salts to adjust the strength of the hydrophobic effect.

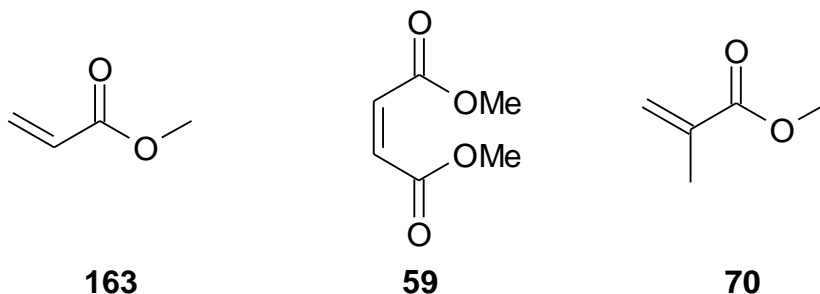


Figure 56

Table 12: Cycloadduct *endo/exo* ratios⁸⁶ for the reactions of cyclopentadiene **156** with selected dipolarophiles in various solvents

Solvent	Methyl vinyl ketone 157	Methyl acrylate 163	Dimethyl maleate 59	Methyl methacrylate 70
Cyclopentadiene	3.85	2.9	2.8	0.4
Ethanol	8.5	5.2	4.5	0.6
Water	21.4	9.3	13.7	1.4

Engberts⁸⁸ has used the term “enforced” hydrophobic interactions to distinguish the bonding of reactants during the activation process from other hydrophobic interactions which may lead to complexes of different geometries. The enforced hydrophobic aggregation of organic molecules results in an increase in the Gibbs free enthalpy of the starting materials. However the activated complexes and transition states of these reactions remain unaffected by hydrophobic effect and so overall there is a reduction in activation energy.^{89, 90} Engberts⁹¹ has also demonstrated that in addition to the hydrophobic effect, changes in hydrogen bonding effects during the activation process play a key role in rate enhancements.

3.1.2 Special hydrogen bonding

Water molecules will form H-bonds with reactants that contain hydrogen bond acceptors, both in the initial and reaction transition states. H-bonding lowers the energy of frontier molecular orbitals by reducing electron density and inter-orbital repulsion. Water H-bonding therefore has a similar effect to electron withdrawing substituents on frontier molecular orbitals.

The relative lowering of frontier molecular orbital energies impacts on a cycloaddition reaction's HOMO-LUMO energy gap. In cases where the gap is lowered the reaction rate will be increased. However, water H-bonding may also cause an increase in the HOMO-LUMO energy gap, and so lead to a decrease in reaction rate. The impact of H-bonding is therefore governed by the dominant HOMO-LUMO gap and the number and strength of hydrogen bond acceptors on the reactants (**Figure 57**).

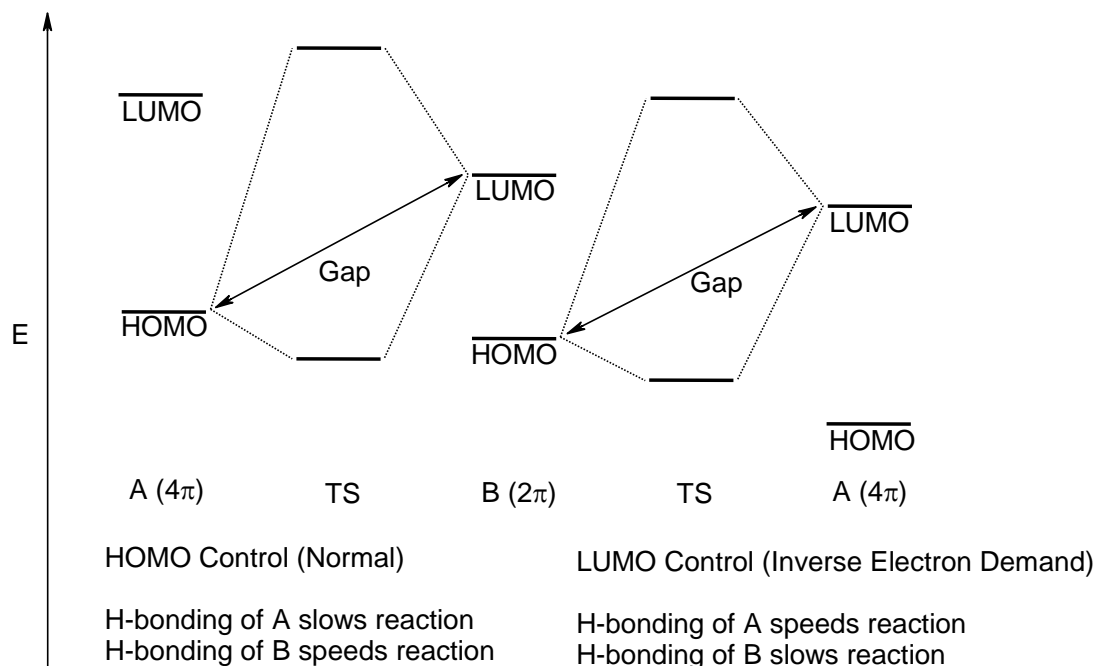
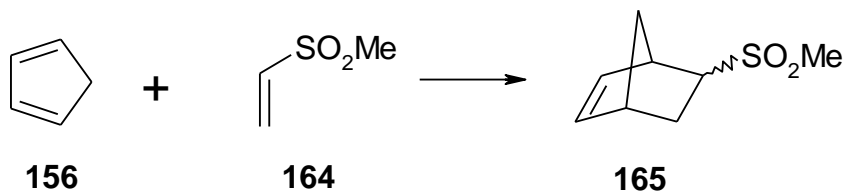


Figure 57

The reactions of cyclopentadiene **156** with two structurally related dienophiles, methyl vinyl ketone **157** (**Scheme 50**) and methyl vinyl sulfone **164** (**Scheme 51**), show the importance of hydrogen bonding interactions. Methyl vinyl sulfone **164** is a weaker H-bond acceptor than methyl vinyl ketone **157** due to the insulating effect of the sulfur atom.^{88, 92} The decreased sensitivity of methyl vinyl sulfone **164** to hydrogen bonds resulted in a smaller water related rate increase than that experienced by methyl vinyl ketone **157**. The reaction of cyclopentadiene **156** with methyl vinyl sulfone **164** also underwent much less pronounced accelerations in ethanol and hexafluoropropanol (**Table 13**).

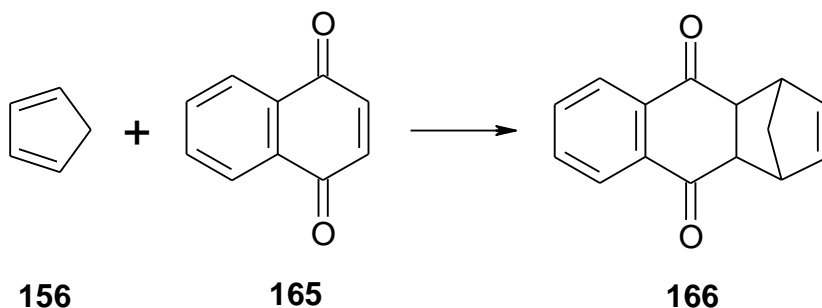


Scheme 51

Table 13: Relative rate constants⁹² of cyclopentadiene **156** with methyl vinyl ketone **157** and methyl vinyl sulfone **164** in water and organic solvents of different hydrogen bonding capacities

Dipolarophile	CH ₃ CN	EtOH	HFP	H ₂ O
methyl vinyl ketone 157	1	4.97	100	290
methyl vinyl sulfone 164	1	2.49	23	71

Jorgenson^{93,94} has stated that the hydrophobic effect contributes a relatively constant rate enhancement while special hydrogen bonding effects in the transition state are primarily responsible for large rate increases. Computer simulations⁹³ have been used to determine that the free energies of activation for the reactions of cyclopentadiene **156** with acrylonitrile **159**, methyl vinyl ketone **157** (Scheme 49) and naphthoquinone **165** (Scheme 52) were reduced by 1.5, 2.8 and 4.4 kcal mol⁻¹ respectively on going from gas phase to water solution. These values are in good agreement with experimental results for transfer from hydrocarbon solvents to water (2.1, 3.8 and 5.0 kcal mol⁻¹ respectively).

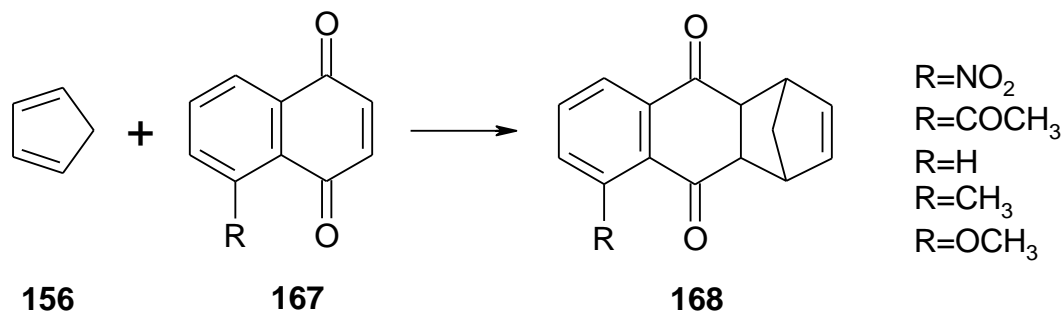


Scheme 52

It was concluded that the rate accelerations observed for these reactions is primarily due to enhanced hydrogen bonding between water molecules and the polarized transition states. The hydrophobic association of reactants was acknowledged as also contributing to the rate accelerations.

3.1.3 Polarity effects

Engberts⁸⁸ has also investigated the possibility that the activated complex in a Diels-Alder reaction may have more polar character in water than in other solvents. Water is a highly polar solvent, and so reactions with transition states more polar than the initial states would be expected to be faster in water. The Hammett rho value⁹⁵ (ρ) may be used to determine the polarity or development of charge in reaction transition states. The Diels-Alder reaction between 5-substituted-1,4-naphthoquinone **167** and cyclopentadiene **156** (Scheme 53) was chosen for investigation.



Scheme 53

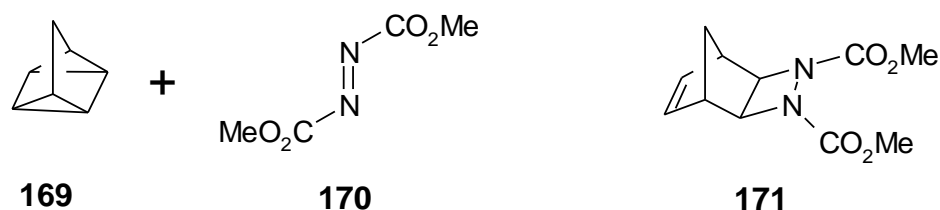
Hammett plots were used to assess the substituents effects on the reaction in water compared with a series of six organic solvents. Larger substituents effects in water than in the other solvents would be expected for an activated complex experiencing a larger build-up of charge in the water.

Considering that the substituents are three bonds away from the reacting double bond, the ρ -values obtained indicate that the activated complex is rather polar, even in organic solvents. Rho values of 1.6 and 1.3 were obtained for *n*-hexane and acetonitrile, respectively. Hammett plots in protic solvents, particularly water and hexafluoro-2-propanol (HFP), were strongly non-linear. This is in part due to unexpected solvent-dependent behaviour associated with the methoxy substituent. This substituent slowed the reaction in *n*-heptane as expected for a HOMO_{diene}-LUMO_{dienophile} controlled reaction. However the reaction was accelerated in water and HFP, possibly due to a solvent-mediated interaction between the methoxy group and the nearby carbonyl group. It was concluded that the charge separation in the activated complex in water was not dissimilar from that in the other solvents studied.

3.1.4 “On Water” reactions

Investigations into the use of water as solvent initially involved dilute, homogenous solutions in which both reactants were in the same phase. This allowed reaction kinetics to be measured directly and also satisfied the widely held belief that reactants must be in solution to react successfully. Breslow⁸⁷ and Grieco⁹⁶ provided rare examples of reactions completed in aqueous suspensions, however overall scant attention was paid to the kinetics of reactions under heterogeneous aqueous conditions.⁹⁷

In 2005, Sharpless⁹⁸ and co-workers demonstrated that a number of reactions involving water insoluble reactants undergo substantial rate accelerations when stirred in aqueous suspension. The reaction of quadricyclane **169** with dimethyl azodicarboxylate **170** (Scheme 54) in toluene or benzene at 80 °C requires 24 h or longer to reach completion. The “on water” reaction is completed in 10 minutes at ambient temperature.



Scheme 54

The “on water” method involves vigorously stirring water insoluble reactants with water to generate an aqueous suspension. As the reactants are initially floating on the surface of water, the term “on water” is used to describe the method. The reaction product is also typically water insoluble, allowing for easy isolation by phase separation or filtration.

It was demonstrated⁹⁸ that both the presence of water and a heterogeneous reaction mixture was crucial for the large rate increases. Methanol could be added to the quadricyclane **169** with dimethyl azodicarboxylate **170** (Scheme 54) reaction mixture with no impact on rate, up until the point the reaction mixture became homogenous. The presence of water in the reaction mixture however led to

significant rate increase compared the reaction completed in pure methanol. Completing the reaction “on perfluorohexane” only led to a modest rate increase relative to the neat reaction, indicating that heterogeneity alone was not the reason for the rate enhancements.

Table 14: Reaction of quadricyclane **169** with dimethyl azodicarboxylate **170** in various solvents⁹⁸

Solvent	Concentration	Time to Completion
Toluene	2	> 120 hours
MeOH	2	18 hours
Neat	4.53	48 hours
On perfluorohexane	4.53	36 hours
On water	4.53	10 min
MeOH/H ₂ O (3:1 homogeneous)	4.53	4 hours
MeOH/H ₂ O (1:1 heterogeneous)	4.53	10 min
MeOH/H ₂ O (1:3 heterogeneous)	4.53	10 min

In 2007, Marcus and Jung⁹⁹ proposed that the rate accelerations associated with “on water” reactions are due to the reactions occurring at the oil-water interface in the aqueous suspensions. In an “on water” reaction, vigorous stirring of the reaction mixture disperses the reactants in the form of oil droplets surrounded by water molecules. Approximately 25% of water molecules at the surface of the oil-water boundary have a free (or “dangling”) -OH group oriented into the organic phase (**Figure 58**). These groups play key role in catalyzing reactions through the formation of H-bonds.

The structural arrangement of water around a small hydrophobic solute in homogenous solution is different as “dangling” -OH groups are no longer found at the boundary. Instead the water molecules are arranged such that H-bonds are formed laterally along the boundary, and so there is no catalytic effect (**Figure 58**). A rate increase⁹⁹ of approximately 1.5×10^5 fold was estimated for the reaction of

quadricyclane **169** with dimethyl azodicarboxylate **170** (Scheme 54) due to the effects of Marcus trans-phase H-bonding.

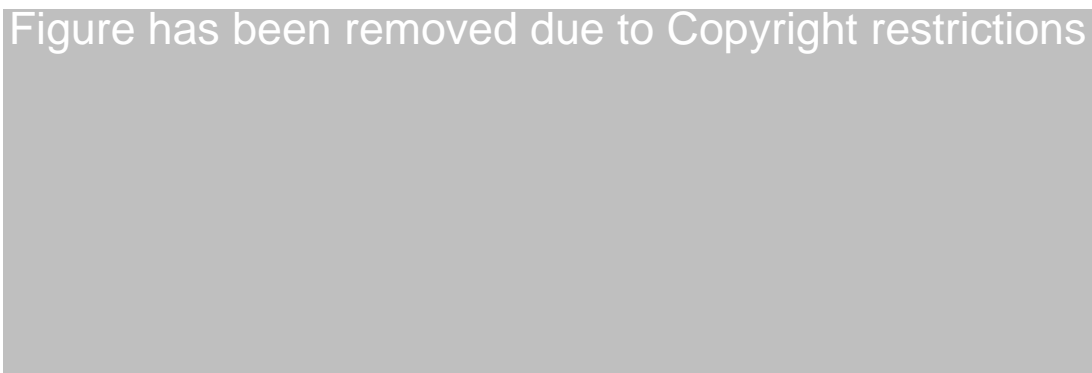


Figure 58: Depiction of the on water catalysis in comparison to the neat and aqueous homogeneous reactions⁹⁹

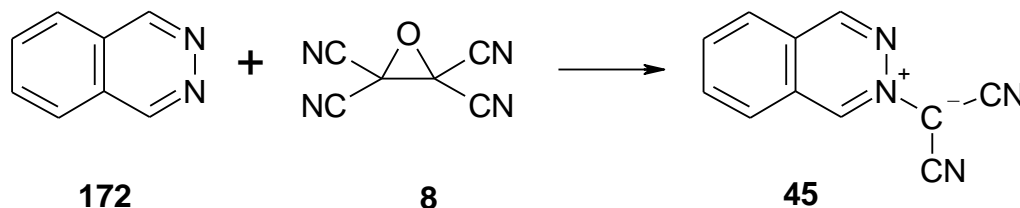
Our long standing interest in the impact of water on 1,3-dipolar reactions led us to explore the phthalazinium-2-dicyanomethanide 1,3-dipole **45** dipole system in more detail. The phthalazinium-2-dicyanomethanide 1,3-dipole **45** has been extensively studied in these laboratories^{31-34, 43}. It has been determined that dipole **45** is a Sustmann type II dipole. It can react *via* normal or inverse electron demand. The change in mechanism³³ is accompanied by a change in regiochemistry (**Section 1.4.2, Scheme 11**). Reactions between 1,3-dipole **45** and electron rich dipolarophiles are LUMO_{dipole} controlled while reactions with electron poor dipolarophiles are HOMO_{dipole} controlled.⁴³

Extensive kinetic studies^{34, 43, 44} have also revealed the beneficial impact of water on the reaction rates of 1,3-dipole **45**. The introduction of water as cosolvent into cycloaddition reactions of phthalazinium-2-dicyanomethanide **45** in acetonitrile gave small initial rate enhancements followed by larger rate increases as the mole fraction of the solvent mixture approached that of pure water. The influence of water on the rates was about 10 times larger for some dipolarophiles than for others, and these dipolarophiles, which were mainly vinyl ketones, were classified as water-super because of this. Other dipolarophiles, such as vinyl esters and vinyl nitriles showed smaller water effects and were classed as water-normal.

This chapter deals with the influence of water on the reactions of 1,3-dipole **45** with various dipolarophiles. Mechanistically, we were interested in determining if water influenced the polarity of cycloaddition transition states involving 1,3-dipole **45**. We were also interested in investigating the “on water” reactions of 1,3-dipole **45**, particularly those involving water-insoluble solids.

3.2 Synthesis of phthalazinium-2-dicyanomethanide 1,3-dipole **45**

A process similar to that used to generate the azolium 1,3 dipoles discussed in Chapter 2 was used to produce compound **45**. A cooled solution of phthalazine **172** in ethyl acetate was treated dropwise with a cooled solution of TCNEO **8** in ethyl acetate (**Scheme 55**). The temperature of the reaction was maintained below 12 °C. When the addition was complete the bright yellow compound **45** precipitated from solution in 92% yield. The structure was supported by IR, ¹H and ¹³C NMR spectra.



Scheme 55

The IR spectrum showed two strong cyano signals at 2191 and 2159cm⁻¹. NMR analysis was carried out using hexadeuteriomethyl sulfoxide (DMSO-d₆) at 80 °C due to the low solubility of **45** in other solvents. The proton adjacent to the quaternised nitrogen was the most deshielded in the H¹ NMR spectrum and appeared at δ 9.60 (**Figure 59**).

In the ¹³C NMR spectrum only one cyano group was observed at 117.2 ppm, the two cyano groups being NMR chemical shift equivalent, similar to the azolium dicyanomethanide 1,3-dipoles (**Section 2.2**). A very weak signal at 63.5 ppm was observed in the ¹³C NMR for the methanide carbon. A pulse delay of 10 seconds was used when the spectrum was being measured.

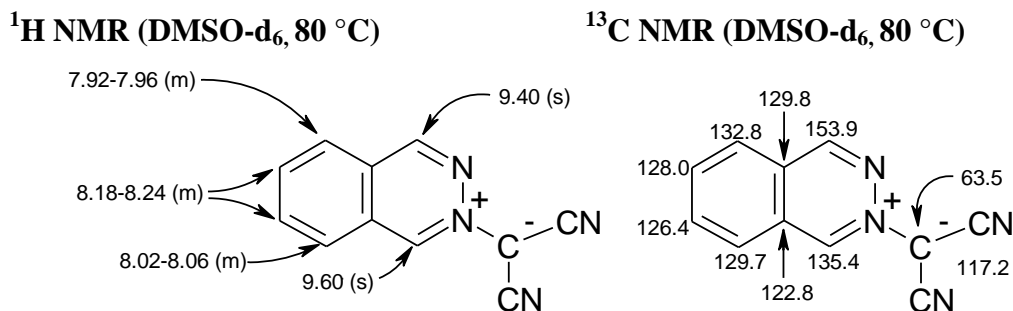
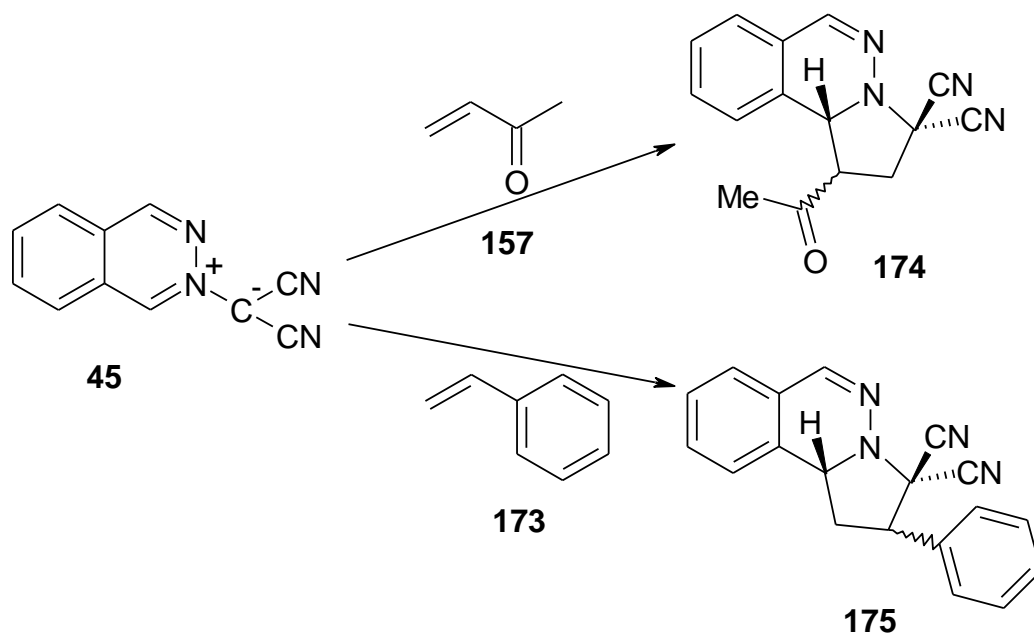


Figure 59: ^1H NMR and ^{13}C NMR assignments for compound **45**

3.3 Synthetic study of the reactions of phthalazinium-2-dicyanomethanide 1,3-dipole **45** with *p*-substituted benzylidene acetone dipolarophiles in acetonitrile

The benzylidene acetone molecule (systematic name: 4-arylbut-3-en-2-one) can be looked upon as comprising of two separate fragments- a styrene and an alkyl vinyl ketone. Styrene **173** is a water-normal dipolarophile while methyl vinyl ketone **157** is a water-super dipolarophile.^{34, 44} The synthetic course⁴³ of the separate reactions of **45** with styrene **173** and methyl vinyl ketone **157** is summarized below (**Scheme 56**).



Scheme 56

When both of the styrene and vinyl ketone features are included in a single dipolarophile (benzylidene acetone), the products **176** and **177** (**Figure 60**) might be expected from transition states comparable to those by which **174** and **175** are formed (**Scheme 56**). However activation energies calculated in collaboration with Prof. Luke Burke⁶³ predicted that the regiochemistry would be reversed.⁶³ The phthalazinium-2-dicyanomethanide 1,3-dipole **45** was reacted with a number of *p*-substituted benzylidene acetones in order to determine the regiochemistry of the reaction.

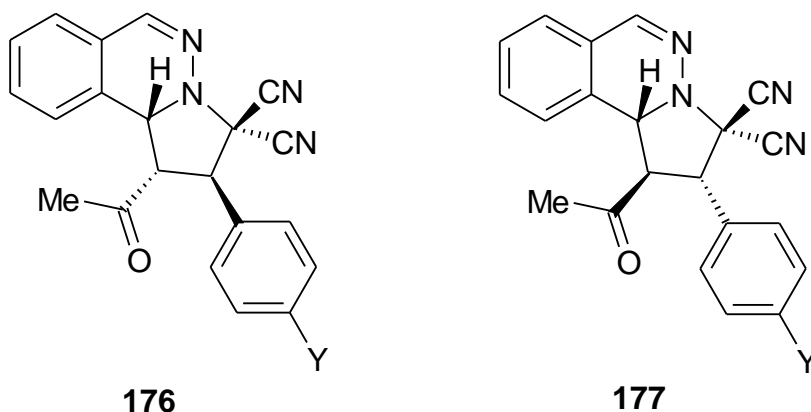
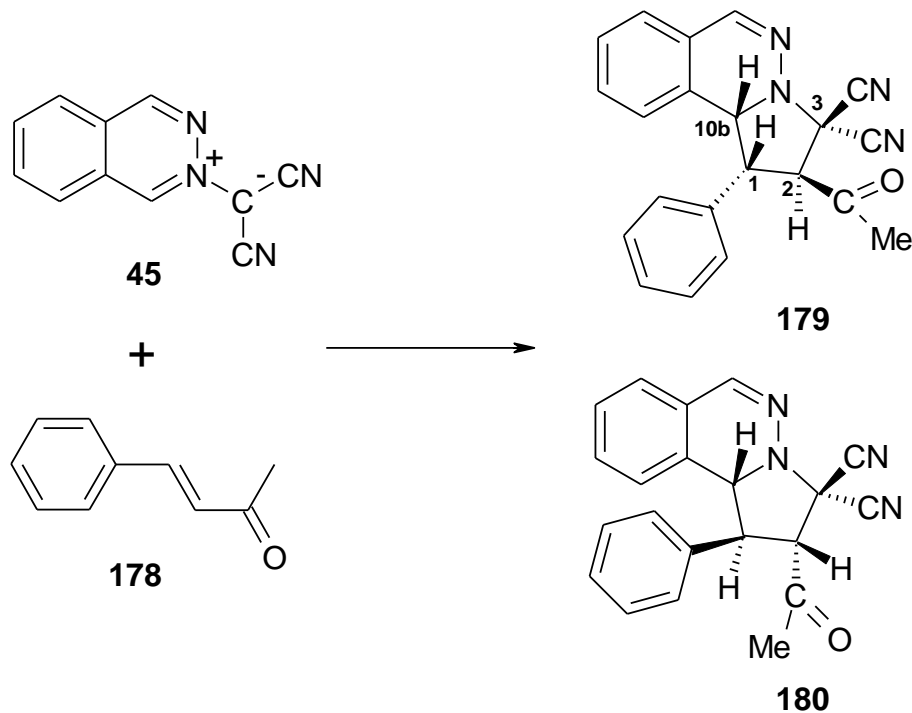


Figure 60

3.3.1 Cycloaddition reaction of phthalazinium-2-dicyanomethanide 1,3-dipole **45** with benzylidene acetone **178**

A suspension of the phthalazinium-2-dicyanomethanide 1,3-dipole **45** in acetonitrile was treated with benzylidene acetone (4-phenyl-3-buten-2-one) **178** and then stirred under reflux for 4.5 h (**Scheme 57**). The solvent was subsequently removed under vacuum and resulting residue taken up in ice-cold ether. This caused the major product **179** to separate as a yellow solid. The ethereal filtrate contained further **179**, the minor product **180**, excess dipolarophile **178** and unreacted 1,3-dipole **45**. Some intractable gum was also generated. The major product **179** was formed in 60% yield, the minor **180** in 6% yield. The expected products, based on the individual fragment reactions, **176** and **177**, were not observed. The structural assignment of the major compound **179** was supported by IR, ¹H NMR and ¹³C NMR spectroscopy.



Scheme 57

The IR spectrum of compound **179** contained a carbonyl band at 1720 cm^{-1} . The pyrrole ring protons were instrumental in determining the regiochemistry of the product. The lowest field signal of the three protons was assigned to H-10b, the highest to H-1, leaving H-2 in between. These pyrrole ring protons displayed a distinctive pattern in the ^1H NMR spectrum (**Figure 61**). H-C(10b) showed as a doublet at δ 5.24, H-C(1) as a doublet of doublets at δ 3.94 and H-C(2) as a doublet at δ 4.27. The structural assignment was found to be in agreement with calculations completed with ACD labs software (**Figure 61**).¹⁰⁰ The ^{13}C NMR spectrum (**Figure 61**) included two signals at 111.3 and 112.2 ppm corresponding to the two cyano groups present.

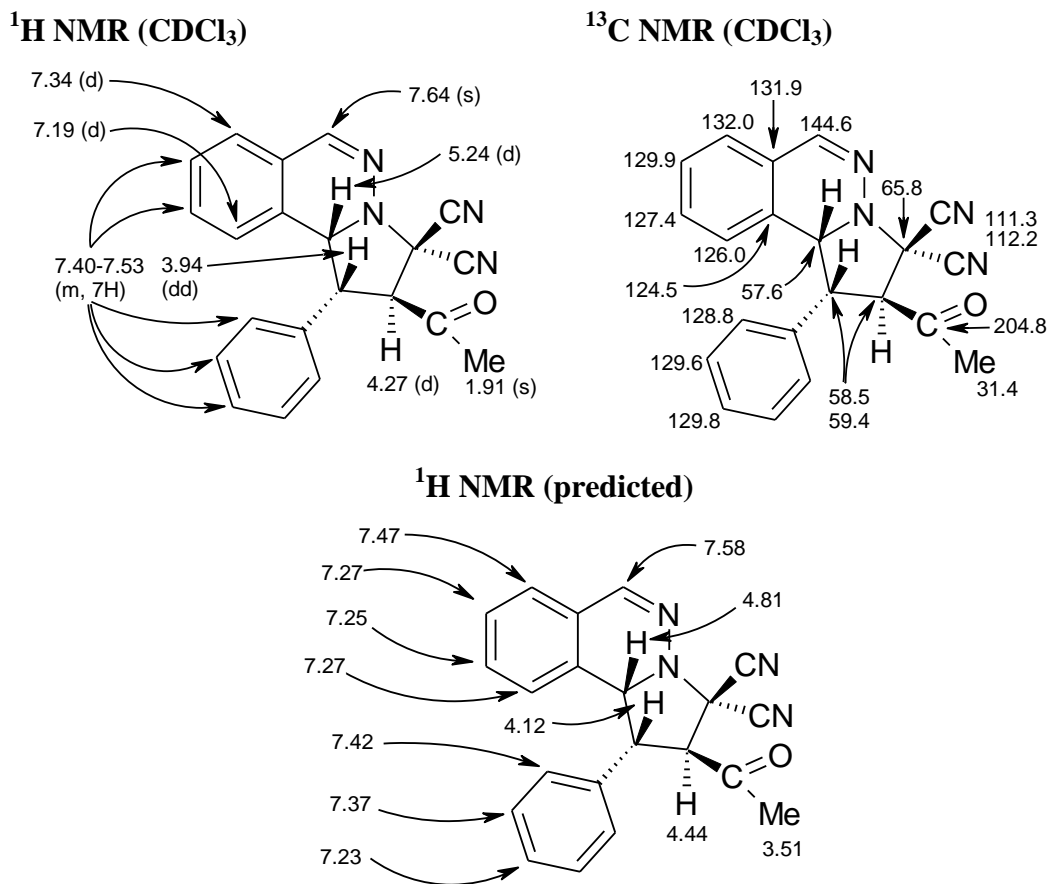


Figure 61: ^1H NMR and ^{13}C NMR assignments for compound **179**

The stereochemistry of **179** was supported by NOEDS. A strong NOE (12-15%) between H-C(10b) and H-C(1), and the absence of an NOE from either of these to H-C(2), indicated that the aryl and the acetyl substituents were in the *endo*- and *exo*-positions, respectively (**Figure 62**).

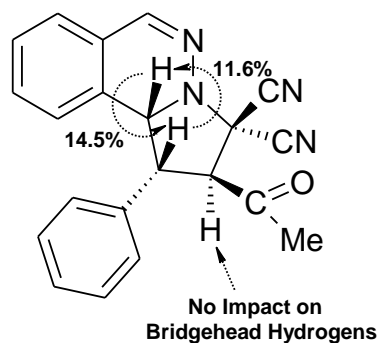


Figure 62: NOEDS enhancements of compound **179** in CDCl_3

Analysis of the ethereal filtrate provided the key pyrrole ring proton signals of the minor product (**Figure 63**). H-C(10b) showed as a doublet at δ 4.64, H-C(1) as a doublet of doublets at δ 3.80 and H-C(2) as a doublet at δ 4.21. The minor product's H-C(10b) proton was shifted upfield relative to the major product due to shielding from the *exo*-aryl group at C(1). The ratio of **179/180** generated in the reaction mixture was \sim 10:1. No interconversion or changes in the products took place under the reaction and workup conditions.

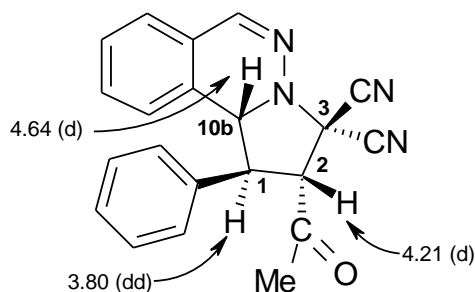
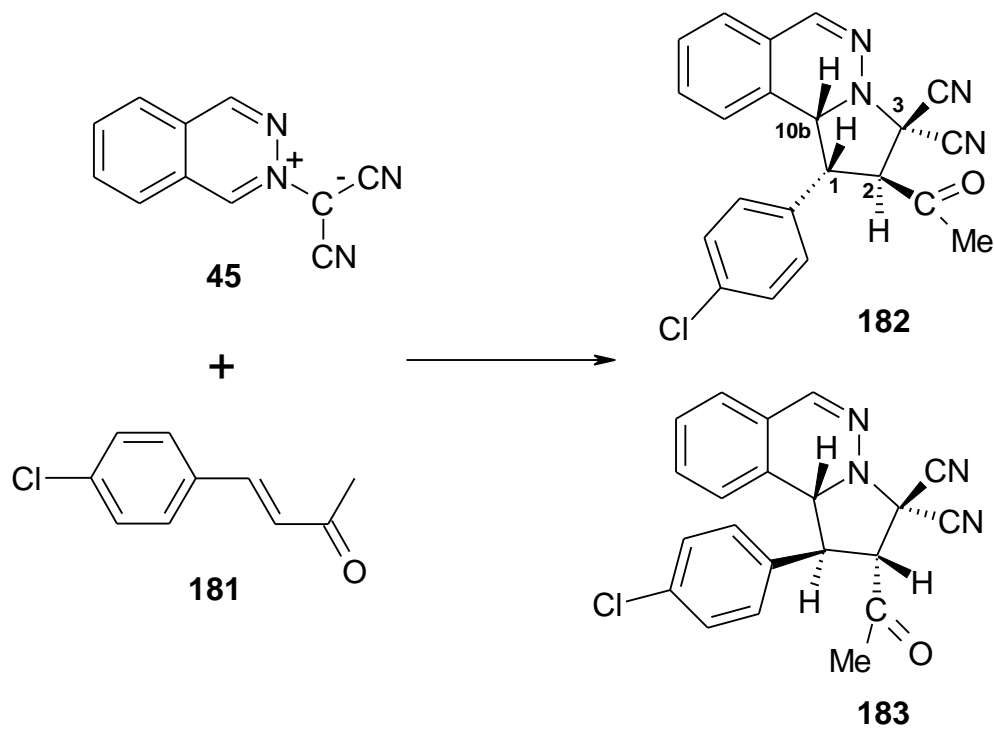


Figure 63: Key ^1H NMR signals of compound **180** in CDCl_3

3.3.2 Cycloaddition reaction of phthalazinium-2-dicyanomethanide 1,3-dipole **45** with *p*-chlorobenzylidene acetone **181**

A suspension of the phthalazinium-2-dicyanomethanide 1,3-dipole **45** in acetonitrile was treated with *p*-chlorobenzylidene acetone (4-(4-chlorophenyl)-3-buten-2-one) **181** and then stirred under reflux for 4 h (**Scheme 58**). The solvent was subsequently removed under vacuum to afford a gummy orange solid. The residue was taken up in ice-cold ether causing the major product **182** to separate as a white solid. The ethereal filtrate contained further **182**, the minor product **183**, excess dipolarophile **181** and unreacted 1,3-dipole **45**. Some intractable gum was also generated. The major product **182** was formed in 52% yield, the minor **183** in 5% yield. The assignment of the major compound **182** was supported by IR, ^1H NMR and ^{13}C NMR spectroscopy.



The IR spectrum of compound **182** contained a carbonyl band at 1725 cm^{-1} . The key pyrrole ring protons displayed a similar pattern in the ^1H NMR spectrum (**Figure 64**) to that observed for compound **182**. H-C(10b) appeared as a doublet at δ 5.25, H-C(1) as a doublet of doublets at δ 3.86 and H-C(2) as a doublet at δ 4.26. The regiochemistry of the product was assigned with reference to **182**. The ^{13}C NMR spectrum (**Figure 64**) included two signals at 111.2 and 111.9 ppm corresponding to the two cyano groups present.

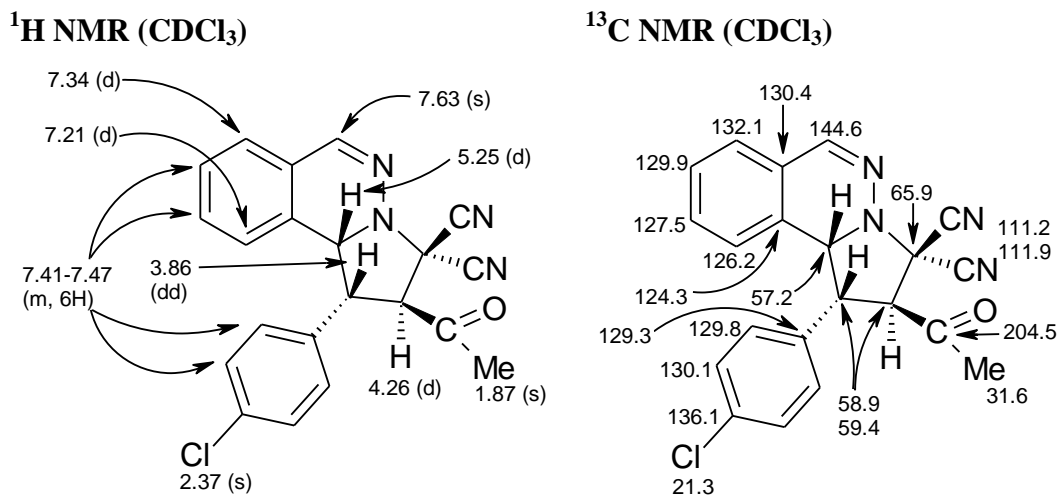


Figure 64: ^1H NMR and ^{13}C NMR assignments for compound **182**

A strong NOE (10-15%) between H-C(10b) and H-C(1), combined with the absence of an NOE from either of these protons to H-C(2), indicated that the aryl and the acetyl substituents were in the *endo*- and *exo*- positions, respectively (**Figure 65**).

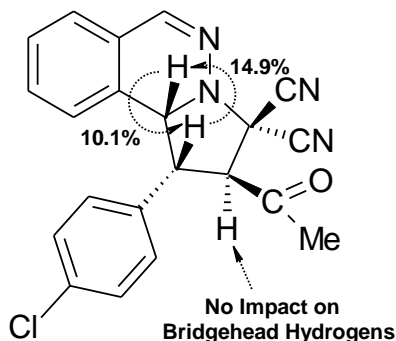


Figure 65: NOEDS enhancements of compound **182** in CDCl_3

Analysis of the ethereal filtrate provided the key pyrrole ring proton signals of the minor product **183** (**Figure 66**). H-C(10b) showed as a doublet at δ 4.66, H-C(1) as a doublet of doublets at δ 3.67 and H-C(2) as a doublet at δ 4.19. The minor product's H-C(10b) proton was shifted upfield relative to the major product due to shielding from the *exo*-aryl group at C(1). The stereochemistry of **183** was supported by NOEDS. An NOE of 7-9% was observed between H-C(2) and H-C(10b), indicating that the aryl and the acetyl substituents were in the *exo*- and *endo*- positions, respectively. The ratio of **182/183** produced in the reaction mixture was ~10:1.

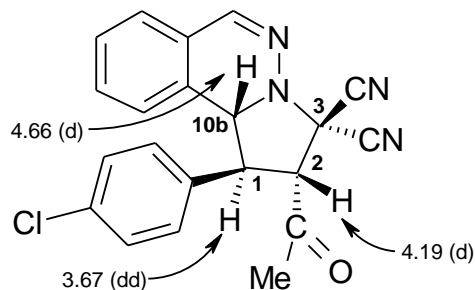
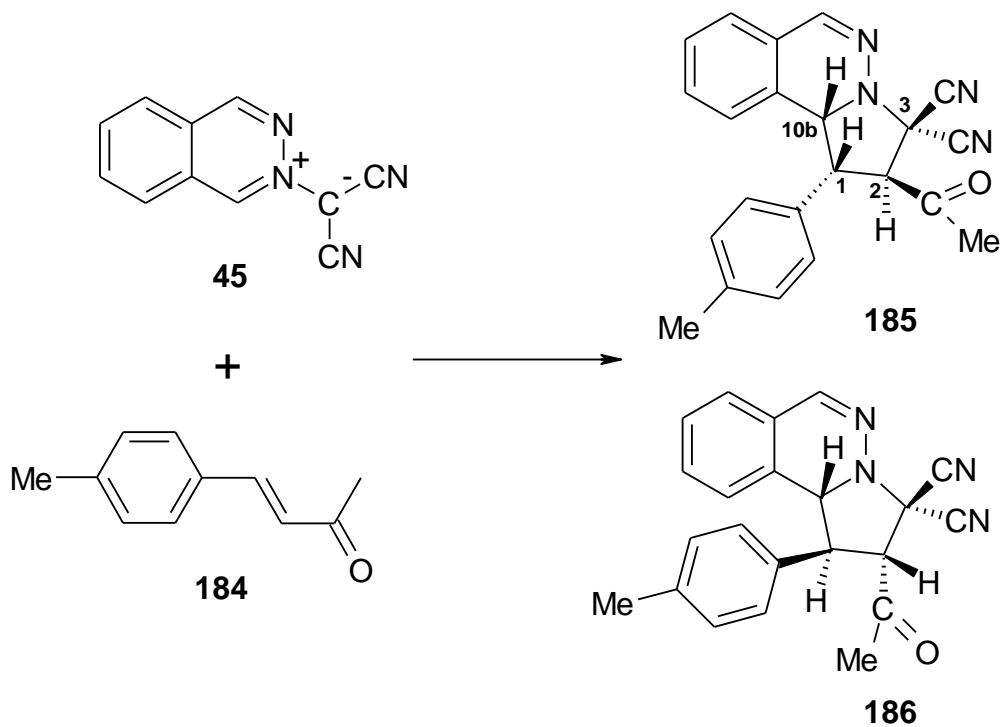


Figure 66: Key ^1H NMR signals of compound **183** in CDCl_3

3.3.3 Cycloaddition reaction of phthalazinium-2-dicyanomethanide 1,3-dipole **45** with *p*-tolylbenzylidene acetone **184**

A suspension of the phthalazinium-2-dicyanomethanide 1,3-dipole **45** in acetonitrile was treated with *p*-tolylbenzylidene acetone (4-(4-methylphenyl)-3-buten-2-one) **184** and then stirred under reflux for 5 h (**Scheme 59**). The solvent was subsequently removed under vacuum to afford a brown gummy residue. The residue was taken up in ice-cold ether causing the major product **185** to separate as a yellow solid. The ethereal filtrate contained further **185**, the minor product **186**, excess dipolarophile **184** and unreacted dipolarophile **45**. Some intractable gum was also generated. The major product **185** was formed in 69% yield, the minor **186** in 8% yield. The assignment of the major compound **185** was supported by IR, ^1H NMR and ^{13}C NMR spectroscopy.



Scheme 59

The IR spectrum of compound **185** contained a carbonyl band at 1725 cm^{-1} . The key pyrrole ring protons were clearly visible in the ^1H NMR spectrum (**Figure 67**). H-C(10b) appeared as a doublet at δ 5.22, H-C(1) as a doublet of doublets at δ 3.93 and H-C(2) as a doublet at δ 4.23. The regiochemistry of the product was assigned with reference to **182**. The ^{13}C NMR spectrum (**Figure 67**) included two signals at 111.3 and 112.3 ppm corresponding to the two cyano groups.

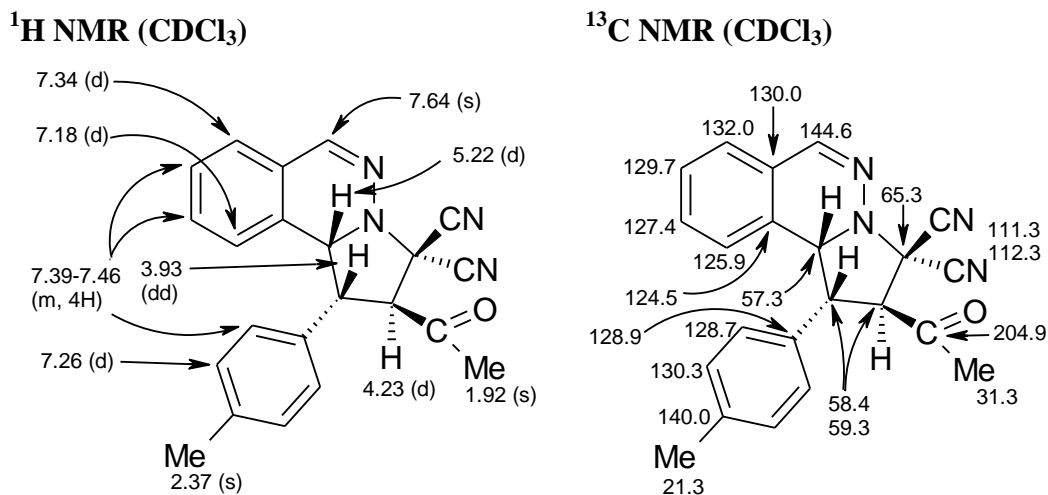


Figure 67: ^1H NMR and ^{13}C NMR assignments for compound **185**

The assignment of **185** was supported by NOEDS. A strong NOE (13-18%) was observed between H-C(10b) and H-C(1). There was no NOE from either of these protons to H-C(2). This supports the assignment of the aryl and the acetyl substituents in the *endo*- and *exo*- positions respectively (**Figure 68**).

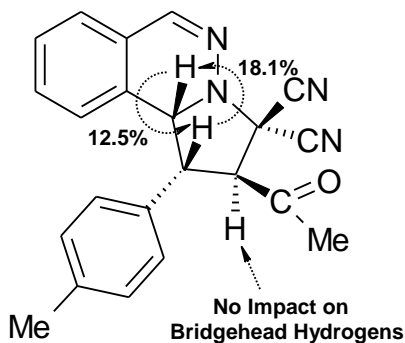


Figure 68: NOEDS enhancements of compound **185** in CDCl_3

Analysis of the ethereal filtrate provided the key pyrrole ring proton signals of the minor product (**Figure 69**). H-C(10b) showed as a doublet at δ 4.63, H-C(1) as a doublet of doublets at δ 3.69 and H-C(2) as a doublet at δ 4.11. The minor product's H-C(10b) proton was shifted upfield relative to the major product due to shielding from the *exo*-aryl group at C(1). The ratio of **185/186** generated in the reaction mixture was \sim 10:1.

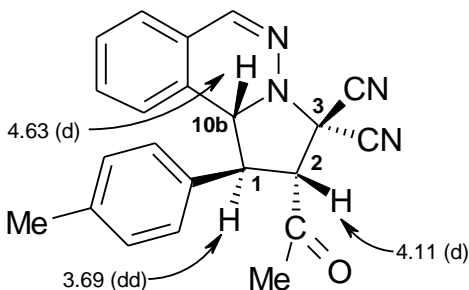


Figure 69: Key ^1H NMR signals of compound **186** in CDCl_3

3.4 Kinetic study of the reactions of phthalazinium-2-dicyanomethanide 1,3-dipole **45** with *p*-substituted benzylidene acetone dipolarophiles

The rates of reaction of 1,3-dipole **45** with a number of benzylidene acetone dipolarophiles were measured by following the disappearance of the dipole using UV-Vis spectroscopy. The wavelength of maximum absorbance (λ_{max}) was 423 nm in acetonitrile and 411 nm in (9:1 mole ratio) water/acetonitrile. The dipolarophile concentration ranged from 20 to 600 molar excess depending on the dipolarophile used. The rates were measured under pseudo-first order conditions at 37 °C for all reactions. Three different concentrations of dipolarophile were used in order to determine the second order rate constant. All kinetic measurements were repeated three times.

Table 15: Rate data for *p*-substituted benzylidene acetones with 1,3-dipole **45** in acetonitrile and aqueous acetonitrile at 37 °C (k_2 : $\text{dm}^3 \text{mol}^{-1} \text{s}^{-1}$)

Dipolarophile	k_2 CH_3CN	k_2 $\text{H}_2\text{O}/\text{CH}_3\text{CN}$ (0.9/0.1)	k_2 ratio ^a
benzylidene acetone 178	7.20×10^{-4}	2.40×10^{-2}	33
<i>p</i> -chlorobenzylidene acetone 181	9.20×10^{-4}	9.98×10^{-3}	11
<i>p</i> -tolylbenzylidene acetone 184	6.35×10^{-4}	7.52×10^{-3}	12

a) Measured k_2 $\text{H}_2\text{O}/\text{CH}_3\text{CN}$ (9.0:1.0 mole ratio) / k_2 CH_3CN

The benzylidene acetone dipolarophile was chosen for study as it contains two distinctive structural fragments- an alkyl vinyl ketone and a styrene. These fragments share the same double bond. Individually, both of these fragments are accelerated in water, but to differing extents. A ketone conjugated to a double bond is a common feature of water-super dipolarophiles.⁴⁴ Styrenes are water-normal dipolarophiles.³⁴ The benzylidene acetones therefore contain elements of both water-super and water-normal dipolarophiles.

The reaction rate measurements indicate that the benzylidene acetones are water-super dipolarophiles^{34, 63} as there is a <10 fold increase in rate on switching from pure acetonitrile to (9:1 mole ratio) water/acetonitrile. Despite containing a water-normal structural fragment, the presence of a ketone conjugated to a double bond is sufficient to ensure that reactions of the benzylidene acetones are strongly accelerated in the presence of water.

3.4.1 Water and polarity of the transition state: Hammett plots

Previous studies on the reactions of the 1,3-dipole **45** in water indicate that the growth of water clusters plays a significant role in accelerating the reactions of water-super dipolarophiles.^{34, 44} In addition to the pervasive hydrophobic effect and special hydrogen bonding effects, transition state polarity changes may contribute to rate accelerations in water. We were therefore interested to see if there was an increase in polarity of the cycloaddition transition states for the reactions of 1,3-dipole **45** and the benzylidene acetones on completing the reactions in water. We wished to explore the possibility that there was a cooperative increase in the polarity of the transition state as each bridging water molecule bound to the growing water cluster.

The Hammett rho value (ρ) has been used extensively to quantify the effect of electron donating and electron withdrawing groups on the transition states of various reactions. This allows the measurement of polarity or charge development in the transition state of a reaction. Hammett plots were measured for the reactions

between 1,3-dipole **45** and the benzylidene acetones in order to identify any changes in transition state polarity on completing the reaction in the presence of water.

On plotting the log of the rate constant against the Hammett σ^+ values,⁹⁵ the ρ value in acetonitrile was found to be +0.35. This ρ value is in good agreement with this reaction being a $\text{HOMO}_{\text{dipole}}$ controlled process where electron withdrawing groups enhance the rate by lowering the $\text{LUMO}_{\text{dipolarophile}}$ energy. The magnitude of this ρ value suggests little charge build up in the transition state. This indicates that the reaction proceeds *via* a concerted orbital controlled cycloaddition mechanism.

The ρ value in water/acetonitrile (9:1 mole ratio) was found to have increased slightly to +0.58. This minor change does not suggest a significant increase in the polarity of the transition state in the presence of water. Therefore the rate accelerations associated with completing these reactions in water are not related to an increase in transition state polarity. Further measurements were hampered by the availability of suitable dipolarophiles, and so a theoretical study was completed to explore this area further.

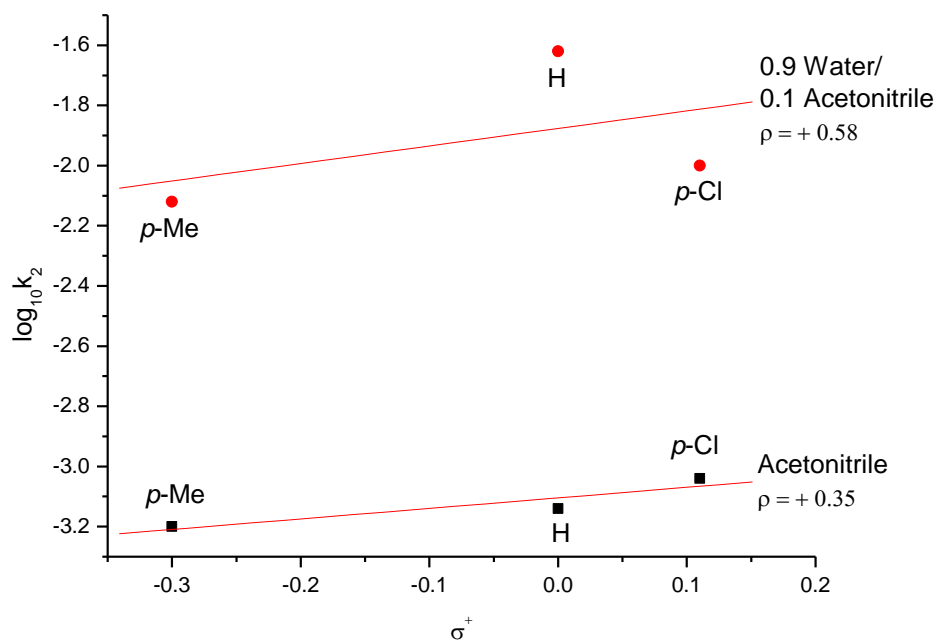


Figure 70: Hammett plot of 1,3-dipole **45** and *p*-substituted benzylidene acetones in acetonitrile and aqueous acetonitrile at 37 °C

3.5 Computational study

3.5.1 Calculations with 0-water and 4-water clusters

A theoretical study was completed in conjunction with Prof. Luke A. Burke of Rutgers University. Calculations were completed with the Gaussian 03 suite of programs using the B3LYP DFT method and the 6-31G(d) basis set. Calculations were carried out on the reactants and the transition state, each with 0 or 4 water molecules in a cage-like structure. Care was taken that the aryl substituents were internally oriented the same way in the reactants and the transition state structures.

The activation energies (E_a), activation entropies (S_a) and activation free energies (G_a) were calculated for the reactions of 1,3-dipole **45** with a series of *p*-substituted benzylidene acetones (**Table 16**). The rate ratios reported are based on the following equation:

$$k_Y/k_H = e^{(E_{a1}/RT)/e^{(E_{a2}/RT)}}$$

The activation energy (E_a), rather than activation free energy (G_a), was used in these calculations as the rate ratios were required for the construction of a Hammett plot.

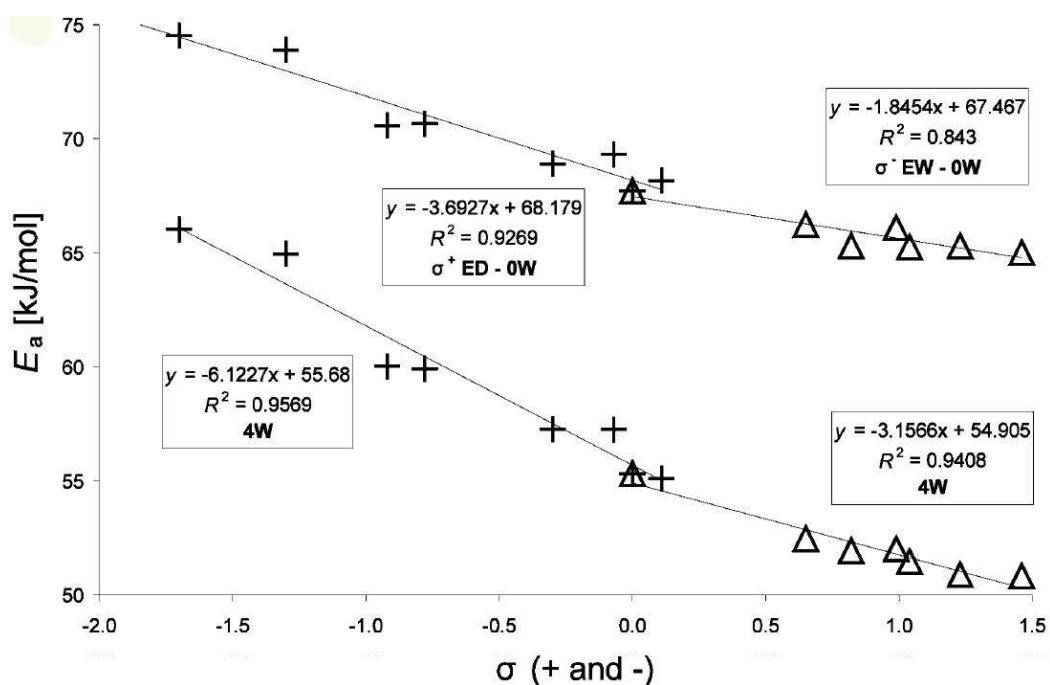
The results indicate that the reactions of dipolarophiles with electron withdrawing substituents have lower activation energies than those with electron donating substituents. This is consistent with the reaction being a $\text{HOMO}_{\text{dipole}}$ controlled process where electron withdrawing groups lower the $\text{LUMO}_{\text{dipolarophile}}$ energy. Activation energies are further reduced when the 4-water cluster is included in the calculations. A water dimer was originally chosen, but the optimisation procedures brought the dimer from a higher energy structure, where two H-atoms of the dimer were bonded to the oxygen of the carbonyl, to another structure in which the dimer fitted in to the notch between the oxygen of the carbonyl and the benzylidene CH group. This structure was not predominant in a previous theoretical study with MVK.⁴⁴ The 4-water cluster remained attached to the oxygen of the carbonyl group throughout the optimization process.

Table 16: Theoretical calculations for *p*-substituted benzylidene acetones. Activation energy E_a in kJ mol^{-1} , activation entropy S_a in $\text{J mol}^{-1} \text{K}^{-1}$, free energy of activation G_a in kJ mol^{-1}

Y	Keto Position	0-Water			Log (k_Y/k_H)	4-Water			Log (k_Y/k_H)
		E_a	$-S_a$	G_a		E_a	$-S_a$	G_a	
H	2-endo	67.71	214.15	134.68	0.000	55.30	228.05	125.63	0.000
	1-endo	74.85	207.13	138.96					
	2-exo	73.34	204.40	136.64		62.81	215.20	129.42	
	1-exo	74.31	203.89	137.45					
Me ₂ N	2-endo	74.54	217.86	142.05	-1.151	66.04	233.26	137.93	-1.810
NH ₂	2-endo	73.90	212.55	140.30	-1.043	64.95	229.07	135.37	-1.625
OH	2-endo	70.57	213.46	137.28	-0.483	60.02	229.02	130.50	-0.785
Me	2-endo	68.90	213.33	135.63	-0.201	57.25	225.15	129.23	-0.329
	1-endo	75.04	203.69	138.10					
	2-exo	74.06	211.16	139.63					
	1-exo	73.91	207.00	138.01					
MeO	2-endo	70.66	211.35	136.59	-0.498	59.91	229.36	130.79	-0.777
	1-endo	75.14	203.84	138.26					
	2-exo	75.17	207.99	139.82					
	1-exo	74.60	202.27	137.26					
F	2-endo	69.31	213.76	136.12	-0.270	57.25	227.47	127.33	-0.328
Cl	2-endo	68.16	210.78	133.91	-0.076	55.08	229.71	126.40	0.037
	1-endo	74.44	206.37	138.20					
	2-exo	72.98	207.84	137.50					
	1-exo	74.08	204.79	137.61					
CHO	2-endo	65.25	212.81	131.61	0.415	51.45	231.81	123.63	0.650
Ac	2-endo	65.30	212.77	131.86	0.406	51.92	230.75	123.77	0.570
CF ₃	2-endo	66.22	215.27	133.33	0.251	52.45	235.73	125.54	0.480
CN	2-endo	66.09	213.30	132.65	0.272	52.00	231.32	123.94	0.556
NO	2-endo	64.99	212.28	131.20	0.458	50.80	232.45	123.32	0.759
NO ₂	2-endo	65.29	209.81	130.79	0.408	50.87	230.88	122.79	0.747
	1-endo	71.98	207.74	136.18					
	2-exo	70.25	208.23	135.04					
	1-exo	70.77	207.38	135.1					

3.5.2 Plot of activation energy versus Hammett constants

A plot of activation energy versus Hammett constants further illustrates the effect of the substituents on the reactions of 1,3-dipole **45** with *p*-substituted benzylidene acetones (**Figure 71**). The best correlation was achieved when the substituents were grouped into σ^+ and σ^- Hammett constants. Electron donating groups by resonance (including *p*-Cl and *p*-F) were assigned σ^+ values while electron withdrawing substituents were assigned σ^- Hammett constants. Both groups gave rise to negative slopes, however the electron donating groups gave larger absolute values.



Note 1: ED and EWD refer to electron donating and electron withdrawing groups (by resonance) respectively

Note 2: 0W and 4W refers to water clusters comprised of zero and four water molecules, respectively

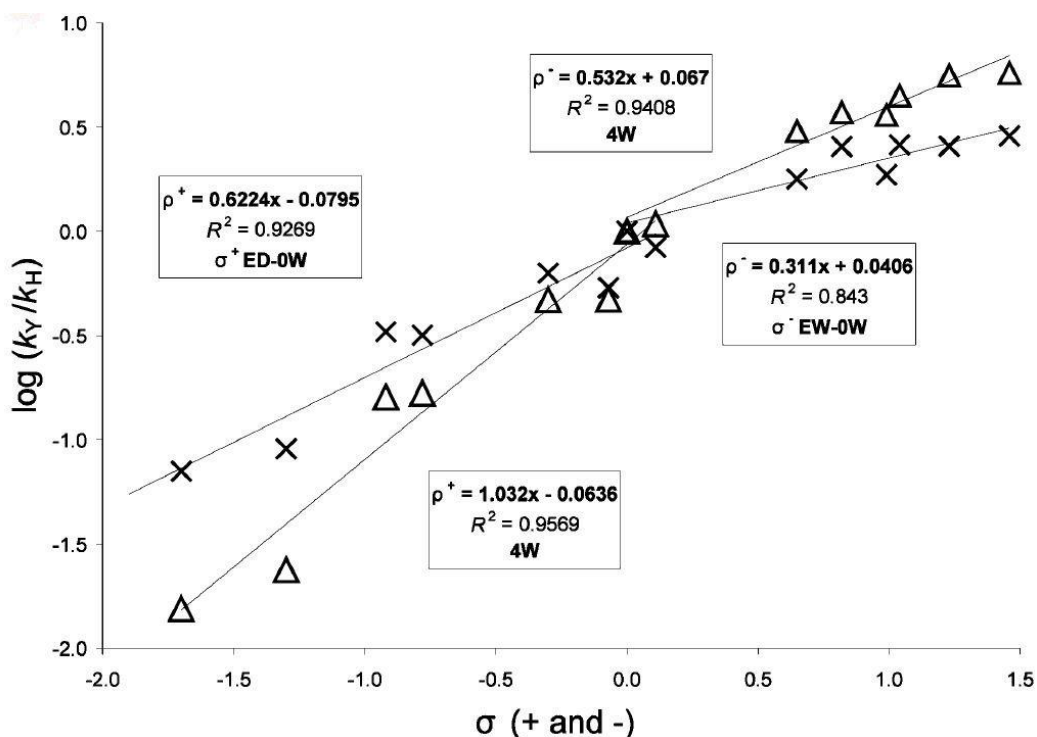
Note 3: Pluses (+) represent electron donating groups, triangles (Δ) electron withdrawing groups

Figure 71: Plot of activation energy (E_a) versus Hammett constants for the reaction of 1,3-dipole **45** with *p*-substituted benzylidene acetones

The plot demonstrates that the presence of the 4-water cluster leads to a reduction in the activation energy of the reaction. Therefore the rate enhancement observed on completing these reactions in water is associated with the presence of H-bonded water clusters attached to the carbonyl group.

3.5.3 Theoretical Hammett plot

A theoretical Hammett plot was also created using calculated reaction rates for a variety of *p*-substituted benzylidene acetones (**Figure 72**). Once again, both σ^+ and σ^- Hammett constants were used depending on the nature of the dipolarophile. This leads to four separate ρ values, two for the reactions with 0 water molecules present and two for the reactions with the 4-water cluster present (**Table 17**).



Note 1: ED and EWD refer to electron donating and electron withdrawing groups (by resonance) respectively

Note 2: 0W and 4W refers to water clusters comprised of zero and four water molecules respectively

Note 3: Crosses (X) represent electron donating groups, triangles (Δ) electron withdrawing groups

Figure 72: Theoretical Hammett plots for the reaction of 1,3-dipole **45** with *p*-substituted benzylidene acetones.

In all cases the ρ values are positive and quite small. The magnitude of the ρ value suggests little charge build up in the transition state. There are slight increases in the ρ values in the presence of the 4-water cluster, however these increases are minor in nature and do not suggest a significant increase in polarity of the transition state. The

theoretical results are in good agreement with the experimentally derived results. Therefore it is concluded that increased polarity of the cycloaddition transition state is not responsible for the rate accelerations observed in the presence of water.

Table 17: Experimental and theoretical ρ values for the reaction of 1,3-dipole **45** with *p*-benzylidene acetones

	Experimental (ρ^+)	Theoretical (ρ^+)	Theoretical (ρ^-)
Water Absent	+ 0.35 ^a	+ 0.62 ^c	+ 0.31 ^c
Water Present	+ 0.58 ^b	+ 1.03 ^d	+ 0.53 ^d

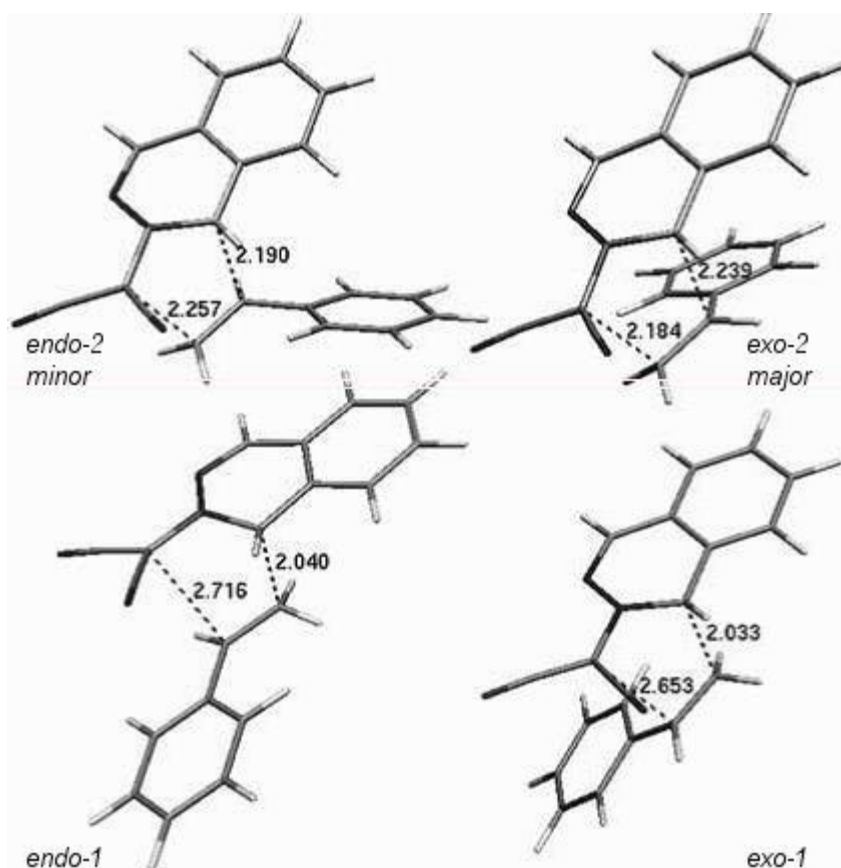
^{a)} Measured in acetonitrile, ^{b)} Measured in 0.9 mole fraction water/acetonitrile,

^{c)} Calculated based on 0-water cluster, ^{d)} Calculated based on 4-water cluster.

3.5.4 Regiochemistry

The regiochemistry of a number of these cycloadditions was determined theoretically, the outcome agreeing with the experimentally observed regiochemistry in all cases. All four potential isomers were investigated for Y= H, Me, MeO, Cl, NO₂. In all cases there was a clear energetic preference for the keto group of the dipolarophile adding in the 2-position. The calculations do not reflect the relative *endo/exo* ratios observed synthetically. The calculations predict that the 2-*endo*-acetyl isomer should be preferentially formed whereas the synthetic reactions completed demonstrated that the major product formed was the 2-*exo*-acetyl isomer in all cases. This may be due to the operation of a solvophobic effect which favours the *endo*-arrangement for the aryl substituent.

Transition state structures were calculated for the four possible isomers derived from **45** and 4-phenyl-3-buten-2-one **178** (**Figure 73**). In all cases the C(2)-C(3) bond is the shorter of the two new bonds being formed, indicating a concerted asynchronous transition state.

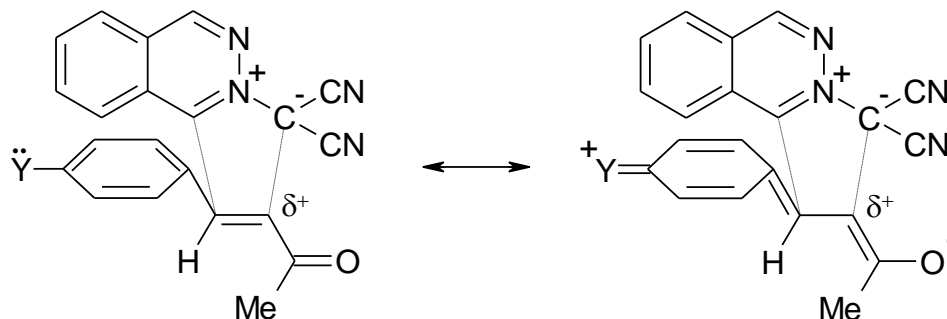


Note 1: Distances of bonds to be formed given in Å

Note 2: Isomer takes its abbreviated name from the position of keto substituent

Figure 73: Calculated transition state structures for the reaction of 1,3-dipole **45** with benzylidene acetone **178**

Calculations also indicated that a dipolar interaction along the developing C(2)-C(3) bond was a key feature of the concerted transition state. Strong resonance electron donating substituents are therefore expected to inhibit the rate by reducing the positive charge at C(2) in the transition state (**Scheme 60**). Conversely electron withdrawing substituents should speed up the reaction.



Scheme 60

3.5.5 Ionisation potential

The ionisation potential of a molecule has traditionally been used as a measure of the energy of the highest occupied molecular orbital. When the measured rates of cycloaddition of a series of dipolarophiles were plotted against the calculated ionisation potential a U-shaped curve was obtained (**Figure 74**).⁴³ This placed the 1,3-dipole **45** in the Sustmann Type II class (normal or inverse demand). Reactions on the left hand side of the curve are $\text{LUMO}_{\text{dipole}}\text{-HOMO}_{\text{dipolarophile}}$ controlled in the transition state. On the right hand side of the curve the reactions are $\text{HOMO}_{\text{dipole}}\text{-LUMO}_{\text{dipolarophile}}$ controlled. The reaction mechanism of the phthalazinium-2-dicyanomethanide 1,3-dipole **45** therefore changes depending on the type of dipolarophile involved in the reaction, leading to variation in the regiochemistry of products.^{33, 43}

The ionisation potential of benzylidene acetone **178** (6.35 eV) was calculated by Prof. Luke Burke of Rutgers University at Camden using methods incorporated into the Gaussian 03 A7 series¹⁰¹ of programs. When combined with a measured reaction constant of $7.2 \times 10^{-4} \text{ dm}^3 \text{ mol}^{-1} \text{ s}^{-1}$, benzylidene acetone **178** is found to sit on the lower left hand side of the curve at point number 27 (**Figure 74**). The position of benzylidene acetone **178** is therefore very close to the point of mechanism change over. Both the experimental and theoretical Hammett plots indicate that the 1,3-dipole **45** reacts with the benzylidene acetones *via* a $\text{HOMO}_{\text{dipole}}\text{-LUMO}_{\text{dipolarophile}}$ controlled process.

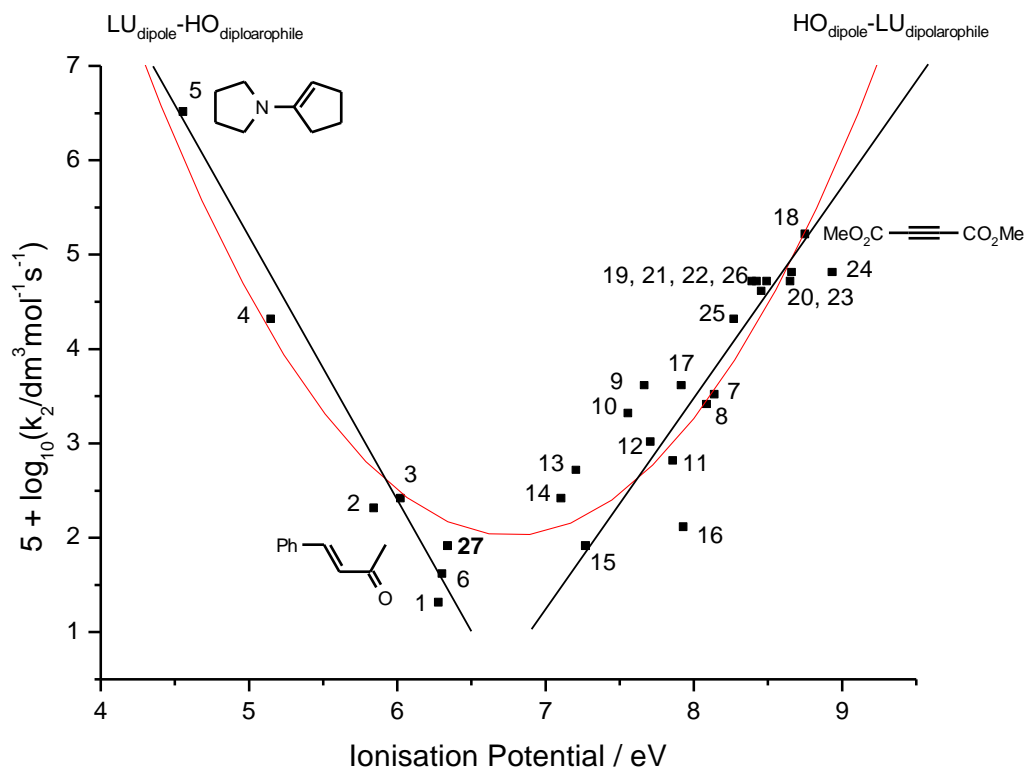


Figure 74: Experimental rates versus calculated (DFT) ionisation potentials for the reactions of phthalazinium-2-dicyanomethanide 1,3-dipole **45** with various dipolarophiles.⁴³ Points 1-26 correspond to the dipolarophiles listed in reference 43. Benzylidene acetone plotted as point 27.

3.6 Synthetic study of “on water” cycloaddition reactions of phthalazinium-2-dicyanomethanide 1,3-dipole **45**

Breslow’s discovery of the acceleration of the Diels-Alder reaction in water⁸² has prompted increased interest in the use of water as a medium for organic reactions. There are both cost and environmental benefits associated with the use of water rather than organic solvents. As indicated previously, Sharpless has suggested that the term “on water” be applied to reactions between insoluble reactants which are suspensions in water⁹⁸. Non-polar liquids that separate from water into a clear organic phase are considered to be good candidates for these reactions. It has been

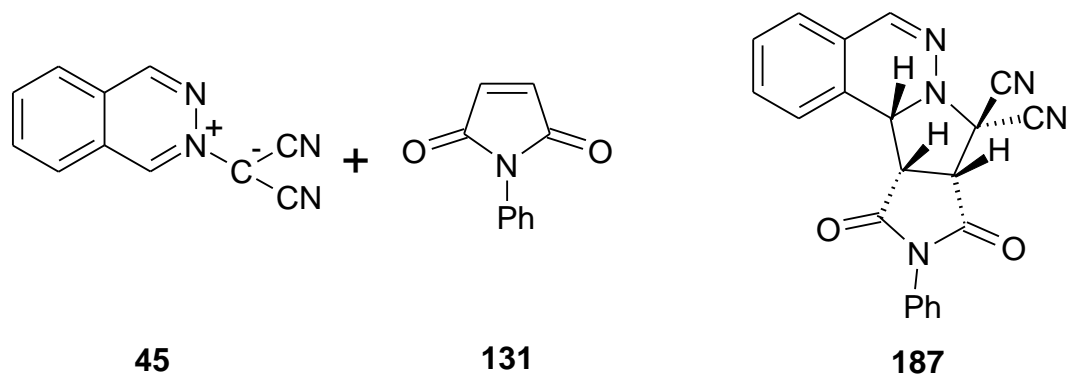
suggested that solids can also be used in these reactions provided one reactant is a liquid.⁹⁸

The solid phthalazinium-2-dicyanomethanide 1,3-dipole **45** is quite water insoluble ($\leq 5 \times 10^{-6}$ mol L⁻¹ at 37 °C). This limit was measured³⁴ from the UV spectra of saturated neat water solutions using the λ_{max} of 413 nm and the extinction coefficient for the solutions of **45** in H₂O-MeCN (9:1 v/v), which were used previously for kinetic studies. The synthetic reactions between aqueous suspensions of compound **45** and insoluble liquid alkene and alkyne dipolarophiles^{44, 63} give high yields of cycloadducts through reactions which can occur in an oily phase at the water-organic interface, or at the solid-liquid interface in the stirred mixture.

It was decided to investigate the impact of reacting phthalazinium-2-dicyanomethanide 1,3-dipole **45** with solid dipolarophiles of decreasing water solubility in water. The water solubilities of the dipolarophiles were obtained from SciFinder. These values were calculated using ACD Labs software¹⁰² and provide a good assessment of the solubilities in water. The dipolarophile *N*-phenylmaleimide **131** has a water solubility in the order of 10⁻³ mol L⁻¹, which we considered to be “sparingly soluble”. The compound *p*-chlorobenzylidene acetone **181** has a water solubility in the order of 10⁻⁴ mol L⁻¹, which we considered to be “very sparingly soluble”. Both dipolarophiles give the appearance of insoluble suspensions in water.

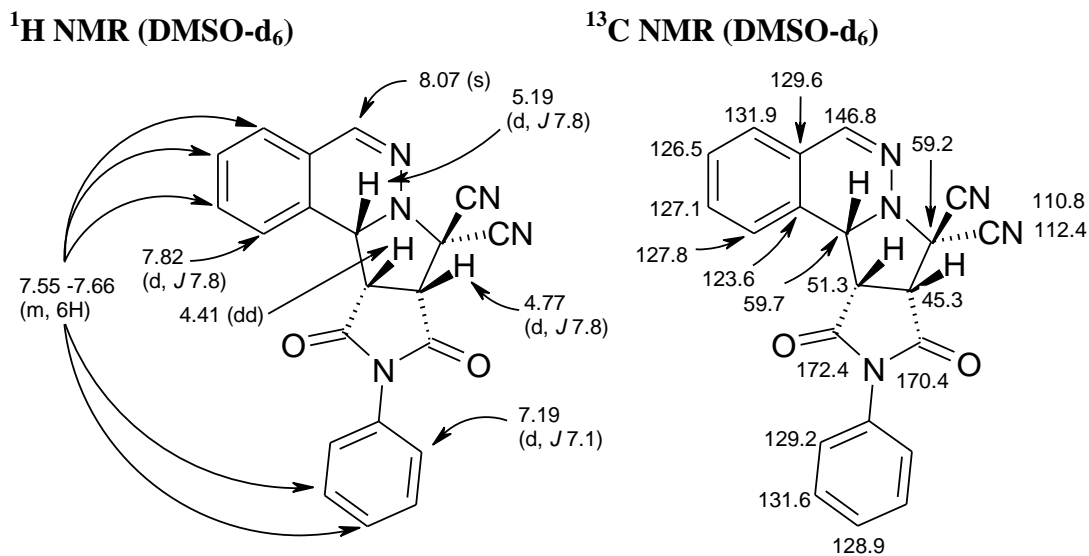
3.6.1 “On water” cycloaddition of phthalazinium-2-dicyanomethanide 1,3-dipole **45** with *N*-phenylmaleimide **131**

Phthalazinium-2-dicyanomethanide dipole **45** was stirred with an equimolar amount of *N*-phenylmaleimide **131** in Millipore water for 24 h at ambient temperature. The highly yellow coloured suspension changed to white/off-white as the dipole **45** was consumed and replaced by product. The insoluble water-wet product stuck to the insides of the flask but could be collected with care. The mixture was filtered to yield compound **187** (Scheme 61) as a pale yellow solid. The structural assignment of the product **187** was supported by IR, ¹H NMR and ¹³C NMR spectroscopy.



Scheme 61

The IR spectrum showed two bands at 1715 and 1795 cm^{-1} corresponding to the two carbonyl groups. NMR spectra were measured in DMSO- d_6 . The H-1 signal appeared as a doublet of doublets at δ 4.41 (**Figure 75**). The H-2 signal occurred as a doublet at δ 4.77 while H-10b appeared as a doublet at δ 5.19. In the ^{13}C NMR, the C-10b signal appeared at 59.7 ppm (**Figure 75**). The two cyano groups occurred at 110.8 and 112.4 ppm. The C-6 signal appeared at 146.8 ppm. The two carbonyl groups appeared at 170.4 and 172.4 ppm. An X-ray crystal structure of the product obtained from the reaction of **45** with *N*-(*t*-butyl) maleimide has previously been obtained in these labs (**Figure 10, Section 1.4.3**).

Figure 75: ^1H NMR and ^{13}C NMR assignments for compound **187**

The stereochemistry of **187** was determined by NOEDS. Irradiation of the H-1 signal resulted in enhancement of both the H-10b and H-2 signals. Irradiation of the H-10b signals caused enhancement of the H-1 signal. Therefore the maleimide ring was determined to be in the *endo* position.

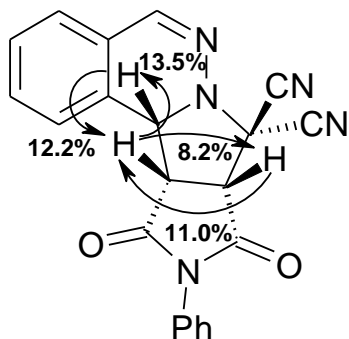


Figure 76: NOEDS enhancements for compound **187** in DMSO- d_6

The compound *N*-phenylmaleimide **131** has a melting point of 89-90 °C and a calculated¹⁰² water solubility of 4.4×10^{-3} mol L⁻¹. The reaction was completed at ambient temperature, well below the melting point of the dipolarophile. Therefore in this case it is not necessary to liquefy a “sparingly soluble” solid dipolarophile in order to allow it to react with a “very sparingly soluble” solid dipole in water.

3.6.2 “On water” cycloaddition of phthalazinium-2-dicyanomethanide 1,3-dipole **45** with *p*-chlorobenzylidene acetone **181**

The phthalazinium-2-dicyanomethanide 1,3-dipole **45** reacts with *p*-chlorobenzylidene acetone **181** in acetonitrile to yield tetrahydropyrrolo[2,1-*a*]phthalazine products (**Scheme 58**). The *p*-chlorobenzylidene acetone **181** dipolarophile has a melting point of 58-62 °C and a calculated¹⁰² water solubility of 1.2×10^{-4} mol L⁻¹. The solubility of **181** in water is therefore an order of magnitude lower than *N*-phenylmaleimide **131**, and so we termed it a “very sparingly soluble” dipolarophile.

The phthalazinium-2-dicyanomethanide 1,3-dipole **45** was treated with a slight excess of *p*-chlorobenzylidene acetone **181** in Millipore water at ambient

temperature, similar to procedure used with *N*-phenylmaleimide **131**. However, in this case the reaction was unsuccessful. There was no visible change in the appearance of the reaction mixture despite the age time being doubled to 48 hours. The yellow suspension was filtered and the resulting precipitate analyzed by ¹H NMR. The precipitate contained unreacted dipole **45**, *p*-chlorobenzylidene acetone **181** and a small amount (<1%) of the expected major product **182**. (Table 18)

Increasing the reaction temperature to 40 °C had a minor beneficial impact, as the yield of the major product **182** increased to 3.5 % after stirring for 48 h (Table 18). However the appearance of the reaction mixture did not change, remaining a yellow suspension during the course of the reaction. It was only when the reaction temperature was raised above the melting point of *p*-chlorobenzylidene acetone **181** that the expected products **182** and **183** were formed in high yield after stirring for 24 h (Table 18). A change in the reaction mixture appearance was observed over the course of the reaction. As the reaction mixture was heated to 75 °C, the yellow suspension became oily. Product began to precipitate from solution, adhering to the inside of the reaction flask and the stir-bar. The reaction mixture was filtered and analyzed by ¹H NMR spectroscopy. A small amount of unreacted dipole **45** and *p*-chlorobenzylidene acetone **181** remained, however the majority of the precipitate was made up of the expected products **182** and **183**. These products were formed in overall 86% yield and in a ratio of 6.2:1 (Table 19). The *endo/exo* product ratio was reduced relative to the reaction in acetonitrile.

Table 18: Reactions of **45** with *p*-chlorobenzylidene acetone **181** in water

Reaction Time (h)	Reaction Temperature (°C)	Total Yield (%)
48	20	< 1
48	40	3.5
24	75	86 ^a

^{a)} Major/minor product ratio (**182:183**) - 6.2:1

Therefore, when both solid reactants are very sparingly soluble, liquefaction of one allows a reaction to occur as expected for an oily-phase process. The solid 1,3-dipole **45** has an intense yellow colour and even trace quantities present in a solution show a yellow colouration. In the reactions at temperatures where the dipolarophile was liquefied the oily phase showed yellow colouration, suggesting that compound **45** was present in this phase.

The reduction in the *endo/exo* ratio for the reaction of 1,3-dipole **45** with *p*-chlorobenzylidene acetone **181** was somewhat unexpected. Breslow^{83, 84} has demonstrated that the *endo/exo* ratio for the Diels-Alder reaction is enhanced when the reaction is completed in water. The same *endo*-effect was expected to occur for the 1,3-dipolar cycloadditions of **45** in water. This effect is suggested to be due to the hydrophobic effect, which favours the more compact transition state associated with the *endo*-transition state. Smaller contributions may also come from polarity effects on the *endo*-favouring secondary orbital interactions and charge transfer contributions to the transition state.^{86, 87}

Table 19: Comparison of yields for the reaction of 1,3-dipole **45** with *p*-chlorobenzylidene acetone **181**

Solvent	Major Isomer 182	Minor Isomer 183	<i>endo/exo</i>
	Yield (%)	Yield (%)	(182/183)
Acetonitrile	52	5	10.4:1
Water	74	12	6.2:1

The results suggest that the reaction of the 1,3-dipole **45** with the sparingly soluble dipolarophile *N*-phenylmaleimide **131** is passing through the water at low concentrations. When the solubilities of both reactants are well below the millimolar threshold, as in the reaction of 1,3-dipole **45** with *p*-chlorobenzylidene acetone **181**, liquefaction of one reactant is necessary. This allows the reaction to pass through a water-penetrated oily phase. In both cases the reactions are subject to the pervasive hydrophobic effect which (i) accelerates the reaction of sparingly soluble reactants

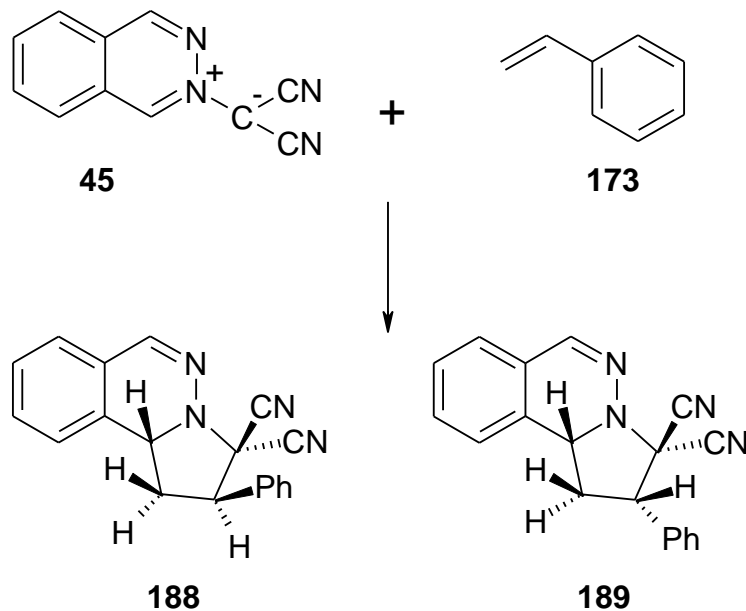
and (ii) immediately expels the more insoluble cycloadducts with larger organic surface areas from the medium as soon as they are formed (when they appear to stick to available surfaces). Hence the entire reaction is rapidly shuttled through the water medium or the oily-phase medium by hydrophobic driven equilibria.

The reduction in the *endo/exo* ratio for the reaction of *p*-chlorobenzylidene acetone **181** with 1,3-dipole **45** in water relative to the reaction in acetonitrile suggests that the hydrophobic effect does not play a significant role in determining the stereochemistry of the reaction. The hydrophobic effect is expected to be strongest when a reaction is occurring within the bulk water medium, and so the reactants are surrounded by water molecules. This suggests therefore the reaction of 1,3-dipole **45** and *p*-chlorobenzylidene acetone **181** is a true “on water” rather than “in water” reaction.

The influence of water on product *endo/exo* ratios is a useful tool in determining if a reaction is proceeding *via* “in water” or “on water” mode. The hydrophobic effect has a significant impact on reactions that proceed “in water”. This results in an increased preference for the *endo*-isomer. Reactions that proceed “on water” are not subject to such a strong hydrophobic effect, and so the *endo*-isomer is not as favoured.

3.7 Comparison with substituted styrenes

The reaction of 1,3-dipole **45** and substituted styrenes are generally LUMO_{dipole} controlled.^{43, 63} Typically two products are formed, both with the aryl substituent in the C-2 position. The main product **188** contains the aryl substituent in the *exo* position, while the minor product **189** has the aryl group in the *endo* position (Scheme 62).



Scheme 62

However, a second minor product was encountered when a strongly electron withdrawing substituent (*m*-NO₂) was investigated.⁶³ This product **192** has the opposite regiochemistry to the major product **190** and the typical minor product **191** (Figure 77). This is the same regiochemistry observed when electron-poor dipolarophiles react with 1,3-dipole **45** in HOMO_{dipole} controlled reactions. This is also the regiochemistry (aryl group attached to C1) observed for the reactions of 1,3-dipole **45** with the benzylidene acetones.

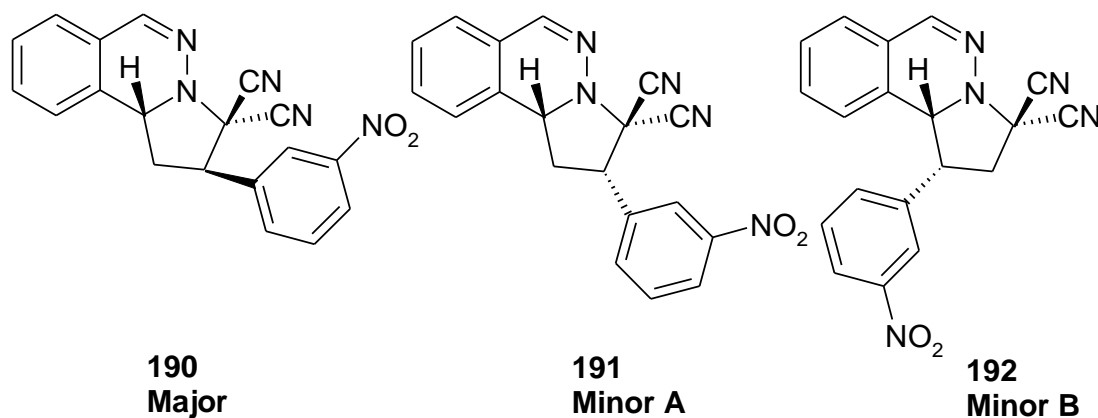


Figure 77

The experimentally measured Hammett plot⁶³ (**Figure 78**) for the reaction of 1,3-dipole **45** with substituted styrenes is v-shaped, indicating that a changeover in mechanism, from LUMO_{dipole} to HOMO_{dipole} control, occurs for this reaction.

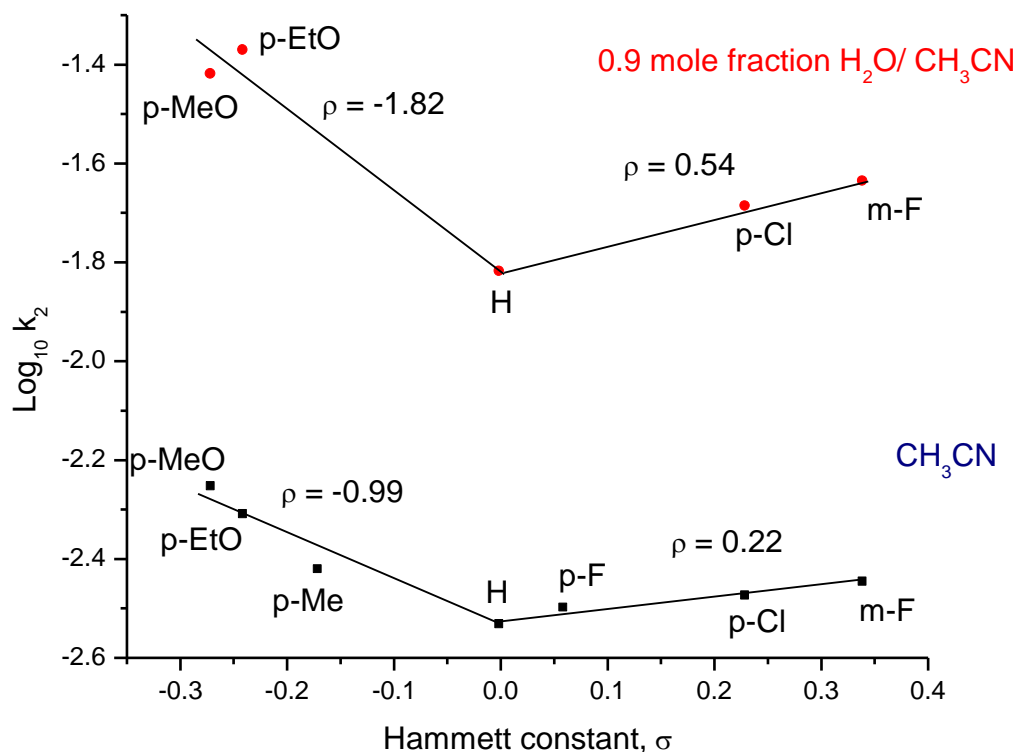


Figure 78: Hammett plot of 1,3-dipole **45** and *p*- and *m*- substituted styrenes in acetonitrile and aqueous acetonitrile at 37 °C

This v-shape indicates a change in mechanism on going from dipolarophiles with electron donating substituents to dipolarophiles with electron withdrawing substituents. The plot of experimental rates versus calculated DFT ionisation potentials (**Figure 74**) for 1,3-dipole **45** with various electron-rich and electron-poor dipolarophiles is a U-shaped curve. A U-shaped curve indicates that dipole **45** is a Sustmann type II dipole. Styrene appears at the bottom of the curve on the left hand side effectively on the borderline for the mechanistic changeover.

From the Hammett plot (**Figure 78**) it is clear that a change of mechanism from LUMO_{dipole} to HOMO_{dipole} control occurs as the substituents are changed. The changeover in mechanism is reflected in a change in regiochemistry. The changeover in mechanism from LUMO_{dipole} to HOMO_{dipole} control occurs once the substituent on the phenyl ring is sufficiently electron withdrawing. The presence of the carbonyl group in the benzyldene acetone dipolarophiles has a similar effect, causing their reactions with 1,3-dipole **45** to be HOMO_{dipole} controlled. Substituted styrenes react equally well with 1,3-dipole **45** in water and acetonitrile (**Table 20**). The reactants appear visually insoluble in water, but react smoothly to generate the expected cycloadducts. There is a slight decrease in the *endo/exo* ratio for the reactions completed using water as solvent. The styrene dipolarophiles listed (**Table 20**) all have solubilities¹⁰² in the range of 10⁻³ mol L⁻¹, and so react “on water”.

Table 20: Comparison of yields (%) and *endo/exo* isomer ratios for the reaction of 1,3-dipole **45** with substituted styrenes⁶³

Dipolarophile	Acetonitrile			Water		
	Major (<i>exo</i>)	Minor (<i>endo</i>)	<i>endo/exo</i>	Major (<i>exo</i>)	Minor (<i>endo</i>)	<i>endo/exo</i>
Styrene 173	74	13	1:6	67	11	1:6
<i>p</i> -MeO styrene	63	8	1:8	78	9	1:9
<i>m</i> -F styrene	76	15	1:5	71	11	1:7
<i>m</i> -NO ₂ styrene	68	11	1:6	72	10	1:7

The reactions of 1,3-dipole **45** and substituted styrenes are accelerated in water and fall into the category of water-normal dipolarophiles (**Table 21**). Water-normal dipolarophiles typically have esters, ethers, sulfones, nitriles or aryl rings conjugated to an alkene or alkyne. In general these give enhancements < 6 in water/acetonitrile (0.9 mole fraction).³⁴ Therefore reactions of 1,3-dipole **45** with *p*-substituted benzyldene acetones are accelerated in water to a greater extent than the reactions of 1,3-dipole **45** with substituted styrenes. This is due to the presence of the carbonyl group conjugated to the double bond in the *p*-substituted benzyldene acetones. The

presence of this group allows special H-bonding to play a significant role in water reactions, and so ensures that the benzylidene acetones are water-super dipolarophiles.

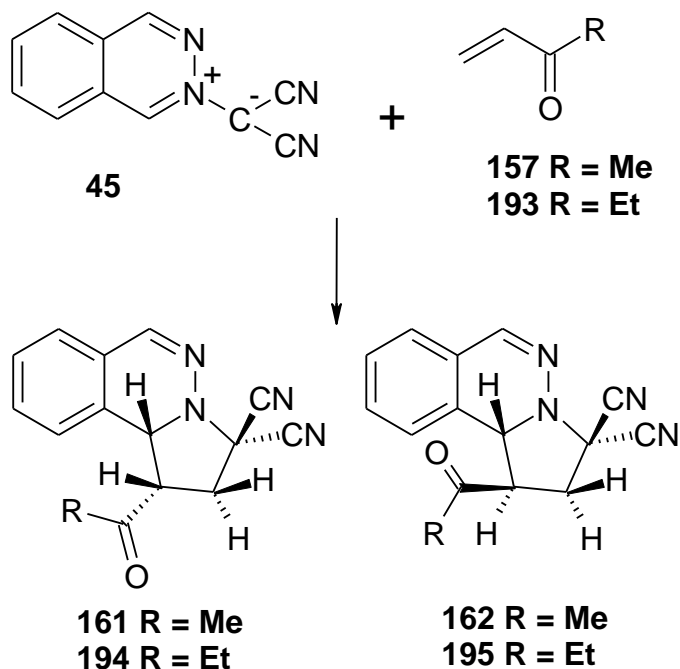
Table 21: Kinetic data for the reaction of 1,3-dipole **45** with substituted styrenes in acetonitrile and aqueous acetonitrile mixtures at 37 °C (k_2 : $\text{dm}^3 \text{mol}^{-1} \text{s}^{-1}$)⁶³

Dipolarophile	k_2 CH ₃ CN	k_2 H ₂ O/CH ₃ CN 0.9 : 0.1 ^a	k_2 Ratio ^b
Styrene 173	2.92×10^{-3}	15.1×10^{-3}	5.2
<i>p</i> -MeO styrene	5.55×10^{-3}	37.8×10^{-3}	6.8
<i>p</i> -EtO styrene	4.98×10^{-3}	42.3×10^{-3}	8.7
<i>p</i> -Me styrene	3.77×10^{-3}	-	-
<i>m</i> -F styrene	3.56×10^{-3}	22.9×10^{-3}	6.4
<i>p</i> -Cl styrene	3.34×10^{-3}	20.4×10^{-3}	6.1
<i>p</i> -F styrene	3.15×10^{-3}	-	-

^a) mole fraction ^b) measured k_2 H₂O-CH₃CN (0.9:0.1)/ k_2 in CH₃CN

3.8 Comparison with alkyl vinyl ketones

The reactions of 1,3-dipole **45** and the alkyl vinyl ketones methyl vinyl ketone **157** and ethyl vinyl ketone **193** are HOMO_{dipole} controlled.^{34, 43} The unsubstituted terminus of the dipolarophile attaches to the 1-CH terminus of the 1,3-dipole. The major products **161** and **194** contain the ketone group in the *endo*-position (**Scheme 63**) (**Table 22**). The minor products **162** and **195** have the same regiochemistry, however the ketone group is in the *exo*-position.



Scheme 63

Table 22: Comparison of yields (%) and *endo/exo* isomer ratios for the reaction of 1,3-dipole **45** with vinyl ketones **157** and **193** in acetonitrile and water at ambient temperature⁷³

Dipolarophile	Acetonitrile			Water		
	Major (<i>endo</i>)	Minor (<i>exo</i>)	<i>endo</i> / <i>exo</i>	Major (<i>endo</i>)	Minor (<i>exo</i>)	<i>endo</i> / <i>exo</i>
Methyl vinyl ketone 157	72	23	3:1	83	12	7:1
Ethyl vinyl ketone 193	71	23	3:1	88	8	11:1

The reaction behaves similarly in water and acetonitrile (**Table 23**). The yields and reaction times are comparable when acetonitrile and water are used as the reaction solvent. However a significant change occurs to the *endo/exo* ratio when the reaction is completed in water. A large increase in the *endo* isomer is observed. This is similar to results obtained by Breslow^{86, 87} for the Diels-Alder reaction. The preference for the *endo* transition state could be due to the fact that it is more

compact than the *exo* transition state, and so is favoured in water. It also indicates that these reactions are taking place “in water”, and so is greatly influenced by the hydrophobic effect.

Table 23: Kinetic data for the reaction of 1,3-dipole **45** with alkyl vinyl ketones **157** and **193** in acetonitrile and aqueous acetonitrile mixtures at 37 °C (k_2 : $\text{dm}^3\text{mol}^{-1}\text{s}^{-1}$)

Dipolarophile	k_2 CH ₃ CN	k_2 H ₂ O/CH ₃ CN 0.9 : 0.1 ^a	k_2 Ratio ^b
Methyl vinyl ketone 157	62.0×10^{-3}	1079×10^{-3}	17.4
Ethyl vinyl ketone 193	76.9×10^{-3}	1044×10^{-3}	13.6

^a)mole fraction ^b) measured k_2 H₂O-CH₃CN (0.9:0.1)/ k_2 in CH₃CN

Both methyl vinyl ketone **157** and ethyl vinyl ketone **193** experience large rate accelerations in aqueous acetonitrile and so are considered water-super dipolarophiles. In general water-super dipolarophiles give rate enhancements > 10 in water/acetonitrile (0.9 mole fraction).³⁴ Water-super dipolarophiles typically feature a ketone C=O conjugated to an alkene or alkyne. The *p*-substituted benzylidene acetones also contain a carbonyl group conjugated to an alkene and so display similar water-super behaviour.

3.9 Conclusion

We have explored the cycloaddition reaction of the phthalazinium-2-dicyanomethanide 1,3-dipole **45** with benzylidene acetone dipolarophiles. New 1,2-substituted tetrahydropyrrolo[2,1-*a*]phthalazine derivatives have been synthesised. The reactions produce two products, both with the aryl substituent on the C-2 position. This regiochemistry was not expected based on the individual reactions of styrenes and alkyl vinyl ketones with the 1,3-dipole **45**. The major product has the aryl substituent in the *endo*-position.

The kinetics of the cycloaddition reaction of 1,3-dipole **45** with benzylidene acetone dipolarophiles was also explored. Large rate accelerations were observed when the reactions were completed in aqueous acetonitrile as opposed to pure acetonitrile. The dipolarophiles are considered to be water-super dipolarophiles, as they experience a rate enhancement of over eleven fold when the reactions are completed in 0.9 mole fraction water/acetonitrile rather than acetonitrile. The water-super nature of these dipolarophiles is associated with the presence of a double bond conjugated to a ketone. This facilitates rate acceleration due to special hydrogen bonding effects. Clusters of water become attached to the carbonyl resulting in stabilization of the transition state relative to the ground state.

A DFT study was completed by Prof. Luke A. Burke of Rutgers University at Camden in a collaborative investigation. The results support a concerted non-synchronous 1,3-dipolar cycloaddition reaction and account for the observed regiochemistry. The theoretical calculations indicate that a dipolar interaction along the developing C(2)-C(3) bond is a key feature of the concerted transition state.

The potential for increases in transition state polarity to contribute to the rate enhancements observed in aqueous acetonitrile was investigated through the use of Hammett plots. The experimental Hammett plots for the reaction of 1,3-dipole **45** with the benzylidene acetones in aqueous acetonitrile and pure acetonitrile had small ρ values of +0.35 and +0.58 respectively. This suggests that little charge build up in

the transition state occurs in either solvent. Theoretical calculations were also completed with a wide variety of benzylidene acetone dipolarophiles to generate a theoretical Hammett plot for this reaction. The theoretical results are in good agreement with the experimentally derived results. Therefore it is concluded that increased polarity of the cycloaddition transition state is not responsible for the rate accelerations observed in the presence of water.

A natural progression of this study was to examine the reactions of 1,3-dipole **45** in pure water. The solid 1,3-dipole **45** was reacted with the solid dipolarophiles *p*-chlorobenzylidene acetone **181** and *N*-phenylmaleimide **131** in pure water. The dipolarophile *p*-chlorobenzylidene acetone required liquefaction to achieve reaction. The *N*-phenylmaleimide **131** dipolarophile has superior solubility in water and so did not need to be liquefied to react. This indicates that successful synthetic reactions can be achieved between two insoluble organic compounds *via* the “on water” methodology if one is liquefied to provide an oily layer in the water mixture. Liquefaction is not required if one of the reactants has sufficient solubility in water to generate an oil layer.

3.10 Future work

The impact of water on endo/exo product ratios for the reactions of **45** with benzylidene acetones remains an area of interest. Comparison of the “on water” product ratios with reactions completed in water/acetonitrile solutions would provide additional insight into the factors that influence reaction selectivity. The reactions of the imidazolium 1,3-dipoles have yet to be completed using water as a reaction solvent. Water would be expected to accelerate the cycloaddition reactions through a combination of the hydrophobic effect and hydrogen bonding, though its polar nature may provide additional stability for the ylide intermediate during the rearrangement step. Finally, advances in process analytical technology, particularly in-line NIR, may also prove to be useful in tracking the cycloaddition reactions and subsequent rearrangements.

3.11 Experimental

Experimental: synthesis

Melting points were measured on an Electrothermal apparatus. IR spectra were measured on a Perkin-Elmer Spectrum 1000 spectrophotometer. Microanalyses were measured on a Perkin-Elmer Model 240 CHN analyser. NMR spectra were measured on a JEOL GXFT 400 instrument with tetramethylsilane as an internal reference. Deuteriochloroform, hexadeuteriomethyl sulphoxide and acetonitrile-d₃ were used as solvents. ¹H NMR assignments were supported by selective proton decoupling and COSY spectra. *J* values are given in Hz. ¹³C NMR assignments were supported by DEPT spectra. The stereochemistry of the cycloadducts was determined using NOEDS. Acetonitrile was HPLC grade and was used without purification.

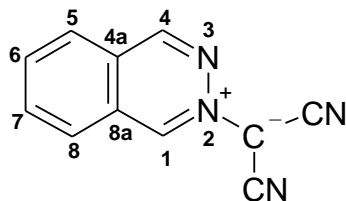
The following chemicals were purchased from:

Sigma-Aldrich: DMSO-d₆, phthalazine, *N*-phenylmaleimide, *trans*-4-phenyl-3-buten-2-one, 4-(4-chlorophenyl)-3-buten-2-one, 4-(4-methylphenyl)-3-buten-2-one.

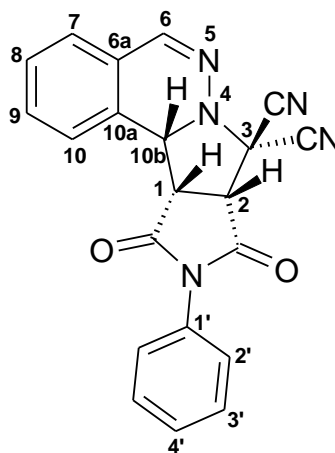
Flourochem: chloroform-d₁.

Chapter 3

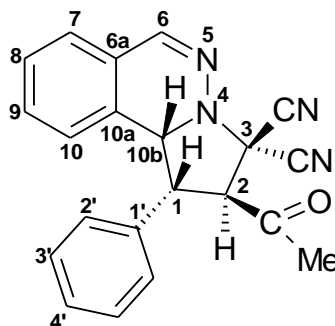
The numbering and naming system below is used in this chapter and has been accepted for publication.



phthalazinium-2-dicyanomethanide 1,3-dipole **45**



endo-1,2-(dicarboxy-*N*-phenylimido)-3,3-dicyano-1,2,3,10b-tetrahydropyrrolo-
[2,1-*a*]phthalazine **187**



1-*endo*-2-*exo*-2-acetyl-1,2,3,10b-tetrahydro-1-phenylpyrrolo
[2,1-*a*]phthalazine-3,3-dicarbonitrile **179**

Synthesis of phthalazinium-2-dicyanomethanide 1,3-dipole **45**

A solution of phthalazine (0.91 g, 7.00 mmol) in ethyl acetate (40 cm³) was cooled to below 0 °C in an ice-bath. This was treated dropwise with a cooled ethyl acetate solution (5 cm³) of TCNEO (1.00 g, 7.00 mmol) such that the reaction temperature was maintained below 12 °C. The yellow product precipitated immediately and was collected by filtration (1.25 g, 92%), mp 263-265 °C (acetonitrile); (Found C, 67.9, H, 3.1; N, 28.7. C₁₁H₆N₄ requires C, 68.0; H, 3.1; N, 28.9%); ν_{\max} (mull)/cm⁻¹ 2191, 2159 (C≡N); δ_{H} (DMSO-d₆, 80 °C), 7.92-7.96 (m, 1H, H-5), 8.02-8.06 (m, 1H, H-8), 8.18-8.24 (m, 2H, H-6 and H-7), 9.40 (s, 1H, H-4), 9.60 (s, 1H, H-1); δ_{C} (DMSO-d₆, 80 °C), 63.5 (methanide C⁻), 117.2 (C≡N), 122.8 (C-8a), 126.4, 128.0 (C-6 and C-7), 129.8 (C-4a), 129.7 (C-8), 132.8 (C-5), 135.4 (C-1), 153.9 (C-4).

Cycloaddition reactions of the phthalazinium-2-dicyanomethanide 1,3-dipole **45** with p-substituted benzylidene acetones

Synthesis of 1-endo-2-exo-2-acetyl-1,2,3,10b-tetrahydro-1-phenylpyrrolo [2,1-a]phthalazine-3,3-dicarbonitrile **179** and 1-exo-2-endo-2-acetyl-1,2,3,10b-tetrahydro-1-phenylpyrrolo[2,1-a]phthalazine-3,3-dicarbonitrile **180**

Phthalazinium-2-dicyanomethanide 1,3-dipole (0.30 g, 1.54 mmol) was added to a solution of *trans*-4-phenyl-3-buten-2-one (0.62 g, 4.62 mmol) in acetonitrile (25 cm³) and stirred under reflux for 4.5 h. After this time the solvent was removed under reduced pressure and the residue was taken up in ice-cold ether which caused the major product **179** to separate as a yellow solid. The ethereal filtrate contained further **179**, the minor product **180**, excess benzylidene acetone, unreacted dipole **45** and some intractable gum. Proton NMR analysis of this mixture gave the reported yields for the products. Compound **179** (0.31 g, 60%), white solid, mp 174-176 °C (from ethanol); (Found: C, 73.6; H, 4.7; N, 16.1. C₂₁H₁₆N₄O requires C, 74.1; H, 4.75; N, 16.45%); ν_{\max} /cm⁻¹ 694, 770 (-Ph) 1720 (C=O); δ_{H} (CDCl₃) 1.91 (s, 3H, CH₃), 3.94 (dd, *J* 7.8, 8.7, 1H, H-1), 4.27 (d, 1H, *J* 7.8, H-2), 5.24 (d, 1H, *J* 8.7, H-

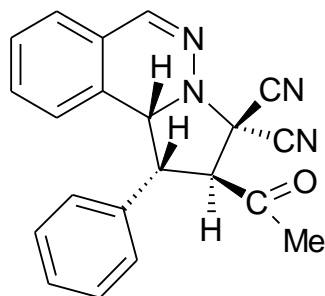
10b), 7.19 (d, 1H, J 7.3, H-10), 7.34 (d, 1H, J 7.3, H-7), 7.40-7.53 (m, 7H, H-8, H-9 and Ph), 7.64 (s, 1H, H-6); δ_C (CDCl₃) 31.4 (CH₃), 57.6 (C-10b), 58.5, 59.4 (C-1, C-2), 65.8 (C-3), 111.3, 112.2 (C≡N), 124.5 (C-10a), 126.0 (C-10), 127.4 (C-9), 128.8 (C-2'), 129.6 (C-3') 129.8 (C-4'), 129.9 (C-8), 131.9 (C-6a), 132.0 (C-7), 144.6 (C-6), 204.8 (C=O) (phenyl C-1' signal overlapped).

Compound **180** (0.03 g, 6%), δ_H (CDCl₃) (from mixture) key signals: 3.80 (dd, 1 H, J 9.2, 7.3, H-1), 4.21 (1H, J 7.3, H-2), 4.64 (d, 1H, J 9.2, H-10b). Other signals overlapped in the mixture.

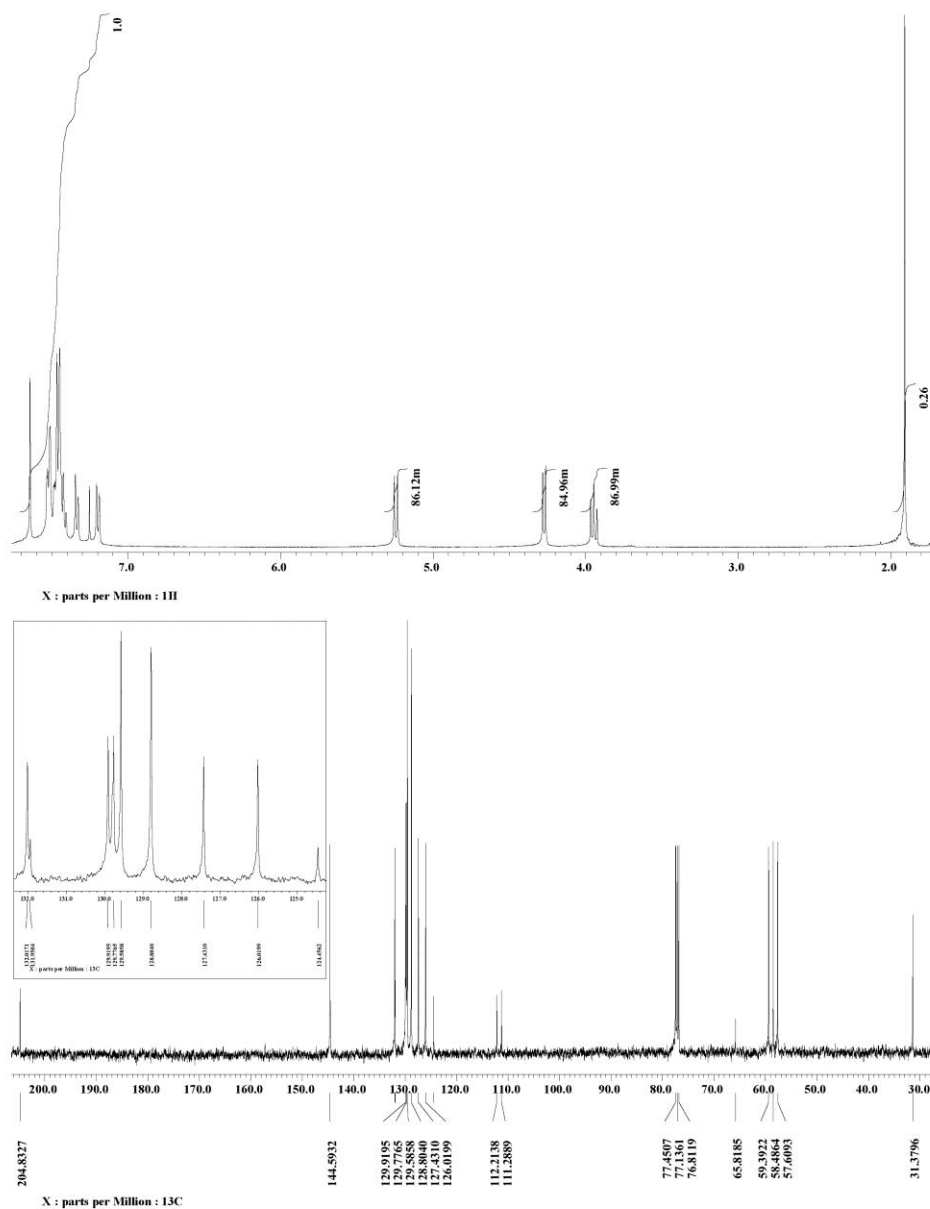
Synthesis of 1-endo-2-exo-2-acetyl-1-(4-chlorophenyl)-1,2,3,10b-tetrahydro pyrrolo[2,1-a]phthalazine-3,3-dicarbonitrile **182 and 1-exo-2-endo-2-acetyl-1-(4-chlorophenyl)-1,2,3,10b-tetrahydropyrrolo[2,1-a]phthalazine-3,3-dicarbonitrile **183****

A suspension of phthalazinium-2-dicyanomethanide 1,3-dipole (0.20 g, 1.03 mmol) in acetonitrile (20 cm³) was treated with 4-(4-chlorophenyl)-3-buten-2-one (0.56 g, 3.10 mmol) and the resulting mixture stirred under reflux for 4 h. The solvent was removed under reduced pressure to afford an orange gummy residue. The residue was taken up in ice-cold ether which caused the major product **182** to separate as a white solid. The ethereal filtrate contained further **182**, the minor product **183**, unreacted dipole **45** and some intractable gum. Proton NMR analysis of this mixture gave the reported yields for the products. Compound **182** (0.19 g, 52%), white solid, mp 162-163 °C (from ethanol); (Found: C, 67.0; H, 3.9; N, 15.4. C₂₁H₁₅ClN₄O requires C, 67.3; H, 4.0; N, 14.95%); $\nu_{\max}/\text{cm}^{-1}$ 1725 (C=O); δ_H (CDCl₃) 1.87 (s, 3H, CH₃), 3.86 (dd, J 7.8, 7.3, 1H, H-1), 4.26 (d, 1H, J 7.8, H-2), 5.25 (d, 1H, J 7.3, H-10b), 7.21 (d, 1H, J 7.3, H-10), 7.34 (d, 1H, J 7.3, H-7), 7.41-7.47 (m, 6H, H-8, H-9 and H-2', H-3'), 7.63 (s, 1H, H-6); δ_C (CDCl₃) 31.6 (CH₃), 57.2 (C-10b), 58.9, 59.4 (C-1, C-2), 65.9 (C-3), 111.2, 111.9 (C≡N), 124.3 (C-10a), 126.2 (C10), 127.5 (C-9), 129.3 (C-1'), 129.8 (C-2'), 129.9 (C-8), 130.1 (C-3'), 130.4 (C-6a), 132.1 (C-7), 136.1 (C-4'), 144.6 (C-6), 204.5 (C=O).

Chapter 3



179



^1H and ^{13}C NMR spectra for product **179** in CDCl_3

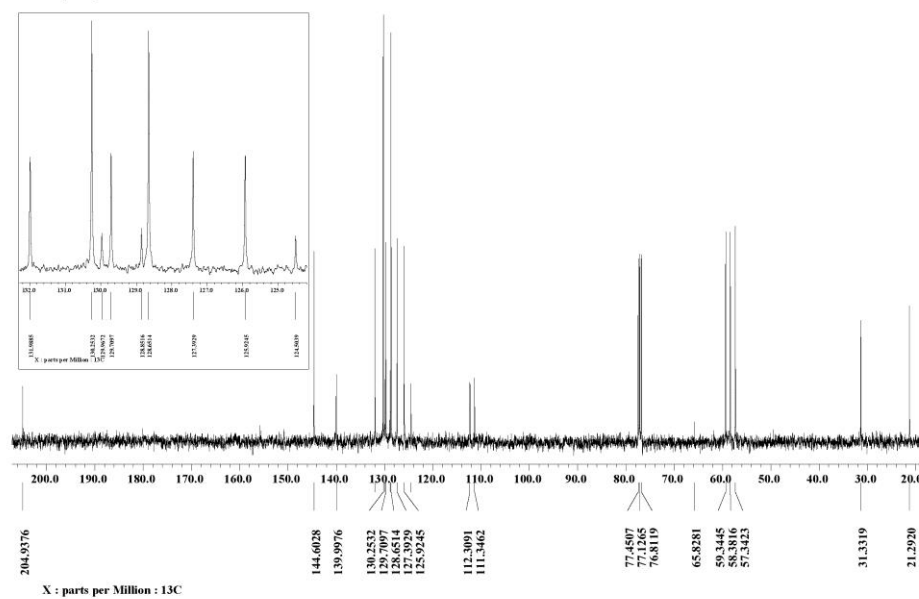
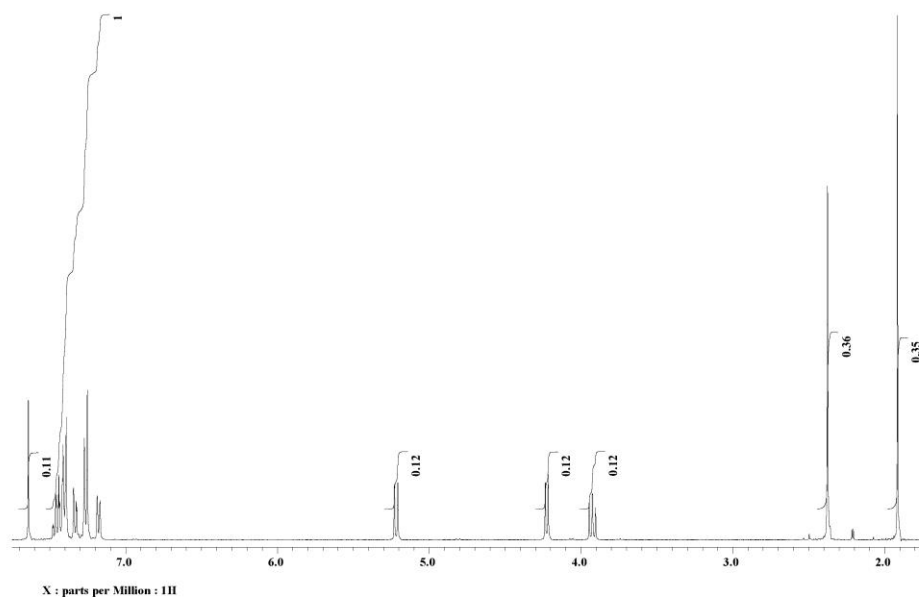
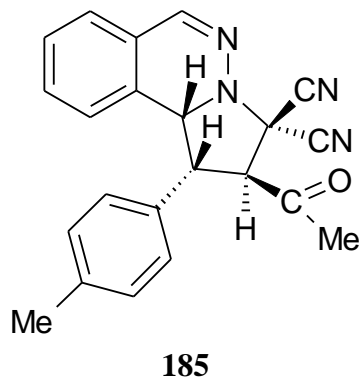
Compound **183** (0.02 g, 5%) δ_{H} (CDCl_3) (from mixture) key signals: 3.67 (dd, 1 H, J 7.1, 9.1 Hz), 4.19 (1H, J 7.1, Hz), 4.66 (d, 1H, J 9.1, Hz). Other signals overlapped in the mixture.

Synthesis of 1-endo-2-exo-2-acetyl-1,2,3,10b-tetrahydro-1-(4-methylphenyl) pyrrolo[2,1-*a*]phthalazine-3,3-dicarbonitrile **185 and 1-exo-2-endo-2-acetyl-1,2,3,10b-tetrahydro-1-(4-methylphenyl)pyrrolo[2,1-*a*]phthalazine-3,3-dicarbonitrile **186****

Phthalazinium-2-dicyanomethanide 1,3-dipole (0.20 g, 1.03 mmol) was added to a solution of 4-(4-methylphenyl)-3-buten-2-one (0.50 g, 3.09 mmol) in acetonitrile (20 cm^3) and stirred under reflux for 5 h. After this time the solvent was removed under reduced pressure to afford a brown gummy residue. The residue was taken up in ice-cold ether which caused the major product **185** to separate as a yellow solid. The ethereal filtrate contained further **185**, the minor product **186**, unreacted dipole and some intractable gum. Proton NMR analysis of this mixture gave the reported yields for the products. Compound **185** (0.25 g, 69%), yellow solid, mp 175-176 °C (from ethanol); (Found: C, 74.4; H, 4.8 N, 15.85. $\text{C}_{22}\text{H}_{18}\text{N}_4\text{O}$ requires C, 74.6; H, 5.1; N, 15.8%); $\nu_{\text{max}}/\text{cm}^{-1}$ 1725 (C=O); δ_{H} (CDCl_3) 1.92 (s, 3H, COCH_3), 2.37 (s, 3H, CH_3 of *p*-tolyl), 3.93 (dd, J 7.8, 8.9, 1H, H-1), 4.23 (d, 1H, J 7.8, Hz), 5.22 (d, 1H, J 8.9, Hz), 7.18 (d, 1H, J 6.9, Hz), 7.26 (d, 2H, J 7.8, Hz), 7.34 (d, 1H, J 7.1, Hz), 7.39-7.46 (m, 4H, H-8, H-9, H-2'), 7.64 (s, 1H, H-6); δ_{C} (CDCl_3) 21.3 (CH_3 of *p*-tolyl), 31.3 (COCH_3), 57.3 (C-10b), 58.4, 59.3 (C-1, C-2), 65.3 (C-3), 111.3, 112.3 ($\text{C}\equiv\text{N}$), 124.5 (C-10a), 125.9 (C-10), 127.4 (C-9), 128.7 (C-2'), 128.9 (C-1'), 129.7 (C-8), 130.0 (C-6a), 130.3 (C-3'), 132.0 (C-7), 140.0 (C-4'), 144.6 (C-6), 204.9 (C=O).

186 (0.03 g, 8%), δ_{H} (CDCl_3) (from mixture) key signals: 3.69 (dd, 1H, J 9.2, 7.3, Hz), 4.11 (1H, J 7.3, Hz), 4.63 (d, 1H, J 9.2, Hz). Other signals overlapped in the mixture.

Chapter 3



^1H and ^{13}C NMR spectra for product **185** in CDCl_3

Cycloaddition reactions of the phthalazinium-2-dicyanomethanide 1,3-dipole **45** in water

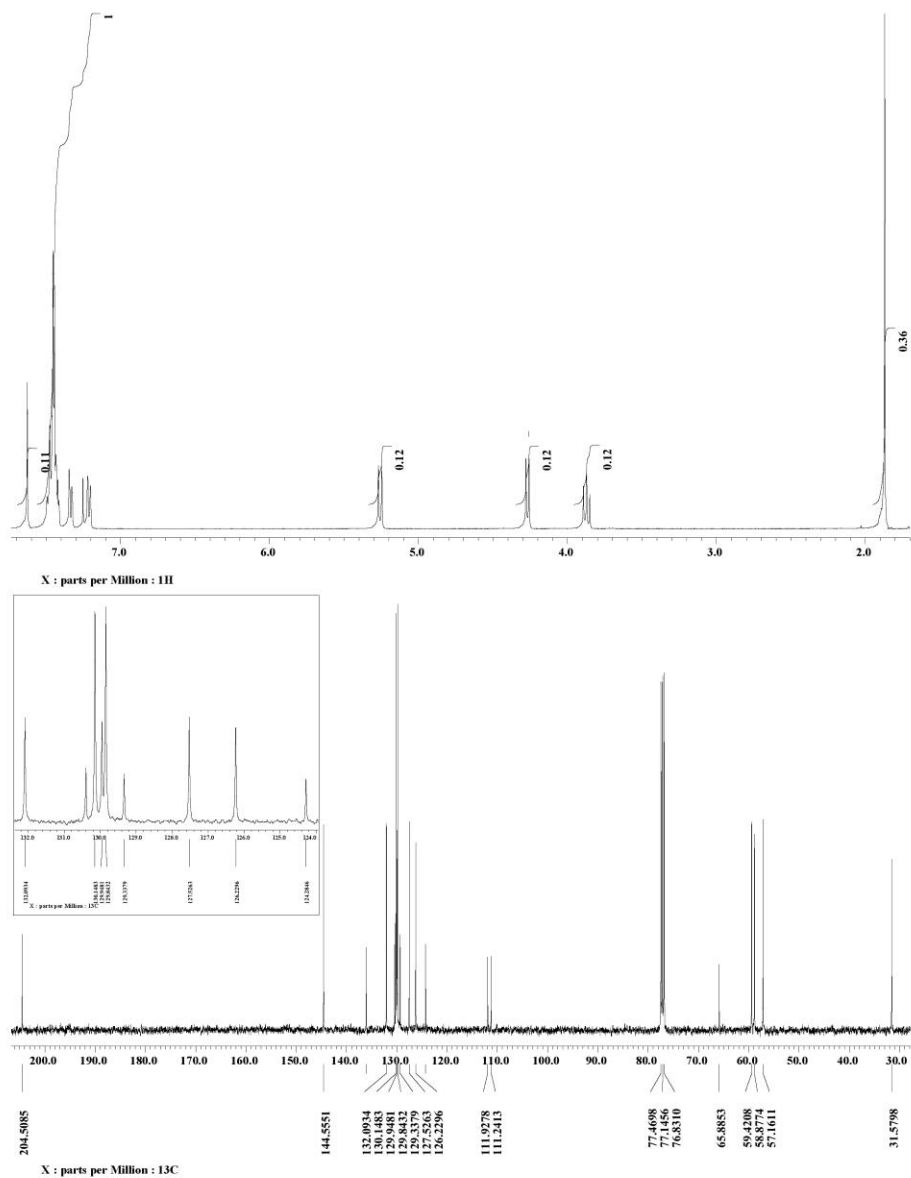
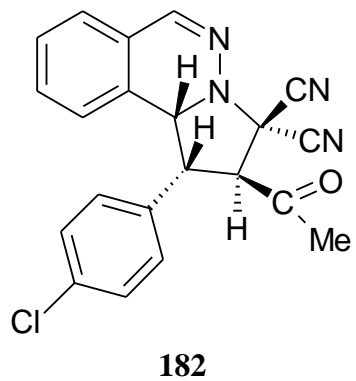
Synthesis of *endo*-1,2-(dicarboxy-*N*-phenylimido)-3,3-dicyano-1,2,3,10b-tetrahydropyrrolo[2,1-*a*]phthalazine **187**

A suspension of phthalazinium-2-dicyanomethanide 1,3-dipole (0.30 g, 1.54 mmol) in water (20 cm³, Millipore grade) was treated with *N*-phenylmaleimide (0.26 g, 1.54 mmol) and stirred at ambient temperature for 24 hours. During this time the product precipitated from solution as a pale yellow solid and was collected by direct filtration to give compound **187** (0.56 g, 96 %); mp 252-253 °C (ethanol); (Found: C, 62.9; H, 3.7 N, 23.2. C₂₁H₂₃N₅O₂ requires C, 62.9; H, 3.6; N, 22.9%); $\nu_{\max}/\text{cm}^{-1}$ 1715, 1795 (C=O); δ_{H} (DMSO-*d*₆) 4.41 (dd, 1H, *J* 7.8, 7.6 H-1), 4.77 (d, 1H, *J* 7.8, H-2), 5.19 (d, 1H, *J* 7.6, H-10b), 7.19 (d, 2H, *J* 7.1, H-2' of *N*-Ph, 7.51-7.66 (m, 6H, H-3' and H-4' of *N*-Ph and H-7 to H-9), 7.82 (d, 1H, *J* 7.8, H-10), 8.07 (s, 1H, H-6); δ_{C} (DMSO-*d*₆) 45.3 (C-2), 51.3 (C-1), 59.2 (C-3), 59.7 (C10-b), 110.8, 112.4 (C≡N), 123.9 (C-10a), 128.9 (C-1' of *N*-Ph), 129.6 (C-6a), 131.9 (C-7), 126.5 (C-8), 127.1 (C-9), 127.8 (C-10), 129.2 (C-2' of *N*-Ph), 131.5 (C-3' of *N*-Ph), 146.8 (C-6), 170.4, 172.4 (C=O).

Synthesis of 1-*endo*-2-*exo*-2-acetyl-1-(4-chlorophenyl)-1,2,3,10b-tetrahydro pyrrolo[2,1-*a*]phthalazine-3,3-dicarbonitrile **182** and 1-*exo*-2-*endo*-2-acetyl-1-(4-chlorophenyl)-1,2,3,10b-tetrahydropyrrolo[2,1-*a*]phthalazine-3,3-dicarbonitrile **183**

A suspension of phthalazinium-2-dicyanomethanide 1,3-dipole (0.20 g, 1.03 mmol) and 4-(4-chlorophenyl)-3-buten-2-one (0.19 g, 1.05 mmol) in water (10 cm³, Millipore grade) was stirred vigorously at 75 °C for 24 h. During this time the suspended solids compacted into a sticky mass surrounding the stir bar and the interior of the reaction flask. The solids were collected by filtration and scraping from the stir bar and flask to give a mixture of compounds **182** and **183**; (0.35 g, 86% total yield); (ratio **182**: **183** determined by ¹H NMR spectroscopy, 6.2:1).

Chapter 3



^1H and ^{13}C NMR spectra for product **182** in CDCl_3

Experimental: kinetics

The phthalazinium-2-dicyanomethanide 1,3-dipole **45** was recrystallized from ethanol before use. The dipolarophiles 4-phenyl-3-buten-2-one (Sigma-Aldrich, $\geq 99\%$), 4-(4-chlorophenyl)-3-buten-2-one (Sigma-Aldrich, 97%) and 4-(p-tolyl)-3-buten-2-one (Sigma-Aldrich, 97%) were used as purchased. Acetonitrile was of spectrophotometric grade (Sigma-Aldrich, $>99.9\%$) and used without further purification. Water was of Millipore grade. The rate constants were measured by recording the disappearance of the phthalazinium-2-dicyanomethanide 1,3-dipole **45** at its maximum wavelength in the solvent mixture. The λ_{\max} was 423 nm in acetonitrile and 411 nm in 0.9 mole fraction water / acetonitrile.

Spectra were measured using a Hewlett Packard Agilent Technologies 8453 UV-Vis spectrophotometer featuring an automatic changer for up to 8 glass cuvettes of path length 1 cm. The temperature (± 0.2 °C) was maintained by means of a thermostat (Haake DC10) controlled water bath, with a separate calibrated thermometer check. The reaction was monitored using pseudo-first-order conditions. The initial concentration of 1,3-dipole **45** was 3.2×10^{-5} M and the dipolarophile concentrations were in excesses ranging from 20 to 600 fold. Kinetic runs were performed at three different concentrations of dipolarophiles and repeated three times. The length of time for the reaction ranged from 36 to 96 h depending on the dipolarophile and conditions. The solution changed from yellow to colourless as the reaction progressed.

In a typical kinetic run 2 cm^3 of the dipole solution was placed in a tightly capped cuvette of path length 1 cm and left to equilibrate to the temperature for 10 min. The dipolarophile solution (1 cm^3) was added and the mixture was shaken, allowed to equilibrate and the absorbance (A) measured. A plot of $\ln (A_t - A_\infty)$ versus time for more than 3 half-lives, gave a line whose slope gave the pseudo-first-order rate constant. These lines typically gave r values of ≥ 0.999 . Plots of the measured pseudo-first-order rate constants, with the origin as an extra point, versus the molarity of the dipolarophile, gave lines where slopes which were the second-order

rate constants quoted. All second-order rate constants were measured at least three times and were reproducible to $\pm 5.0\%$.

Computational Methods

A number of computational methods incorporated into the Gaussian 03 series of programs¹⁰¹ were used in this study. All geometry optimisations were carried out with B3LYP^{103, 104} DFT method. The standard split valence plus polarisation 6-31G(d) basis set was used in all cases. Normal mode analysis was used to ascertain the nature of all structures identified as stationary points. All dipolarophiles were optimised and their lowest energy conformations were used in this study. The geometries of all carbonyl groups were optimised to a *cis* or quasi *cis* configuration to the C=C bond in the transition states as these configurations give lower energies than the *trans* configurations in the separated dipolarophiles. Transition state structures were calculated for all four stereo (*endo/exo*) and regioisomeric products from C=C bond dipolarophiles. In many of the dipolarophiles used in this study there is a possibility for one or more lone pair orbitals to be the HOMO(s). As we are dealing with cycloaddition reactions the highest π -C=C molecular orbital should be considered for the frontier orbital interactions. All dipolarophile LUMO in this study are π -C=C molecular orbitals. It was verified that the HOMO and the LUMO of the 1,3-dipole **45** are composed mainly of the three dipole atoms and do not involve a lone pair of the benzo system.⁶³

References

1. R. Huisgen, *Proc. Chem. Soc.*, 1961, 357.
2. R. Huisgen, *Angew. Chem. Int. Ed.*, 1963, **2**, 565.
3. T. L. Gilchrist, in 'Heterocyclic Chemistry', Pittman Publishing, London, 1992, **2**, 85.
4. W. J. Linn, R. E. Benson, O. W. Webster, *J. Am. Chem. Soc.*, 1963, **85**, 2032.
5. W. J. Linn, O. W. Webster, R. E. Benson, *J. Am. Chem. Soc.*, 1965, **87**, 3651.
6. V. Boekelheide, N. A. Fedoruk, *J. Am. Chem. Soc.*, 1968, **90**, 3830.
7. E. Diez-Barra, M. del Carmen Pardo, J. Elguero, *J. Org. Chem.*, 1982, **47**, 4409.
8. J. A. Zoltewicz, L. W. Deady, *Adv. Heterocyclic Chem.*, 1978, **22**, 71.
9. C. Leonte, I. Zugravescu, *Tetrahedron Lett.*, 1972, 2027.
10. E. Hatzigrigoriou, M. Bakolachristianopoulou, A. Varvoglis, *J. Chem. Res. (S)*, 1987, 374.
11. C. Bugg, R. L. Sass, R. Desiderato, *J. Am. Chem. Soc.*, 1964, **86**, 3157.
12. C. Bugg, R. L. Sass, *Acta Crystallogr.*, 1965, **18**, 591.
13. B. B. De More, W. S. Wilcox, J. H. Goldstein, *J. Chem. Phys.*, 1954, **22**, 876.
14. Y. Karzazi, G. Vergoten, G. Surpateanu, *J. Mol. Struct.*, 1999, **476**, 121.
15. Y. I. Binev, B. A. Stamboliyska, I. G. Binev, *Spectrochim. Acta A*, 2001, **57**, 95.
16. J. Coates, in 'Encyclopedia of Analytical Chemistry', ed. R. A. Meyers, John Wiley and Sons Ltd., Chichester, 2000, 10815.
17. Y. Karzazi, G. Vergoten, G. Surpateanu, *J. Mol. Struct.*, 1997, **435**, 35.
18. G. Surpateanu, J. P. Catteau, P. Karafiloglou, A. Lablachecombier, *Tetrahedron*, 1976, **32**, 2647.
19. R. C. F. Jones, J. R. Nichols, M. T. Cox, *Tetrahedron Lett.*, 1990, **31**, 2333.
20. E. Vedejs, G. R. Martinez, *J. Am. Chem. Soc.*, 1979, **101**, 6452.
21. E. Vedejs, S. Larsen, F. G. West, *J. Org. Chem.*, 1985, **50**, 2170.
22. K. Matsumoto, T. Uchida, M. Toda, N. Hayashi, Y. Ikemi, K. Aoyama, A. Kakehi, *Supramol. Chem.*, 2001, **13**, 93.

23. K. Matsumoto, H. Katsura, T. Uchida, K. Aoyama, T. Machiguchi, *Heterocycles*, 1997, **45**, 2443.
24. N. Basketter, A. O. Plunkett, *J. Chem. Soc., Chem. Comm.*, 1971, 1578.
25. Y. Kobayashi, T. Kutsuma, Y. Sekine, *Tetrahedron Lett.*, 1972, 3325.
26. M. Mattner, H. Neunhoeffler, *Eur. J. Org. Chem.*, 2004, 4234.
27. K. Matsumoto, T. Uchida, K. Aoyama, M. Nishikawa, T. Kuroda, T. Okamoto, *J. Heterocyclic Chem.*, 1988, **25**, 1793.
28. K. Matsumoto, R. Ohta, T. Uchida, H. Nishioka, M. Yoshida, A. Kakehi, *J. Heterocyclic Chem.*, 1997, **34**, 203.
29. T. Sasaki, K. Kanematsu, Y. Yukimoto, S. Ochiai, *J. Org. Chem.*, 1971, **36**, 813.
30. K. Matsumoto, Y. Ikemi, H. Konishi, X. L. Shi, T. Uchida, K. Aoyama, *J. Heterocyclic Chem.*, 1988, **25**, 689.
31. R. N. Butler, D. M. Farrell, C. S. Pyne, *J. Chem. Res. (S)*, 1996, 418.
32. R. N. Butler, D. M. Farrell, *J. Chem. Res. (S)*, 1998, 214.
33. R. N. Butler, A. G. Coyne, P. McArdle, D. Cunningham, L. A. Burke, *J. Chem. Soc., Perkin Trans. I*, 2001, 1391.
34. R. N. Butler, A. G. Coyne, W. J. Cunningham, L. A. Burke, *J. Chem. Soc., Perkin Trans. 2*, 2002, 1807.
35. E. Diez-Barra, C. Pardo, J. Elguero, J. Arriau, *J. Chem. Soc., Perkin Trans. 2*, 1983, 1317.
36. K. Matsumoto, T. Uchida, M. Toda, K. Aoyama, A. Kakehi, A. Shigihara, J. W. Lown, *Tetrahedron Lett.*, 1992, **33**, 7643.
37. O. Tsuge, H. Shimoharada, M. Noguchi, S. Kanemasa, *Chem. Lett.*, 1982, 711.
38. O. Tsuge, Y. Shimizu, H. Shimoharada, S. Kanemasa, *Heterocycles*, 1982, **19**, 2259.
39. O. Tsuge, S. Kanemasa, S. Takenaka, *B. Chem. Soc. Jpn.*, 1983, **56**, 2073.
40. O. Tsuge, H. Shimoharada, *Chem. Pharm. Bull.*, 1982, **30**, 1903.
41. O. Tsuge, S. Kanemasa, S. Takenaka, *Chem. Lett.*, 1983, 519.
42. K. Elender, P. Riebel, A. Weber, J. Sauer, *Tetrahedron*, 2000, **56**, 4261.

43. R. N. Butler, A. G. Coyne, L. A. Burke, *J. Chem. Soc., Perkin Trans. 2*, 2001, 1781.
44. R. N. Butler, W. J. Cunningham, A. G. Coyne, L. A. Burke, *J. Am. Chem. Soc.*, 2004, **126**, 11923.
45. O. Diels, K. Alder, *Justus Liebigs Ann. Chem.*, 1928, **98**, 260.
46. M. J. S. Dewar, R. C. Dougherty, in 'The PMO Theory of Organic Chemistry', Plenum Press, New York, 1975, 345.
47. R. B. Woodward, R. Hoffmann, *Angew. Chem. Int. Ed.*, 1969, **8**, 781.
48. R. Huisgen, L. Mobius, G. Muller, H. Stangl, G. Szeimies, J. M. Vernon, *Chem. Ber.-Recl.*, 1965, **98**, 3992.
49. R. Huisgen, *Angew. Chem. Int. Ed. Engl.*, 1963, **2**, 633.
50. R. Huisgen, G. Szeimies, L. Mobius, *Chem. Ber.-Recl.*, 1967, **100**, 2494.
51. R. A. Firestone, *J. Org. Chem.*, 1968, **33**, 2285.
52. R. Huisgen, *J. Org. Chem.*, 1968, **33**, 2291.
53. J. Baran, H. Mayr, *J. Am. Chem. Soc.*, 1987, **109**, 6519.
54. R. Huisgen, G. Mloston, E. Langhals, *J. Am. Chem. Soc.*, 1986, **108**, 6401.
55. R. Huisgen, in '1,3-Dipolar Cycloadditions: Concertedness, Yes or No?' ed. V. G. Kartsev, IBS Press, Moscow, 2003, 83.
56. R. Sustmann, *Tetrahedron Lett.*, 1971, 2717.
57. R. Sustmann, *Tetrahedron Lett.*, 1971, 2721.
58. R. N. Butler, L. M. Wallace, *J. Chem. Soc., Perkin Trans. 1*, 2000, 4335.
59. R. N. Butler, D. F. O' Shea, *Heterocycles*, 1994, **37**, 571.
60. R. N. Butler, M. O. Cloonan, P. McArdle, D. Cunningham, *J. Chem. Soc., Perkin Trans. 1*, 1998, 1295.
61. R. N. Butler, A. M. Evans, A. M. Gillan, J. P. James, E. M. McNeela, D. Cunningham, P. McArdle, *J. Chem. Soc., Perkin Trans. 1*, 1990, 2537.
62. R. N. Butler, D. M. Colleran, *J. Chem. Soc., Perkin Trans. 1*, 1992, 2159.
63. R. N. Butler, A. G. Coyne, W. J. Cunningham, E. M. Moloney, L. A. Burke, *Helv. Chim. Acta*, 2005, **88**, 1611.
64. R. N. Butler, F. A. Lysaght, L. A. Burke, *J. Chem. Soc., Perkin Trans. 2*, 1992, 1103.

65. R. N. Butler, D. M. Colleran, F. A. Lysaght, D. F. O' Shea, *J. Chem. Res. (S)*, 1993, 78.
66. R. N. Butler, A. M. Fahy, A. Fox, J. C. Stephens, P. McArdle, D. Cunningham, A. G. Ryder, *Tetrahedron Lett.*, 2006, **47**, 1721.
67. R. N. Butler, A. M. Fahy, A. Fox, J. C. Stephens, P. McArdle, D. Cunningham, A. Ryder, *J. Org. Chem.*, 2006, **71**, 5679.
68. H. Ogura, K. Kikuchi, *J. Org. Chem.*, 1972, **37**, 2679.
69. I. Zugravescu, J. Herdan, I. Druta, *Rev. Roum. de Chim.*, 1974, **19**, 649.
70. O. Meth-Cohn, *Tetrahedron Lett.*, 1975, 413.
71. H. A. Gavin, Ph. D. Thesis, NUI Galway, 1992.
72. T. Itoh, Y. Matsuya, K. Nagata, M. Miyazaki, N. Tsutsumi, A. Ohsawa, *J. Chem. Soc., Perkin Trans. 1*, 1998, 1637.
73. A. G. Coyne, Ph. D. Thesis, NUI Galway, 2002.
74. B. Abarca, R. Ballesteros, F. Mojarrad, M. R. Metni, S. Garciagrande, E. Perezcarreno, G. Jones, *Tetrahedron*, 1991, **47**, 5277.
75. T. Stevens, E. Creighton, A. Gordon, M. MacNicol, *J. Chem. Soc.*, 1928, **0**, 3193.
76. A. M. Van Leusen, B. E. Hoogenboom, H. A. Houwing, *J. Org. Chem.*, 1976, **41**, 711.
77. R. G. Micetich, P. Spevak, T. W. Hall, B. K. Bains, *Heterocycles*, 1985, **23**, 1645.
78. H. J. Cristau, P. P. Cellier, J. F. Spindler, M. Taillefer, *Chem. Eur. J.*, 2004, **10**, 5607.
79. L. Burke, R. Butler, *J. Org. Chem.*, 2009, **74**, 5199.
80. A. I. Vogel, 'Vogel's Textbook of Practical Organic Chemistry', ed. A. J. H. E. B. S. Furniss; Ed., P. W. Smith; Ed., A. R. Tatchell, Prentice Hall, 1989.
81. M. Sekiya, S. Ishikawa, *Yakugaku Zasshi*, 1958, **78**, 549.
82. D. C. Rideout, R. Breslow, *J. Am. Chem. Soc.*, 1980, **102**, 7816.
83. R. Breslow, *Acc. Chem. Res.*, 1991, **24**, 159.
84. R. Breslow, R. Connors, Z. Zu, *Pure Appl. Chem.*, 1996, **68**, 1527.
85. R. Breslow, C. J. Rizzo, *J. Am. Chem. Soc.*, 1991, **113**, 4340.

86. R. Breslow, U. Maitra, D. Rideout, *Tetrahedron Lett.*, 1983, **24**, 1901.
87. R. Breslow, U. Maitra, *Tetrahedron Lett.*, 1984, **25**, 1239.
88. S. Otto, W. Blokzijl, J. B. F. N. Engberts, *J. Org. Chem.*, 1994, **59**, 5372.
89. S. Otto, J. B. F. N. Engberts, *Org. Biomol. Chem.*, 2003, **1**, 2809.
90. A. Meijer, S. Otto, J. B. F. N. Engberts, *J. Org. Chem.*, 1998, **63**, 8989.
91. J. B. F. N. Engberts, *Pure Appl. Chem.*, 1995, **67**, 823.
92. S. Otto, J. B. F. N. Engberts, *Pure Appl. Chem.*, 2000, **72**, 1365.
93. J. Chandrasekhar, S. Shariffskul, W. J. Jorgensen, *J. Phys. Chem. B*, 2002, **106**, 8078.
94. J. F. Blake, D. Lim, W. L. Jorgensen, *J. Org. Chem.*, 1994, **59**, 803.
95. C. Hansch, A. Leo, R. W. Taft, *Chem. Rev.*, 1991, **91**, 165.
96. P. A. Grieco, P. Garner, Z. He, *Tetrahedron Lett.*, 1983, **24**, 1897.
97. J. E. Klijjn, J. B. F. N. Engberts, *Nature*, 2005, **435**, 746.
98. S. Narayan, J. Muldoon, M. G. Finn, V. V. Fokin, H. C. Kolb, K. B. Sharpless, *Angew. Chem. Int. Ed.*, 2005, **44**, 3275.
99. Y. Jung, R. A. Marcus, *J. Am. Chem. Soc.*, 2007, **129**, 5492.
100. ACD/C+H NMR Predictors, version 14.00, Advanced Chemistry Development, Inc., 2016
101. Gaussian 03, Revision A.1, M. J. Frisch, G. W. Trucks, H. B. Schlegel, G. E. Scuseria, M. A. Robb, J. R. Cheeseman, J. A. Montgomery, T. V. Jr., K. N. Kudin, J. C. Burant, J. M. Millam, S. S. Iyengar, J. Tomasi, V. Barone, B. Mennucci, M. Cossi, G. Scalmani, N. Rega, G. A. Petersson, H. Nakatsuji, M. Hada, M. Ehara, K. Toyota, R. Fukuda, J. Hasegawa, M. Ishida, T. Nakajima, Y. Honda, O. Kitao, H. Nakai, M. Klene, X. Li, J.E. Knox, H. P. Hratchian, J. B. Cross, C. Adamo, J. Jaramillo, R. Gomperts, R. E. Stratmann, O. Yazyev, A. A. J., R. Cammi, C. Pomelli, J. W. Ochterski, P. Y. Ayala, K. Morokuma, G. A. Voth, P. Salvador, J. J. Dannenberg, V. G. Zakrzewski, S. Dapprich, A. D. Daniels, M. C. Strain, O. Farkas, D. K. Malick, A. D. Rabuck, K. Raghavachari, J. B. Foresman, J. V. Ortiz, Q. A. G. Cui, S. Clifford, J. Cioslowski, B. B. Stefanov, G. Liu, A. Liashenko, P. Piskorz, I. Komaromi, R. L. Martin, D. J. Fox, T. Keith., M. A. Al-Laham, C.

- Y. Peng, A. Nanayakkara, M. Challacombe, P. M. W. Gill, B. Johnson, W. Chen, M. W. Wong, C. Gonzalez, J. A. Pople., Gaussian, Inc., Pittsburgh PA, 2003.
102. Reported values from SciFinder, calculated using Solaris, version 8.15, Advanced Chemistry Development, Inc., Toronto ON, 2006.
 103. C. Lee, W. Yang, W. G. Parr, *Phys. Rev. B*, 1988, **37**, 785.
 104. A. D. Becke, *Phys. Rev. A*, 1988, **38**, 3098.

Publications

Publications

1. Water and the Huisgen cycloaddition reaction: A focus on polar contributions to the transition state in the reactions of dicyano(phthalazinium)methanide with substituted styrenes and benzylidene acetones.
R. N. Butler, A. G. Coyne, W. J. Cunningham, E. M. Moloney, L. A. Burke, *Helv. Chim. Acta.*, 2005, **88**, 1611.
2. Spirally twisted ylide structures from 1,2-rearrangements in reactions of imidazolium dicyanomethanide 1,3-dipoles with maleic anhydride: new perspectives on the Boekelheide-Fedoruk ring expansions
R. N. Butler, H. A. Gavin, E. M. Moloney, P. McArdle, D. Cunningham, L. A. Burke, *Tetrahedron Lett*, 2006, **47**, 6107.
3. Organic synthesis in water: 1,3-dipolar cycloaddition reactions at ambient temperature with aqueous suspensions of solid reactants
R. N. Butler, A. G. Coyne, E. M. Moloney, *Tetrahedron Lett*, 2007, **48**, 3501.
4. Water and organic synthesis: A focus on the in-water and on-water border. Reversal of the in-water Breslow hydrophobic enhancement of the normal *endo*-effect on crossing to on-water conditions for Huisgen cycloadditions with increasingly insoluble organic liquid and solid 2π -Dipolarophiles
R. N. Butler, A. G. Coyne, W. J. Cunningham, E. M. Moloney, *J. Org. Chem.*, 2013, **78**, 3276.